

Final Report

NATURAL PRODUCT-BASED DRUG DISCOVERY FROM THAI AND CHINESE MEDICINAL PLANTS

การค้นพบยาที่ได้จากผลิตภัณฑ์ธรรมชาติจากสมุนไพรไทยและจีน

Apichart Suksamrarn

Principal Investigator

NATURAL PRODUCT-BASED DRUG DISCOVERY FROM THAI AND CHINESE MEDICINAL PLANTS

การค้นพบยาที่ได้จากผลิตภัณฑ์ธรรมชาติจากสมุนไพรไทยและจีน

Investigators

1. Apichart Suksamrarn	Ramkhamhaeng University
2. Pawinee Piyachaturawat	Mahidol University
3. Sunit Suksamrarn	Srinakharinwirot University
4. Boon-ek Yingyongnarongkul	Ramkhamhaeng University
5. Vachiraporn Ajavakom	Ramkhamhaeng University
6. Moltira Promkan	Mahidol University
7. Sumana Dakeng	Mahidol University
8. Guolin Zhang	Chengdu Institute of Biology
9. Fei Wang	Chengdu Institute of Biology

Supported by The Thailand Research Fund

(The views and opinions of the researchers expressed in this report do not necessarily state or reflect those of The Thailand Research Fund)

ACKNOWLEDGEMENTS

The researchers are grateful to The Thailand Research Fund (TRF) for the Directed Basic Research Grant entitled Natural Product-based Drug Discovery from Thai and Chinese Medicinal Plants, which also includes a collaborative research project with Professor Dr. Gaolin Zhang and Professor Fei Wang, Chengdu Institute of Biology, Chinese Academy of Sciences, China. Supports from the Golden Jubilee Ph.D. Program of TRF, and Center of Excellence for Innovation in Chemistry (PERCH-CIC), Office of the Higher Education Commission are gratefully acknowledged. We also acknowledge the Bioassay Research Facility, National Center for Genetic Engineering and Biotechnology (BIOTEC) for partial support on bioassay tests.

The researchers are indebted to Miss Nattisa Niyomtham, Miss Parichat Suebsakwong and Miss Waraluck Chaichompoo for recording the nuclear magnetic resonance spectra, to Miss Kanyarat Chanchang for recording the mass spectra, to Mr. Archawin Nakaew and Miss Sukanya Kunkaewom for recording the infrared spectra, and to Miss Nilubon Sornkaew for measurement of the optical rotation.

The researchers are grateful to Professor Dr. Fei Wang, Chengdu Institute of Biology and Associate Professor Dr. Tanapat Palaka, Department of Microbiology, Faculty of Science, Chulalongkorn University for some bioassay evaluations.

Finally, the researchers acknowledge supports from Ramkhamhaeng University, Mahidol University and Srinakharinwirot University.

Apichart Suksamrarn

Principal Investigator

บทคัดย่อ

โครงการวิจัยนี้เกี่ยวข้องกับการค้นพบยาจากผลิตภัณฑ์ธรรมชาติ ประกอบด้วยโครงการจำนวน 6 โครงการ แต่ละโครงการประกอบด้วยโครงการย่อยจำนวนต่างกัน โครงการที่ 1 การเลือกสารผลิตภัณฑ์ ธรรมชาติออกฤทธิ์เพื่อการค้นพบยา เป็นการตรวจหาส่วนประกอบทางเคมีที่มีฤทธิ์ทางยา เช่นฤทธิ์ ปกป้องการเกิดภาวะกระดูกพรุน โครงการที่ 2 เป็นการปรับเปลี่ยนโครงสร้างสารนำบางชนิดเพื่อให้มี ฤทธิ์ทางชีวภาพสูงขึ้น โครงการนี้ประกอบด้วยโครงการย่อย 2 โครงการย่อย โครงการย่อยที่ 1 เป็น การศึกษาแอนาลอกเคอร์คิวมินอยด์ที่มีฤทธิ์ยับยั้งเอนไซม์ phosphodiesterase-5 และการขยายหลอด เลือดแดงในปอดของหนู เพื่อหายาลดความดันโลหิตในปอด และได้พบสารกลุ่มนี้จำนวนหนึ่งที่มีฤทธิ์ ้ ดังกล่าวนี้ โครงการย่อยที่ 2 เป็นการปรับเปลี่ยนโครงสร้างของ chalcones ให้มีฤทธิ์ยับยั้งการสร้าง biofilm ของแบคที่เรีย และพบว่า 3-hydroxychalcone มีฤทธิ์ดังกล่าวนี้ดีกว่า azithromycin ซึ่งเป็นยา อ้างอิงถึง 6 เท่า โครงการที่ 3 เป็นการศึกษาผลิตภัณฑ์ธรรมชาติที่มีฤทธิ์ต้านเซลล์มะเร็ง โดยทำการแยก หาสูตรโครงสร้าง ปรับเปลี่ยนโครงสร้าง สังเคราะห์แอนาลอก และการทดสอบฤทธิ์ทางชีวภาพ ประกอบด้วย 3 โครงการย่อย โครงการย่อยที่ 1 เป็นการสังเคราะห์ ศึกษาความสัมพันธ์ระหว่าง โครงสร้างกับฤทธิ์ในการยับยั้งเซลล์มะเร็งในช่องปาก ได้สังเคราะห์แอนา ลอก trienones จำนวน 16 สาร พบว่ามีจำนวนหนึ่งที่แสดงฤทธิ์นี้สูง และบางสารมีฤทธิ์สูง กว่า ellipticine ซึ่ง เป็นยาต้านมะเร็งอ้างอิง โครงการย่อยที่ 2 เป็นการศึกษาฤทธิ์ต้านมะเร็งท่อน้ำดีของสารอัลคาลอยด์จากย่านาง พบว่า สารที่มีอยู่มาก สามารถยับยั้งการเพิ่มจำนวนของเซลล์มะเร็งท่อน้ำดีได้อย่างมี tiliacorinine ซึ่งเป็น นัยสำคัญ และสามารถลดการเจริญของมะเร็งในหนูทดลองได้ดี โครงการย่อยที่ 3 เป็นการศึกษาแอนา ลอกของเคอร์คิวมินอยด์ที่มีฤทธิ์ในการเพิ่มฤทธิ์การเจริญของ teromerase โดยพบว่า แอนาลอกของ เคอร์คิวมินอยด์ที่มีสายโซ่ด้านข้างเป็น alkylpyridinium บางสารแสดงฤทธิ์นี้ งานวิจัยนี้เป็นการค้นพบ teromerase activators ชนิดใหม่ที่ไปกระทำต่อ teromerase โดยตรงหรือโดยอ้อม มากกว่าที่จะไป กระทำที่ยืน telomerase reverse transcriptase ตามที่ได้มีผู้รายงานไว้

โครงการที่ 4 เป็นการปรับเปลี่ยนโครงสร้างและทดสอบฤทธิ์ทางชีวภาพและกลไกการออกฤทธิ์ของ สารต้านการอักเสบที่ไม่ใช่สเตียรอยด์จากผลิตภัณฑ์ธรรมชาติ ประกอบด้วย 2 โครงการย่อย โครงการ ย่อยที่ 1 เป็นไดเอริลเฮปทานอยด์ซึ่งมีฤทธิ์ยับยั้งการสร้างในตริกออกไซด์จากว่านชักมดลูก โครงการ ย่อยนี้ได้ศึกษาส่วนประกอบทางเคมีของเหง้าของพืชตระกูลว่านชักมดลูก ซึ่งมีพบทั้งในไทยและในจีน สำหรับว่านชักมดลูก ได้พบไดเอริลเฮปทานอยด์ชนิดใหม่จำนวน 8 ชนิดและที่ได้เคยทราบโครงสร้างมา ก่อนแล้วอีก 13 ชนิด งานวิจัยนี้ผู้ร่วมวิจัยทางประเทศจีน คือศาสตราจารย์ กัวลิน จาง และ ศาสตราจารย์ เฟย หวาง ได้ศึกษาพืชในสกุลนี้ในจีนเปรียบเทียบด้วย ผลการวิจัยพบว่าไดเอริลเฮปทานอยด์ 2 ชนิด แสดงฤทธิ์ต้านการอักเสบโดยยับยั้งการสร้างในตริกออกไซด์ในเซลล์ RAW264.7 ที่ถูกกระตุ้นด้วย LPS โครงการที่ 5 เป็นการหาสารออกฤทธิ์ในการบำบัดโรคของผู้สูงอายุจากผลิตภัณฑ์ธรรมชาติ โครงการนี้มี

4 โครงการย่อย โครงการย่อยที่ 1 เป็นการศึกษาผลการยับยั้งของสารไดเอริลเฮปทานอยด์จากว่านชัก มดลูกต่อการเกิดกระดูกพรุนในหนูเพศเมียที่ถูกตัดรังไข่ออก พบว่าสาร (3R)-1,7-diphenyl-(4E,6E)-4,6heptadien-3-ol สามารถยับยั้งการสูญเสียมวลกระดูกในหนูที่ตัดรังไข่ออกได้ โดยใช้สาร 17β-estradiol เป็นฮอร์โมนควบคุม สารนี้จึงน่าจะเป็นสารที่มีศักยภาพในการรักษามวลและโครงสร้างของกระดูกในสตรี ที่ขาดฮอร์โมนเอสโตรเจนเพื่อลดการเกิดกระดูกพรุนหลังวัยหมดประจำเดือน โครงการย่อยที่ 2 เป็น การศึกษาผลของแอนาลอกของไอโซสเตวิออล คือ 16-O-acetyldihydroisosteviol ต่อการขยายหลอด เลือดของหนู พบว่าสารนี้สามารถขยายหลอดเลือดของหนูได้โดยผ่านกลไกที่ไม่ขึ้นกับเอนโดทีเลียม โครงการย่อยที่ 3 เป็นผลของแอนาลอกของเคอร์คิวมินอยด์ คือ di-O-demethylcurcumin ในการปกป้อง ไม่ให้เกิด apoptosis ในเซลล์ประสาท ซึ่งเนื่องมาจากการเหนี่ยวนำด้วยเอมัยลอยด์เบตา พบว่าสารนี้ สามารถป้องกันการตายของเซลล์ประสาทได้ โดยการยับยั้ง apoptosis อันเนื่องมาจากการตายของไมโต คอนเดรียและ endoplasmic reticulum (ER) stress โครงการย่อยที่ 4 เป็นการศึกษาผลของ *O*demethyldemethoxycurcumin ต่อการลด apoptosis ที่ถูกเหนี่ยวนำโดย thapsigargin ที่มีต่อเซลล์ neuroblastoma (SK-N-SH) โดยมีกลไกผ่าน ER stress signaling ผลที่ได้แสดงให้เห็นว่าสารนี้เพิ่มการ มีชีวิตของเซลล์ประสาทที่เกิดการตายแบบ apoptosis ที่ถูกเหนี่ยวนำโดย thapsigargin สารนี้จึงอาจเป็น ทางเลือกหนึ่งสำหรับการป้องกันโรคการเสื่อมของเซลล์ประสาทได้ โครงการที่ 6 เป็นการออกแบบและ สังเคราะห์ระบบนำส่งยาสำหรับผลิตภัณฑ์ธรรมชาติที่มีฤทธิ์เป็นพิษต่อเซลล์ และสารออกฤทธิ์อื่นไปยัง เซลล์เป้าหมาย โครงการย่อยที่ 1 เป็นการพัฒนา cationic lipids ที่มีส่วนหัว ส่วนกลาง และส่วนหาง จาก การออกแบบโดยใช้ส่วนต่างๆ ดังกล่าวร่วมกันโดยมีลิปิดอื่นด้วยได้นำไปสู่การค้นพบสารนำยาเข้าสู่เซลล์ ที่มีประสิทธิภาพสูงมากและมีความเป็นพิษต่ำ โครงการย่อยที่ 2 เป็นการสังเคราะห์และศึกษา ประสิทธิภาพของการนำสารเข้าสู่เซลล์ของ cationic lipids ที่มีสารหลักเป็น spermine โครงการย่อยนี้ได้ สังเคราะห์ cationic lipids ที่มีส่วนหัว ส่วนกลาง และส่วนหางแตกต่างกัน พบว่าไลโปโซมที่มีลิปิดและ DOPE สามารถนำดีเอ็นเอเข้าสู่ HeLa เซลล์ได้ปานกลางถึงดี ไลโปโซมที่ลิปิดมีหมู่ dioxypropyl อยู่ตรงส่วนกลางมีความสามารถในการนำส่งสารได้ดีที่สุด ส่วนลิปิดที่มีหมู่ 2 -amino-1,3dioxypropyl อยู่ตรงส่วนกลางมีความสามารถในการนำส่งสารได้ดีที่สุดภายใต้สภาวะ 10% ซีรัม

ในการวิจัยโครงการนี้ ได้มีการค้นพบสารผลิตภัณฑ์ ธรรมชาติและแอนาลอกของสารผลิตภัณฑ์ ธรรมชาติที่มีฤทธิ์ทางชีวภาพสูงเป็นจำนวนมาก โดยบางสารมีฤทธิ์สูงกว่ายามาตรฐานที่ใช้กัน การวิจัย ในอนาคตจึงควรพิจารณาหาทางนำสารที่มีฤทธิ์สูงเหล่านี้ไปต่อยอด เพื่อที่จะได้สารที่ศักยภาพในการ พัฒนาเป็นยารักษาโรคต่อไป

คำสำคัญ: สารผลิตภัณฑ์ธรรมชาติ, การค้นพบยา, การปรับเปลี่ยนโครงสร้าง, ฤทธิ์ความเป็นพิษต่อ เซลล์, ฤทธิ์ต้านแบคทีเรีย, ฤทธิ์ต้านกระดูกพรุน, ฤทธิ์ต้านความดันสูง, ฤทธิ์ต้านการอักเสบ, ฤทธิ์ ต้านอัลไซเมอร์, แคตไอออนนิกลิปิด

ABSTRACT

The project deals with natural product-based drug discovery. It consists of six projects and each project contained a number of subprojects. The first project is Selection of Bioactive Natural Products for Drug Discovery and the subproject involves Screening of Anti-Osteoporosis Constituents from Plants. The second project is Structural Modification of Some Lead Compounds for Higher Biological Activities. This project consists of two subprojects, the first one of which is Curcuminoid Analogues with Phosphodiesterase-5 (PDE5) Inhibitory Activity and Rat Pulmonary Artery Dilating Property, which led to the discovery of a number of curcuminoid analogues that inhibited PDE5 and dilated rat pulmonary arteries. The second subproject is Structural Modification of Chalcones to Analogues with Potent Inhibitory Activity against Biofilm Formation by Bacteria and it was found that 3-hydroxychalcone exhibited the most potent inhibitory activity; its mean minimum biofilm inhibitory concentration was 6-fold more active than the reference drug, azithromycin. The third project deals with Natural Products with Cytotoxic Activity. Isolation, Structural Elucidation, Structural Modification, Synthesis of Analogues, in vitro and in vivo Activity Evaluations. There are three subprojects in this project. The first one is Synthesis, Cytotoxicity against Human Oral Cancer KB Cells and Structure-Activity Relationship Studies of Trienone Analogues of Curcuminoids. In his subproject, sixteen trienone analogues have been synthesized for cytotoxicty against KB cell line. A number of the analogues exhibited very high anti-KB activity and some of them showed higher cytotoxicy than that of ellipticine, the reference anti-cancer drug. The second subproject is Anti-cholangiocarcinoma Activity of Bisbenzylisoquinoline Alkaloid from *Tiliacora triandra*. The major alkaloid, tiliacorinine, significantly inhibited proliferations of human cholangiocarcinoma (CCA) cell lines and considerably reduced tumor growth in CCA xenografted mice. The third subproject is Curcuminoid Analogues Enhance Teromerase Activity in an in vitro TRAP Assay. In this subproject, a number of curcuminoid analogues with alkylpyridinium side chain were found to enhance telomerase activity in an in vitro TRAP assay. The finding might lead to a new class of telomerase activators that act directly or indirectly on telomerase, rather than through the reactivation of the telomerase reverse transcriptase (TERT) gene associated with other telomerase activators found in the literature.

The fourth project is Structural Modification and Biological Evaluation of Nonsteroidal Antiinflammatory Natural Products and Analogues and Study of Mechanism of Action. This project consists of two subprojects. The first subproject is Diaryheptanoids of Curcuma comosa with Nitric Oxide Inhibitory Activity. This subproject involved the investigation of chemical constituents of the rhizomes of Curcuma comosa. Eight new diaryheptanoids and thirteen known diaryheptanoids were isolated. A number of Curcuma and other species of Chinese origins have also been studied by Professor Guolin Zhang and Professor Fei Wang, our Chinese collaborators in comparison with those of the Thai origins. Two diarylheptanoids were found to show anti-inflammatory effect by inhibiting NO production in LPS-stimulated RAW264.7 cells. The fifth project is Natural Product-based Therapeutic Agents for Diseases of the Elderly. This project consists of four subprojects. The first one is Bone Sparing Effect of Diarylheptanoid from Curcuma comosa in Ovariectomized Rats. In this subproject, the diarylheptanoid, (3R)-1,7-diphenyl-(4E,6E)-4,6-heptadien-3-ol, have been demonstrated to protect ovariectomy-induced bone loss in adult female rats with 17β-estradiol as a positive control. This compound appears to be a promising candidate for preserving bone mass and structure in the estrogen deficient women with a potential role in reducing postmenopausal The Vasorelaxation **Effects** of 16-*O*osteoporosis. second subproject is acetyldihydroisosteviol, an Analogue of Isosteviol, on Isolated Rat Thoracic Aorta. The chemically modified analogue of isosteviol, 16-O-acetyldihydroisosteviol, induced potent relaxation of rat aortic rings through endothelium-independent pathway. The third subproject is Protective Effect of a Curcuminoid Analogue against Amyloid Beta-Induced Apoptosis in Neuronal Cells. The mechanisms and effects of di-O-demethylcurcumin in preventing Aβinduced apoptosis have been investigated. It could be concluded that this compound is a candidate protectant against neuronal death through its suppression of the apoptosis mediated mitochondrial death and ER stress pathway. The fourth subproject is O-Demethyldemethoxycurcumin Exerts Suppression Effects on Thapsigargin Triggered on Endoplasmic Reticulum Stress in SK-N-SH Cells. The work aimed to evaluate the potential involvement of O-demethyldemethoxycurcumin on thapsigargin-induced apoptosis in cultured neuroblastoma (SK-N-SH) cells through the endoplasmic reticulum (ER) stress signaling The results showed that this curcuminoid analogue improved SK-N-SH cell pathway. viability by decreasing the apoptotic cell death induced by thapsigargin. Other related beneficial effects have also been found. This compound offers potential as an alternative therapeutic agent for protection against neurodegenerative diseases. The sixth project deals with Design and Synthesis of Delivery System for Cytotoxic and Other Bioactive Natural Products and Analogues to Targeted Cells. The first subproject involved Development of Cationic Lipids with Different Polarheads, Central Core Structures and Hydrophobic Tails. The combination of lipids with different polarheads, central core structures and hydrophobic tails in the presence of helper lipid has allowed the discovery of highly efficient transfection agents with minimal cytotoxicity. The second subproject is Synthesis and *in vitro* Transfection Efficiency of Spermine-based Cationic Lipids with Different Central Core Structures and Lipophilic Tails. In this subproject, spermine-based cationic lipids with four different central core structures and three hydrophobic tails were synthesized. The liposomes containing lipids and DOPE showed moderate to good *in vitro* DNA delivery into HeLa cells. Liposomes composed of lipids with 3-amino-1,2-dioxypropyl as a central core structure exhibited highest transfection efficiency under serum-free condition. Lipid with 2-amino-1,3-dioxypropyl core structure showed highest transfection under 10% serum condition.

Several bioactive natural products and analogues have been discovered in this project and some of them exhibited higher biological activities than the references drugs. In the future research, these bioactive compounds should be considered as potential candidates for the development of therapeutic drugs.

Keywords: Natural products, drug discovery, structural modification, cytotoxicity, anti-bacteria, anti-osteoporosis, anti-hypertension, anti-inflammation, anti-Alzheimer's disease, cationic lipids

CONTENTS

	Page
Acknowledgements	i
Abstract (Thai)	ii
Abstract (English)	iv
Contents	vii
1. Executive Summary	1
1.1. Objectives	1
1.2. Work Accomplished	1
Project 1. Project 1. Selection of Bioactive Natural Products for Drug	
Discovery	1
Project 1.1. Project 1.1 Screening of Anti-Osteoporosis Constituents from	
Plants	1
Project 2. Structural Modification of Some Lead Compounds for Higher	
Biological Activities	2
Project 2.1. Curcuminoid Analogues with Phosphodiesterase-5 (PDE5)	
Inhibitory Activity and Rat Pulmonary Artery Dilating Property	2
Project 2.2. Structural Modification of Chalcones to Analogues with	
Potent inhibitory Activity against Biofilm Formation by Bacteria	2
Project 3. Natural Products with Cytotoxic Activity. Isolation, Structural	
Elucidation, Structural Modification, Synthesis of Analogues, in vitro	
and in vivo Activity Evaluations	3
Project 3.1. Synthesis, Cytotoxicity against Human Oral Cancer KB	
Cells and Structure-Activity Relationship Studies of Trienone	
Analogues of Curcuminoids	3
Project 3.2. Analogues of Curcuminoids with Enhanced Biological	
Activities	3
Project 3.3 Curcuminoid Analogues Enhance Teromerase Activity in	
an in vitro TRAP Assay	4

	Page
Project 4. Structural Modification and Biological Evaluation of Nonsteroidal	
Antiinflammatory Natural Products and Analogues and Study of	
Mechanism of Action	5
Project 4.1. Diaryheptanoids of Curcuma comosa with Nitric Oxide	
Inhibitory Activity	5
Project 5. Natural Product-based Therapeutic Agents for Diseases of the	
Elderly	6
Project 5.1. Bone Sparing Effect of Diarylheptanoid from Curcuma	
comosa in Ovariectomized Rats	6
Project 5.2. Vasorelaxation Effects of 16-O-acetyldihydroisosteviol,	
an Analogue of Isosteviol, on Isolated Rat Thoracic Aorta	6
Project 5.3. Protective Effect of a Curcuminoid Analogue against	
Amyloid Beta-Induced Apoptosis in Neuronal Cells	7
Project 5.4. O-Demethyldemethoxycurcumin Exerts Suppression Effects	
on Thapsigargin Triggered on Endoplasmic Reticulum Stress in	
SK-N-SH Cells	8
Project 6. Design and Synthesis of Delivery System for Cytotoxic and	
Other Bioactive Natural Products and Analogues to Targeted Cells	9
Project 6.1. Development of Cationic Lipids with Different Polarheads,	
Central Core Structures and Hydrophobic Tails	9
Project 6.2. Synthesis and in vitro transfection efficiency of spermine-	
based cationic lipids with different central core structures and	
lipophilic tails	10
2. Research Achievements	11
2.1. Objectives	11
2.2. Work Accomplished	11
Project 1. Selection of Bioactive Natural Products for Drug Discovery	11
Project 1.1. Project 1.1 Screening of Anti-Osteoporosis Constituents from	
Plants	12

	Page
Project 2. Structural Modification of Some Lead Compounds for Higher	
Biological Activities	15
Project 2.1. Curcuminoid Analogues with Phosphodiesterase-5 (PDE5)	
Inhibitory Activity and Rat Pulmonary Artery Dilating Property	15
Project 2.2. Structural Modification of Chalcones to Analogues with	
Potent inhibitory Activity against Biofilm Formation by Bacteria	19
Project 3. Natural Products with Cytotoxic Activity. Isolation, Structural	
Elucidation, Structural Modification, Synthesis of Analogues, in vitro	
and in vivo Activity Evaluations	21
Project 3.1. Synthesis, Cytotoxicity against Human Oral Cancer KB	
Cells and Structure-Activity Relationship Studies of Trienone	
Analogues of Curcuminoids	21
Project 3.2. Analogues of Curcuminoids with Enhanced Biological	
Activities	23
Project 3.3 Curcuminoid Analogues Enhance Teromerase Activity in	
an in vitro TRAP Assay	27
Project 4. Structural Modification and Biological Evaluation of Nonsteroidal	
Antiinflammatory Natural Products and Analogues and Study of	
Mechanism of Action	28
Project 4.1. Diaryheptanoids of Curcuma comosa with Nitric Oxide	
Inhibitory Activity	29
Project 5. Natural Product-based Therapeutic Agents for Diseases of the	
Elderly	40
Project 5.1. Bone Sparing Effect of Diarylheptanoid from Curcuma	
comosa in Ovariectomized Rats	41
Project 5.2. Vasorelaxation Effects of 16-O-acetyldihydroisosteviol,	
an Analogue of Isosteviol, on Isolated Rat Thoracic Aorta	45
Project 5.3. Protective Effect of a Curcuminoid Analogue against	
Amyloid Beta-Induced Apoptosis in Neuronal Cells	47

	Page
Project 5.4. O-Demethyldemethoxycurcumin Exerts Suppression Effects	
on Thapsigargin Triggered on Endoplasmic Reticulum Stress in	
SK-N-SH Cells	52
Project 6. Design and Synthesis of Delivery System for Cytotoxic and	
Other Bioactive Natural Products and Analogues to Targeted Cells	55
Project 6.1. Development of Cationic Lipids with Different Polarheads,	
Central Core Structures and Hydrophobic Tails	56
Project 6.2. Synthesis and in vitro transfection efficiency of spermine-	
based cationic lipids with different central core structures and	
lipophilic tails	74
2.3. Outputs	78
2.4. Future Plans	78
3. Other Related Activities	78
3.1. International Publications	78
3.2. Other Research Outputs	80
3.3 Utilization of Research Outputs	80
3.4. Activities of Members as Invited Speakers	80
3.5. Research Networking with the Experts outside the University and Abroad	81
3.6. Research Networking within the University	82
3.7. Awards and Honors	82
4. Problems and Obstacles (if any)	82
5. Comments and Suggestions	82
Appendix. Publications	83

Contact No. DBG5680006

NATURAL PRODUCT-BASED DRUG DISCOVERY FROM THAI AND CHINESE MEDICINAL PLANTS

การค้นพบยาที่ได้จากผลิตภัณฑ์ธรรมชาติจากสมุนไพรไทยและจีน Final Report

September 30, 2013 - September 29, 2015

1. Executive Summary

1.1 Objectives

The objectives of the proposed project are as followed:

- 1. To select bioactive natural products for drug discovery
- 2. To modify the structures of some lead compounds for higher biological activities
- 3. To isolate, elucidate the structures, to modify the structures of natural products with cytotoxic activity.
- 4. To modify the structures and evaluate antiinflammatory natural products and analogues and study of mechanism of action.
- 5. To find natural product-based therapeutic agents for diseases of the elderly.
- 6. To design and synthesize delivery system for cytotoxic and other bioactive natural products and analogues to targeted cells.

1.2 Work Accomplished

Project 1. Selection of Bioactive Natural Products for Drug Discovery

Project 1.1 Screening of Anti-Osteoporosis Constituents from Plants

In order to search for compounds with anti-osteoporosis activity, thirty-nine compounds isolated from the following plant species have been screened for cytotoxicity against RAW264.7 cell line and anti-inflammatory activity: *Curcuma comosa, Dioscorea bulbifera, Vitex glabrata, Zingiber officinale, Murraya koenigii, Andrographis paniculata, Stevia rebaudiana, Momordica charantia, Trigonostemon reidioides, Croton crassifolius, Ziziphus cambodiana, Garcinia cowa and Artocarpus lakoocha*. Some of the tested compounds will be selected for anti-osteoporosis evaluation.

Project 2. Structural Modification of Some Lead Compounds for Higher Biological Activities

Project 2.1 Curcuminoid Analogues with Phosphodiesterase-5 (PDE5) Inhibitory Activity and Rat Pulmonary Artery Dilating Property

Pulmonary arterial hypertension is a relatively rare lung disorder with a poor prognosis. Pulmonary arteries become constricted, thus reducing blood flow to the lungs and increasing pulmonary arterial pressure. This led to increase in the load on the right ventricle, leading to right heart failure and death. Three natural curcuminoids and six synthetic curcuminoid analogues were synthesized and these compounds were tested for PDE5 and PDE6 inhibitory activities using enzymatic radioassay. Their vasorelaxation was measured using freshly-isolated segments of rat pulmonary artery and aorta. The natural curcuminoids mildly inhibited PDE5 (IC $_{50}$ =18 μ M). Some compounds were PDE5 selective over PDE6. All analogues possessed concentration-dependent vasorelaxant activity on pulmonary arteries (EC $_{40}$ 29-90 μ M, maximum response 60-90% at 300 μ M). Activity profiles suggest actions through additional cell pathways for promoting vasorelaxation.

Output. This project has led to the following publication:

Kruangtip, O., Chootip, K., Temkitthawon, P., Changwichit, K., Chuprajob, T., Changtam, C., Suksamrarn, A., Khorana, N., Scholfield, C. N., Ingkaninan, K., 2014. Curcumin analogues inhibit phosphodiesterase-5 and dilate rat pulmonary arteries. *J. Pharm. Pharmacol.* 67, 87-95.

Project 2.2 Structural Modification of Chalcones to Analogues with Potent inhibitory Activity against Biofilm Formation by Bacteria

Two natural chalcones and eleven synthetic analogues were evaluated in vitro for their antibiofilm activity against strong biofilm-forming strains of NTHi. It was found that 3-hydroxychalcone exhibited the most potent inhibitory activity, its mean minimum biofilm inhibitory concentration (MBIC50) being 16mg/mL (71.35mM), or approximately sixfold more active than the reference drug, azithromycin (MBIC50 419.68mM). This chalcone significantly inhibited biofilm formation by all studied NTHi strains, indicating that the antibiofilm activities of this compound occur across multiple strong-biofilm forming NTHi isolates of different clinical origins. These findings indicate that 3-hydroxychalcone has

powerful antibiofilm activity and suggest the potential application of this compound as a new therapeutic agent for control of NTHi biofilm-associated infections.

Output. This project has led to the following collaborative publication:

Kunthalert, D., Baothong, S., Khetkam, P., Chokchaisiri, S., Suksamrarn, A., 2014. A chalcone with potent inhibiting activity against biofilm formation of nontypeable *Haemophilus influenzae*. *Microbiol. Immunol.* 58, 581-589.

Project 3. Natural Products with Cytotoxic Activity. Isolation, Structural Elucidation, Structural Modification, Synthesis of Analogues, in *vitro* and *in vivo* Activity Evaluations Project 3.1 Synthesis, Cytotoxicity against Human Oral Cancer KB Cells and Structure-Activity Relationship Studies of Trienone Analogues of Curcuminoids

Sixteen trienone analogues have been synthesized for cytotoxicty against oral cancer cell line. A number of the analogues exhibited very high anti-KB activity and some of them showed higher cytotoxicy than that of ellipticine, the reference anti-cancer drug.

Output. This project has led to the following publication:

Chuprajob, T., Changtam, C., Chokchaisiri, R., Chunglok, W., Sornkaew, N., Suksamrarn, A., 2014. Synthesis, cytotoxicity against human oral cancer KB cells and structure-activity relationship studies of trienone analogues of curcuminoids. *Bioorg. Med. Chem. Lett.* 24, 2839-2844.

Project 3.2 Anti-cholangiocarcinoma Activity of Bisbenzylisoquinoline Alkaloid from *Tiliacora triandra*

Plant-derived compounds are gaining interest as potential cancer therapeutics, particularly for treatment-refractory cancers such as cholangiocarcinoma (CCA). *Tiliacora triandra*, or "Ya nang" in Thai, contained a number of bisbenzylisoquinoline alkaloids including tiliacorinine as the major alkaloid. This compound was investigated for antitumor activity in CCA cell lines *in vitro* and *in vivo*. Antiproliferative effect of tiliacorinine on human CCA cell lines was investigated using SRB assay. Tiliacorinine significantly inhibited proliferations of human CCA cell lines with IC₅₀ 4.5-7 μM by inducing apoptosis through caspase activation,

up-regulation of BAX, down-regulation of Bcl_{xL} and XIAP. This alkaloid considerably reduced tumor growth in CCA xenografted mice. These results demonstrated the antitumor effects of **3.2(1)** on human CCA *in vitro* and *in vivo*. Tiliacorinine may be an effective agent for CCA treatment.

Output. This project has led to the following publication:

Janeklang, S.; Nakaew, A., Vaeteewoottacharn, K., Seubwai, W., Boonsiri, P., Kismali, G., Suksamrarn, A., Okada, S., Wongkham, S., 2014. *In vitro* and *in vivo* antitumor activity of tiliacorinine in human cholangiocarcinoma. *Asian Pac. J. Cancer Prev.* 15, 7473–7478.

Project 3.3 Curcuminoid Analogues Enhance Teromerase Activity in an *in vitro* TRAP Assay

We have found for the first time that a number of curcuminoid analogues especially those with alkylpyridinium side chain enhanced telomerase activity in an in vitro TRAP assay. A preliminary analysis of structure-activity relationships found that the minimal requirement for this enhanced telomerase activity is a curcuminoid core with at least one suitable, while curcuminoids with two such side chains exhibit even greater activity. The finding here might lead to a new class of telomerase activators that act directly or indirectly on telomerase, rather than through the reactivation of the telomerase reverse transcriptase (TERT) gene associated with other telomerase activators found in the literature.

Output. This project has led to the following publication:

Taka, T., Changtam, C., Thaichana, P., Kaewtunjai, N., Suksamrarn, A., Lee, T. R., Tuntiwechapikul, W., 2014. Curcuminoid derivatives enhance telomerase activity in an in vitro TRAP assay. *Bioorg. Med. Chem. Lett.* 24, 5242-5246.

Project 4. Structural Modification and Biological Evaluation of Nonsteroidal Antiinflammatory Natural Products and Analogues and Study of Mechanism of Action Project 4.1 Diaryheptanoids of *Curcuma comosa* with Nitric Oxide Inhibitory Activity

Curcuma comosa Roxb. (Zingiberaceae), has been used in indigenous medicine in Thailand. The rhizome of this plant species has known as an anti-inflammatory agent and has been used for the treatment of postpartum uterine bleeding and as an aromatic stomachic. Investigation of the chemical constituents of the rhizomes of this plant species collected from Sawangdaendin district, Sakon Nakorn province revealed the presence of eight new diaryheptanoids, together with thirteen known diaryheptanoids. A number of Curcuma and other species of Chinese origins have also been studied by Professor Guolin Zhang and Professor Fei Wang, our Chinese collaborators in comparison with those of the Thai origins. To examine the biological effect of the isolated compounds, the mouse macrophage RAW 264.7 cells were treated with different concentrations of the diarylheptanoids. Some diarylheptanoids were found to be active to the test. The calculated IC₅₀ concentration of the two active compounds for the inhibition of NO production in LPS-stimulated RAW264.7 cells was 6.56 μ M and 4.15 μ M, respectively. The anti-inflammatory effect of the diarylheptanoids not only help for the understanding of traditional medicinal use of C. comosa rhizomes, but also validate further development of the two compounds as therapeutic tools for the prevention and treatment of inflammatory diseases.

Output. This project has led to the following publication:

Sornkaew, N., Lin, Y., Wang, F., Zhang, G., Chokchaisiri, R., Zhang, A., Wongkrajang, K., Suebsakwong, P., Piyachaturawat, P., Suksamrarn, A., 2015. Diarylheptanoids of *Curcuma comosa* with inhibitory effects on nitric oxide production in macrophage RAW 264.7 cells. *Nat. Prod. Commun.* 10, 89-93.

Project 5. Natural Product-based Therapeutic Agents for Diseases of the Elderly

Project 5.1 Bone Sparing Effect of Diarylheptanoid from *Curcuma comosa* in Ovariectomized Rats

Osteoporosis is a serious worldwide health problem that primarily effect middle-aged and elderly women. Efforts to reduce bone loss in menopausal osteoporosis have been focused on compounds with the potential to preserve bone mass through inhibition of osteoclastic bone resorption or stimulation bone formation. Among therapeutic agents, estrogen is the most effective compound and is capable of limiting bone loss and reducing the rate of bone fractures in postmenopausal women. However, long-term treatment with estrogen is limited due to its carcinogenic risk and feminizing effects. Phytoestrogens, non-steroidal plant-derived compounds with estrogenic activity, have received increased interest as estrogen alternatives to alleviate bone loss. Studies have suggested that a diet rich in phytoestrogen may relieve menopausal symptoms and protect against estrogen-associated diseases, including breast cancers, cardiovascular diseases, and osteoporosis. Curcuma comosa has been widely used as a dietary supplement for relieving postmenopausal symptoms in Thailand. In the present study, the diarylheptanoid, (3R)-1,7-diphenyl-(4E,6E)-4,6-heptadien-3-ol (DPHD), have been demonstrated to protect ovariectomy-induced bone loss (OVX) in adult female Sprague-Dawley rats with 17b-estradiol (E2, 10 mg/kg Bw) as a positive control. DPHD appears to be a promising candidate for preserving bone mass and structure in the estrogen deficient women with a potential role in reducing postmenopausal osteoporosis.

Output.

Tantikanlayaporn, D., Wichit, P., Weerachayaphorn, J., Chairoungdua, A., Chuncharunee, A., Suksamrarn, A., Piyachaturawat, P. Bone sparing effect of a novel phytoestrogen diarylheptanoid from *Curcuma comosa* Roxb. in ovariectomized rats. *PLoS ONE*, 2013, 8, e78739. doi:10.1371/journal.pone.0078739.

Project 5.2 Vasorelaxation Effects of 16-O-acetyldihydroisosteviol, an Analogue of Isosteviol, on Isolated Rat Thoracic Aorta

The chemical modification of isosteviol was performed by sodium borohydride reduction of isosteviol, followed by acetylation to give 16-O-acetyldihydroisosteviol (ADIS). The

vasorelaxant effects of ADIS were investigated and it was found that ADIS (0.1 μ M–3 mM) induced relaxation of aortic rings pre-contracted by phenylephrine (PE, 10 μ M) and KCl (80 mM) with intact-endothelium ($E_{max}=79.26\pm3.74$ and 79.88 ± 3.79 , respectively) or denuded-endothelium ($E_{max}=88.05\pm3.69$ and 78.22 ± 6.86 , respectively). In depolarization Ca^{2+} -free solution, ADIS inhibits $CaCl_2$ -induced contraction in endothelium-denuded rings in a concentration-dependent manner. In addition, ADIS attenuates transient contractions in Ca^{2+} -free medium containing EGTA (1 mM) induced by PE (10 μ M) and caffeine (20 mM). By contrast, relaxation was not affected by tetraethylammonium (TEA, 5 mM), 4-aminopyridine (4-AP, 1 mM), glibenclamide (10 μ M), barium chloride (BaCl₂, 1 mM), and 1H-[1,2,3]oxadiazolo[4,3- α]quinoxalin-1-one (ODQ, 1 μ M). These findings reveal the vasorelaxant effect of ADIS, through endothelium-independent pathway. It acts as a Ca^{2+} channel blocker through both intracellular and extracellular Ca^{2+} release.

Output. This project has led to the following publication:

Pantan, R., Onsa-ard, A., Tocharus, J., Wonganan, O., Suksamrarn, A., Tocharus, C., 2014. Endothelium-independent vasorelaxation effects of 16-*O*-acetyldihydroisosteviol on isolated rat thoracic aorta. *Life Sci.* 116, 31-36.

Project 5.3 Protective Effect of a Curcuminoid Analogue against Amyloid Beta-Induced Apoptosis in Neuronal Cells

Alzheimer's disease (AD) is a neurodegenerative and progressive disorder. The distinctive appearance of pathological AD is amyloid plaque which is the accumulation of amyloid β (A β) in extracellular neuronal cells and neurofibrillary tangles (NFT) in neuronal cells, which lead to neurotoxicity via reactive oxygen species (ROS) generation related apoptosis. Loss of synapses and synaptic damage resulted in the decline in AD. Neuronal cell death is the main cause of brain dysfunction and cognitive impairment. A β activates neuronal death via endoplasmic reticulum (ER) stress and mitochondria apoptosis pathway. This work has been done in collaboration with Assistant Professor Dr. Jiraporn Tocharus, Department of Physiology, Faculty of Medicine, Chiang Mai University. The mechanisms and effects of di-O-demethylcurcumin in preventing A β -induced apoptosis has been investigated. Pretreatment with di-O-demethylcurcumin, followed by A β 25-35 in human neuroblastoma SK-N-SH cells

improved cell viability and decreased neuronal cell apoptosis. Pretreatment with the compound attenuated the number of nuclear condensations and number of apoptotic cells in A β 25-35-induced group in a concentration-dependent manner by using transmission electron microscope (TEM) and flow cytometry, respectively. Di-O-demethylcurcumin also increased the ratio of Bcl-XL/Bax protein, and reduced intracellular ROS level, cytochrome c protein expression, cleaved caspase-9 protein expression, and cleaved caspase-3 protein expression. Additionally, treatment of this compound also reduced the expression of ER stress protein markers, including protein kinase RNA like endoplasmic reticulum kinase (PERK) phosphorylation, eukaryotic translation initiation factor 2 alpha (eIF2 α) phosphorylation, inositol-requiring enzyme 1 (IRE1) phosphorylation, X-box-binding protein-1 (XBP-1), activating transcription factor (ATF6), C/EBP homologous protein (CHOP), and cleaved caspase-12 protein. CHOP and cleaved caspase-12 protein are the key mediators of apoptosis. Therefore, this compound is a candidate protectant against neuronal death through its suppression of the apoptosis mediated by mitochondrial death and ER stress pathway.

Output. This project has led to the following publication:

Pinkaew, D., Changtam, C., Tocharus, C., Thummayot, S., **Suksamrarn, A.**, Tocharus, J., 2015. Di-*O*-demethylcurcumin protects SK-N-SH cells against mitochondrial and endoplasmic reticulum-mediated apoptosis cell death induced by Ab25-35. *Neurochem. Int.* 80, 110-119.

Project 5.4 *O*-Demethyldemethoxycurcumin Exerts Suppression Effects on Thapsigargin Triggered on Endoplasmic Reticulum Stress in SK-N-SH Cells

Endoplasmic reticulum (ER) stress is a common cause of neurodegenerative disease, including Alzheimer's disease and Parkinson's disease. Therefore, interventions that attenuate ER stress may contribute to a reduction in apoptotic cell death. This work aimed to evaluate the potential involvement of *O*-demethyldemethoxycurcumin, an analogue of curcuminoids, on thapsigargin-induced apoptosis in cultured neuroblastoma (SK-N-SH) cells through the ER stress signaling pathway. The results showed that *O*-demethyldemethoxycurcumin improved SK-N-SH cell viability by decreasing the apoptotic cell death induced by thapsigargin. Consistent with these findings, *O*-demethyldemethoxycurcumin inhibited the thapsigargin-

induced activation of cleavage caspase-12. Moreover, *O*-demethyldemethoxycurcumin attenuated the intracellular Ca²⁺ level and the expression of the calpain protein. *O*-demethyldemethoxycurcumin also downregulated the expression of ER stress signaling proteins, including the phosphorylation of PKR-like endoplasmic reticulum kinase (p-PERK), the phosphorylation of inositol-requiring enzyme 1(p-IRE1), activating transcription factor 6 (ATF6), binding immunoglobulin protein (BiP) and C/EBP homologous protein (CHOP). The findings suggest that *O*-demethyldemethoxycurcumin could protect against thapsigargin-induced ER stress in SK-N-SH cells. Therefore, *O*-demethyldemethoxycurcumin offers potential as an alternative therapeutic agent for protection against neurodegenerative diseases.

Output. This project has led to the following publication:

Janyou, A., Changtam, C., Suksamrarn, A., Tocharus, C., Tocharus, C., 2015. Suppression effects of *O*-demethyldemethoxycurcumin on thapsigargin triggered on endoplasmic reticulum stress in SK-N-SH cells. *Neurotoxicol.* 50, 92-100.

Project 6. Design and Synthesis of Delivery System for Cytotoxic and Other Bioactive Natural Products and Analogues to Targeted Cells

Project 6.1 Development of Cationic Lipids with Different Polarheads, Central Core Structures and Hydrophobic Tails

The combination of lipids with different polarheads, central core structures and hydrophobic tails in the presence of helper lipid, DOPE, has allowed the discovery of highly efficient transfection agents with minimal cytotoxicity. These mixture lipids showed high efficiency to deliver DNA into HEK293, MCF-7 and HeLa cells than that of a commercially available transfection agent. The strategy developed is useful for the development of cationic lipid-based gene delivery. Employing the synergistic effect of these lipids may be a promising approach for successful non-viral gene transfection.

Output. This project has led to the following publication:

Niyomtham, N., Apiratikul, N., Chanchang, K., Opanasopit, O., Yingyongnarongkul, B., 2014. Synergistic effect of cationic lipids with different polarheads, central core structures and hydrophobic tails on gene transfection efficiency. *Biol. Pharm. Bull.* 37, 1534-1542.

Project 6.2 Synthesis and in vitro transfection efficiency of spermine-based cationic lipids with different central core structures and lipophilic tails

Twelve spermine-based cationic lipids with four different central core structures (di(oxyethyl)amino, di(oxyethyl)amino carboxy, 3-amino-1,2-dioxypropyl and 2-amino-1,3-dioxypropyl) and three hydrophobic tails (lauric acid, myristic acid and palmitic acid) were synthesized. The liposomes containing lipids and DOPE showed moderate to good *in vitro* DNA delivery into HeLa cells. GFP expression experiments revealed that liposomes composed of lipids with 3-amino-1,2-dioxypropyl as a central core structure exhibited highest transfection efficiency under serum-free condition. Whereas, lipid with 2-amino-1,3-dioxypropyl core structure showed highest transfection under 10% serum comdition. Moreover, the liposomes and lipoplexes composted of these cationic lipids exhibited low cytotoxicity.

Output. This project has led to the following publication:

Niyomtham, N., Apiratikul, N., Suksen, K., Opanasopit, P., Yingyongnarongkul, B., 2015. Synthesis and in vitro transfection efficiency of spermine-based cationic lipids with different central core structures and lipophilic tails. *Bioorg. Med. Chem. Lett.* 25, 496-503.

2. Research Achievements (ผลงานวิจัยที่ทำสำเร็จ)

2.1 Objectives (วัตถุประสงค์)

The objectives of the proposed project are as followed:

- 1. To select bioactive natural products for drug discovery
- 2. To modify the structures of some lead compounds for higher biological activities
- 3. To isolate, elucidate the structures, to modify the structures of natural products with cytotoxic activity.
- 4. To modify the structures and evaluate antiinflammatory natural products and analogues and study of mechanism of action.
- 5. To find natural product-based therapeutic agents for diseases of the elderly.
- 6. To design and synthesize delivery system for cytotoxic and other bioactive natural products and analogues to targeted cells.

General objectives

- 1. To carry out the proposed project as stipulated.
- 2. To publish research results in international peer-reviewed journals.
- 3. To strengthen the research team that has already been established and the new collaborators to be recruited for this project.
- 4. To train and produce research scientists for the future.

2.2 Work Accomplished

Project 1. Selection of Bioactive Natural Products for Drug Discovery

The work in this project involves selection of plants for the study based on local use, the chemical constituents of the plant in the same genus or family, or/and preliminary biological evaluation. Extraction of plant materials. Screening for biological activities. Bioassay-guided isolation of bioactive compounds. Identification and structural elucidation of the isolated compounds by spectroscopic analysis. Chemical reactions may also be employed to gain more information of the structure of the isolated compounds. In some special cases, X-ray crystallographic analysis will also be used. Structural modification of lead compounds. Biological evaluation of the isolated compounds using available bioassays.

Project 1.1 Screening of Anti-Osteoporosis Constituents from Plants

Osteoporosis is a systemic skeletal disease characterized by low bone mineral density and microarchitectural deterioration of bone tissue, leading to a consequent increase in bone fragility and fracture risk. Hypogonadism is the most well-established cause of osteoporosis, which is usually thought to be an age-adjusted symptom. ^{1.1[1]} In recent years, osteoporosis has become a major health problem of more than 200 million people worldwide and has one of the highest incidence of all diseases in the elderly population. ^{1.1[2]} Estrogen, bisphosphonates, calcitonin, calcium products, ipriflavone, and anabolic steroids are clinically used as effective medications. ^{1.1[3]} However, each of them has established some side effects. Many medicinal plants have long been used to prevent and treat osteoporosis in many countries. These natural medicines from plants have fewer side effects and are more suitable for long-term use than most synthesized drugs. Plant natural medicines may provide alternatives for the prevention and treatment of osteoporosis. ^{1.1[4]}

In order to search for compounds with anti-osteoporosis activity, thirty-nine compounds isolated from the following plant species have been screened for cytotoxicity against RAW264.7 cell line and anti-inflammatory activity: *Curcuma comosa, Dioscorea bulbifera, Vitex glabrata, Zingiber officinale, Murraya koenigii, Andrographis paniculata, Stevia rebaudiana, Momordica charantia, Trigonostemon reidioides, Croton crassifolius, Ziziphus cambodiana, Garcinia cowa and Artocarpus lakoocha*. The results are presented in Table 1.1(1). Some of the tested compounds will be selected for anti-osteoporosis evaluation.

Table 1.1 Screening for cytotoxicity against RAW264.7 cell line and anti-inflammatory activity of pure compounds isolated from plants

	Cytotoxicity	Anti-inflammatory Acivity
Sample No.	$IC_{50} (\mu M)$	% Inhibition, IC ₅₀ (μ M)
ASTP 001	~ 12	~ 10
ASTP 002	> 50	> 50
ASTP 003	> 50	> 50
ASTP 004	> 50	> 50
ASTP 005	> 50	> 50
ASTP 006	> 50	> 50
ASTP 007	> 50	> 50
ASTP 008	> 50	> 50
ASTP 009	> 50	> 50
ASTP 010	~ 25	~ 2.5
ASTP 011	> 50	> 50
ASTP 012	> 50	> 50
ASTP 013	> 50	> 50
ASTP 014	> 50	> 50
ASTP 015	> 50	> 50
ASTP 016	*	*
ASTP 017	> 50	> 50
ASTP 018	> 50	> 50
ASTP 019	~ 10	~ 7
ASTP 020	> 50	~ 30
ASTP 021	> 50	> 50
ASTP 022	> 50	> 50
ASTP 023	~ 17	~ 1
ASTP 024	> 50	> 50
ASTP 025	> 50	> 50
ASTP 026	> 50	> 50
ASTP 027	> 50	> 50
ASTP 028	> 50	> 50

^{*}Sample did not dissolve in DMSO

Table 1.1 (continued)

Sample No.	Cytotoxicity	Anti-inflammatory Acivity
	$IC_{50} (\mu M)$	% Inhibition, IC_{50} (μM)
ASTP 029	> 50	~ 25
ASTP 030	> 50	> 50
ASTP 031	> 50	> 50
ASTP 032	*	*
ASTP 034	> 50	> 50
ASTP 035	> 50	> 50
ASTP 036	> 50	~ 20
ASTP 037	> 50	> 50
ASTP 038	> 50	> 50
ASTP 039	~ 14	~8

^{*}Sample did not dissolve in DMSO

References

- 1.1[1] Sambrook, P., Cooper, C., 2006. Osteoporosis. *Lancet*, 367, 2010–2018.
- 1.1[2] Rachner, T. D., Khosla, S., Hofbauer, L. C., 2011. Osteoporosis: now and the future. *Lancet*, 377, 1276–1287.
- 1.1[3] Compston, J., 2012. The use of combination therapy in the treatment of postmenopausal osteoporosis. *Endocrine*, 41, 11–18.
- Jia, M., Nie, Y., Cao, D.-P., Xue, Y.-Y., Wang, J.-S., Zhao, L., Rahman, K., Zhang, Q.-Y., Qin, L.-P., 2012. Potential antiosteoporotic agents from plants: a comprehensive review. *Evid. Compl. Altern. Med.*, 2012, Article ID 364604, 28 pages; doi:10.1155/2012/364604.

Project 2. Structural Modification of Some Lead Compounds for Higher Biological Activities

This project involves the selection of lead compound derived from the project 1, or from prior phytochemical investigations, for further study. Bioactive compound will be selected based on the SAR study, its biological activity, chemical structure and functional groups present in the molecule. Chemical modification of the lead compound will then follow. The selected lead compound will be subjected to structural modification, starting from preparation of derivatives of functional groups present in the molecule. Further modification of functional groups or skeleton will also be considered, depending on individual compound. Finally, biological evaluation of the modified compound will be carried out. If the modified compound is more active than the parent lead compound, further modification may be repeated to obtain the most active one.

Project 2.1 Curcuminoid Analogues with Phosphodiesterase-5 Inhibitory Activity and Rat Pulmonary Artery Dilating Property

Pulmonary arterial hypertension (PAH) is a relatively rare lung disorder with a poor prognosis. Pulmonary arteries become constricted, thus reducing blood flow to the lungs and increasing pulmonary arterial pressure. This led to increase in the load on the right ventricle, leading to right heart failure and death.^{2,1[1]} Several mechanisms for the disease have been proposed and shown to produce PAH in animal models, but none appear to reflect the human condition. Because of this unclear etiology, current drug treatments have focused on symptomatic treatment in the form of vasodilators. Sildenafil, tadalafil, vardenafil and similar drugs have received the most widespread application. These compounds are inhibitors of phosphodiesterase-5 (PDE5) which is found in many cells including the smooth muscle cells of pulmonary vascular tree expressed as PDE5A. 2.1[2] This enzyme is upregulated in pulmonary hypoxia and PAH making it an attractive drug target for treatment of these pathologies.^{2.1[3]} The target substrate for PDE5 is the inactivation of guanine 3',5'-cyclic monophosphate (cGMP) via hydrolysis. Cytosolic cGMP constituatively activates in particular, ATP- and BK-channels^[5] and the resulting increased K-permeability maintains vasorelaxant tone. 2.1[4] Inhibiting PDE5 favours cGMP accumulation thus promoting vasodilatation. ^{2.1[5,6]} Sildenafil was initially registered as an oral drug for erectile dysfunction,

then later approved for PAH treatment.^{2.1[5]} There is a growing list of successful clinical trials with PDE5 inhibitors^[8] which may lead to extended licencing by regulatory bodies.^{2.1[6,7]} Clearly, these inhibitors also cause vasodilatation in other tissues^{2.1[7]} and more especially have retinal-related complications most commonly associated with additional PDE6 blockade.^{2.1[8]} Therefore, investigations for drugs specific for diseased targets including the pulmonary arterial circulation are going on.

Several *Curcuma* species are known to be vasorelaxant including *Curcuma longa*,^{2.1[9]} while curcumin (**2.1(1)**) reduces pulmonary arterial pressure.^{2.1[10]} This implies that curcuminoids might provide leads for the development of a new generation of selective PDE5 inhibitors. We therefore aimed to explore the activities of both natural and synthetic curcuminoid analogues on the inhibition of PDE5 in cell-free assay and on the vasorelaxation of freshly isolated rat pulmonary arteries *in vitro*. This work has been done in collaboration with Associate Professor Dr. Kornkanok Ingkaninan and colleagues, Naresuan University.

Three natural curcuminoids (2.1(1)-2.1(3)) were used in this study. Six synthetic curcuminoid analogues (2.1(4)-2.1(9)) were synthesized and the detail of synthesis can be seen in the published work given below. These compounds were tested for PDE5 and PDE6 inhibitory activities using enzymatic radioassay. Their vasorelaxation was measured using freshly-isolated segments of rat pulmonary artery and aorta. The curcuminoids 2.1(1)-2.1(3) mildly inhibited PDE5 (IC₅₀=18µM): the *meta*-methoxyl of curcumin was important for PDE5 inhibition. But hydroxyl rearrangements, removing both methoxyls and one ketomethylene yielded the potent 2.1(7) and 2.1(9) (IC₅₀ 4μ M) (compared to sildenafil, IC₅₀ 0.03μ M). Only 2.1(1), 2.1(3), and 2.1(4) were PDE5 selective over PDE6. Triazole-carboxylic addition provided water-solubility while preserving potency. All analogues possessed concentrationdependent vasorelaxant activity on pulmonary arteries (EC₄₀ 29-90 µM, maximum response 60-90% at 300 µM), while compounds (1-8) were weakly acting in a rta (maximum response<40%). Only demethoxycurcumin (2) and analogues 2.1(5), 2.1(8) and 2.1(9) had endothelium-dependent actions. The reference drug sildenafil was highly potent (EC₄₀ 0.04 μM) and highly endothelium-dependent in pulmonary artery but weak on intact aorta (EC₄₀ 1.8µM). Activity profiles suggest actions through additional cell pathways for promoting vasorelaxation.

Output. This project has led to the following publication:

Kruangtip, O., Chootip, K., Temkitthawon, P., Changwichit, K., Chuprajob, T., Changtam, C., Suksamrarn, A., Khorana, N., Scholfield, C. N., Ingkaninan, K., 2014. Curcumin analogues inhibit phosphodiesterase-5 and dilate rat pulmonary arteries. *J. Pharm. Pharmacol.* 67, 87-95.

References

- 2.1[1] Barst, R. J., McGoon, M., Torbicka, A., Sitbon, O., Krowka, M. J., Olschewski, H., Gaine, S., 2004. Diagnosis and differential assessment of pulmonary arterial hypertension. *J. Am. Coll. Cardiol.*, 43(12 Suppl S): 40S–47S.
- 2.1[2] Sebkhi, A., Strange, J. W., Phillips, S. C., Wharton, J., Wilkins, M. R., 2003.

- Phosphodiesterase type 5 as a target for the treatment of hypoxia-induced pulmonary hypertension. *Circulation* 107, 3230–3235.
- 2.1[3] Scipioni, A., Giorgi, M., Nuccetelli, V., Stefanini, S., 2009. Immunohistochemical localisation of PDE5 in rat lung during pre- and postnatal development. *J. Biomed. Biotechnol.* 2009, Article ID 932961. doi:10.1155/2009/932961.
- 2.1[4] Schoeffter, P., Lugnier, C., Demesy-Waeldele, F., Stoclet, J. C., 1987. Role of cyclic AMP- and cyclic GMP-phosphodiesterases in the control of cyclic nucleotide levels and smooth muscle tone in rat isolated aorta. A study with selective inhibitors. *Biochem. Pharmacol.* 36, 3965–3972.
- 2.1[5] Galiè, N., Torbicki, A., Barst, R., Dartevelle, P., Haworth, S., Higenbottam, T., Olschewski, H., Peacock, A., Pietra, G., Rubin, L. J., Simonneau, G., 2004. Guidelines on diagnosis and treatment of pulmonary arterial hypertension The Task Force on Diagnosis and Treatment of Pulmonary Arterial Hypertension of the European Society of Cardiology. *Eur. Heart J.* 25, 2243–2278.
- 2.1[6] Chrysant, S. G., 2013. Effectiveness and safety of phosphodiesterase 5 inhibitors in patients with cardiovascular disease and hypertension. *Curr. Hypertens. Rep.* 15, 475–483.
- 2.1[7] Kukreja, R. C., Salloum, F. N., Das, A., Koka, S., Ockaili, R. A., Xi, L., 2011. Emerging new uses of phosphodiesterase-5 inhibitors in cardiovascular diseases. *Exp. Clin. Cardiol.*16, e30–e35.
- 2.1[8] Kerr, N. M., Danesh-Meyer, H. V., 2009. Phosphodiesterase inhibitors and the eye. *Clin. Experiment Ophthalmol.* 37, 514–523.
- 2.1[9] Adaramoye, O. A., Anjos, R. M., Almeida, M. M., Veras, R. C., Silvia, D. F., Oliveira, F. A., Cavalcante, K. V., Araújo, I. G., Oliveira, A. P., Medeiros, I. A., 2009. Hypotensive and endothelium-independent vasorelaxant effects of methanolic extract from *Curcuma longa* L. in rats. *J. Ethnopharmacol*. 124, 457–462.
- 2.1[10] Lin, Q., et al., 2006. Effect of curcumin on pulmonary hypertension and wall collagen of pulmonary arterioles of chronic hypoxic hypercapnic rats. *Chin. J. Appl. Physiol.* 22, 257–261.

Project 2.2 Structural Modification of Chalcones to Analogues with Potent inhibitory Activity against Biofilm Formation by Bacteria

Nontypeable *Haemophilus influenzae* (NTHi), an important human respiratory pathogen, frequently causes biofilm infections. Currently, resistance of bacteria within the biofilm to conventional antimicrobials poses a major obstacle to effective medical treatment on a global scale. ^{2.2[1-3]} Novel agents that are effective against NTHi biofilm are therefore urgently required. This work has done in collaboration with Assistant Professor Dr. Duangkamol Kunthalert and colleagues, Naresuan University.

In this study, the natural chalcones 2.2(1) and 2.2(2) were evaluated in vitro for their antibiofilm activity against strong biofilm-forming strains of NTHi. A number of synthetic analogues of chalcones (2.2(3) - 2.2(13)) was synthesized and evaluated. Of the test chalcones, 3-hydroxychalcone (chalcone 2.2(8)) exhibited the most potent inhibitory activity, its mean minimum biofilm inhibitory concentration (MBIC50) being 16mg/mL (71.35mM), or approximately sixfold more active than the reference drug, azithromycin (MBIC50 419.68mM). The inhibitory activity of chalcone 2.2(8), which is a chemically modified chalcone, appeared to be superior to those of the natural chalcones tested. Significantly, chalcone 2.2(8) inhibited biofilm formation by all studied NTHi strains, indicating that the antibiofilm activities of this compound occur across multiple strong-biofilm forming NTHi isolates of different clinical origins. According to antimicrobial and growth curve assays, chalcone 2.2(8) at concentrations that decreased biofilm formation did not affect growth of NTHi, suggesting the biofilm inhibitory effect of chalcone 2.2(8) is non-antimicrobial. In terms of structure-activity relationship, the possible substituent on the chalcone backbone required for antibiofilm activity is discussed. These findings indicate that 3-hydroxychalcone (chalcone 2.2(8)) has powerful antibiofilm activity and suggest the potential application of chalcone 2.2(8) as a new therapeutic agent for control of NTHi biofilm-associated infections. The detail of this work can be seen in the following paper.

Output. This project has led to the following collaborative publication:

Kunthalert, D., Baothong, S., Khetkam, P., Chokchaisiri, S., Suksamrarn, A., 2014. A chalcone with potent inhibiting activity against biofilm formation of nontypeable *Haemophilus influenzae*. *Microbiol. Immunol.* 58, 581-589.

References

- 2.2[1] Kochanek, K. D., Murphy, S. L., Anderson, R. N., Scott, C., 2004. Deaths: final data for 2002. *Natl. Vital Stat. Rep.* 53, 1–115.
- 2.2[2] Sullivan, S. D., Ramsey, S. D., Lee, T. A., 2000. The economic burden of COPD. *Chest* 117, 5S–9S.
- 2.2[3] Gates, G. A., 1996. Cost-effectiveness considerations in otitis media treatment. *Otolaryngol. Head Neck Surg.* 114, 525–30.

Project 3. Natural Products with Cytotoxic Activity. Isolation, Structural Elucidation, Structural Modification, Synthesis of Analogues, in *vitro* and *in vivo* Activity Evaluations

This project involves (1) Selection of lead compound with cytotoxic activity for further study. Cytotoxic compound will be selected based on the SAR study, its cytotoxic activity, chemical structure and functional groups present in the molecule. (2) Chemical modification The selected lead compound will be subjected to structural of the lead compound. modification, starting from preparation of derivatives of functional groups present in the molecule. Further modification of functional groups or skeleton will also be conducted, depending on individual compound. (3) Biological evaluation of the modified compounds. If the modified compounds exhibit more cytotoxic activity than the parent lead compound, structural optimization (or further structural modification) may be conducted to obtain the most active and suitable one. (4) Evaluation for toxicity to normal cell (Vero cell, for example). Determination of selectivity index (the ratio between toxicity to normal cell and toxicity to cancer cell). Potent analogue with high selectivity index will be selected for further study. Analogue which is very high cytotoxic activity, but with high toxicity to Vero cell will be considered to subject to different further modification. (5) Selection of potent analogue for further in depth study. Normally it is the most active and high selectivity index.

Project 3.1 Synthesis, Cytotoxicity against Human Oral Cancer KB Cells and Structure-Activity Relationship Studies of Trienone Analogues of Curcuminoids

Curcuminoids are the major constituents of turmeric (*Curcuma longa* L., Zingiberaceae) and have been used for centuries as a dietary pigment, spice and traditional medicine in India and China. The major curcuminoid isolated from this plant species is curcumin (**3.1(1)**), with demethoxycurcumin (**3.1(2)**) and bisdemethoxycurcumin (**3.1(3)**) as the minor constituents. Curcuminoids exhibited many interesting biological activities, ^{3.1[1]} Recently, a new curcuminoid analogue, 1,7-bis(4-hydroxyphenyl)-1,4,6-heptatrien-3-one (**3.1(4)**), which is structurally related to the curcuminoid **3.1(3)**, has been isolated as a minor component of *C. longa*. ^{3.1[2]} This compound inhibited the production of TNF- α by lipopolysaccharide-activated macrophages. ^{3.1[3]} Another new curcuminoid analogue, 1,7-bis(4-hydroxy-3-methoxyphenyl)-1,4,6-heptatrien-3-one (**3.1(5)**), which is structurally related to the curcuminoid **3.1(1)**, has later been isolated. ^{3.1[4]} It is interesting to note that these two compounds possess a 1E,4E,6E-

heptatrien-3-one functionality, which is a rare group of naturally occurring curcuminoid analogue and has not much been studied, especially the biological activities of this type of compounds. The structural diversity of the trienones **3.1(4)** and **3.1(5)** has prompted us to investigate their biological activities. However, the scarcity of these compounds in natural sources has prevented us from obtaining them for biological activity evaluations. We therefore decided to synthesize the natural trienones **3.1(4)** and **3.1(5)** and other analogues of these two trienones. The cytotoxic activity we would like to explore was oral cancer. Oral cancer was estimated to account for 2.7% of all cancers. There were about 300,000 oral cancer cases in 2012 worldwide and about 50% of patients died from this type of cancer. The five-year relative survival rate of oral cancer patients is less than 35% in advanced stage of disease at initial diagnosis.

3.1[6]

R¹ 3'
$$R^2$$
 R^2 R^2 R^2 R^2 R^2 R^3 R^4 R^2 R^4 R^4 R^4 R^4 R^4 R^2 R^4 R^4 R^4 R^2 R^4 R^4 R^2 R^4 R^4 R^2 R^4 R^4 R^2 R^4 R^4 R^4 R^2 R^4 R^4 R^2 R^4 $R^$

In the previous work, ^{3.1[7]} we have synthesized a number of trienones for cytotoxicty against a number of cancer cell lines, including oral cancer. However, when we planned to prepare a manuscript on cytotoxicity of the synthesized compounds, we found that the number and diversity of the synthesized compounds were not sufficient for structure-activity relationship study. In this TRF project, we therefore decided to synthesize more of the trienones analogues and it was found that a number of the analogues exhibited very high anti-KB activity and some of them showed higher cytotoxicy than that of ellipticine, the reference anti-cancer drug. The detail is in the following published work.

Output. This project has led to the following publication:

Chuprajob, T., Changtam, C., Chokchaisiri, R., Chunglok, W., Sornkaew, N., Suksamrarn, A., 2014. Synthesis, cytotoxicity against human oral cancer KB cells and structure-activity relationship studies of trienone analogues of curcuminoids. *Bioorg. Med. Chem. Lett.* 24, 2839-2844.

References

- 3.1[1] Maheshwari, R. K., Singh, A. K., Gaddipatti, J., Srimal, R. C., 2006. Multiple biological activities of curcumin: a short review. *Life Sci.* 78, 2081–2087.
- 3.1[2] Nakayama, R., Tamura, Y., Yamanaka, H., Kikuzaki, H., Nakatani, N., 1993. Curcuminoid pigments from *Curcuma domestica*. *Phytochemistry 33*, 501–502.
- 3.1[3] Jang, M. K., Sohn, D. H., Ryu, J.-H., 2001. A curcuminoid and sesquiterpenes as inhibitors of macrophage TNF-alpha release from *Curcuma zedoaria*. *Planta Med*. 67, 550–552.
- 3.1[4] Park, S.-Y., Kim, D. S. H. L., 2002. Discovery of natural products from *Curcuma longa* that protect cells from beta-amyloid insult: A drug discovery effort against Alzheimer's disease. *J. Nat. Prod.* 65, 1227–1231.
- 3.1[5] Ferlay, J., Soerjomataram, I., Ervik, M., Dikshit, R., Eser, S., Mathers, C., Rebelo, M., Parkin, D. M., Forman, D., Bray, F., 2013. GLOBOCAN 2012 v1.0, Cancer Incidence and Mortality Worldwide: IARC CancerBase No. 11 [Internet]. Lyon, France: International Agency for Research on Cancer. Available from: http://globocan.iarc.fr, accessed on 4/4/2014.
- 3.1[6] Siegel, R., Naishadham, D., Jemal, A., 2012. Cancer statistics, 2012. *CA Cancer J. Clin.* 62, 10–29.
- 3.1[7] Suksamrarn, A., Piyachaturawat, P., Rukachaisirikul, T., Suksamrarn, S., Sukcharoen, O., Sangvichien, E., Yingyongnarongkul, B., Ajavakom, V., 2012. Structural modification of natural products for drug discovery. Final report. Bangkok: The Thailand Research Fund, March 31, 2013.

Project 3.2 Anti-cholangiocarcinoma Activity of Bisbenzylisoquinoline Alkaloid from *Tiliacora triandra*

Cholangiocarcinoma (CCA) is a malignant cancer arising from bile duct epithelium. It is a liver cancer and is a serious public health problem in the northeast of Thailand as it has the highest incidence and mortality rate.^{3.2[1]} Only about 10% of patients with early-stage disease are considered surgical operation^{3.2[2]} and chemotherapy is the option left for inoperable patients.^{3.2[3]} However, the outcome of the chemo-drug treatment is unfavorable with the five

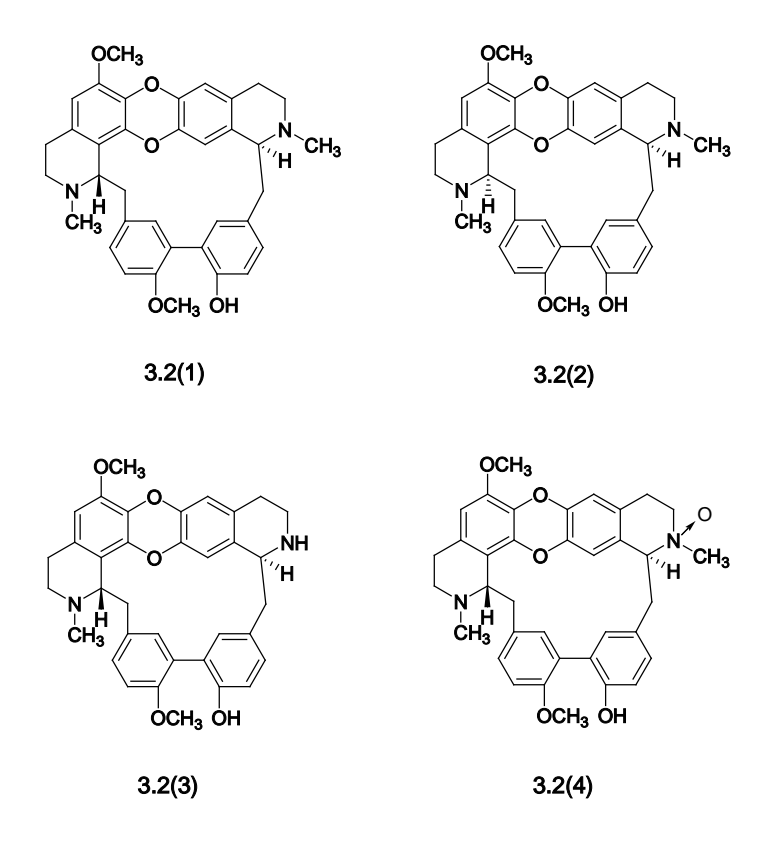
year survival lesser than 10%.^{3.2[4-6]} To reduce the mortality rate of CCA, new effective treatment strategies are needed.

Plant-derived compounds are gaining interest as potential cancer therapeutics, ^{3.2[7,8]} particularly for treatment-refractory cancers such as CCA. ^{3.2[9]} *Tiliacora triandra* (Colebr.) Diels, or "Ya nang" in Thai, is a tropical medicinal plant in the Menispermaceae family. ^{3.2[10]} It is an edible plant and it is used as an ingredient in Thai cuisines. A number of bisbenzylisoquinoline alkaloids including tiliacorinine **3.2(1)**, tiliacorine **3.2(2)**, nortiliacorinine **3.2(3)** and tiliacorinine-2′-*N*-oxide **3.2(4)** have been isolated from the roots of this plant species. ^{3.2[11-15]}

In this study, tiliacorinine (3.2(1)), the major alkaloid, was investigated for antitumor activity in CCA cell lines *in vitro* and *in vivo*. The work has been done in collaboration with Professor Sopit Wongkham and colleagues, Khon Kaen University. Antiproliferative effect of 3.2(1) on human CCA cell lines was investigated using SRB assay. Acridine orange/ethidium bromide staining, flow cytometric analysis and DNA laddering assay were used for apoptotic determination. Apoptotic related proteins were verified by Western blotting. Antitumor activity of 3.2(1) *in vivo* was demonstrated in CCA xenografted mice. Compound 3.2(1) significantly inhibited proliferations of human CCA cell lines with IC₅₀ 4.5-7 μM by inducing apoptosis through caspase activation, up-regulation of BAX, down-regulation of Bcl_{xL} and XIAP. The alkaloid 3.2(1) considerably reduced tumor growth in CCA xenografted mice. These results demonstrated the antitumor effects of 3.2(1) on human CCA *in vitro* and *in vivo*. Tiliacorinine (3.2(1)) may be an effective agent for CCA treatment. For the detail of this work, please see the following published paper.

Output. This project has led to the following publication:

Janeklang, S.; Nakaew, A., Vaeteewoottacharn, K., Seubwai, W., Boonsiri, P., Kismali, G., Suksamrarn, A., Okada, S., Wongkham, S., 2014. *In vitro* and *in vivo* antitumor activity of tiliacorinine in human cholangiocarcinoma. *Asian Pac. J. Cancer Prev.* 15, 7473–7478.



References

- 3.2[1] Sripa, B., Pairojkul, C., 2008. Cholangiocarcinoma: lessons from Thailand. *Curr. Opin. Gastroenterol.*, 24, 349–356.
- 3.2[2] Han, S. L., Zhu, G. B., Yao, J. G., Lan, S. H., Shao, Y. F., 2005. Diagnosis and surgical treatment of primary hepatic cholangiocarcinoma. *Hepatogastroenterology*, 52, 348–351.
- 3.2[3] Chou, T. C., Talalay, P., 1984. Quantitative analysis of dose-effect relationships: the combined effects of multiple drugs or enzyme inhibitors. *Adv. Enzyme Regul.*, 22, 27–55.
- 3.2[4] Butthongkomvong, K., Sirachainan, E., Jhankumpha, S., et al., 2013. Treatment outcome of palliative chemotherapy in inoperable cholangiocarcinoma in Thailand. *Asian Pac. J. Cancer Prev.*, 14, 3565–3568.
- 3.2[5] Rizvi, S., Gores, G. J., 2013. Pathogenesis, diagnosis, and management of cholangiocarcinoma. *Gastroenterology*, 145, 1215–1229.

- 3.2[6] Thunyaharn, N., Promthet, S., Wiangnon, S., et al., 2013. Survival of cholangiocarcinoma patients in northeastern Thailand after supportive treatment. *Asian Pac. J. Cancer Prev.*, 14, 7029–7032.
- 3.2[7] Shukla, Y., 2007. Tea and cancer chemoprevention: a comprehensive review. *Asian Pac. J. Cancer Prev.*, 8, 155–166.
- 3.2[8] Aras, A., Khokhar, A. R., Qureshi, M. Z., et al., 2014. Targeting cancer with nanobullets: Curcumin, EGCG, resveratrol and quercetin on flying carpets. *Asian Pac. J. Cancer Prev.*, 15, 3865–3871.
- 3.2[9] Naus, P. J., Henson, R., Bleeker, G., Wehbe, H., Meng, F., Patel, T., 2007. Tannic acid synergizes the cytotoxicity of chemotherapeutic drugs in human cholangiocarcinoma by modulating drug efflux pathways. *J. Hepatol.*, 46, 222–229.
- 3.2[10] Smitinand, T., 2014. Thai Plant Names, Revised Edition. Department of Natural Park, Wildlife and Plant Conservation, Ministry of Natural Resources and Environment, Bangkok.
- 3.2[11] Wiriyachitra, P., Phuriyakorn, B., 1981. Alkaloids of *Tiliacora triandra. Aust. J. Chem.* 34, 2001–2004.
- 3.2[12] Pachaly, P., Khosravian, H., 1988. New bisbenzylisoquinoline alkaloids from *Tiliacora triandra. Planta Med.* 54, 433–437.
- 3.2[13] Markmee, S., Saiin, C., 2003. Isolation of anti-malarial active compound from Yanang (*Tiliacora triandra* Diels). *Kasetsart J. Nat. Sci.* 37, 47–51.
- 3.2[14] Pavanand, K. Webster, H. K., Yongvanitchit, K., Dechatiwongse, T., 1981.

 Antimalarial activity of *Tiliacora triandra* Diels against *Plasmodium falciparum* in vitro. *Phytother. Res.* 3, 215–217.
- 3.2[15] Nakaew, A., Janeklang, S., Wongkham, S., Suksamrarn, A., 2014. Anti-cholangiocarcinoma activity of alkaloids and their analogues from *Tiliacora triandra*. Pure and Applied Chemistry International Conference 2014 (PACCON 2014), Centara Hotel & Convention Centre, Khon Kaen, 8–10 January.

Project 3.3 Curcuminoid Analogues Enhance Teromerase Activity in an *in vitro* TRAP Assay

Telomerase expression is associated with cell immortalization and tumorigenesis. ^{3.3[1]} Most human somatic cells do not express telomerase; and therefore, their telomeres are gradually shortened with each cell division due to the 'end-replication' problem. 3.3[2] Once a few telomeres are shortened to a critical length, they signal the cell to enter growth arrest known as replicative senescence. 3.3[3] Cancer cells evade replicative senescence by maintaining their telomeres, mostly by reactivating telomerase reverse transcriptase (TERT) expression. 3.3[4] Inhibition of telomerase is thus a selective cancer therapy with the capacity to render cancer cells to replicative senescence. ^{3.3[5]} Telomerase is a multi-subunit ribonucleoprotein enzyme comprised of the telomerase reverse transcriptase (TERT), the telomerase RNA (TR), and species-specific accessory proteins.^{3,3[6]} TERT catalyzes the addition of a short repetitive telomeric sequence onto the 30-end of telomeres using a section of TR as the template in a process known as repeat addition processivity. 3.3[7] The work has been performed in collaboration with Assistant Professor Dr. Wirote Tuntiwechapikul and colleagues, Chiang Mai University. In this work, we have found for the first time that a number of curcuminoid analogues that enhance telomerase activity in an in vitro TRAP assay. A preliminary analysis of structure-activity relationships found that the minimal requirement for this enhanced telomerase activity is a curcuminoid core with at least one suitable alkylpyridinium side chain, while curcuminoids with two such side chains exhibit even greater activity. The finding here might lead to a new class of telomerase activators that act directly or indirectly on telomerase, rather than through the reactivation of the telomerase reverse transcriptase (TERT) gene associated with other telomerase activators found in the literature. The detail of this work can be seen in the paper mentioned below.

Output. This project has led to the following publication:

Taka, T., Changtam, C., Thaichana, P., Kaewtunjai, N., Suksamrarn, A., Lee, T. R., Tuntiwechapikul, W., 2014. Curcuminoid derivatives enhance telomerase activity in an in vitro TRAP assay. *Bioorg. Med. Chem. Lett.* 24, 5242-5246.

References

- 3.3[1] (a) Shay, J. W., Wright, W. E., 2011. Role of telomeres and telomerase in cancer. Semin. Cancer Biol. 21, 349-353; (b) Autexier, C., Greider, C. W.,1996. Telomerase and cancer: revisiting the telomere hypothesis. Trends Biochem. Sci. 21, 387-391.
- 3.3[2] Olovnikov, A. M., 1996. Telomeres, telomerase, and aging: origin of the theory. *Exp. Gerontol.* 31, 443-448.
- 3.3[3] Shay, J. W., Wright, W. E., 2005. Telomere dynamics are a critical component of both aging and cancer. *Carcinogenesis* 26, 867-874.
- (a) Deng, Y., Chan, S. S., Chang, S., 2008. Telomere dysfunction and tumour suppression: the senescence connection. *Nat. Rev. Cancer* 8, 450-458; (b) Kim, N. W., Piatyszek, M. A., Prowse, K. R., Harley, C. B., West, M. D., Ho, P. L. C., Coviello, G. M., Wright, W. E., Weinrich, S. L., Shay, J. W., 1994. Specific association of human telomerase activity with immortal cells and cancer. *Science* 266, 2011-2015.
- 3.3[5] Ouellette, M. M., Wright, W. E., Shay, J. W. J., 2011. Targeting telomerase-expressing cancer cells. *Cell. Mol. Med.* 15, 1433-1442.
- 3.3[6] Wyatt, H. D., West, S. C., Beattie, T. L., 2010. InTERTpreting telomerase structure and function. *Nucleic Acids Res.* 38, 5609-5622.
- (a) Greider, C. W., 1991. Teromerase is processive. *Mol. Cell. Biol.* 11, 4572-4580;
 (b) Hardy, C. D., Schultz, C. S., Collins, K. J., 2001. Requirements for the dGTP-dependent repeat addition processivity of recombinant Tetrahymena telomerase. *Biol. Chem.* 276, 4863-4871;
 (c) Moriarty, T. J., Marie-Egyptienne, D. T., Autexier, C., 2004. Functional organization of repeat addition processivity and DNA ynthesis determinants in the human telomerase multimer. *Mol. Cell. Biol.* 24, 3720-3733.

Project 4. Structural Modification and Biological Evaluation of Nonsteroidal Antiinflammatory Natural Products and Analogues and Study of Mechanism of Action

The work involves (1) selection of lead compound that exhibits antiinflammatory activity for further study. Antiinflammatory compound will be selected based on the SAR study, its antiinflammatory activity, chemical structure and functional groups present in the molecule.

(2) chemical modification of the lead compound. The selected lead compound will be subjected to structural modification, starting from preparation of derivatives of functional groups present in the molecule. Further modification of functional groups or skeleton will also be conducted, depending on individual compound. All the compounds synthesized or modified will be subjected to structural confirmation. (3) antiinflammatory evaluation of the modified compound. If the modified compound exhibits higher antiinflammatory activity than the parent lead compound, further modification may be repeated to obtain the most active one. (4) evaluation for toxicity to normal cell (Vero cell, for example). (5) analogues with high activity will be subjected to further antiinflammatory evaluation. This project is also a collaborative research with Professor Guolin Zhang and Professor Fei Wang, Chengdu Institute of Biology, Chinese Academy of Sciences, China.

Project 4.1 Diaryheptanoids of *Curcuma comosa* with Nitric Oxide Inhibitory Activity

Curcuma comosa Roxb. (Zingiberaceae), has been used in indigenous medicine in Thailand. The rhizome of this plant species has known as an anti-inflammatory agent and has been used for the treatment of postpartum uterine bleeding and as an aromatic stomachic. A number of diarylheptanoids with nematocidal^{4.1[1]} and estrogenic activity,^{4.1[2]} and a phloracetophenone glucoside with choleretic activity^{4.1[3]} have been isolated. The aerial parts of this plant species contained labdane diterpenes, 4.1[4] flavonoid glycosides and diarylheptanoids. 4.1[5] Unlike C. longa, this plant species exists with high biodiversity. Investigation of C. comosa collected from cultivation sites in different parts of Thailand revealed that the rhizome morphology is highly variable. Chromosome numbers, together with inflorescent, floral and leaf morphology were used to separate this plant species into different cultivars. The study revealed that chromosome numbers can be used to accurately verify the taxonomic identification of C. comosa. 4.1[6] The amplified fragment length polymorphism (AFLP) marker was used to identify and elucidate the phylogenetic relationships of this plant species. 4.1[7] We have recently investigated the constituents of the rhizomes of C. comosa collected from Kampaengsaen district, Nakhon Pathom province, central Thailand. 4.1[2] Further phytochemical studies of this plant species collected from different parts of the country have been explored. Preliminary investigation of the chemical constituents of the rhizomes of this plant species collected from Sawangdaendin district, Sakon Nakorn province, northeastern Thailand revealed that the diarylheptanoid contents, especially the minor components, are different.

Partial chemical constituents and biological evaluation of C. comosa rhizomes have been investigated. 4.1[8] The hexane and ethanol extracts of *C. comosa* rhizomes from Sakon Nakorn province were subjected to repeated column chromatography and eight new diaryheptanoids, **4.1(1)–4.1(5)**, together with thirteen known diaryheptanoids, 1,7-diphenyl-(6E)-6-hepten-3one (4.1(6)), (5R)-1,7-diphenyl-5-hydroxy-(6E)-6-hepten-3-one (4.1(7)), $^{4.1[1,9]}$ 1,7-diphenyl-(4E,6E)-4,6-heptadien-3-one (4.1(8)), $^{4.1[10]}$ (3*R*)-1,7-diphenyl-(4*E*,6*E*)-4,6-heptadien-3-ol (**4.1(9**)), 1-(4-hydroxyphenyl)-7-phenyl-(6*E*)-6-hepten-3-one (**4.1(10**)), 1-(4-hydroxyphenyl)-7-phenyl-(4E,6E)-4,6-heptadien-3-one (4.1(11)), $^{4.1[2]}$ (3S,5S)-1,7-diphenylheptan-3,5-diol (4.1(12)), 4.1[11] a 3:1 mixture of (3S)- and (3R)-1-(4-hydroxyphenyl)-7-phenyl-(6E)-6-hepten-3-ol (3S)-1-(3,4-dihydroxyphenyl)-7-phenyl-(6E)-6-hepten-3-ol (4.1(13a and 13b)), (**4.1(14**)), ^{4.1[2,3,12]} 1-(3-methoxy-4-hydroxyphenyl)-7-phenylheptan-3,5-diol (**4.1(15**)), ^{4.1[13]} 1-(4-hydroxyphenyl)-7-phenylheptan-3,5-diol (**4.1(16**)), 4.1[13,14] and 1,7-bis-(4-hydroxyphenyl)-(4E,6E)-4,6-heptadien-3-one $(4.1(17))^{4.1[15]}$ were isolated. The configurations of **4.1(7)** and **4.1(9)** were determined to be R by the modified Mosher's method (data not shown). The absolute configurations of compounds 4.1(13) and 4.1(14) were determined to be a 3:1 mixture of 3S and 3R 4.1(13a) and 4.1(13b) and 3S, respectively (data note shown). It is noteworthy that the absolute stereochemistry and enantiomeric ratio of compounds 4.1(9), 4.1(13) and 4.1(14) is the same as those isolated from Kampaengsaen district, Nakhon Pathom province.

A number of *Curcuma* and other species of Chinese origins have also been studied by Professor Guolin Zhang and Professor Fei Wang in comparison with those of the Thai origins.

Compound **4.1(1)** was obtained as a white solid, m.p. 110–112 °C. The HR-TOFMS (ES⁻) showed the [M–H]⁻ peak at m/z 279.1835, compatible with the molecular formula C₁₉H₁₉O₂. The IR absorption band at 3233 cm⁻¹ revealed the presence of a hydroxyl group. The presence of $\alpha, \beta, \gamma, \delta$ -unsaturated system was evident from the ¹H NMR signals (Table 1) at $\delta_{\rm H}$ 5.83 (dd, J = 15.1, 6.8 Hz, 1H, H-4), $\delta_{\rm H}$ 6.37 (dd, J = 15.1, 10.6 Hz, 1H, H-5), 6.54 (d, J = 15.6 Hz, 1H, H-7), 6.76 (partially overlapping signal, 1H, H-6), which corresponded to the ¹³C NMR signals at $\delta_{\rm C}$ 136.1, 131.0, 132.6 and 128.1, respectively (Table 1). The COSY spectrum between H-1 ($\delta_{\rm H}$ 2.65, m, 2H) and H-2 ($\delta_{\rm H}$ 1.87, m, 2H), H-2 and H-3 ($\delta_{\rm H}$ 4.21, m, 1H), and H-3 and H-4 determined the present of a hydroxyl at C-3. The attachment of the phenyl group to the 7-position of the heptyl chain was confirmed from the HMBC correlations between H-6 and C-1" ($\delta_{\rm C}$ 137.0), H-7 and C-2"/C-6" ($\delta_{\rm C}$ 126.3), and H-2"/H-6" ($\delta_{\rm H}$ 7.38, br d, J = 7.5 Hz, 2H) and C-7 ($\delta_{\rm C}$ 132.6), whereas that of the 4-hydroxyphenyl moiety to the 1-position was confirmed by the HMBC correlations between H-1 and C-2 ($\delta_{\rm C}$ 38.8), C-3 ($\delta_{\rm C}$ 72.0), C-1' ($\delta_{\rm C}$ 133.7), C-2'/6' ($\delta_{\rm C}$ 129.4), and H-2'/H-6' ($\delta_{\rm H}$ 7.05, d, d = 8.2 Hz, 2H) and C-1 ($\delta_{\rm C}$ 30.7) (Table

1). The low optical rotation ($[\alpha]_D^{29} - 3.84$, c 1.37, EtOH) suggested that this compound existed as a mixture of two enantiomers, since it has been observed that diarylheptanoids with a 4,6-dien-3-ol system exhibited high optical rotation. ^{4.1[2]} The absolute stereochemistry at C-3 and the enantiomeric ratio were determined by the modified Mosher's method. ^{4.1[2,16,17]} Thus, upon treatment with (R)-(-)-MTPA chloride and (S)-(+)-MTPA chloride, the diarylheptanoids **4.1(1a)** and **4.1(1b)** mixture was transformed to a mixture of the corresponding (S)-MTPA esters **1ax** and **1bx**, and (R)-MTPA esters **4.1(1ay)** and **4.1(1by)**, respectively (Figure 1). Analysis of the ¹H-NMR spectra of the two Mosher ester mixtures established the absolute configuration at C-3 of the diarylheptanoid mixture as S and R in a ratio of 1.2:1. The diarylheptanoid **4.1(1)** was thus concluded as a 1.2:1 mixture of (S)- and (S)-1-(S)-1-(4-hydroxyphenyl)-7-phenyl-(S)-4,6-heptadien-3-ol **4.1(1a)** and **4.1(1b)**.

Figure 4.1(1) $\Delta \delta = (\Delta \delta_S - \Delta \delta_R)$ values obtained from the MTPA esters of compounds 4.1(1a) and 4.1(1b) mixture and 4.1(4) in CDCl₃

Compound **4.1(2)** was obtained as a colorless sticky solid. The HR-TOFMS (ES⁻) showed the [M–H]⁻ peak at m/z 293.1541, consistent with the molecular formula $C_{20}H_{22}O_2$. The IR spectrum showed an absorption band for a hydroxyl group at 3321 cm⁻¹. The ¹H NMR data (Table 1) of **2** were similar to those of **4.1(1)** except that **4.1(2)** showed the presence of a methoxyl signal at δ_H 3.29 (3H, s) and δ_C 56.1, which could be placed at C-3 (δ_C 81.2) from the HMBC correlations between OCH₃-3/C-3, and between H-3/C-1 (δ_C 30.5), C-2 (δ_C 37.3),

OCH₃, and C-5 ($\delta_{\rm C}$ 132.9). Compound **2** exhibited low optical rotation, $[\alpha]_{\rm D}^{29}$ –0.33 (c 0.68 EtOH), suggesting that this compound should exist as a racemic mixture. Compounds **4.1(2a)** and **4.1(2b)** are thus assumed to exist as racemic mixture of (3S)- and (3R)-1-(4-hydroxyphenyl)-3-methoxy-7-phenyl-(4E,6E)-4,6-heptadiene.

Compound **4.1(3)** was isolated as a colorless sticky solid. The molecular formula was determined as $C_{21}H_{24}O_3$ by HR-TOFMS (ES⁻) at m/z 323.1698 [M–H]⁻. The IR spectrum showed an absorption band for a hydroxyl group at 3308 cm⁻¹. The ¹H and ¹³C NMR spectra of **3** (Table 1) were found to be similar to those of **4.1(2)**, with an additional signal for a methoxyl group at C-3' (δ_C 143.6). The aromatic proton signals at δ_H 6.67 (s, 1H, H-2'), 6.81 (d, J = 7.6 Hz, 1H, H-5') and 6.66 (d, J = 7.6 Hz, 1H, H-6') revealed a 1,3,4-trisubstituted aromatic ring. The location of a methoxyl group at C-3' and a hydroxyl group at C-4' were confirmed by the HMBC correlations between H-2'/C-3', C-4' (δ_C 146.3), and C-6' (δ_C 121.0), H-5'/C-1' (δ_C 133.8), C-3', C-4', and C-6', H-6'/C-2' (δ_C 111.0), C-3', and C-4'. Diaryheptanoid **4.1(3)** exhibited low optical rotation ($[\alpha]_D^{25}$ +2.20, c 1.52, EtOH) indicating that this compound should exist as a ca. 1:1 mixture of (3S)- and (3R)-1-(3-hydroxy-4-methoxyphenyl)-3-methoxy-7-phenyl-(4E,6E)-4,6-heptadiene (**4.1(2a)** and **4.1(2b)**).

Compound **4.1(4)** was isolated as a colorless sticky solid, $[\alpha]_D^{29}$ +5.38 (c 1.31, EtOH). The HR-TOFMS (ES $^-$) at m/z 357.1716 [M–H] $^-$ established the molecular formula as $C_{21}H_{26}O_5$. The IR spectrum showed an absorption band for hydroxyl and acetoxyl groups at 3370 and 1705 cm $^{-1}$, respectively. The assignment for the proton signals at δ_H 6.63 (br s, 1H, H-2'), 6.74 (d, J = 8.0 Hz, 1H, H-5') and 6.54 (br d, J = 8.0 Hz, 1H, H-6') revealed a 1,3,4-trisubstitued benzene ring system. The 13 C NMR data (Table 1) displayed 21 signals including two carbinolic (δ_C 66.8, and 71.4), five methylene (δ_C 31.1, 32.0, 36.4, 38.4, and 42.6), one acetoxy (δ_C 21.0 and 173.0), and twelve aromatic ring carbons, suggesting an acetylated diarylheptanoid structure. The structure deduction of **4.1(4)** was confirmed by COSY, DEPT, HMQC, and HMBC spectra. The attachment of the phenyl group to the 7-position of the heptyl chain was confirmed by the HMBC correlations between H-7 (δ_H 2.64 and 2.77, m, 2×1H) and C-1" (δ_C 141.8) and C-2"/C-6" (δ_C 128.3). In addition, the absolute stereochemistry at C-5 was deduced to be R configuration by the modified Mosher's method (Figure 4.1(1)). However, the existing

data did not permit the assignment the absolute configuration at C-3. Compound **4.1(4)** was therefore identified as (5R)-1-(3,4-dihydroxyphenyl)-7-phenyl-3-acetoxy-5-hydroxyheptane.

Compound **4.1(5)** was isolated as a colorless amorphous solid, m.p. 52–53 °C, $[\alpha]_D^{21}$ –43.12 (c 0.48, EtOH). The molecular formula was determined as C₁₉H₂₀O₃ by HR-TOFMS (ES⁻) at m/z 295.1338 [M-H]. The IR spectrum showed an absorption band for hydroxyl groups at 3328 cm⁻¹. The 13 C NMR data (Table 1) displayed 19 signals including a carbinolic ($\delta_{\rm C}$ 74.9), four methylene (δ_C 24.0, 27.5, 28.7, and 34.8), two methine (δ_C 130.0 and 130.2), and twelve aromatic ring carbons, suggesting a diarylheptanoid structure. The presence of the transolefinic protons was evident from the double triplet signal at $\delta_{\rm H}$ 6.23 (J=15.9, 7.2 Hz, H-6) and the doublet signal at $\delta_{\rm C}$ 6.41 (J=15.9 Hz, H-7) in the ¹H-NMR spectrum, which corresponded to the 13 C NMR signals at $\delta_{\rm C}$ 130.0 and 130.2, respectively. The 1 H-NMR spectrum of compound **4.1(5)** was similar to those of (3S)-1-(3,4-dihydroxyphenyl)-7-phenyl-(6E)-6-hepten-3-ol 4.1(14). However, the significant difference was based on the molecular weight of 4.1(5) with 2 amu lower than that of 4.1(14) and the presence of aromatic singlet signals of H-3' at δ_H 6.37 (δ_C 103.8), and H-6' at δ_H 6.52 (δ_C 115.5) indicated the connectivity between an aromatic ring at C-3 with an ether bond. The large W_{1/2} value (24 Hz) of H-3 suggested its axial relationship with H-1ax. In our previous work, the absolute configuration at C-3 of **4.1(5)** has not been established. ^{4.1[8]} In the present work, the absolute configuration was determined by circular dichroism (CD) spectroscopy. The C-3 configuration was determined to have an R-configuration based on the helecity rule for P-helecity of the chiral chromane ring system, $^{4.1[18-21]}$ which showed negative Cotton effect for the $1L_b$ band at 250-270nm. $^{4.1[22-24]}$ The NOE correlation of H-1 and H-3 confirmed the C-3 (Figure 2). Compound **4.1(5)** was thus elucidated as (3R)-1-(4,5-dihydroxyphenyl)-7-phenyl-(6E)-6-hepten-3,2'epoxide.

Figure 4.1(2) NOE correlation of H-3 with H-1ax of compound 4.1(5)

The high biodiversity of the chemical constituents of *C. comosa* should be noted. The contents of a number of diarylheptanoids from *C. comosa* rhizomes collected from Sakon Nakorn province, northeastern Thailand according to the present work were found to be different from those isolated from *C. comosa* from Kampaengsaen district, Nakhon Pathom province, central Thailand. ^{4.1[2]} Apart from the new compounds **4.1(1)–4.1(5)**, the known compounds **4.1(12)**, **4.1(15)–4.1(17)** have not been reported previously in the Kampaengsaen cultivar.

To examine the biological effect of the isolated compounds, the mouse macrophage RAW 264.7 cells were treated with different concentrations of the diarylheptanoids. Compounds 4.1(1a) and 4.1(1b) mixture and 4.1(14) were found to be active to the test. As shown in Figure 4.1(2), lipopolysaccharide (LPS) treatment significantly promoted the production of nitric oxide (NO), a well-known proinflammatory cytokine involving in many inflammatory diseases. 4.1[25] BAY 11-7082, a NF-kB inhibitor, which was used as a positive control 4.1[26] (Guzik et al., 2003), significantly inhibited the production of NO in the LPS-treated RAW264.7 cells. Furthermore, at 0.1-10 μ g/ml, compounds **4.1(1a)** and **4.1(1b)** mixture and 4.1(14) could inhibit the production of NO in the LPS-treated RAW264.7 cells in a concentration-dependent manner. The calculated IC₅₀ concentration of compounds **4.1(1a)** and 4.1(1b) mixture and 4.1(14) for the inhibition of NO production in LPS-stimulated RAW264.7 cells was 1.84 μ g/l (6.56 μ M) and 1.24 μ g/l (4.15 μ M), respectively. The antiinflammatory effect of the diarylheptanoids not only help for the understanding of traditional medicinal use of C. comosa rhizomes, but also validate further development of compounds **4.1(1a)** and **4.1(1b)** mixture and **4.1(14)** as the apeutic tools for the prevention and treatment of inflammatory diseases.

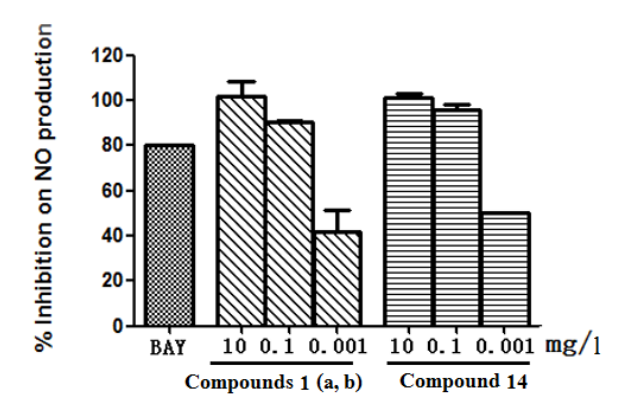


Figure 4.1(2) Effects of compounds **4.1(1a)** and **4.1(1b)** mixture and **4.1(14)** on inhibiting NO production. Mouse macrophage RAW264.7 cells were pretreated with compounds at indicated concentrations for 2 h and then treated with LPS (1 mg/l). After 24, NO levels were determined in conditioned medium by the Griess reaction.

Output. This project has led to the following publication:

Sornkaew, N., Lin, Y., Wang, F., Zhang, G., Chokchaisiri, R., Zhang, A., Wongkrajang, K., Suebsakwong, P., Piyachaturawat, P., Suksamrarn, A., 2015. Diarylheptanoids of *Curcuma comosa* with inhibitory effects on nitric oxide production in macrophage RAW 264.7 cells. *Nat. Prod. Commun.* 10, 89-93.

References

- 4.1[1] Jurgens, T. M., Frazier, E. G., Schaeffer, J. M., Jones, T. E., Zink, D. L., Borris, R. P., Nanakorn, W., 1994. Novel nematocidal agents from *Curcuma comosa. J. Nat. Prod.* 57, 230–235.
- 4.1[2] Suksamrarn, A., Ponglikitmongkol, M., Wongkrajang, K., Chindaduang, A., Kittidanairak, S., Jankam, A., Yingyongnarongkul, B., Kittipanumat, N., Chokchaisiri, R., Khetkam, P., Piyachaturawat, P., 2008. Diarylheptanoids, new phytoestrogens from the rhizomes of *Curcuma comosa*: isolation, chemical modification and estrogenic activity evaluation. *Bioorg. Med. Chem.* 16, 6891–6902.

- 4.1[3] Suksamrarn, A., Eiamong, S., Piyachaturawat, P., Byrne, L. T., 1997. A phloracetophenone glucoside with choleretic activity from *Curcuma comosa*. Phytochemistry 45, 103–105.
- 4.1[4] Chokchaisiri, R., Chaneiam, N., Svasti, S., Fucharoen, S., Vadolas, J., Suksamrarn, A., 2010. Labdane diterpenes from the aerial parts of *Curcuma comosa* enhance fetal hemoglobin production in an erythroid cell line. *J. Nat. Prod.* 73, 724–728.
- 4.1[5] Chokchaisiri, R., Innok, P., Suksamrarn, A., 2012. Flavonoids glycosides from the aerial parts of *Curcuma comosa*. *Phytochemistry Lett.* 5, 361–366.
- 4.1[6] Soontornchainaksaeng, P., Jenjittikul, T., 2010. Chromosome number variation of phytoestrogen-producing *Curcuma* (Zingiberaceae) from Thailand. *J. Nat. Med.* 64, 370–377.
- 4.1[7] Keeratinijakal, V., Kladmook, M., Laosatit, K., 2010. Identification and characterization of *Curcuma comosa* Roxb., phytoestrogens-producing plant, using AFLP markers and morphological characteristics. *J. Med. Plants Res.* 4, 2651–2657.
- 4.1[8] Suksamrarn, A., Piyachaturawat, P., Rukachaisirikul, T., Suksamrarn, S., Sukcharoen, O., Sangvichien, E., Yingyongnarongkul, B., Ajavakom, V., 2012. Structural modification of natural products for drug discovery. Final report. Bangkok: The Thailand Research Fund, March 31, 2013.
- 4.1[9] Kuronayaki, M., Noro, T., Fukushima, S., Aimaya, R., Ikuta, A., Itokawa, H., Morita, M., 1983. Studies on the constituents of the seeds of *Alpinia katsumadai* Hayata. *Chem. Pharm. Bull.* 31, 1544-1550.
- 4.1[10] Claeson, P., Panthong, A, Tuchinda, P., Reutrakul, V., Kanjanapothi, D., Taylor, W.
 C., Santisuk, T., 1993. Three non-phenolic diarylheptanoids with anti-inflammatory activity from *Curcuma xanthorrhiza*. *Planta Med.* 59, 451–454.
- 4.1[11] Hashimoto, T., Tori, M., Asakawa, Y., 1986. Five new diarylheptanoids from the male flowers of *Alnus sieboldiana*. Chem. Pharm. Bull. 34, 1846–1849.
- 4.1[12] Suksamrarn, A., Eiamong, S., Piyachaturawat, P., Charoenpiboonsin, J., 1994. Phenolic diarylheptanoids from *Curcuma xanthorrhiza*. *Phytochemistry* 36, 1505–1508.

- 4.1[13] Shin, D., Kinoshita, K., Koyama, K., Takahashi, K., 2002. Antiemetic principles of *Alpinia officinarum*. J. Nat. Prod. 65, 1315–1318.
- 4.1[14] Uehara, S. I., Yasuda, I., Akiyama, K., Morita, H., Takeya, K., Itokawa, H., 1987. Diarylheptanoids from the rhizomes of *Curcuma xanthorrhiza* and *Alpinia officinarum*. *Chem. Pharm. Bull.* 35, 3298–3304.
- 4.1[15] Li, J., Zhao, F., Li, M. Z., Chen, L. X., Qiu, F., 2010. Diarylheptanoids from the rhizomes of *Curcuma kwangsiensis*. *J. Nat. Prod.* 73, 1667–1671.
- 4.1[16] Dale, J. A., Dull, D. L., Mosher, H. S., Chen, 1969. α–Methoxy-α-trifluoromethylphenylacetic acid, a versatile reagent for the determination of enantiomeric composition of alcohols and amines. *J. Org. Chem.* 34, 2543–2549.
- 4.1[17] Ohtani, I., Kusumi, T., Kashman, Y., Kakisawa, H., 1991. High-filed FT NMR application of Mosher's method. The absolute configurations of marine terpenoids. *J. Am. Chem. Soc.* 113, 4092–4096.
- 4.1[18] Slade, D., Ferreira, D., Marais, J. P. J., 2005. Circular dichroism, a powerful tool for the assessment of absolute configuration of flavonoids. *Phytochemistry* 66, 2177-2215.
- 4.1[19] Antus, S., Kurtan, T., Juhasz, L., Kiss, L., Hollosi, M., Majer, Z.S., 2001. Chiroptical properties of 2,3-dihydrobenzo[b]furan and chromane chromophores in naturally occurring *O*-heterocycles. *Chirality* 13, 493–506.
- 4.1[20] Francesco, M., Gennaro, P., Lorenzo, D. B., Thomas, N., Piero, S., 2009. Circular dichroism of tocopherols versus tocotrienols. *Chirality* 21, 35-43.
- 4.1[21] Asaf, A. Q., Huanbiao, M. Lester, P., Devid, M. P., 2000. Isolation and identification of novel tocotrienols from rice bran with hypocholesterolemic, antioxidant, and antitumor properties. *J. Agic. Food Chem.* 48, 3130-3140.
- 4.1[22] Sashida, Y., Yamatoto, T., Koike, C., Shimomura, H., 1976. A new flavan glycoside from *Buckleya lanceolata* leaves. *Phytochemistry* 15, 1185-1186.
- 4.1[23] Cardillo, G., Merlini. L., Nasini. G., 1971. Constituents of dragon's blood. Part I. Structure and absolute configuration of new optically active flavans. *J. Chem. Soc.*(*C*), 3967-3970.

- 4.1[24] Chiara, C., Simona, B., Susanna, M., 2005. Computational study of conformational and chiroptical properties of (2*R*,3*S*,4*R*)-(+)-3,3',4,4',7-flavanpentol. *Chirality* 17, 577–589.
- 4.1[25] Mendes Sdos, S., Candi, A., Vansteenbrugge, M., Pignon, M. R., Bult, H., Boudjeltia, K. Z., Munaut, C., Raes, M., 2009. Microarray analyses of the effects of NF-kappaB or PI3K pathway inhibitors on the LPS-induced gene expression profile in RAW264.7 cells: synergistic effects of rapamycin on LPS-induced MMP9-overexpression. *Cell Signal*. 21, 1109–1122.
- 4.1[26] Guzik T. J., Korbut, R., Adamek-Guzik, T., 2003. Nitric oxide and superoxide in inflammation and immune regulation. *J. Physiol. Pharmacol.* 54, 469–487.

Project 5. Natural Product-based Therapeutic Agents for Diseases of the Elderly

Three types of natural product-based therapeutic agents for diseases of the elderly will be focused. They are antihypertensive, acetylcholinesterase inhibitory, and osteoporosis inhibitory activities. (1) Antihypertensive activity evaluation of the isolated compounds. (2) Structure-activity relationship (SAR) study of the tested compounds. (3) Selection of lead compound for further study. Bioactive compound will be selected based on the SAR study, its biological activity, chemical structure and functional groups present in the molecule. (4) Chemical modification of the lead compound. The selected lead compound will be subjected to structural modification, starting from preparation of derivatives of functional groups present in the molecule. Further modification of functional groups or skeleton will also be considered, depending on individual compound. (5) Synthesis of analogues of estrogenic compound. If the structure of the lead compound is not complicated, chemical synthesis or combinatorial synthesis of analogues will be used to obtain more analogues for biological evaluation. (6) Biological evaluation of the modified/synthesized compounds. (7) Selection of analogue with high estrogenic activity for further studies (mechanism of action, etc). (8) The process for acetylcholinesterase inhibitory activity will be conducted (steps 1-7). (9) The process for osteoporosis inhibitory activity will be conducted (steps 1-7).

Project 5.1 Bone Sparing Effect of Diarylheptanoid from *Curcuma comosa* in Ovariectomized Rats

This work is the continuing study of diarylheptanoids isolated from the rhizomes of *Curcuma comosa* Roxb.

Osteoporosis is a serious worldwide health problem that primarily effect middle-aged and elderly women.^{5,1[1,2]} It is characterized by reduced bone mass and the deterioration of bone microarchitecture leading to increase the risk of bone fragility and fracture. ^{5.1[3]} An accelerated rate of bone resorption in menopausal and post-menopausal women is associated with reduced levels of the hormone estrogen.^{5.1[4]} Recently, efforts to reduce bone loss in menopausal osteoporosis have been focused on compounds with the potential to preserve bone mass through inhibition of osteoclastic bone resorption or stimulation bone formation. ^{5.1[5]} Among therapeutic agents, estrogen is the most effective compound and is capable of limiting bone loss and reducing the rate of bone fractures in postmenopausal women.^{5.1[6,7]} However, longterm treatment with estrogen is limited due to its carcinogenic risk and feminizing effects. Phytoestrogens, non-steroidal plant-derived compounds with estrogenic activity, have received increased interest as estrogen alternatives to alleviate bone loss. Studies have suggested that a diet rich in phytoestrogen may relieve menopausal symptoms and protect against estrogenassociated diseases, including breast cancers, cardiovascular diseases, and osteoporosis. 5.1[8,9] Isoflavones, such as genistein and daidzein, the major phytoestrogens in soybeans, are the most extensively studies phytoestrogens. These compounds inhibit osteoclast bone resorption and suppress osteoclast activity and survival in vitro. ^{5.1[10,11]} In addition, isoflavones have been identified as naturally occurring selective estrogen receptor modulators (SERMs) and as bonesparing agents.^{5.1[12,13]} The known properties of phytoestrogens suggest that these compounds may be alternatives to estrogen for preventing and treating osteoporosis in postmenopausal women. Curcuma comosa Roxb., a plant in Zingiberaceae family, has been widely used as a dietary supplement for relieving postmenopausal symptoms in Thailand. ^{5.1[14]} Consistent with the presence of a phytoestrogen, hexane extract of C. comosa rhizomes prevent bone loss in estrogen deficient mice. $^{5.1[15]}$ The diarylheptanoid, (3R)-1,7-diphenyl-(4E,6E)-4,6-heptadien-3ol (DPHD), the phytoestrogen isolated from C. comosa^{5.1[16]} has several pharmacological properties including estrogenic-like activity^{5.1[17,18]} and anti-inflammatory effects.^{5.1[19]} Recently, DPHD was found to activate Wnt/b-catenin signaling and promote mouse preosteoblastic (MC3T3-E1) cell proliferation through the estrogen receptor pathway. ^{5.1[20]} Similarly, human osteoblast cell differentiation and function were also enhanced upon DPHD treatment ^{5.1[21]} suggesting that DPHD may have a beneficial effect in preventing bone loss in patients experiencing estrogen deficiency. The biological activities of DPHD appear to be selective with anabolic effects predominantly on osteoblasts. We hypothesized that DPHD may have a beneficial effect in preventing bone loss due to estrogen deficiency.

In the present study, we demonstrated the protective effect of DPHD on ovariectomy-induced bone loss (OVX) in adult female Sprague-Dawley rats with 17b-estradiol (E2, 10 mg/kg Bw) as a positive control. Treatment of OVX animals with DPHD at 25, 50, and 100 mg/kg Bw for 12 weeks markedly increased bone mineral density (BMD) of tibial □etaphysic as measured by peripheral Quantitative Computed Tomography (pQCT). Histomorphometric analysis of bone structure indicated that DPHD treatment retarded the ovariectomy-induced deterioration of bone microstructure. Ovariectomy resulted in a marked decrease in trabecular bone volume, number and thickness and these changes were inhibited by DPHD treatment, similar to that seen with E2. Moreover, DPHD decreased markers of bone turnover, including osteocalcin and tartrate resistant acid phosphatase (TRAP) activity. These results suggest that DPHD has a bone sparing effect in ovariectomy-induced trabecular bone loss and prevents deterioration of bone microarchitecture by suppressing the rate of bone turnover. Therefore, DPHD appears to be a promising candidate for preserving bone mass and structure in the estrogen deficient women with a potential role in reducing postmenopausal osteoporosis.

The detail of this study is in the following published work.

Output. This project has led to the following publication:

Tantikanlayaporn, D., Wichit, P., Weerachayaphorn, J., Chairoungdua, A., Chuncharunee, A., Suksamrarn, A., Piyachaturawat, P. Bone sparing effect of a novel phytoestrogen diarylheptanoid from *Curcuma comosa* Roxb. in ovariectomized rats. *PloS ONE*, 2013, 8, e78739. doi:10.1371/journal.pone.0078739.

References

5.1[1] Cummings, S. R., Melton, L. J., 2002. Epidemiology and outcomes of osteoporotic fractures. *Lancet* 359, 1761–1767.

- 5.1[2] Cauley, J. A., Thompson, D. E., Ensrud, K. C., Scott, J. C., Black, D., 2000. Risk of mortality following clinical fractures. *Osteoporos. Int.* 11, 556–561.
- 5.1[3] Raisz, L. G., 2005. Pathogenesis of osteoporosis: concepts, conflicts, and prospects. *J. Clin. Invest.* 115, 3318–3325.
- 5.1[4] Lerner, U. H., 2006. Bone remodeling in post-menopausal osteoporosis. *J. Dental Res.* 85, 584–595.
- 5.1[5] Downey, P. A., Siegel, M. I., 2006. Bone biology and the clinical implications for osteoporosis. *Phys. Ther.* 86, 77–91.
- 5.1[6] Stevenson, M., Lloyd-Jones, M., Nigris, E. D., Brewer, N., Davis, S., Oakley, J., 2005. A systematic review and economic evaluation of alendronate, etidronate, risedronate, raloxifene and teriparatide for the prevention and treatment of postmenopausal osteoporosis. *Health Tech. Assess.* 9, 1–160.
- 5.1[7] Felson, D. T., Zhang, Y., Hannan, M. T., Kiel, D. P., Wilson, P. W. F., Anderson, J. J., 1993. The effect of postmenopausal estrogen therapy on bone density in elderly women. *N. Engl. J. Med.* 329, 1141–1146.
- 5.1[8] Tham, D. M., Gardner, C. D., Haskell, W. L., 1998. Potential health benefits of dietary phytoestrogens: a review of the clinical, epidemiological, and mechanistic evidence. *J. Clin. Endocrinol. Metab.* 83, 2223–2235.
- 5.1[9] Messina, M. J., Wood, C. E., 2008. Soy isoflavones, estrogen therapy, and breast cancer risk: analysis and commentary. *Nutr. J.* 7, 17.
- 5.1[10] Blair, H. C., Jordan, S. E., Peterson, T. G., Barnes, S., 1996. Variable effects of tyrosine kinase inhibitors on avian osteoclastic activity and reduction of bone loss in ovariectomized rats. *J. Cell Biochem.* 61, 629–637.
- 5.1[11] Sugimoto, E., Yamaguchi, M., 2000. Stimulatory effect of daidzein in osteoblastic MC3T3-E1 cells. *Biochem. Pharmacol.* 59, 471–475.
- 5.1[12] Dang, Z. C., Lowik, C., 2005. Dose-dependent effects of phytoestrogens on bone. *Trends Endocrinol. Metab.* 16, 207–213.
- 5.1[13] Ren, P., Ji, H., Shao, Q., Chen, X., Han, J., Sun, Y., 2007. Protective effects of sodium daidzein sulfonate on trabecular bone in ovariectomized rats. *Pharmacology* 79, 129–136.
- 5.1[14] Piyachaturawat, P., Ercharuporn, S., Suksamrarn, A., 1995. Uterotrophic effect of

- Curcuma comosa in rats. Pharmaceut. Biol. 33, 334–338.
- 5.1[15] Weerachayaphorn, J., Chuncharunee, A., Mahagita, C., Lewchalermwongse, B., Suksamrarn, A., Piyachaturawat, P., 2011. A protective effect of *Curcuma comosa* Roxb. on bone loss in estrogen deficient mice. *J. Ethnopharmacol*. 137, 956–962.
- 5.1[16] Suksamrarn, A., Ponglikitmongkol, M., Wongkrajang, K., Chindaduang, A., Kittidanairak, S., Jankam, A., Yingyongnarongkul, B., Kittipanumat, N., Chokchaisiri, R., Khetkam, P., Piyachaturawat, P., 2008. Diarylheptanoids, new phytoestrogens from the rhizomes of *Curcuma comosa*: Isolation, chemical modification and estrogenic activity evaluation. *Bioorg Med. Chem.* 16, 6891–6902.
- 5.1[17] Winuthayanon, W., Suksen, K., Boonchird, C., Chuncharunee, A., Ponglikitmongkol, M., Suksamrarn, A.; Piyachaturawat, P., 2009. Estrogenic activity of diarylheptanoids from *Curcuma comosa* Roxb. Requires metabolic activation. *J. Agric. Food Chem.* 57, 840–845.
- 5.1[18] Winuthayanon, W., Piyachaturawat, P., Suksamrarn, A., Ponglikitmongkol, M., Arao, Y., Hewitt, S. C., Korach, K. S., 2009. Diarylheptanoid phytoestrogens isolated from the medicinal plant *Curcuma comosa*: biologic actions in vitro and in vivo indicate estrogen receptor dependent mechanisms. *Environ. Health Perspect*. 117, 1155–1161.
- 5.1[19] Thampithak, A., Jaisin, Y., Meesarapee, B., Chongthammakun, S., Piyachaturawat, P., Govitrapong, P., Sanvarinda, Y., 2009. Transcriptional regulation of iNOS nd COX-2 by a novel compound from *Curcuma comosa* in lipopolysaccharide-induced microglial activation. *Neurosci. Lett.* 462, 171–175.
- 5.1[20] Bhukhai, K., Suksen, K., Bhummaphan, N., Janjorn, K., Thongon, N., Tantikanlayaporn, D., Piyachaturawat, P., Suksamrarn, A., Chairoungdua, A., 2012. A phytoestrogen diarylheptanoid mediates estrogen receptor/Akt/glycogen synthase kinase 3beta protein-dependent activation of the Wnt/beta-catenin signaling pathway. *J. Biol. Chem.* 287, 36168–36178.
- 5.1[21] Tantikanlayaporn, D., Robinson, L. J., Suksamrarn, A., Piyachaturawat, P., Blair, H. C., 2013. A diarylheptanoid phytoestrogen from *Curcuma comosa*, 1,7-diphenyl-4,6-heptadien-3-ol, accelerates human osteoblast proliferation and differentiation. *Phytomedicine* 20, 676–682.

Project 5.2 Vasorelaxation Effects of 16-O-acetyldihydroisosteviol, an Analogue of Isosteviol, on Isolated Rat Thoracic Aorta

Stevioside is a diterpene glycoside isolated from the leaves of the plant Stevia rebaudiana (Bertoni) Bertoni, and it has been used as an artificial sweetener worldwide. ^{5.2[1-3]} Stevioside has shown the property on arterial pressure and renal function as a calcium antagonist^{5.2[4]} and lowering blood pressure via intravenous injection in anesthetized spontaneously hypertensive rats.^{5.2[5]} Isosteviol (ent-16-oxobeyeran-19-oic acid, **5.2(1)**), a tetracyclic diterpenoid obtained by acid hydrolysis of stevioside, has been reported as exhibiting pharmacological activity. Isosteviol attenuates myocardial damage induced by ischemia-reperfusion in isolated perfused guinea pig heart, ^{5.2[6]} rat heart in vivo, ^{5.2[7]} and rat brain in vivo. ^{5.2[8]} Moreover, isosteviol also shows the vasorelaxant effect via opening the K⁺ channels in rat aorta.^{5.2[9]} Recently, the chemical modification of isosteviol was performed by sodium borohydride reduction of isosteviol, followed by acetylation to give 16-O-acetyldihydroisosteviol (ADIS, 5.2(3)) (Figure 5.2(1)). The vasorelaxant effect in rat aortic rings was found to be greater in the case of ADIS than in the case of isosteviol about 12-fold. ^{5.2[10]} This is of special interest as far as evaluating the mechanism of ADIS on the vasorelaxant effect is concerned. Thus, the purpose of this study is to investigate the mechanism of ADIS as regards vasorelaxant activity, as it would be beneficial in evaluating natural products, which may be considered as an alternative modality for hypertensive patients. This work has been done in collaboration with Assistant Professor Dr. Chainarong Tocharus, Chiang Mai University and was supported by the Higher Education Research Promotion (HERP) Program, Office of the Higher Education Commission and supported in part by The Thailand Research Fund.

The vasorelaxant effects of ADIS were investigated by means of isometric tension recording experiment. It was found that ADIS (0.1 μ M–3 mM) induced relaxation of aortic rings pre-contracted by phenylephrine (PE, 10 μ M) and KCl (80 mM) with intact-endothelium ($E_{max} = 79.26\pm3.74$ and 79.88 ± 3.79 , respectively) or denuded-endothelium ($E_{max} = 88.05\pm.3.69$ and 78.22 ± 6.86 , respectively). In depolarization Ca^{2+} -free solution, ADIS inhibits $CaCl_2$ -induced contraction in endothelium-denuded rings in a concentration-dependent manner. In addition, ADIS attenuates transient contractions in Ca^{2+} -free medium containing EGTA (1 mM) induced by PE (10 μ M) and caffeine (20 mM). By contrast, relaxation was not affected by tetraethylammonium (TEA, 5 mM), 4-aminopyridine (4-AP, 1 mM),

glibenclamide (10 μ M), barium chloride (BaCl₂, 1 mM), and 1H-[1,2,3]oxadiazolo[4,3- α]quinoxalin-1-one (ODQ, 1 μ M). These findings reveal the vasorelaxant effect of ADIS, through endothelium-independent pathway. It acts as a Ca²⁺ channel blocker through both intracellular and extracellular Ca²⁺ release.

Figure 5.2(1) Preparation of 16-*O*-acetyldihydroisosteviol (ADIS, **5.2(3)**) from isosteviol (**5.2(1)**)

The detail of this study is in the following published work.

Output. This project has led to the following publication:

Pantan, R., Onsa-ard, A., Tocharus, J., Wonganan, O., Suksamrarn, A., Tocharus, C., 2014. Endothelium-independent vasorelaxation effects of 16-*O*-acetyldihydroisosteviol on isolated rat thoracic aorta. *Life Sci.* 116, 31-36.

References

- 5.2[1] Geuns, J. M. C., 2003. Stevioside. *Phytochemistry* 64, 913-921.
- 5.2[2] Chatsudthipong, V., Muanprasat, C., 2009. Stevioside and related compounds: Therapeutic benefits beyond sweetness. *Pharmacol. Therapeut.* 121, 41-54.
- 5.2[3] Goyal, S. K., Samsher, Goyal, R.K., 2010. Stevia (*Stevia rebaudiana*) a biosweetener: a review. *Int. J. Food Sci. Nutri.* 61, 1-10.
- 5.2[4] Melis, M. S., 1992. Influence of calcium on the blood pressure and renal effects of stevioside. *Braz. J. Med. Biol. Res.* 25, 943-949.

- Chan, P., Xu, D. Y., Liu, J. C., Chen, Y. J., Tomlinson, B., Huang, W. P., Cheng, J. T., 1998. The effect of stevioside on blood pressure and plasma catecholamines in spontaneously hypertensive rats. *Life Sci.* 63, 1679-1684.
- 5.2[6] Xu, D., Li, Y., Wang, J., Davey, A. K., Zhang, S., Evans, A. M., 2007. The cardioprotective effect of isosteviol on rats with heart ischemia-reperfusion injury. *Life Sci.* 80, 269-274.
- 5.2[7] Xu, D., Zhang, S., Foster, D., Wang, J., 2007. The effects of isosteviol against myocardium injury induced by ischaemia-reperfusion in the isolated guinea pig heart. *Clin. Exp. Pharmacol. Physiol.* 34, 488-493.
- 5.2[8] Xu, D., Du, W., Zhao, L., Davey, A. K., Wang, J., 2008. The neuroprotective effects of isosteviol against focal cerebral ischemia injury induced by middle cerebral artery occlusion in rats. *Planta Med.* 74, 816-821.
- 5.2[9] Wong, K.-L., Chan, P., Yang, H.-Y., Hsu, F.-L., Liu, I. M., Cheng, Y.-W., Cheng, J.-T., 2004. Isosteviol acts on potassium channels to relax isolated aortic strips of Wistar rat. *Life Sci.* 74, 2379-2387.
- 5.2[10] Wonganan, O., Tocharus, C., Puedsing, C., Homvisasevongsa, S., Sukcharoen, O., Suksamrarn, A., 2013. Potent vasorelaxant analogs from chemical modification and biotransformation of isosteviol. *Eur. J. Med. Chem.* 62, 771-776.

Project 5.3 Protective Effect of a Curcuminoid Analogue against Amyloid Beta-Induced Apoptosis in Neuronal Cells

Alzheimer's disease (AD) is a progressive neurodegenerative disease of the central nervous system (CNS), generally affecting the elderly. AD is one of the most common forms of dementia, which is determined clinically by diagnosing for multiple cognitive deficits including memory loss, emotional disturbance, etc.^{5.3[1]} The distinctive appearance of pathological AD are amyloid plaques and neurofibrillary tangles (NFT)^{5.3[2,3]} that cause loss of neurons and synapses in the brain. Amyloid β (A β) is derived from the proteolytic cleavage of the amyloid precursor protein (APP) by β - and γ -secretase enzymes, and accumulate in the extracellular neuronal cells.^{5.3[4]} NFT is accumulated within the neurons as a result of abnormal phosphorylation of the microtubules-associated tau-protein. Recent studies suggest that A β accumulation has been causatively implicated in the neuronal dysfunction and

neuronal loss that underlie the clinical manifestations of AD.^{5,3[5]} Furthermore, several lines of research have suggested that Aβ exerts neuronal toxicity through the production of reactive oxygen species (ROS), ^{5.3[6]} which leads to neuronal apoptosis ^{5.3[7]} due to the involvement of the mitochondrial death pathway and the endoplasmic reticulum (ER) stress.^{5,38]} ER is an intracellular organelle related to protein folding, intracellular calcium homeostasis, lipid synthesis, steroids and cholesterol. Cellular conditions in ER, such as depletion of calcium, alter glycosylation, and the oxidative stress leads to unfolded protein. Unfolded protein accumulation in ER lumen is termed as ER stress; 5.3[9] this accumulation activates unfolded protein response (UPR), thereby signaling responses for ER homeostasis by decreasing protein synthesis, and increasing chaperone and degradation. ^{5.3[10]} However, prolonged ER stress is associated with apoptotic cell death, 5.3[11] which is caused by activating three signal transducers that are protein kinase RNA like endoplasmic reticulum kinase (PERK), activating transcription factor (ATF6) and inositol-requiring enzyme 1 (IRE1); then, upregulates the expression of the C/EBP homologous protein (CHOP), ^{5.3[12]} caspase-12 protein, ^{5.3[9]} and glucose related protein 78 (Grp78). ^{5.3[13]} Moreover, apoptosis mainly involves excessive ROS-induced mitochondrial dysfunction upon the increase in the permeability of mitochondria membrane.^{5.3[14]} These results in the inducing of proapoptotic protein such as Bax translocate from the cytoplasm to the mitochondria membrane and a decrease in the antiapoptotic proteins (Bcl-2, Bcl-XL). Thereafter, cytochrome c gets released to the cytoplasm and combines with apoptotic protease activating factor 1 (APAF-1) and procaspase-9 to become the active form of caspase-9 protein which stimulates the caspase-3 protein, and this leads to cell death. ^{5.3[15]} Evidences, therefore, suggest that suppression of Aβ-mediated neuronal apoptosis would be a target to attenuate progressive neuronal damages and provide a strategy for the given approach to the development and treatment of AD.

Curcumin is the major constituent of curcuminoids isolated from turmeric (*Curcuma longa* L.), with demethoxycurcumin and bisdemethoxycurcumin being the minor constituents. Previous studies have shown that curcumin has a wide range of beneficial properties, including antioxidant activity, anti-inflammatory, anticancer, neuroprotective, and antiviral activities. ^{5.3[16-20]} Structural modifications of curcuminoids to analogues that exhibit higher physiological activities and pharmacological activities than the parent curcumininoids have been reported by our group. ^{5.3[21,22]} Recently, we reported our research finding that di-*O*-

demethylcurcumin (5.3(1)), a chemically modified demethylated analogue of curcumin obtained from the rhizomes of *Curcuma longa*, showed a potent anti-inflammatory activity greater than that of the parent curcumin.^{5.3[23]} However, it remains unclear whether compound 5.3(1)) exerts neuroprotection against A β -induced neuronal damage. Considering the important role of A β in the pathogenesis of AD, elucidation of the effects of 5.3(1)) against A β -induced toxicity may provide a new insight into its potential application to the prevention or treatment of AD. It is, therefore, of interest to investigate whether 5.3(1)) would protect against A β -induced cytotoxicity in SK-N-SH cells. This work has been done in collaboration with Assistant Professor Dr. Jiraporn Tocharus, Department of Physiology, Faculty of Medicine, Chiang Mai University.

We have investigated the mechanisms and effects of di-O-demethylcurcumin (5.3(1)), a demethylated analogue of curcumin obtained from the rhizomes of Curcuma longa, in preventing Aβ-induced apoptosis. Pretreatment with di-O-demethylcurcumin, followed by Aβ25-35 (10 μM) in human neuroblastoma SK-N-SH cells improved cell viability by using MTS assay and decreased neuronal cell apoptosis. Pretreatment with compound 5.3(1) attenuated the number of nuclear condensations and number of apoptotic cells in Aβ25-35induced group in a concentration-dependent manner by using transmission electron microscope (TEM) and flow cytometry, respectively. Compound 5.3(1) also increased the ratio of Bcl-XL/Bax protein, and reduced intracellular ROS level, cytochrome c protein expression, cleaved caspase-9 protein expression, and cleaved caspase-3 protein expression. Additionally, compound 5.3(1) treatment also reduced the expression of ER stress protein markers, including protein kinase RNA like endoplasmic reticulum kinase (PERK) phosphorylation, eukaryotic translation initiation factor 2 alpha (eIF2 α) phosphorylation, inositol-requiring enzyme 1 (IRE1) phosphorylation, X-box-binding protein-1 (XBP-1), activating transcription factor (ATF6), C/EBP homologous protein (CHOP), and cleaved caspase-12 protein. CHOP and cleaved caspase-12 protein are the key mediators of apoptosis.

Our data suggest that compound **5.3(1)** is a candidate protectant against neuronal death through its suppression of the apoptosis mediated by mitochondrial death and ER stress pathway. Details of the work can be seen in the published paper.

Output. This project has led to the following publication:

Pinkaew, D., Changtam, C., Tocharus, C., Thummayot, S., Suksamrarn, A., Tocharus, J., 2015. Di-*O*-demethylcurcumin protects SK-N-SH cells against mitochondrial and endoplasmic reticulum-mediated apoptosis cell death induced by Ab25-35. *Neurochem. Int.* 80, 110-119.

References

- 5.3[1] Hauptmann, S., Keil, U., Scherping, I., Bonert, A., Eckert, A., Muller, W.E., 2006. Mitochondrial dysfunction in sporadic and genetic Alzheimer's disease. *Exp. Gerontol.* 41, 668–673.
- 5.3[2] Hardy, J., Selkoe, D.J., 2002. The amyloid hypothesis of Alzheimer's disease: progress and problems on the road to therapeutics. *Science* 297, 353–356.
- 5.3[3] Selkoe, D.J., 2001. Alzheimer's disease: genes, proteins, and therapy. Physiol. Rev. 81, 741–766.
- 5.3[4] Sisodia, S.S., Annaert, W., Kim, S.H., De Strooper, B., 2001. Gamma-secretase: never more enigmatic. *Trends Neurosci.* 11, 2–6.
- 5.3[5] Dante, S., Hauss, T., Dencher, N.A., 2003. Insertion of externally administered amyloid beta peptide 25-35 and perturbation of lipid bilayers. *Biochemistry* 42, 13667–13672.
- 5.3[6] Butterfield, D.A., Reed, T., Newman, S.F., Sultana, R., 2007. Roles of amyloid betapeptide-associated oxidative stress and brain protein modifications in the pathogenesis of Alzheimer's disease and mild cognitive impairment. *Free Radic. Biol. Med.* 43, 658–677.
- 5.3[7] Ramalingam, M., Kim, S.J., 2012. Reactive oxygen/nitrogen species and their functional correlations in neurodegenerative diseases. *J. Neural Transm.* 119, 891–910.

- 5.3[8] Takuma, K., Yan, S.S., Stern, D.M., Yamada, K., 2005. Mitochondrial dysfunction, endoplasmic reticulum stress, and apoptosis in Alzheimer's disease. *J. Pharmacol. Sci.* 97, 312–316.
- 5.3[9] Nakagawa, T., Zhu, H., Morishima, N., Li, E., Xu, J., Yankner, B.A., et al., 2000. Caspase-12 mediates endoplasmic-reticulum-specific apoptosis and cytotoxicity by amyloidbeta. *Nature* 403, 98–103.
- 5.3[10] Vembar, S.S., Brodsky, J.L., 2008. One step at a time: endoplasmic reticulum-associated degradation. *Nat. Rev. Mol. Cell Biol.* 9, 944–957.
- 5.3[11] Boyce, M., Yuan, J., 2006. Cellular response to endoplasmic reticulum stress: a matter of life or death. *Cell Death Differ*. 13, 363–373.
- 5.3[12] Chen, C.M., Wu, C.T., Chiang, C.K., Liao, B.W., Liu, S.H., 2012. C/EBP homologous protein (CHOP) deficiency aggravates hippocampal cell apoptosis and impairs memory performance. *PLoS ONE* 7, e40801.
- 5.3[13] Kim, I., Xu,W., Reed, J.C., 2008. Cell death and endoplasmic reticulum stress: disease relevance and therapeutic opportunities. *Nat. Rev. Drug Discov.* 7, 1013–1030.
- 5.3[14] Chen, J.X., Yan, S.D., 2007. Amyloid-beta-induced mitochondrial dysfunction. *J. Alzheimers Dis.* 12, 177–184.
- 5.3[15] Slee, E.A., Harte, M.T., Kluck, R.M., Wolf, B.B., Casiano, C.A., Newmeyer, D.D., et al., 1999. Ordering the cytochrome c-initiated caspase cascade: hierarchical activation of caspases-2, -3, -6, -7, -8, and -10 in a caspase-9-dependent manner. *J. Cell Biol.* 144, 281–292.
- 5.3[16] Bandgar, B.P., Kinkar, S.N., Chavan, H.V., Jalde, S.S., Shaikh, R.U., Gacche, R.N., 2014. Synthesis and biological evaluation of asymmetric indole curcumin analogs as potential anti-inflammatory and antioxidant agents. *J. Enzyme Inhib. Med. Chem.* 29, 7–11.
- 5.3[17] Belviranli, M., Okudan, N., Atalik, K.E., Oz, M., 2013. Curcumin improves spatial memory and decreases oxidative damage in aged female rats. Biogerontology 14, 187–196.

- 5.3[18] Bhullar, K.S., Jha, A., Youssef, D., Rupasinghe, H.P., 2013. Curcumin and its carbocyclic analogs: structure-activity in relation to antioxidant and selected biological properties. *Molecules* 18, 5389–5404.
- 5.3[19] Morsy, M.A., El-Moselhy, M.A., 2013. Mechanisms of the protective effects of curcumin against indomethacin-induced gastric ulcer in rats. *Pharmacology* 91, 267–274.
- 5.3[20] Rath, K.S., McCann, G.A., Cohn, D.E., Rivera, B.K., Kuppusamy, P., Selvendiran, K., 2013. Safe and targeted anticancer therapy for ovarian cancer using a novel class of curcumin analogs. *J. Ovarian Res.* 11, 35–47.
- 5.3[21] Changtam, C., de Koning, H.P., Ibrahim, H., Sajid, M.S., Gould, M.K., Suksamrarn, A., 2010. Curcuminoid analogs with potent activity against Trypanosoma and Leishmania species. *Eur. J. Med. Chem.* 45, 941–956.
- 5.3[22] Aroonrerk, N., Changtam, C., Kirtikara, K., Suksamrarn, A., 2012. Inhibitory effects of di-*O*-demethylcurcumin on interleukin-1B-induced interleukin-6 production from human gingival fibroblasts. *J. Dent. Sci.* 7, 350–358.
- 5.3[23] Tocharus, J., Jamsuwan, S., Tocharus, C., Changtam, C., Suksamrarn, A., 2012. Curcuminoid analogs inhibit nitric oxide production from LPS-activated microglial cells. *J. Nat. Med.* 66, 400–405.

Project 5.4 *O*-Demethyldemethoxycurcumin Exerts Suppression Effects on Thapsigargin Triggered on Endoplasmic Reticulum Stress in SK-N-SH Cells

Neurodegenerative diseases, such as Alzheimer's disease (AD), Parkinson's disease (PD) and Huntington's disease (HD), account for a significant and increasing proportion of morbidity and mortality worldwide. Several lines of evidence suggest that endoplasmic reticulum (ER) stress plays a critical role in the development or pathology of many neuro-degenerative diseases. These diseases share a common pathogenetic mechanism the aggregation and deposition of unfolded proteins that leads to progressive central nervous system (CNS) degeneration. The ER is a main organelle that regulates protein folding and calcium signaling. When the ER is disturbed, unfolded proteins accumulate in the ER lumen and Ca²⁺ is released from the ER to the cytoplasm, leading to ER stress on the cells. Several stimuli interference with N-linked protein glycosylation, viral infection and depletion

of Ca²⁺ in the ER, lead to an accumulation of unfolded proteins in the ER that triggers the unfolded protein response (UPR).^{5,4[7]} The UPR is mediated through ER transmembrane receptors, including double-stranded RNA-activated protein kinase (PKR), the PKR-like ER kinase (PERK), inositol-requiring protein-1 (IRE1) and activating transcription factor 6 (ATF6). Excessive and prolonged stresses ultimately lead to apoptosis by inducing expression of the C/EBP homologous protein (CHOP), a Bcl-2 inhibitor.^{5,4[8-11)} In addition, previous studies suggested that ER stress is involved with many neurodegenerative diseases. Therefore, interventions that attenuate ER stress may contribute to reduced apoptosis ^{5,4[12]}

Curcumin is a major chemical component of curcuminoids, which is isolated from turmeric (Curcuma longa L) and the details are summarized in Project 5.3. Our study reported that the analogs of curcumin exhibited higher physiological and pharmacological activities than the parent curcumin itself by inhibiting nitric oxide and proinflammatory cytokines production. Among them, O-demethyldemethoxycurcumin was a more potent anti-inflammatory than its parent compounds (Tocharus et al., 2012).^{5.4[13]} It is therefore of interest to investigate whether chemical modification of the curcuminoids would improve their neuroprotective property. In this study, we evaluated whether O-demethyldemethoxycurcumin (5.4(1)), the demethylated analog of the natural demethoxycurcumin, protects SK-N-SH cells from thapsigargin-induced cell death mediated by ER stress. Using this model, we determined the effects of Odemethyldemethoxycurcuminon expression of proteins involved in ER stress-induced cell death. The results showed that O-demethyldemethoxycurcumin improved SK-N-SH cell viability by decreasing the apoptotic cell death induced by thapsigargin. Consistent with these findings, O-demethyldemethoxycurcumin inhibited the thapsigargin-induced activation of cleavage caspase-12. Moreover, O-demethyldemethoxycurcumin attenuated the intracellular Ca²⁺ level and the expression of the calpain protein. *O*-demethyldemethoxycurcumin also downregulated the expression of ER stress signaling proteins, including the phosphorylation of PKR-like endoplasmic reticulum kinase (p-PERK), the phosphorylation of inositol-requiring enzyme 1(p-IRE1), activating transcription factor 6 (ATF6), binding immunoglobulin protein (BiP)and C/EBP homologous protein (CHOP). Our findings suggest that Odemethyldemethoxycurcumin could protect against thapsigargin-induced ER stress in SK-N-SH cells. Therefore, O-demethyldemethoxycurcumin offers potential as an alternative

therapeutic agent for protection against neurodegenerative diseases. Details of the work can be seen in the published paper.

Output. This project has led to the following publication:

Janyou, A., Changtam, C., Suksamrarn, A., Tocharus, C., Tocharus, C., 2015. Suppression effects of *O*-demethyldemethoxycurcumin on thapsigargin triggered on endoplasmic reticulum stress in SK-N-SH cells. *Neurotoxicol.* 50, 92-100.

References

- 5.4[1] Emerit, J., Edeas, M.. Bricaire, F., 2004. Neurodegenerative diseases and oxidative stress. *Biomed. Pharmacother.* 58, 39-46.
- 5.4[2] Brown, M.K., Naidoo, N.. 2012. The endoplasmic reticulum stress response in aging and age-related diseases. *Front. Physiol.* 3, 3389-3399.
- 5.4[3] Hugo, V., Hetz, C.. 2013. The unfolded protein response in Alzheimer's disease. Semin. Immunopathol. 35, 277-292.
- 5.4[4] Halliday, M., Mallucci, G.R., 2014. Targeting the unfolded protein response in neurodegeneration: a new approach to therapy. *Neuropharm.* 76, 169-174.
- 5.4[5] Hamman, B.D., Hendershot, L.M., 1998. Bip maintains the permeability barrier of the ER membrane by sealing the luminal end of the translocon pore before and early in translocation. *Cell* 92, 747-758.
- 5.4[6] Kleizen, B., Braakman, I., 2004. Protein folding and quality control in endoplasmic reticulum. *Cell Biol.* 16, 343-349.
- 5.4[7] Bernales, S., Soto M.M., McCullagh, E., 2012. Unfolded protein stress in the endoplasmic reticulum and mitochondria: a role in neurodegeneration. Front. Aging Neurosci. 4.1-13.
- 5.4[8] Harding, H.P., Zhang, Y., Zeng, H., Novoa, I., Lu, P.D., Calfon, M., Sadri, N., Yun, C., Popko, B., Paules, R., Stojdl, D.F., Bell, J.C., Hettmann, T., Leiden, J.M., Ron,

- D., 2003. An integrated stress response regulates amino acid metabolism and resistance to oxidative stress. *Mol. Cell.* 11, 619-633.
- 5.4[9] Xu, C., Maitre, B.B., Reed, J.C., 2005. Endoplasmic reticulum stress: cell life and death decisions. *J. Clin. Invest.* 115, 2656-2664.
- 5.4[10] Hetz, C., Bernasconi, P., Fisher, J., Lee, A.-H., Bassik, M.C., Antonsson, B., Brandt, G.S., Iwakoshi, N.N., Schinzel, A., Glimcher, L.H., Korsmeyer, S.J., 2006. Proapoptotic BAX and BAK modulate the unfolded protein response by a direct interaction with IRE1α. Science 312, 572-576.
- 5.4[11] Lai, E., Teodoro, T., Volchuk, A., 2007. Endoplasmic reticulum stress: signaling the unfolded protein response. *Physiol.* 22, 193-201.
- 5.4[12] Nagai, K., 2012. Bovine milk phospholipid fraction protects Neuro2a cells from endoplasmic reticulum stress via PKC activation and autophagy. *J. Biosci. Bioeng.* 114, 466-471.
- 5.4[13] Tocharus, J., Jamsuwan, S., Tocharus, C., Changtam, C., Suksamrarn, A., 2012. Curcuminoid analogs inhibit nitric oxide production from LPS-activated microglial cells. J. Nat. Med. 66, 400-405.

Project 6. Design and Synthesis of Delivery System for Cytotoxic and Other Bioactive Natural Products and Analogues to Targeted Cells

The work under this project includes: (1) Selection of lead compound with high cytotoxic activity for further study. Bioactive compound will be selected based on the SAR study, its biological activity, chemical structure and functional groups present in the molecule. (2) Design of delivery system for the selected lead compound. A number of drug delivery systems will be designed and used for each selected lead compound. Examples of the design of delivery system include the drug targeting to hypoxic tissue using self-inactivating bioreductive delivery system, tumor-homing cell-penetrating peptide and cationic lyposome for the delivery of drug. (3) Design of prodrug system for the delivery of drug at selected site. (4) Synthesis of the conjugate part of the lead compound and construction of delivery system for the lead compound. (5) Evaluation of cytotoxicity of the conjugated system and comparison of cytotoxicity of the lead compound with that of the conjugated system. Evaluation of toxicity to the normal cell (e.g. Vero cell) of the lead compound with that of the

conjugated system. (6) Evaluation of the efficiency of delivery of the lead compound to the targeted cancer cell. In order to facilitate and complement our drug discovery work, design of delivery system for lead compound and development of the carriers to protect and deliver of drugs into targeted cells will also be undertaken.

Project 6.1 Development of Cationic Lipids with Different Polarheads, Central Core Structures and Hydrophobic Tails

Many efforts are focus on developing carriers to protect and deliver drugs and genetic materials into targeted cells. Two delivery systems namely viral and non-viral vectors are currently developed to solve the problems. However, the limitation of viral vectors concerning toxicity, immunogenicity, scale-up procedures and their relatively small capacity for therapeutic DNA has prompted the development non-viral vectors. Delivery systems based on non-viral vectors, for example cationic lipids, dendrimers or cationic polymers, have been the focus of recent research. 6.1[1] Non-viral systems have proved to be generally less toxic or immunogenic, more easily to produce and a greater stability. Cationic liposomes are one of the most extensively studied of non-viral vectors because of their lesser immunogenic nature, ease of production and handle, and ability to deliver large pieces of DNA. Cationic liposomes, like other non-viral vectors bearing positive charge, interact with the negatively charged phosphate backbone of nucleic acids to form a compact structure and facilitate cellular uptake by endocytic routes. 6.1[2-5] Since the first application of cationic lipid in DNA delivery, 6.1[6] numerous cationic lipids have been synthesized and demonstrated the capability of delivering genetic materials into various cells. ^{6.1[1]} Some of cationic liposomes-mediated gene transfers have been used in gene therapy clinical trials. ^{6.1[7]} However, significant limitations of cationic liposomes are low transfection efficiency and much research activity has been focused on increase efficiency. The main approach to improving the transfection properties was to synthesize new kinds of cationic lipids. The alternative strategy, apart from employing the helper lipids such as DOPE or cholesterol, to improve tansfection efficiency is the use of mixture cationic lipids. Previous studies have shown that the use of a mixture of cationic lipids with the same head group but with different chain lengths dramatically enhances the transfection of human umbilical artery endothelial cells (HUAEC). The synergistic effect was not only limited to the homologous, but it also exhibited to cationic lipids with different polarhead and hydrophobic tails. ^{6.1[9]} Mixture of multi-components to form lipoplexes has also been reported. Asymmetric vesicles formulated with lipids having very different headgroups have been prepared. This vesicle is expected to be a delivery system with increase in biocompatibility and flexibility. ^{6.1[11]} Recently, we described the cationic lipids **6.1(1)** ^{6.1[12]} and **6.1(2)** ^{6.1[13,14]} (Figure 6.1(1)) which exhibited transfection efficiency higher than and comparable to the commercially available transfection reagents. These lipids contain different polarheads, central core structure, and hydrophobic tails; **6.1(1)** comprise of the commonly used template, aminoglycerol, primary amino headgroup and dodecanoyl tails whereas **6.1(2)** has di(hydroxyethyl)amino core structure, polyamine polarhead and myristoyl tails. Therefore, to investigate how transfection changes with the liposome comprised of cationic lipids with different polarheads, central core structures and hydrophobic tails, cationic liposome consisting of **6.1(1)** and **6.1(2)** was prepared and tested for transfection efficiency in mammalian cells. The size and zeta potential of the prepared liposome were also evaluated.

$$H_2N \sim \prod_{1}^{N} \prod_{1}^{N} \bigcap_{0}^{N} \bigcap_{0}^{$$

Figure 6.1(1) Structures of cationic lipids 6.1(1) and 6.1(2)

Synthesis of Cationic Lipids 6.1(1) and 6.1(2) Combinatorial synthesis provides a library of bioactive compounds to discover the lead. Lipid **6.1(1)**, which was one of the lead components found from a 60-compound library, $^{6.1[12]}$ exhibited higher transfection efficiency than the commercially available transfection agent, Effecene TM. To obtain this compound in high purity and quantity, the lipid **6.1(1)** was synthesized by a conventional method (Scheme 6.1(1)). The synthesis was started by the preparation of N-(tert-butoxycarbonyl)-1,2-diaminoethane (**6.1(4)**) by high dilution method. The reaction of **6.1(4)** with 4-nitrophenyl chloroformate followed by treatment with (\pm)-3-amino-1,2-propanediol afforded diol **6.1(5)** in 53% yield over three steps. The diol **6.1(5)** was then esterified with dodecanoic

acid using DCC as coupling agent to provide compound **6.1(6)** in 82% yield. Removal of the Boc-protecting group by the standard method yielded the lipid **6.1(1)** in quantitative yield.

Scheme 6.1(1) Synthesis of cationic lipid **6.1(1)**. Reagents and conditions: *a*) Di-*tert*-butyl dicarbonate, DCM, 24 h; *b*) 4-nitrophenyl chloroformate, pyridine, CH_2Cl_2 , 8 h; *c*) (\pm)-3-amino-1,2-propanediol, CH_2Cl_2 :MeOH (1:1), 12 h; *d*) dodecanoic acid , DCC, DMAP, CH_2Cl_2 , 16 h; *e*) 20% TFA/ CH_2Cl_2 , 1 h.

The lipid **6.1(2)** which consisted of spermine polarhead was synthesized by solid phase chemistry (Scheme 6.1(2)). The protected spermine having one free primary amino group was prepared using the modified literature method. Firstly, the active carbonate Wang resin **6.1(7)** was reacted with an excess of spermine to give the resin **6.1(8)**. The primary amino group was selectively protected over the presence of secondary amine with 2-acetyldimedone (Dde-OH). This reaction is highly selective most likely due to the stabilization provided by a strong intramolecular H-bond. The remaining secondary amines were then protected with *tert*-butyloxycarbonyl (Boc) groups and the Dde protecting group was selectively removed under mild condition with 2% hydrazine hydrate in DMF to obtain the resin **6.1(9)**. The liberated amine was converted to the desired di(hydroxyethyl)amino by treating the resin **6.1(9)** with excess 2-bromoethanol in the presence of DIPEA to generate the diol resin **6.1(10)**. The assembly of the lipid was accomplished by reacting the alcohols with myristic acid using DIC as coupling agent in the presence of DMAP as a catalyst. The final product was cleaved from the resin by treatment with 20% TFA in CH₂Cl₂. The filtrate was collected and concentrated *in vacuo*; the resulting lipid was further purified by Sephadex LH20 column

chromatography. The structures of the synthesized cationic lipids were confirmed by spectroscopic means (IR, NMR and HRMS).

Scheme 6.1(2) Synthesis of cationic lipid **6.1(2)**. Reagents and conditions: *a*) spermine, DMF:CH₂Cl₂ (1:1), 16 h; *b*) Dde-OH, CH₂Cl₂, 16 h; *c*) di-*tert*-butyl dicarbonate, pyridine, CH₂Cl₂, 16 h; *d*) 5% hydrazine /DMF, 1 h; *e*) bromoethanol, DIPEA, DMF, 16 h; *f*) myristic acid, DIC, DMAP, CH₂Cl₂, 16 h; *g*) 20% TFA/CH₂Cl₂, 2 h.

Characterization of the Cationic Liposomes/DNA Complexes The lipoplex formation between the cationic liposome preparing from single lipid and mixture lipids was analyzed by varying the lipid/DNA weight ratio using agarose gel retardation assays (Figure 6.1(2)). The results from the agarose gel electrophoresis illustrated that cationic liposomes were able to

form lipoplexes. Excess DNA was barely detectable using lipid-to-DNA ratio of 5 in all of the cationic assemblies. The results indicated that liposome in the presence of lipids **6.1(1)** and **6.1(2)** did not change the DNA binding property to form the lipoplexes.

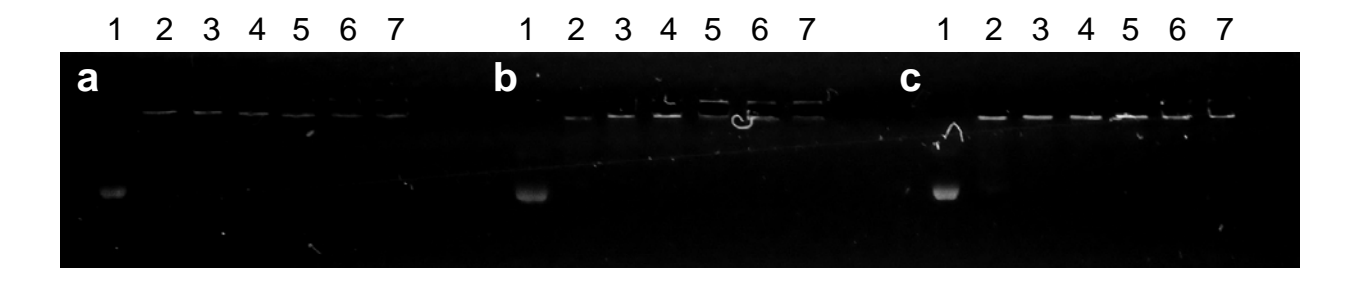
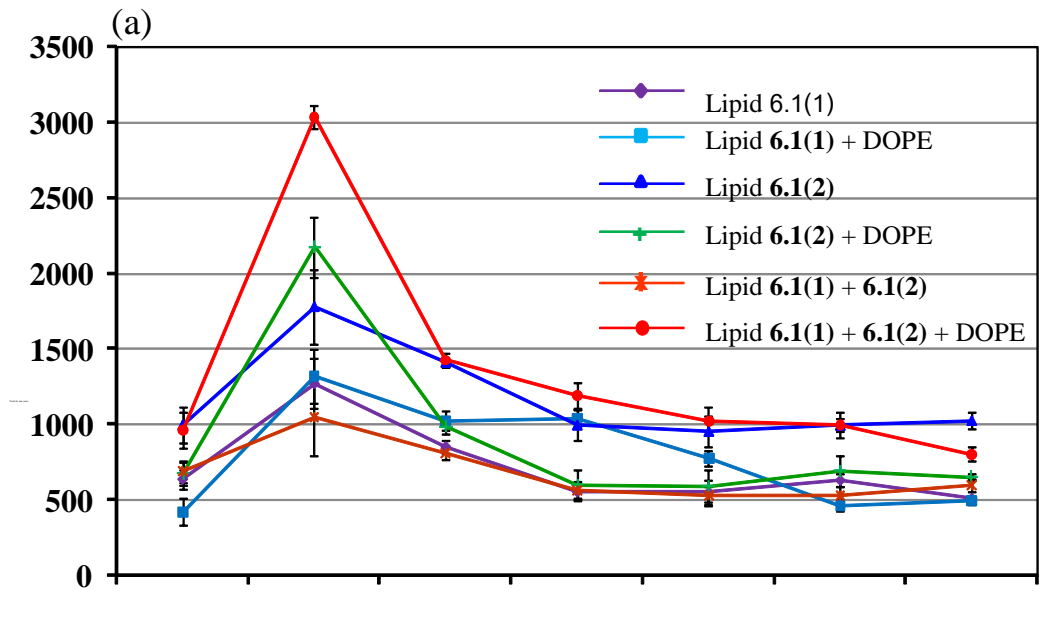


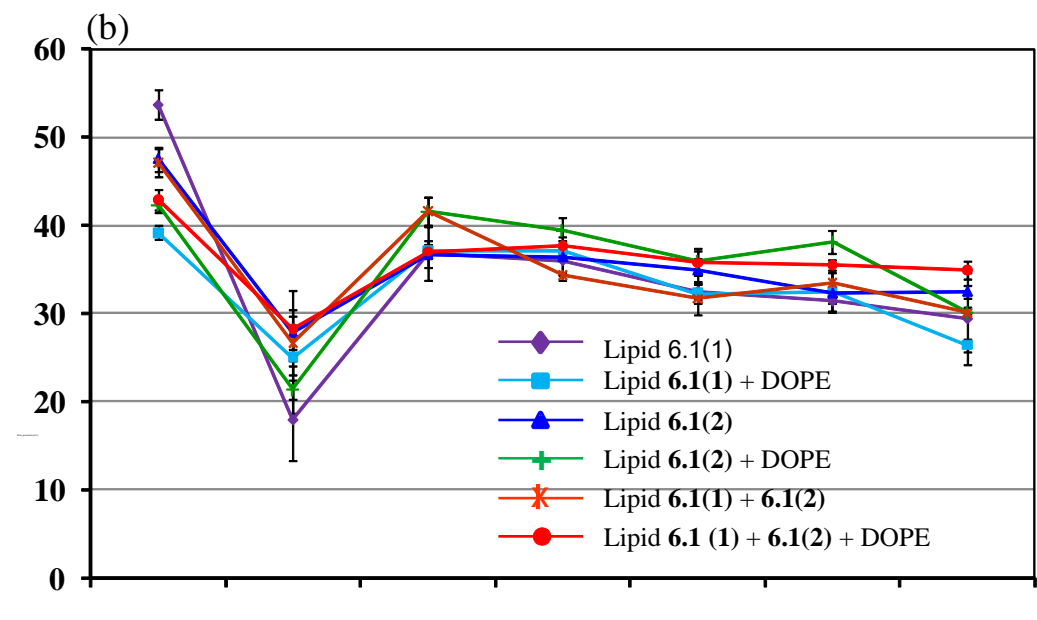
Figure 6.1(2) Gel retardation assay of liposomes/DNA complexes. Lane 1, DNA (pCMV-encoding β -galactosidase); lanes 2–7, liposomes /DNA complexes at weight ratios of 5, 10, 15, 20, 25 and 30 for a) liposomes-lipid **6.1(1)**, b) liposomes-lipid **6.1(2)**, and c) liposomes-lipids **6.1(1)**+ **6.1(2)** at weight ratio of 1:1.

Further investigations of the particle size and zeta potentials of the liposomes and liposomes/DNA complexes were performed across the entire weight ratios of 2 to 40. As shown in Figure 6.1(3)a, the particle size of the liposome **6.1(1)** (636±67 nm) was smaller than that of liposome 2 (997±120 nm). The particle sizes of these liposomes consisting of DOPE were smaller than those without DOPE. However, the mixture of lipids 6.1(1), 6.1(2) and DOPE formed larger liposome (1428±46 nm) than that of the mixture of lipids 6.1(1) and **6.1(2)** alone (810±46 nm). The particle size of the formed lipoplexes with the cationic liposomes/DNA weight ratio varied from 2 to 40 was studied. It was found that most of the liposomes could bind and compact DNA into particles of cationic liposomes/DNA at the weight ratio of 5. The mean diameters of 6.1(1)/DNA, 6.1(1)-DOPE/DNA, 6.1(2)-DOPE/DNA and 6.1(1)-6.1(2)/DNA lipoplexes were 500-600 nm, whereas the diameters of **6.1(2)**/DNA and **6.1(1)**- **6.1(2)**-DOPE/DNA lipoplexes were 800-1000 nm. The zeta potential, which is a measure of the electrical field of cationic liposomes in an aqueous environment, is one of the important factors that controls their DNA binding ability. High zeta potential is preferred for higher DNA binding ability. From Figure 6.1(3)b, it was found that the liposomes of the lipids 6.1(1) and 6.1(2) have a zeta potential of 53.7 ± 1.7 and 47.5 ± 1.4 mV,

respectively. The inclusion of DOPE as the helper lipid in the lipids **6.1(1)** and **6.1(2)** leads to an decrease in the zeta potential which is observed to be 39.2±0.8 and 43.3±0.8 mV, respectively. The zeta potential of the liposomes prepared by the mixture of lipids **6.1(1)** and **6.1(2)** was 47.1±1.6 mV. Addition of DOPE in the mixture of the lipids **6.1(1)** and **6.1(2)**, the zeta potential (42.9±1.1 mV) was not much decreased. As shown in Figure 6.1(3)b, the zeta potential was slightly decreased along with the increase in cationic liposome/DNA weight ratio. Most of the cell membranes usually show negative charge, so it is expected that the high positively charged liposomes formulated by the mixture lipids **6.1(1)** and **6.1(2)** alone or with the combination of DOPE will significantly enhance the interaction between liposomes and cells and facilitate cellular uptake.



Cationic liposome/DNA weight ratio



Cationic liposome/DNA weight ratio

Figure 6.1(3) (a) Particle size and (b) zeta potential at varying weight ratios of liposomes/DNA complexes; (\clubsuit) liposomes-lipid **6.1(1)**, (\blacksquare) liposomes-lipid **6.1(1)**+DOPE (1:1), (\blacktriangle) liposomes-lipid **6.1(2)**, (+) liposomes-lipid **6.1(2)**+DOPE (1:1), (*) liposomes-lipids **6.1(1)**+**6.1(2)** (1:1), and (\clubsuit) liposomes-lipids **6.1(1)**+**6.1(2)**+DOPE (0.5:0.5:1). Each value represents the mean \pm S.D. of three measurements.

Transfection Activity Most of the cationic lipid carriers studied so far are liposomes composed of cationic lipid alone or a mixture of cationic lipid and a helper lipid, which was usually DOPE, ^{6.1[19]} DOPC^{6.1[20]} or cholesterol. ^{6.1[21]} The alternative approach can be the use of combination of cationic lipids having the same headgroup but with tails of different chain lengths^{6.1[8]} or cationic lipids with different polarhead and hydrophobic tails.^{6.1[9]} To study the synergistic effect of cationic lipids with different polarheads, central core structures and hydrophobic tails, the lipids 6.1(1) and 6.1(2) were mixed at various weight ratios and tested for DNA delivery to human embryonic kidney cells (HEK293) using β -galactosidase as a reporter gene. The liposomes prepared from the lipids 6.1(1) and 6.1(2) were also evaluated for transfection efficiency. The transfection activity was reported as number of transfected cells per cm². Figure 6.1(4) displays data generated from an assay employing plasmid DNA (0.1 µg/well) at liposomes/DNA weight ratio of 20 under serum-free condition. Liposomes comprises of the lipid 6.1(1) and 6.1(2) alone exhibited low transfection efficiency than the LipofectamineTM 2000. As shown in Figure 6.1(4), the weight ratio of **6.1(1)** and **6.1(2)** is important for higher transfection efficiency; the optimal ratio was 1:1. Combining the lipid **6.1(1)** with **6.1(2)** at weight ratio of 1:1 enhances about 10 and 3.5-fold the extent of transfection of HEK293 cells, compared with liposomes prepared from each of lipid 6.1(1) and **6.1(2)**, respectively. At this ratio, the transfection efficiency was about 2-fold higher than that of the commercially available transfection agent, LipofectamineTM 2000. When the ratio of the lipids **6.1(1)** to **6.1(2)** decreases the transfection efficiency was also decreased. It has been shown that the synergistic effect of cationic liposomes on treansfection efficiency depended on the lipid composition. The minor change in cationic lipid component significantly effected on the transfection efficiency. 6.1[10] Thus, our finding confirmed this observation. It has also been revealed that liposomes compose of very different lipid headgroups and/or aliphatic tails has been shown to produce asymmetric liposomes. ^{6.1[11]} This was expected to increase the biocompatibility and flexibility of liposomes as delivery system. The liposomes comprised of lipids 6.1(1) and 6.1(2) which have different polarheads, central core structures and hydrophobic tails may be construct asymmetric liposomes, in particular at weight ratio of 1:1, and resulted in highly transfection efficiency. On the basis of the results (Figure 6.1(4)), the mixture of lipids **6.1(1)** and **6.1(2)** at weight ratio of 1:1 was chosen to further optimize transfection.

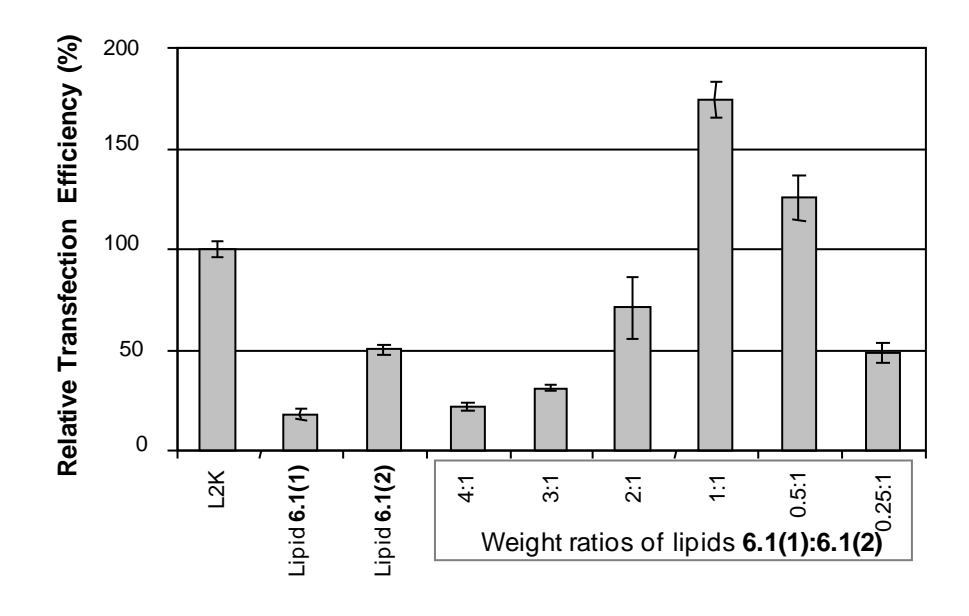


Figure 6.1(4) *In vitro* transfection efficiency of liposomes/DNA complexes with weight ratio of 20 in HEK293 cells. The transfection efficiencies of the liposomes were compared to that of the commercially available reagent, the Lipofectamine2000TM (L2K) which calculated as 100% transfection efficiency. Each value represents the mean \pm S.D. of triplicate experiments.

The helper lipid, DOPE, has been known to increase the transfection efficiency of cationic liposomes to transfer and release DNA into the cytoplasm.^{6.1[22]} To evaluate the effect of DOPE on gene delivery of the mixture of cationic lipids **6.1(1)** and **6.1(2)**, this mixture lipids (**6.1(1)**/ **6.1(2)** at weight ratio of 1:1) was mixed with different amounts of DOPE to form cationic liposomes. In order to find out the most effective formulation, transfection with identical liposomes/DNA weight ratio of 20 was used. Their ability to deliver a plasmid encoding β -galactosidase into HEK293 cells was studied (Figure 6.1(5)). A synergistic effect on the transfection efficiency was clearly demonstrated by the combined use of mixture of lipids **6.1(1)** and **6.1(2)** with the helper lipid, DOPE. The highest transfection efficiency was achieved by using the combination of mixture of lipids **6.1(1)** and **6.1(2)**/DOPE at the weight ratio of 1:1. This formulation dramatically increased the transfection efficiency for 11.5- and 2.3-fold, which was higher than those of liposomes comprised of lipid **6.1(1)**-DOPE and lipid **6.1(2)**-DOPE formulations, respectively. This optimal formulation exhibited 2.5-fold higher

transfection efficiency than that of LipofectamineTM 2000. Thus, the liposomes composed of mixture lipids/DOPE at weight ratio of 1:1 was chosen for further study.

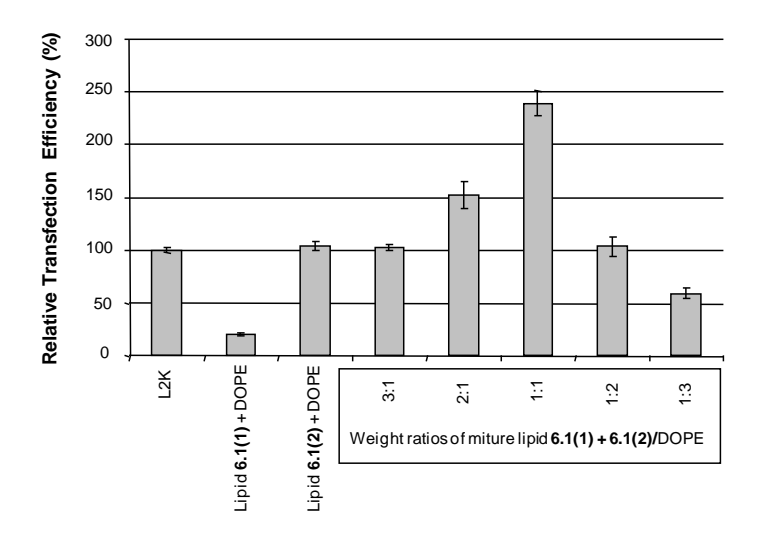


Figure 6.1(5) *In vitro* transfection efficiency of liposomes/DNA complexes with weight ratio of 20 in HEK293 cells. The liposomes were formulated at various weight ratios of mixture lipids **6.1(1)**+**6.1(2)** and DOPE. The transfection efficiencies of the liposomes were compared to that of the commercially available reagent, Lipofectamine2000TM (L2K) which calculated as 100% transfection efficiency. Each value represents the mean \pm S.D. of triplicate experiments.

The transfection efficiency of the cationic liposome also depends on the cationic lipisomes/DNA ratio as previously reported by our group^{6.1[12,23,24]} and others.^{6.1[25-27]} To find out the optimal liposomes/DNA ratio, transfection experiments were performed against HEK293 cells by using mixture lipids/DOPE ratio of 1:1. As shown in Figure 6.1(6), the liposomes formulations with mixture lipids/DOPE at 1:1 weight ratio showed maximum transfection efficiency at liposomes/DNA weight ratio of 5 and transfection profiles followed a bell-shaped graph. At this optimal liposomes/DNA weight ratio, liposome comprised of mixture lipids having different polarheads, central core structures and hydrophobic tails showed nearly 3-fold higher transfection efficiency than LipofectamineTM 2000.

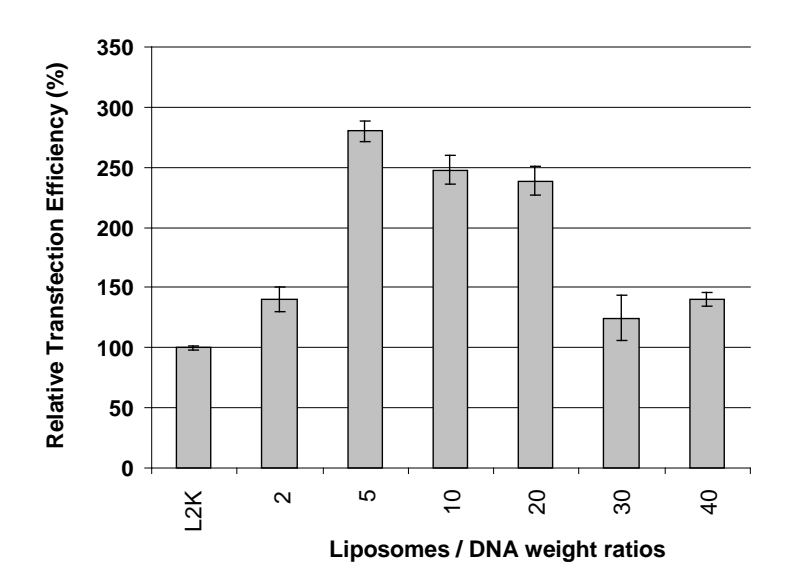


Figure 6.1(6) *In vitro* transfection efficiency of liposomes/DNA complexes across the cationic liposome/DNA weight ratios of 2 to 40 in HEK293 cells. Transfection efficiency of the mixture lipids was compared to that of the commercial reagent, Lipofectamine2000TM (L2K), which calculated as 100% transfection efficiency. Each value represents the mean \pm S.D. of triplicate experiments.

One of the major drawbacks of cationic liposomes for their *in vivo* use is the inhibition of the transfection efficiency in the presence of serum. Most of cationic liposomes including many commercially available transfection reagents which exhibited high transfection activity in the absence of serum lost their efficiency when transfected in the presence of serum. 6.1[24,28] In order to investigate the effect of serum on gene transfection efficiencies of mixture lipids, transfection experiments with our optimized lipid formulations were therefore performed in the presence of 10, 20, 30 and 40% serum. The results are shown in Figure 6.1(7). The transfection efficiency of mixture lipids gradually decreased when the amount of serum increase. Interestingly, the transfection efficiency of mixture lipids at high serum condition (30-40%) showed comparable transfection efficiency to LipofectamineTM 2000. It has been reported that size of the lipoplexes may be one of the factors contributing the serum resistance. 6.1[29,30] Large lipoplexes (>700 nm) showed transfection efficiency in the presence or absence of serum, but small lipoplexes (<250 nm) exhibited transfection efficiency only in the absence of serum. Thus, high transfection efficiency of optimized lipoplexes

formulation, total lipids/DNA ratio of 5, under high serum condition may be due to the large size of our lipoplexes aggregates (1428±46 nm, Figure 6.1(3)a).

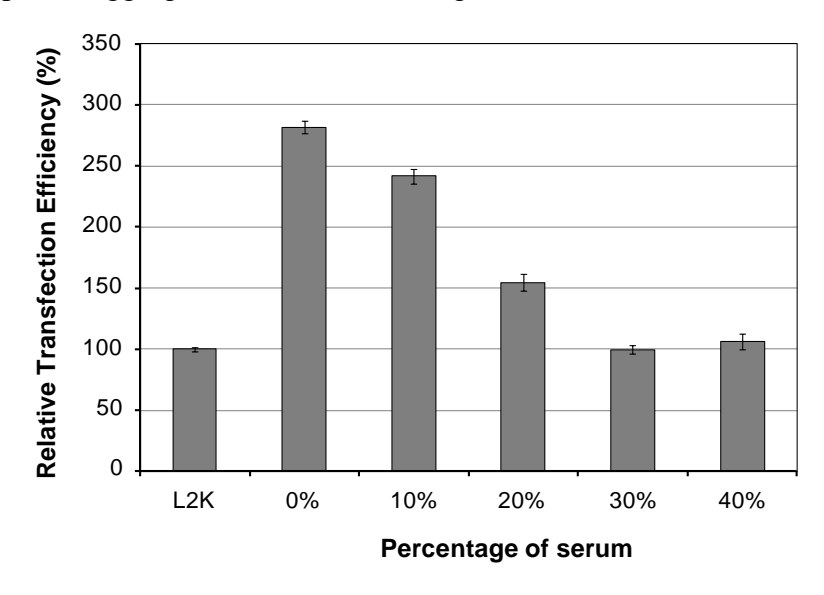


Figure 6.1(7) Transfection efficiency of mixture lipids using optimized mixture lipids/DOPE ratio of 1:1 and liposome/DNA ratio of 5 in HEK293 cells at various amount of serum. Transfection efficiency of the mixture lipids was compared to that of the commercial reagent, Lipofectamine 2000^{TM} , which calculated as 100% transfection efficiency. Each value represents the mean \pm S.D. of triplicate experiments.

It is known that transfection agents have the ability to specifically deliver DNA into different cell types. ^{6.1[12,23,24]} To evaluate the transfection efficiency of these mixture lipids toward the different cell lines, human breast adenocarcinoma (MCF-7) and cervical epithelial adenocarcinoma (HeLa) cells, the experiments were performed by using optimum condition under serum-free conditions. The transfection efficiency of mixture lipids was compared with the commercially available transfection agent, Lipofectamine TM 2000, which was calculated as 100%. The results are illustrated in Figure 6.1(8). The optimal liposome and lipoplexes formulations of mixture lipids that work well in HEK293 cells can be applied to MCF-7 and HeLa cells. The liposome comprised of mixture lipids **6.1(1)** and **6.1(2)/DOPE** at 1:1 weight ratio exhibited 2-fold higher transfection efficiency to deliver DNA into HeLa cells than that of the Lipofectamine TM 2000. However, the ability of these lipids and Lipofectamine TM 2000 to transfer DNA into MCF-7 cells was comparable.

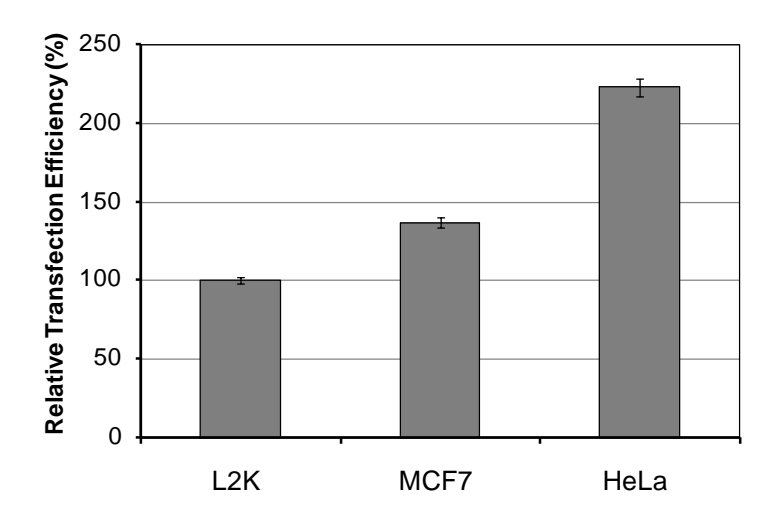
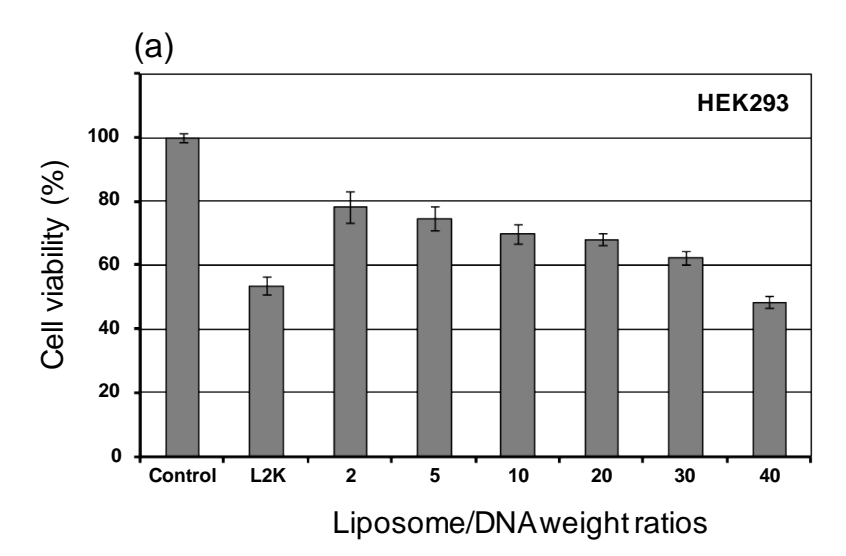
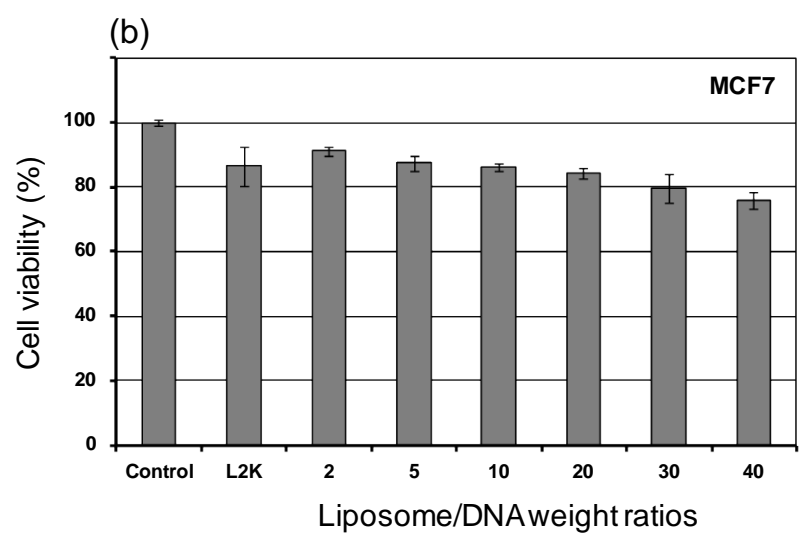


Figure 6.1(8) *In vitro* transfection efficiency of liposomes comprised of mixture lipids **6.1(1)** and **6.1(2)**/DOPE (1:1 weight ratio) in MCF7 and HeLa cells using optimum conditions. Transfection efficiency of the mixture lipids was compared to that of the commercial reagent, Lipofectamine2000TM (L2K), which calculated as 100% transfection efficiency. Each value represents the mean \pm S.D. of triplicate experiments.

Transfection Toxicity Two mostly concerned criteria for gene delivery carriers are transfection efficiency and their cytotoxicity. To assess the relationship between cytotoxicity and gene expression efficiency, the toxicity of the liposomes/DNA complexes at weight ratios of 2 to 40 was determined by measuring changes in cell metabolic activity (MTT assay) and was shown as % cell viability as compared to the control cells in the presence of DNA. The results are shown in Figure 6.1(9). It was found that the optimal lipoplexes formulation (liposomes/DNA weight ratio of 5) of the mixture lipids showed low toxicity (cell viability more than 80%) in MCF-7 and HeLa cells. The cell viability of these lipids against HEK293 cell was slightly lower than 80%. This result was in contrast to the high transfection efficiency of these lipids. The cell viability of Lipofectamine2000TM against MCF-7 and HeLa cell was higher and slightly lower than 80%, respectively. However, the cytotoxicity of the LipofectamineTM 2000 was relatively high for HEK293 cell line and the cell viability was approximately 60%. Thus, a slight reduction in metabolic activity of these mixture lipids should not prevent it from further *in vivo* study as transfection agent.





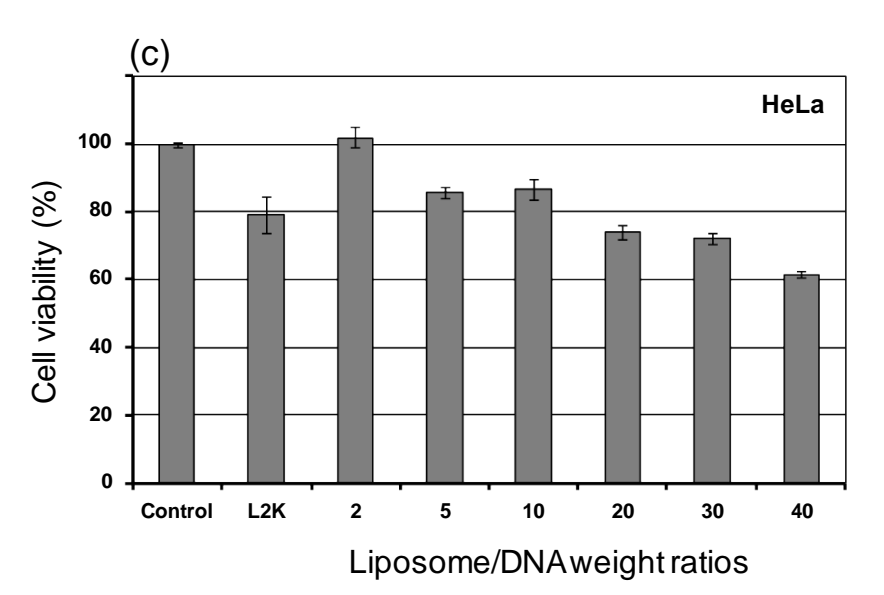


Figure 6.1(9) Cell viability of (a) HEK293, (b) MCF7 and (c) HeLa cells in the presence of lipoplexes formulated at various liposome/DNA weight ratios of 2 to 40 using the constant amount of DNA at 0.1 μ g per well. The commercially available agent, Lipofectamine2000TM was also tested for comparison. Cell metabolic activity was determined by an MTT assay. Each value represents the mean \pm S.D. of triplicate experiments.

In conclusion we have demonstrated that the combination of lipids with different polarheads, central core structures and hydrophobic tails in the presence of helper lipid, DOPE, has allowed the discovery of highly efficient transfection agents with minimal cytotoxicity. These mixture lipids showed high efficiency to deliver DNA into HEK293, MCF-7 and HeLa cells than that of a commercially available transfection agent. We hope that the strategy illustrated here is useful for the development of cationic lipid-based gene delivery. Employing the synergistic effect of these lipids may be a promising approach for successful non-viral gene transfection.

Output. This project has led to the following publication:

Niyomtham, N., Apiratikul, N., Chanchang, K., Opanasopit, O., Yingyongnarongkul, B., 2014. Synergistic effect of cationic lipids with different polarheads, central core structures and hydrophobic tails on gene transfection efficiency *Biol. Pharm. Bull.* 37, 1534–1542.

References

- 6.1[1] Mintzer, M. A., Simanek, E. E., 2009. Nonviral vectors for gene delivery. *Chem. Rev.*, 109, 259–302.
- 6.1[2] Xu, D., Hong, J., Sheng, K., Dong, L., Yao, S., 2007. Preparation of polyethyleneimine nanogels *via* photo-Fenton reaction. *Radiat. Phys. Chem.*, 76, 1606–1611.
- 6.1[3] Xu, D. M., Yao, S. D., Liu, Y. B., Sheng, K. L., Hong, J., Gong, P. J., Dong, L., 2007. Size-dependent properties of M-PEIs nanogels for gene delivery in cancer cells. *Int. J. Pharm.*, 338, 291–296.

- 6.1[4] Kopatz, I., Remy, J. S., Behr, J. P., 2004. A model for non-viral gene delivery: through syndecan adhesion molecules and powered by actin. *J. Gene Med.*, 6, 769–776.
- 6.1[5] Mounkes, L. C., Zhong, W., Cipres-Palacin, G., Heath, T. D., Debs, R. J., 1998.
 Proteoglycans mediate cationic liposome-DNA complex-based gene delivery in vitro and in vivo. J. Biol. Chem., 273, 26164–26170.
- 6.1[6] Felgner, P. L., Gadex, T. R., Holm, M., Roman, R., Chan, H. W., Wenz, M., Northrop, J. P., Ringold, G. M., Danielsen, M., 1987. Lipofection: a highly efficient, lipid-mediated DNA-transfection procedure. *Proc. Natl. Acad. Sci. USA*, 84, 7413–7417.
- 6.1[7] Edelstein, M. L., Abedi, M. R., Wixon, J., 2007. Gene therapy clinical trials worldwide to 2007-an update. *J. Gene Med.*, **9**, 833–842.
- 6.1[8] Wang, L., MacDonald, R. C., 2004. New strategy for transfection: mixtures of medium-chain and long-chain cationic lipids synergistically enhance transfection. *Gene Ther.*, 11, 1358–1362.
- 6.1[9] Wang, L., MacDonald, R. C., 2007. Synergistic effect between components of mixtures of cationic amphipaths in transfection of primary endothelial cells. *Mol. Pharmaceutics*, 4, 615–623.
- 6.1[10] Caracciolo, G., Pozzi, D., Caminiti, R., Marchini, C., Montani, M., Amici, A., Amenitsch, H., 2007. Transfection efficiency boost by designer multicomponent lipoplexes. *Biochim. Biophys. Acta*, 1768, 2280–2292.
- 6.1[11] Pautot, S., Frisken, B. J., Weitz, D. A., 2003. Engineering asymmetric vesicles. *Proc. Natl. Acad. Sci. USA*, 100, 10718–10721.
- 6.1[12] Yingyongnarongkul, B., Radchatawedchakoon, W., Krajarng, A., Watanapokasin, R., Suksamrarn, A, 2009.. High transfection efficiency and low toxicity cationic lipids with aminoglycerol-diamine conjugate. *Bioorg. Med. Chem.*, 17, 176–188.
- 6.1[13] Paecharoenchai, O., Niyomtham, N., Ngawhirunpat, T., Rojanarata, T., Yingyongnarongkul, B., Opanasopit, P., 2012. Cationic niosomes composed of spermine-based cationic lipids mediate high gene transfection efficiency. *J. Drug Targeting*, 20, 783–792.

- 6.1[14] Paecharoenchai, O., Niyomtham, N., Apirakaramwong, A., Ngawhirunpat, T., Rojanarata, T., Yingyongnarongkul, B., Opanasopit, P., 2012. Structure relationship of cationic lipids on gene transfection mediated by cationic liposomes. *AAPS Pharm. Sci. Tech.*, 13, 1302–1308.
- 6.1[15] Unciti-Broceta, A., Diezmann, F., Ou-Yang, C. Y., Fara, M. A., Bradley, M., 2009. Synthesis, penetrability and intracellular targeting of fluorescein-tagged peptoids and peptide-peptoid hybrids. *Bioorg. Med. Chem.*, 17, 959–966.
- 6.1[16] Oliver, M., Jorgensen, M. R., Miller, A., 2004. The facial solid-phase synthesis of cholesterol-based polyamine lipids. *Tetrahedron Lett.*, 45, 3105–3107.
- 6.1[17] Yingyongnarongkul, B., Apiratikul, N., Aroonrerk, N., Suksamrarn, A., 2006. Solid phase synthesis and antibacterial activity of hydroxycinnamic acid amides and analogues against methicillin-resistant *Staphylococcus aureus* and vancomycin-resistant *S. aureus. Bioorg. Med. Chem. Lett.*, 16, 5870–5873.
- 6.1[18] Nash, I. A., Bycroft, B. W., Chan, W. C., 1996. Dde-a selective primary amine protecting group: a facile solid phase synthetic approach to polyamine conjugates. *Tetrahedron Lett.*, 37, 2625–2628.
- 6.1[19] Fahood, H., Serbina, N., Huang, L., 1995. The role of dioleoyl phosphatidyl ethanolamine in cationic liposome-mediated gene-transfer. *Biochim. Biophys. Acta Biomembranes*, 1235, 289–295.
- 6.1[20] Caracciolo, G., Pozzi, D., Caminiti, R., Marchini, C., Montani, M., Amlci, A., Amenitsch, H., 2007. Transfection efficiency boost by designer multicomponent lipoplexes. *Biochim. Biophys. Acta Biomembranes*, 1768, 2280–2292.
- 6.1[21] Li, S., Tseng, W. C., Stolz, D. B., Wu, S. .P, Watkins, S. C., Huang, L., 1999. Dynamic changes in the characteristics of cationic lipidic vectors after exposure to mouse serum: implications for intravenous lipofection. *Gene Ther.*, 6, 585–594.
- 6.1[22] Hui, S. W., Langner, M., Zhao, Y.-L., Ross, P., Hurley, E., Chan, K., 1996. The role of helper lipids in cationic liposome-mediated gene transfer. *Biophys. J.*, 71, 590–599.

- 6.1[23] Radchatawedchakoon, W., Watanapokasin, R., Krajarng, A., Yingyongnarongkul, B., 2010. Solid phase synthesis of novel asymmetric hydrophilic head cholesterol-based cationic lipids with potential DNA delivery. *Bioorg. Med. Chem.*, 18, 330–342.
- 6.1[24] Radchatawedchakoon, W., Krajarng A., Niyomtham, N., Watanapokasin, R., Yingyongnarongkul, B., 2011. Transfection efficiency of cationic lipids with asymmetric acyl-cholesteryl hydrophobic tails. *Chem. Eur. J.*, 17, 3287–3295.
- 6.1[25] Bajaj, A., Kondaiah, P., Bhattacharya, S., 2008. Effect of the nature of the spacer on gene transfer efficacies of novel thiocholesterol derived gemini lipids in different cell lines: a structure–activity investigation. *J. Med. Chem.*, 51, 2533–2540.
- 6.1[26] Kim, B.-K., Bae, Y.-U., Doh, K.-O., Hwang, G.-B., Lee, S.-H., Kang, H., Seu, Y.-B., 2011. The synthesis of cholesterol-based cationic lipids with trimethylamine head and the effect of spacer structures on transfection efficiency. *Bioorg, Med. Chem. Lett.*, 21, 3734–3737.
- 6.1[27] Goldring, W. P. D., Jubeli, E., Downs, R.A., Johnston, A. J. S., Khalique, N. A., Raju, L., Wafadari, D., Pungente, M. D., 2012. Novel macrocyclic and acyclic cationic lipids for gene transfer: synthesis and in vitro evaluation. *Bioorg, Med. Chem. Lett.*, 22, 4686–4692.
- 6.1[28] Ghosh, K. Y., Visweswariah, S. S., Bhattacharya, S., 2000. Nature of linkage between the cationic headgroup and cholesteryl skeleton controls gene transfection efficiency *FEBS Lett.*, 473, 341–344.
- 6.1[29] Turek, J., Dubertret, C., Jaslin, G., Antonakis, K., Scherman, D., Pitard, B., 2000. Formulations which increase the size of lipoplexes prevent serum-associated inhibition of transfection. *J. Gene Med.*, 2, 32–40.
- 6.1[30] Lian, T., Ho, R. J.Y., 2003. Design and characterization of a novel lipid-DNA complex that resists serum-induced destabilization. *J. Pharm. Sci.*, 92, 2373–2385.

Project 6.2 Synthesis and in vitro transfection efficiency of spermine-based cationic lipids with different central core structures and lipophilic tails

Gene therapy has been receiving much attention due to its promise to prevent and treat many acquired and inherited diseases such as cancers, cystic fibrosis and AIDS. 6.2[1] Viruses are the most effective DNA delivery vehicle for gene therapy, but they suffer from a number of undesirable properties for therapeutic applications, such as uncertainties about safety, immunogenicity, limited packaging capacity for genetic material and manufacturing difficulties. Non-viral DNA delivery vehicles have, therefore, also been under development in an effort to overcome these barriers. There are many classes of compounds used for the nonviral delivery of DNA including cationic polymers, cationic peptides, cationic dendrimers and cationic lipids. 6.2[2] Cationic lipids are small molecules which can easily be designed and studied structure-activity relationships. ^{6.2[3-7]} Cationic lipids are commonly comprised of three main parts including polarhead, linker and lipophilic domain. Cationic lipids with double hydrocarbon chains as lipophilic tails have been widely studied and used as the non-viral gene delivery. These lipids usually have glycerol or aminoglycerol as central core structure. ^{6.2[8-10]} Since the first reported of cationic lipid having aminoglycerol backbone, N-[1-(2,3dioleolyloxy)propyl]-*N*,*N*,*N*-trimethylammonium chloride (DOTMA), ^{6.2[8]} aminoglycerol-based cationic lipids have been synthesized for gene delivery. These include 1,2-dimyristyloxypropyl-3-dimethyl-hydroxyethyl ammonium bromide (DMRIE), 6.2[9] 1,2dioleoyloxypropyl-3-dimethyl-hydroxyethyl ammonium bromide (DORIE), 6.2[9] N-(1-(2.3dioleoyloxy)propyl)-N,N,N-trimethylammonium methyl sulphate (DOTAP)^{6.2[10]} and 2,3dioleyloxy-N-[2(sperminecarboxamido)ethyl]-N,N-dimethyl-1-propanaminium pentatrifluoro acetate (DOSPA).^{6.2[11]} Previously, structure-activity relationship study of cationic lipids having aminoglycerol as a central core structure has been investigated. ^{6.2[11]} The polarhead of aminoglycerol-based cationic lipids was mainly monocationic group. 6.2[8-12] Naturally occurring polyamine, especially spermine, has been used as polarhead of numerous cationic lipids due to its ability to condense with DNA. However, the use of spermine as a polarhead of aminoglycerol-based cationic lipid has not been reported. Moreover, the central core structure of cationic lipid, rather than aminoglycerol, has not been much attention. We are therefore interested to synthesize new cationic lipids which exhibit high transfection efficiency.

In this study, twelve spermine-based cationic lipids with four different central core structures (di(oxyethyl)amino, di(oxyethyl)amino carboxy, 3-amino-1,2-dioxypropyl and 2-amino-1,3-dioxypropyl) and three hydrophobic tails (lauric acid, myristic acid and palmitic acid) were synthesized (Figure 6.2(1)). The liposomes containing lipids and DOPE showed moderate to good *in vitro* DNA delivery into HeLa cells. GFP expression experiments revealed that liposomes composed of lipids with 3-amino-1,2-dioxypropyl as a central core structure exhibited highest transfection efficiency under serum-free condition. Whereas, lipid with 2-amino-1,3-dioxypropyl core structure showed highest transfection under 10% serum comdition. Moreover, the liposomes and lipoplexes composted of these cationic lipids exhibited low cytotoxicity. The detail of the work can be seen in the published paper.

Figure 6.2(1) Structures of cationic lipids having different central core structures and lipophilic tails.

Output. This project has led to the following publication:

Niyomtham, N., Apiratikul, N., Suksen, K., Opanasopit, P., Yingyongnarongkul, B., 2015. Synthesis and in vitro transfection efficiency of spermine-based cationic lipids with different central core structures and lipophilic tails. *Bioorg. Med. Chem. Lett.* 25, 496-503.

References

- Yang, Z. R., Wang, H. F., Zhao, J., Peng, Y. Y., Wang, J., Guinn, B.-A., Huang, L.
 Q., 2007. Recent developments in the use of adenoviruses and immunotoxins in cancer gene therapy. *Cancer Gene Ther.* 14, 599-615.
- 6.2[2] Mintzer, M. A., Simanek, E. E., 2009. Nonviral vectors for gene delivery. *Chem. Rev. 109*, 259-302.
- 6.2[3] Kim, B.-K., Doh, K.-O., Nam, J. H., Kang, H., Park, J.-G., Moon, I.-J., Seu, Y.-B., 2009. *Bioorg. Med. Chem. Lett.* 19, 2986-2989.
- 6.2[4] Zhang, Q.-F., Yang, W.-H., Yi, W.-J., Zhang, J., Ren, J., Luo, T.-Y., Zhu, W., Yu, X.-Q., 2011. TACN-containing cationic lipids with ester bond: Preparation and application in gene delivery *Bioorg. Med. Chem. Lett.* 21, 7045-7049.
- 6.2[5] Yingyongnarongkul, B., Radchatawedchakoon, W., Krajarng, A., Watanapokasin, R., Suksamrarn, A., 2009. High transfection efficiency and low toxicity cationic lipids with aminoglycerol-diamine conjugate. *Bioorg. Med. Chem.* 17, 176-188.
- 6.2[6] Radchatawedchakoon, W., Watanapokasin R., Krajarng, A., Yingyongnarongkul, B., 2010. Solid phase synthesis of novel asymmetric hydrophilic head cholesterol-based cationic lipids with potential DNA delivery. *Bioorg. Med. Chem.* 18, 330-342.
- 6.2[7] Radchatawedchakoon, W., Krajarng, A., Niyomtham, N., Watanapokasin R., Yingyongnarongkul, B., 2011. High transfection efficiency of cationic lipids with asymmetric acyl-cholesteryl hydrophobic tails. *Chem. Eur. J.* 17, 3287-3295.

- 6.2[8] Felgner, P. L., Gadex, T.R., Holm, M., Roman, R., Chan, H.W., Wenz, M., Northrop, J.P., Ringold, G.M., Danielsen, M., 1987. Lipofection: a highly efficient, lipid-mediated DNA-transfection procedure. *Proc. Natl. Acad. Sci. USA* 84, 7413-7417.
- 6.2[9] Felgner, J. H., Kumar, R., Sridhar, C. N., Wheeler, C. J., Tsai, Y. J., Border, R., Ramsey, P., Martin, M., Felgner. P. L., 1994. Enhanced gene delivery and mechanism studies with a novel series of cationic lipid formulations. *J. Biol. Chem.* 269, 2550-2561.
- 6.2[10] Leventis, R., Silvius, J. R., 1990. Interactions of mammalian cells with lipid dispersions containing novel metabolizable cationic amphiphiles. *Biochim. Biophys. Acta* 1023, 124-132.
- 6.2[11] Heyes, J. A., Niculescu-Duvaz, D., Cooper, R. G., Springer, C., 2002. Synthesis of novel cationic lipids: effect of structural modification on the efficiency of gene transfer. *J. Med. Chem.* 45, 99-114.
- 6.2[12] Zhi, D., Zhang, S., Qureshi, F., Zhao, Y., Cui, S., Wang, B., Chen, H., Wang, Y., Zhao, D., 2012. Synthesis and biological activity of carbamate-linked cationic lipids for gene delivery in vitro. *Bioorg. Med. Chem. Lett.* 22, 3837-3841.

2.3 Output (ผลที่ได้รับ)

Apart from the research progress that has been accomplished according to the proposed work plan, 12 international publications have been achieved (please see **3.1 International publications**). Five M.Sc. and three Ph.D. students participating in this project have graduated.

2.4 Future Plans (งานที่จะทำต่อในอนาคต)

Future work will be the selection of some of the structure leads for indept or in vivo work.

3. Other Related Activities (กิจกรรมอื่น ๆ ที่เกี่ยวข้อง)

3.1 International Publications (ผลงานวิจัยที่ตีพิมพ์ในวารสารวิชาการระดับนานาชาติ)

Parts of the work have been published in the following refereed international journals:

- 3.1.1 Tantikanlayaporn, D., Wichit, P., Weerachayaphorn, J., Chairoungdua, A., Chuncharunee, A., Suksamrarn, A., Piyachaturawat, P. Bone sparing effect of a novel phytoestrogen diarylheptanoid from *Curcuma comosa* Roxb. in ovariectomized rats. *PloS ONE*, 2013, 8, e78739. doi:10.1371/journal.pone.0078739.
- 3.1.2 Chuprajob, T., Changtam, C., Chokchaisiri, R., Chunglok, W., Sornkaew, N., Suksamrarn, A., 2014. Synthesis, cytotoxicity against human oral cancer KB cells and structure-activity relationship studies of trienone analogues of curcuminoids. *Bioorg. Med. Chem. Lett.* 24, 2839-2844.
- 3.1.3 Kruangtip, O., Chootip, K., Temkitthawon, P., Changwichit, K., Chuprajob, T., Changtam, C., Suksamrarn, A., Khorana, N., Scholfield, C. N., Ingkaninan, K., 2014. Curcumin analogues inhibit phosphodiesterase-5 and dilate rat pulmonary arteries. *J. Pharm. Pharmacol.* 67, 87-95.
- 3.1.4 Kunthalert, D., Baothong, S., Khetkam, P., Chokchaisiri, S., Suksamrarn, A., 2014. A chalcone with potent inhibiting activity against biofilm formation of nontypeable *Haemophilus influenzae*. *Microbiol. Immunol.* 58, 581-589.

- 3.1.5 Janeklang, S.; Nakaew, A., Vaeteewoottacharn, K., Seubwai, W., Boonsiri, P., Kismali, G., Suksamrarn, A., Okada, S., Wongkham, S., 2014. *In vitro* and *in vivo* antitumor activity of tiliacorinine in human cholangiocarcinoma. *Asian Pac. J. Cancer Prev.* 15, 7473–7478.
- 3.1.6 Taka, T., Changtam, C., Thaichana, P., Kaewtunjai, N., Suksamrarn, A., Lee, T. R., Tuntiwechapikul, W., 2014. Curcuminoid derivatives enhance telomerase activity in an in vitro TRAP assay. *Bioorg. Med. Chem. Lett.* 24, 5242-5246.
- 3.1.7 Pantan, R., Onsa-ard, A., Tocharus, J., Wonganan, O., Suksamrarn, A., Tocharus, C., 2014. Endothelium-independent vasorelaxation effects of 16-O-acetyldihydroisosteviol on isolated rat thoracic aorta. *Life Sci.* 116, 31-36.
- 3.1.8 Niyomtham, N., Apiratikul, N., Chanchang, K., Opanasopit,O., Yingyongnarongkul, B., 2014. Synergistic effect of cationic lipids with different polarheads, central core structures and hydrophobic tails on gene transfection efficiency. *Biol. Pharm. Bull.* 37, 1534–1542.
- 3.1.9 Sornkaew, N., Lin, Y., Wang, F., Zhang, G., Chokchaisiri, R., Zhang, A., Wongkrajang, K., Suebsakwong, P., Piyachaturawat, P., Suksamrarn, A., 2015. Diarylheptanoids of *Curcuma comosa* with inhibitory effects on nitric oxide production in macrophage RAW 264.7 cells. *Nat. Prod. Commun.* 10, 89-93.
- 3.1.10 Pinkaew, D., Changtam, C., Tocharus, C., Thummayot, S., Suksamrarn, A., Tocharus, J., 2015. Di-O-demethylcurcumin protects SK-N-SH cells against mitochondrial and endoplasmic reticulum-mediated apoptosis cell death induced by Ab25-35. *Neurochem. Int.* 80, 110-119.
- 3.1.11 Niyomtham, N., Apiratikul, N., Suksen, K., Opanasopit, P., Yingyongnarongkul, B., 2015. Synthesis and in vitro transfection efficiency of spermine-based cationic lipids with different central core structures and lipophilic tails. *Bioorg. Med. Chem. Lett.* 25, 496-503.
- 3.1.12 Janyou, A., Changtam, C., Suksamrarn, A., Tocharus, C., Tocharus, C., 2015. Suppression effects of *O*-demethyldemethoxycurcumin on thapsigargin triggered on endoplasmic reticulum stress in SK-N-SH cells. *Neurotoxicol.* 50, 92-100.

3.2 Other Research Outputs (ผลงานวิจัยอื่น ๆ)

-

3.3 Utilization of Research Outputs (การนำผลงานไปใช้ประโยชน์)

-

3.4 Activities of Members as Invited Speakers (จำนวนและรายละเอียดการได้รับเชิญไปเป็น วิทยากร)

The numbers and details of invitations of principal investigator and investigators of the project to give lectures in scientific meetings are the followings:

- 3.4.1 Apichart Suksamrarn, "Structural modification: a promising strategy in natural products drug discovery", invited lecture presented at 74th FIP World Congress of Pharmacy and Pharmaceutical Sciences 2014, BITEC Bangkok, September 1, 2014.
- 3.4.2 Apichart Suksamrarn, "Biological activity enhancement of natural products by chemical modification and microbial transformation", invited lecture presented at The International Bioscience Conference, Phuket Graceland Resource and Spa, Phuket, September 29, 2014.
- 3.4.3 Apichart Suksamrarn, "Structural modification as a promising strategy to enhance cytotoxic activity of natural products", invited lecture presented at Pure and Applied Chemistry Conference 2015 (PACCON 2015), Amari Watergate Hotel, Bangkok, January 22, 2015.

3.5 Research Networking with the Experts outside the University and Abroad (การ เชื่อมโยงทางวิชาการกับนักวิชาการอื่น ๆ ทั้งในประเทศและต่างประเทศ)

Apart from the researchers recruited from other universities as investigators of this project, we have established the linkages with the following Thai scientists in the areas of our research:

- 3.5.1 Professor Suthat Fucharoen, Thalassemia Research Center, Institute of Molecular Biosciences, Mahidol University, Salaya Campus, Nakhon Pathom, Thailand
- 3.5.2 Professor Dr. Supa Hannongbua, Faculty of Science, Kasetsart University, Bangkok, Thailand
- 3.5.3 Professor Dr. Sopit Wongkham, Department of Biochemistry, Faculty of Medicine, Khon Kaen University, Khon Kaen, Thailand
- 3.5.4 Associate Professor Dr. Natthida Weerapreeyakul, Faculty of Pharmaceutical Sciences, Khon Kaen University, Khon Kaen, Thailand
- 3.5.5 Associate Professor Dr. Kornkanok Inkaninan, Department of Pharmaceutical Chemistry and Pharmacognosy, Faculty of Pharmaceutical Sciences, Naresuan University, Pitsanulok, Thailand
- 3.5.6 Associate Professor Dr. Siritron Samosorn, Department of Chemistry, Faculty of Science, Srinakharinwirot University, Bangkok, Thailand
- 3.5.7 Assistant Professor Dr. Duangkamol Kunthalert, Department of Microbiology and Parasitology, Faculty of Medical Sciences, Naresuan University, Pitsanulok, Thailand
- 3.5.8 Assistant Professor Dr. Rungnapha Saeeng, Department of Chemistry, Faculty of Science, Burapha University, Chonburi, Thailand
- 3.5.9 Assistant Professor Dr. Chainarong Tocharus, Department of Anatomy, Faculty of Medicine, Chiang Mai University, Chiang Mai, Thailand
- 3.5.10 Assistant Professor Dr. Jiraporn Tocharus, Department of Biochemistry, Faculty of Medical Sciences, Naresuan University, Pitsanulok, Thailand
- 3.5.11 Assistant Professor Dr. Wirote Tantiwechapikul, Department of Biochemistry, Faculty of Medicine, Chiang Mai University, Chiang Mai, Thailand
- 3.5.12 Assistant Professor Dr. Chatchai Muanprasat, Department of Physiology, Faculty of Science, Mahidol University, Bankok, Thailand

3.5.13 Dr. Ratchanaporn Chokchaisiri, Department of Chemistry, School of Science, University of Phayao, Phayao, Thailand

We have also established the linkages with foreign scientists in the areas of our research.

- 3.5.14 Professor Guolin Zhang, Chengdu Institute of Biology, Chinese Academy of Sciences, Chengdu, China
- 3.5.15 Professor Fei Wang, Chengdu Institute of Biology, Chinese Academy of Sciences, Chengdu, China
- 3.5.16 Professor Alexander I. Gray, Division of Pharmaceutical Sciences, Strathclyde Institute of Pharmacy & Biomedical Sciences, University of Strathclyde, Scotland

3.6 Research Networking within the University (การเชื่อมโยงทางวิชาการกับนักวิชาการ ภายในสถาบันเดียวกัน)

The staff members of the Faculty of Science, Ramkhamhaeng University, i.e. from the Department of Chemistry (Associate Professor Dr. Thitima Rukachaisirikul and Dr. Vachiraporn Ajavakom), Department of Biology (Assistant Professor Dr. Ek Sangvichien) and Department of Biotechnology (Associate Professor Oratai Sukcharoen) have been invited to be the collaborators of the project.

3.7 Awards and Honors (รางวัลที่ได้รับ)

4. Problems and Obstacles (if any) (ปัญหาและอุปสรรค (ถ้ามี))

-

5. Comments and Suggestions (ความเห็นและข้อเสนอแนะ)

_

APPENDIX

Publications

Publications

- 1. Tantikanlayaporn, D., Wichit, P., Weerachayaphorn, J., Chairoungdua, A., Chuncharunee, A., Suksamrarn, A., Piyachaturawat, P. Bone sparing effect of a novel phytoestrogen diarylheptanoid from *Curcuma comosa* Roxb. in ovariectomized rats. *PloS ONE*, 2013, 8, e78739. doi:10.1371/journal.pone.0078739.
- Chuprajob, T., Changtam, C., Chokchaisiri, R., Chunglok, W., Sornkaew, N., Suksamrarn, A., 2014. Synthesis, cytotoxicity against human oral cancer KB cells and structure-activity relationship studies of trienone analogues of curcuminoids. *Bioorg. Med. Chem. Lett.* 24, 2839-2844.
- 3. Kruangtip, O., Chootip, K., Temkitthawon, P., Changwichit, K., Chuprajob, T., Changtam, C., Suksamrarn, A., Khorana, N., Scholfield, C. N., Ingkaninan, K., 2014. Curcumin analogues inhibit phosphodiesterase-5 and dilate rat pulmonary arteries. *J. Pharm. Pharmacol.* 67, 87-95.
- 4. Kunthalert, D., Baothong, S., Khetkam, P., Chokchaisiri, S., Suksamrarn, A., 2014. A chalcone with potent inhibiting activity against biofilm formation of nontypeable *Haemophilus influenzae*. *Microbiol. Immunol.* 58, 581-589.
- Janeklang, S.; Nakaew, A., Vaeteewoottacharn, K., Seubwai, W., Boonsiri, P., Kismali, G., Suksamrarn, A., Okada, S., Wongkham, S., 2014. *In vitro* and *in vivo* antitumor activity of tiliacorinine in human cholangiocarcinoma. *Asian Pac. J. Cancer Prev.* 15, 7473–7478.
- 6. Taka, T., Changtam, C., Thaichana, P., Kaewtunjai, N., Suksamrarn, A., Lee, T. R., Tuntiwechapikul, W., 2014. Curcuminoid derivatives enhance telomerase activity in an in vitro TRAP assay. *Bioorg. Med. Chem. Lett.* 24, 5242-5246.
- 7. Pantan, R., Onsa-ard, A., Tocharus, J., Wonganan, O., Suksamrarn, A., Tocharus, C., 2014. Endothelium-independent vasorelaxation effects of 16-*O*-acetyldihydroisosteviol on isolated rat thoracic aorta. *Life Sci.* 116, 31-36.
- 8. Niyomtham, N., Apiratikul, N., Chanchang, K., Opanasopit,O., Yingyongnarongkul, B., 2014. Synergistic effect of cationic lipids with different polarheads, central core structures and hydrophobic tails on gene transfection efficiency. *Biol. Pharm. Bull.* 37, 1534–1542.

- 9. Sornkaew, N., Lin, Y., Wang, F., Zhang, G., Chokchaisiri, R., Zhang, A., Wongkrajang, K., Suebsakwong, P., Piyachaturawat, P., **Suksamrarn, A.**, 2015. Diarylheptanoids of *Curcuma comosa* with inhibitory effects on nitric oxide production in macrophage RAW 264.7 cells. *Nat. Prod. Commun.* 10, 89-93.
- Pinkaew, D., Changtam, C., Tocharus, C., Thummayot, S., Suksamrarn, A., Tocharus, J., 2015. Di-O-demethylcurcumin protects SK-N-SH cells against mitochondrial and endoplasmic reticulum-mediated apoptosis cell death induced by Ab25-35. *Neurochem. Int.* 80, 110-119.
- Niyomtham, N., Apiratikul, N., Suksen, K., Opanasopit, P., Yingyongnarongkul, B., 2015. Synthesis and in vitro transfection efficiency of spermine-based cationic lipids with different central core structures and lipophilic tails. *Bioorg. Med. Chem. Lett.* 25, 496-503.
- 12. Janyou, A., Changtam, C., Suksamrarn, A., Tocharus, C., Tocharus, C., 2015. Suppression effects of *O*-demethyldemethoxycurcumin on thapsigargin triggered on endoplasmic reticulum stress in SK-N-SH cells. *Neurotoxicol.* 50, 92-100.



Bone Sparing Effect of a Novel Phytoestrogen Diarylheptanoid from *Curcuma comosa* Roxb. in Ovariectomized Rats

Duangrat Tantikanlayaporn¹, Patsorn Wichit¹, Jittima Weerachayaphorn¹, Arthit Chairoungdua¹, Aporn Chuncharunee², Apichart Suksamrarn³, Pawinee Piyachaturawat¹*

1 Department of Physiology, Faculty of Science, Mahidol University, Bangkok, Thailand, 2 Department of Anatomy, Faculty of Medicine, Siriraj Hospital, Mahidol University, Bangkok, Thailand, 3 Department of Chemistry, Faculty of Science, Ramkhamhaeng University, Bangkok, Thailand

Abstract

Phytoestrogens have been implicated in the prevention of bone loss in postmenopausal osteoporosis. Recently, an active phytoestrogen from *Curcuma comosa* Roxb, diarylheptanoid (DPHD), (3R)-1,7-diphenyl-(4E,6E)-4,6-heptadien-3-ol, was found to strongly promote human osteoblast function *in vitro*. In the present study, we demonstrated the protective effect of DPHD on ovariectomy-induced bone loss (OVX) in adult female Sprague-Dawley rats with 17 β -estradiol (E_2 , 10 μ g/kg Bw) as a positive control. Treatment of OVX animals with DPHD at 25, 50, and 100 mg/kg Bw for 12 weeks markedly increased bone mineral density (BMD) of tibial metaphysis as measured by peripheral Quantitative Computed Tomography (pQCT). Histomorphometric analysis of bone structure indicated that DPHD treatment retarded the ovariectomy-induced deterioration of bone microstructure. Ovariectomy resulted in a marked decrease in trabecular bone volume, number and thickness and these changes were inhibited by DPHD treatment, similar to that seen with E_2 . Moreover, DPHD decreased markers of bone turnover, including osteocalcin and tartrate resistant acid phosphatase (TRAP) activity. These results suggest that DPHD has a bone sparing effect in ovariectomy-induced trabecular bone loss and prevents deterioration of bone microarchitecture by suppressing the rate of bone turnover. Therefore, DPHD appears to be a promising candidate for preserving bone mass and structure in the estrogen deficient women with a potential role in reducing postmenopausal osteoporosis.

Citation: Tantikanlayaporn D, Wichit P, Weerachayaphorn J, Chairoungdua A, Chuncharunee A, et al. (2013) Bone Sparing Effect of a Novel Phytoestrogen Diarylheptanoid from *Curcuma comosa* Roxb. in Ovariectomized Rats. PLoS ONE 8(11): e78739. doi:10.1371/journal.pone.0078739

Editor: Brenda Smith, Oklahoma State University, United States of America

Received April 18, 2013; Accepted September 16, 2013; Published November 11, 2013

Copyright: © 2013 Tantikanlayaporn et al. This is an open-access article distributed under the terms of the Creative Commons Attribution License, which permits unrestricted use, distribution, and reproduction in any medium, provided the original author and source are credited.

Funding: This study was supported by the Thailand Research Fund (TRF) through the Royal Golden Jubilee Ph.D. Program (grant PHD/0103/2549 to DT and PP), the Strategic Basic Research Grant of TRF (to PP and to AS), the Office of the Higher Education Commission and Mahidol University under the National Research and Universities Initiative, and The National Research Council of Thailand. The funders had no role in study design, data collection and analysis, decision to publish, or preparation of the manuscript.

1

Competing Interests: The authors have declared that no competing interests exist.

* E-mail: pawinee.pia@mahidol.ac.th

Introduction

Osteoporosis is a serious worldwide health problem that primarily effect middle-aged and elderly women [1,2]. It is characterized by reduced bone mass and the deterioration of bone microarchitecture leading to increase the risk of bone fragility and fracture [3]. An accelerated rate of bone resorption in menopausal and post-menopausal women is associated with reduced levels of the hormone estrogen [4]. Recently, efforts to reduce bone loss in menopausal osteoporosis have been focused on compounds with the potential to preserve bone mass through inhibition of osteoclastic bone resorption or stimulation bone formation [5]. Among therapeutic agents, estrogen is the most effective compound and is capable of limiting bone loss and reducing the rate of bone fractures in postmenopausal women [6,7]. However, long-term treatment with estrogen is limited due to its carcinogenic risk and feminizing effects.

Phytoestrogens, non-steroidal plant-derived compounds with estrogenic activity, have received increased interest as estrogen alternatives to alleviate bone loss. Studies have suggested that a diet rich in phytoestrogen may relieve menopausal symptoms and

protect against estrogen-associated diseases, including breast cancers, cardiovascular diseases, and osteoporosis [8,9]. Isoflavones, such as genistein and daidzein the major phytoestrogens in soybeans, are the most extensively studies phytoestrogens. These compounds inhibit osteoclast bone resorption and suppress osteoclast activity and survival *in vitro* [10,11]. In addition, isoflavones have been identified as naturally occurring selective estrogen receptor modulators (SERMs) and as bone-sparing agents [12,13]. The known properties of phytoestrogens suggest that these compounds may be alternatives to estrogen for preventing and treating osteoporosis in postmenopausal women.

Curcuma comosa Roxb. (C. comosa), a plant in Zingiberaceae family, has been widely used as a dietary supplement for relieving postmenopausal symptoms in Thailand [14]. Consistent with the presence of a phytoestrogen, hexane extract of C. comosa rhizomes prevent bone loss in estrogen deficient mice [15]. Diarylheptanoid, (3R)-1,7-diphenyl-(4E,6E)-4,6-heptadien-3-ol (hereafter DPHD), a novel phytoestrogen isolated from C. comosa [16] has several pharmacological properties including estrogenic-like activity [17,18] and anti-inflammatory effects [19]. Recently, DPHD was found to activate Wnt/β-catenin signaling and promote mouse

preosteoblastic (MC3T3-E1) cell proliferation through the estrogen receptor pathway [20]. Similarly, human osteoblast cell differentiation and function were also enhanced upon DPHD treatment [21] suggesting that DPHD may have a beneficial effect in preventing bone loss in patients experiencing estrogen deficiency.

The biological activities of DPHD appear to be selective with anabolic effects predominantly on osteoblasts. We hypothesized that DPHD may have a beneficial effect in preventing bone loss due to estrogen deficiency. In the present study, we investigated the bone sparing effect of DPHD in ovariectomized-rats that exhibit estrogen deficiency. The effect of DPHD on bone mineral density (BMD), changes to bone microarchitecture, and biochemical markers of bone turnover were determined after a 12-week course of treatment. Our analysis provides mechanistic insight into the beneficial effects of the phytoestrogen DPHD in reducing bone loss in estrogen deficient rats and suggests a potential clinical use for DPHD in menopausal women.

Materials and Methods

The animal experimental protocol was approved by the committee on Animal Care and Use, Faculty of Science, Mahidol University (approval protocol number: MUSC-171). All animal experiments were performed in accordance with the guidelines of National Laboratory Animal Center, Mahidol University.

Chemicals and Plant Materials

Preparation of phytoestrogen diarylheptanoid (3R)-1,7-diphenyl-(4E,6E)-4,6-heptadien-3-ol (DPHD) from C. comosa was performed as previously described [16,21]. Rhizomes of C. comosa were purchased from the Kampaengsaen district, Nakhon Pathom province, Thailand. No specific permission is required for these activities and the field study did not involve endangered or protected species. Briefly, rhizomes were cut into small pieces, dried and ground to powder then extracted with n-hexane in a Soxhlet extractor. After removal of the solvent in vacuo, a pale brown viscous oil was obtained. The DPHD was isolated from the hexane extract as a major component (23.9%) by repeated silica gel column chromatography. DPHD was eluted with hexanedichloromethane and each step utilized an increasing quantity of the more polar solvent. The structure of DPHD was confirmed and the absolute stereochemistry at the 3-position was determined to be R by nuclear magnetic resonance and mass spectroscopy, the same as that of DPHD previously isolated [16]. The purity of the isolated material was assessed by TLC and NMR spectroscopy and estimated to be 99% pure. The chemical structure is shown in Figure 1A.

 17β -estradiol (E₂) and p-nitrophenyl phosphate were purchased from Sigma-Aldrich Chemical Company (MO, USA). Methyl methacrylate, 2-ethoxyethyl acetate and orange G were obtained from Merck Company (Darmstadt, Germany). Haematoxylin, fushin acid, and DePex mounting medium were purchased from VWR International Ltd. (Poole, England). All compounds were initially dissolved in 5% DMSO and diluted in olive oil to the final doses.

Animals and Treatments

Eight-week-old female Sprague-Dawley rats, weighing 200–220 g, were supplied by the National Laboratory Animal Centre of Thailand (Salaya, Nakornpathom, Thailand). Animals were housed in standard stainless steel cages under controlled conditions: temperature at $25\pm2^{\circ}\mathrm{C}$, relative humidity of 50–60%, a 12-h light/dark cycle, and allowed free access to food (rat pellets, C.P.

rat feed, Pokphand Animal Fed Co. Ltd., Bangkok, Thailand) and water. Rats were randomly assigned to sham-operated control and ovariectomized (OVX) groups. In OVX animals, both sites of ovaries, which are the primary source of endogenous estrogen, were removed under general anesthesia using pentobarbital sodium (50 mg/kg Bw, i.p.). Animals were allowed to recover from surgery for one week prior to use in experiments. Rats were divided into six groups of six to eight animals each as follows: sham operated control receiving vehicle (olive oil); OVX rats receiving vehicle (olive oil, i.p.); OVX rats receiving DPHD at doses of 25, 50 and 100 mg/kg Bw (i.p.); OVX rats receiving 17β-estradiol (E₂) at a dose of 10 μ g/kg Bw (s.c.) as a positive control. DPDH and E₂ were daily administered for 12 weeks and body weights were recorded weekly. All rats were given subcutaneous injections of 10 mg/kg calcein, a fluorochrome bone marker, on Day 7 and Day 1 before animals were sacrificed. At the end of treatments, animals were euthanized with an overdose of sodium pentobarbital. Serum was collected and stored at −70°C until use and the uterus was removed and weighed. Tibial bones were excised, kept in saline-soaked gauze, covered with plastic and stored at -20° C prior to analysis.

Measurement of Bone Mineral Density (BMD)

The bone mineral density of left tibia was measured *ex vivo* by peripheral Quantitative Computed Tomography (pQCT; XCT Research SA⁺, Stratec Medizintechnik GmbH., Germany) according to a previously protocol [22]. In brief, both the trabecular and cortical bone density were scanned in cross-sectional plane at metaphyseal sites of tibias. Proximal tibial metaphysis was measured 2 mm below the growth plate. All bones were scanned at 0.5 mm intervals using a voxel size of 0.09 mm×0.09 mm×0.09 mm. The trabecular bone was determined using contour mode 2 and peel mode 2 with a threshold value of 720 mg/cm³. The cortical bone was determined using separation mode 2 with a threshold value of 900 mg/cm³. All parameters were analyzed using XCT-5.50E software (Stratec Medizintechnik GmbH., Germany).

Bone Histomorphometric Analysis

All bone histomorphometries were conducted at the proximal metaphyseal region of the right tibia. The adhering tissues and bone marrow were removed from tibias followed by fixation for 3 days in 70% (vol/vol) ethanol, as previously described [23]. Bones were then dehydrated in 95, and 100% (vol/vol) ethanol for 3 and 2 days, respectively, followed by embedding and undecalcification in methyl methacrylate resin at 42°C for 48 h. To obtain 7 µm and 12 µm thick sections, the embedded tibia was cut in longitudinal section using a microtome (model RM2255; Leica, Nussloch, Germany). The region of tibial studied was the secondary spongiosa, the trabecular part of proximal tibia, at 1-2 mm distal to the epiphysial plate and extending to 6 mm. The 7 μm sections were deplasticified in 2-ethoxyethyl acetate and stained with Goldner's trichrome then analyzed under bright field microscopy. The structural variables were examined using the histology section and parameters measured include trabecular bone volume, normalized by tissue volume (BV/TV, %), trabecular number (Tb.N, mm⁻¹), trabecular thickness (Tb.Th, μ m) and trabecular separation (Tb.Sp, μ m). The 12 μ m sections of proximal tibia were left unstained to determine the mineral apposition rate (MAR), an index of osteoblastic activity, calculated by dividing the mean distance between double labels of the calcein with time interval between the administration of the two labels. Bone formation rate (BFR/TV) is another dynamic parameter that is an index of bone turnover in general and bone formation in

((3R)-1,7-diphenyl-(4E,6E)-4,6-heptadien-3-ol)

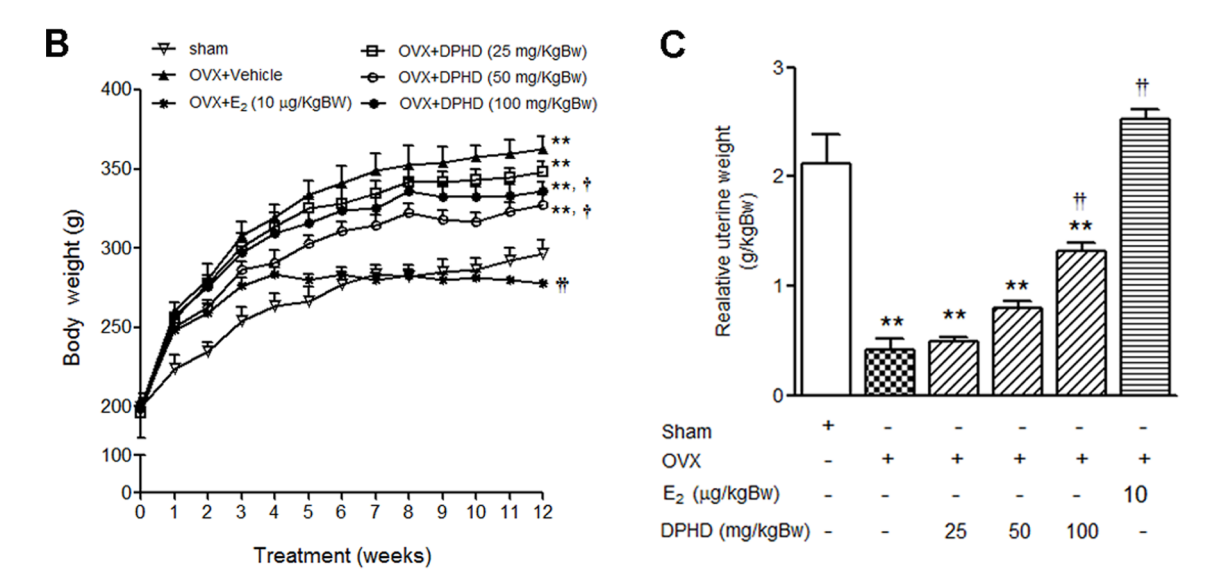


Figure 1. Estrogenic activity of DPHD compared to E₂. Structure of the phytoestrogen diarylheptanoid DPHD, (3*R*)-1,7-diphenyl-(4*E*,6*E*)-4,6-heptadien-3-ol, isolated from the rhizome of *C. comosa* (A). Effects of DPHD on body weight (B) and uterine weight (C) of sham-operated and ovariectomized (OVX) rats receiving vehicle and various doses of DPHD (25, 50 and 100 mg/kg Bw) or 17β-estradiol (E₂, 10 μg/kg Bw) for 12 weeks. Results are expressed as the mean \pm SEM, n = 6–8. **p<0.01, significantly different from sham rats. † p<0.05 and †† p<0.01, significantly different from OVX rats.

doi:10.1371/journal.pone.0078739.g001

particular and allows for the determination of the age of bone [24]. All slides were analyzed under a light/fluorescent microscope using a computer assisted Osteomeasure system (Osteometric, Atlanta, GA), software version 4.1. Bone histomorphometric parameters were reported according to the American Society for Bone and Mineral Research Nomenclature Committee [25].

Serum Bone Biomarkers Assay

Tartrate-resistant acid phosphatase (TRAP) activity, a bone resorption marker, was determined by using microplate assay method. 4-nitrophenyl phosphate (4-NPP) was used as the substrate according to the procedure of Lau et al. with modification [26]. Serum was incubated for 30 min at 37°C with a substrate solution consisting of 7.6 μ mol/L 4-NPP in 100 μ mol/L sodium acetate buffer containing 50 μ mol/L sodium tartrate (pH 5.5). 1 μ mol/L NaOH was added to stop the reaction and the absorbance at 405 nm was monitored to detect product formation. Serum osteocalcin concentration, a bone turnover marker, was measured using an enzyme immunoassay (EIA) kit specific for rat osteocalcin (Biomedical Technology, Staughton, IN, USA).

Statistical Analysis

All data are expressed as means ± SEM and were analyzed using one-way analysis of variance (ANOVA) and Newman–Keuls post-hoc test using SPSS for Windows, Version 17.0 (Chicago, IL, USA). A non parametric Wilcoxon-type test for trend (Cuzick's

Test for Trend) was employed for evaluation of the trend across the groups. Differences were considered statistical significant at p < 0.05.

Results

Effects of Ovariectomy and DPHD Treatment on Body Weight and Uterine Weight

All rats exhibited an increase in body weight during the 12 weeks of treatment, particularly in OVX rats. As shown in Figure 1B, at the end of experiment, the body weight gain was consistently highest in OVX control. However, the increases in body weights of OVX rats was suppressed by treatment with E₂ (10 µg/kg Bw) to levels similar to the sham controls. Treatments of OVX rats with DPHD at doses of 50 and 100 mg/kg BW also significantly decreased body weight compared to OVX controls. However, the effect of DPHD on body weight was not as pronounced as that seen with E₂ (Figure 1B). These results indicate that DPHD partially suppressed body weight gain in OVX rats. The uterine weights of OVX rats was also changed but in this case a significant decrease was observed when compared to sham controls (p<0.01). Uterine weight was increased in OVX rats following treatment with estrogen and DPHD, though a significant increase was only observed at 100 mg/kg Bw of DPHD (p<0.01) (Figure 1C).

Effects of DPHD on ex vivo Bone Mineral Density (BMD)

Both total and trabecular bone mineral density (BMD) of tibial metaphysis were markedly decreased in OVX rats (at 12 weeks) compared to those of sham controls (Figure 2A and 2B, respectively). E_2 treatment (10 $\mu g/kg$ Bw) effectively prevented the decreases in total and trabecular BMD. Treatments with DPHD at doses of 25, 50, and 100 mg/kg Bw also prevented the decrease in total and trabecular BMD compared to the OVX group given the vehicle control. Similar to the effect observed for body weight, treatment with DPDH did not restore BMD to the level seen in the sham-operated group. Interestingly, DPHD had no effect on the cortical BMD of tibial metaphysis though a protective effect was observed with E_2 (Figure 2C). These findings suggest that DPHD predominantly only protects against trabecular bone loss, while E_2 effectively prevents the loss of both trabecular and cortical bones.

Effects of DPHD on Bone cross Sectional Area and Thickness

In Table 1, the total, trabecular and cortical bone cross sectional areas (CSA) of tibia are shown. In OVX rats, total and trabecular CSA of tibia were increased by 12% and 20%, respectively, compared to sham controls. Treatment with E_2 , and DPHD at doses of 50 and 100 mg/kg Bw prevented the increases in cross sectional area. However, there was no significant change in cortical area and thickness.

Effects of DPHD on Trabecular Bone Microarchitectural Changes

Both static and dynamic changes in histomorphometry of the proximal tibial metaphysis were evaluated. The growth plate and spongiosa region of the proximal tibia of sham, OVX, OVX+DPHD (100 mg/kg Bw), and OVX+E₂ (10 µg/kg Bw) rats are shown in Figure 3A. Compared to the sham rats, a decrease in trabecular bone and connectivity was observed in OVX rats indicating that ovariectomy resulted in the deterioration of trabecular bone microstructure. However, treatment with E₂ completely protected against this deterioration with partial protection observed with DPHD treatment. Ovariectomy also induced a marked decrease in the trabecular bone volume (BV/ TV) compared to that of the sham rats (73% reduction) (Figure 3C) and again treatment with E2 completely restored trabecular bone volume to levels seen in the sham controls. All doses of DPHD significantly increased BV/TV (Figure 3C) and trabecular number (Tb.N) (p<0.05) (Figure 3D) in OVX rats but these values were reduced compared to the sham and E2 treated animals. DPHD treatment also increased trabecular thickness (Tb.Th) in OVX rats but significant difference was not observed at low dose of DPHD (25 mg/Kg Bw)-treated group (Figure 3E). Trabecular separation (Tb.Sp), another important structural index for static microstructural changes of bone, was markedly increased in OVX rats compared to sham controls. E2 treatment was capable of significantly decreasing the separation of bone to the level seen in the sham controls. The Tb.Sp in animals treated with DPHD was also significantly reduced but were significantly higher than that for the sham control group (Figure 3F). These results suggest that DPHD treatment improved the connectivity of trabecular bone in the ovariectomized rats though to a lesser degree than treatment with E_2 .

The dynamic bone histomophometry was assessed using fluorescence microscopy to monitor the uptake of calcein, a fluorochrome bone marker (Figure 3B). Bone formation and mineralization, expressed as mineral apposition rate (MAR), were

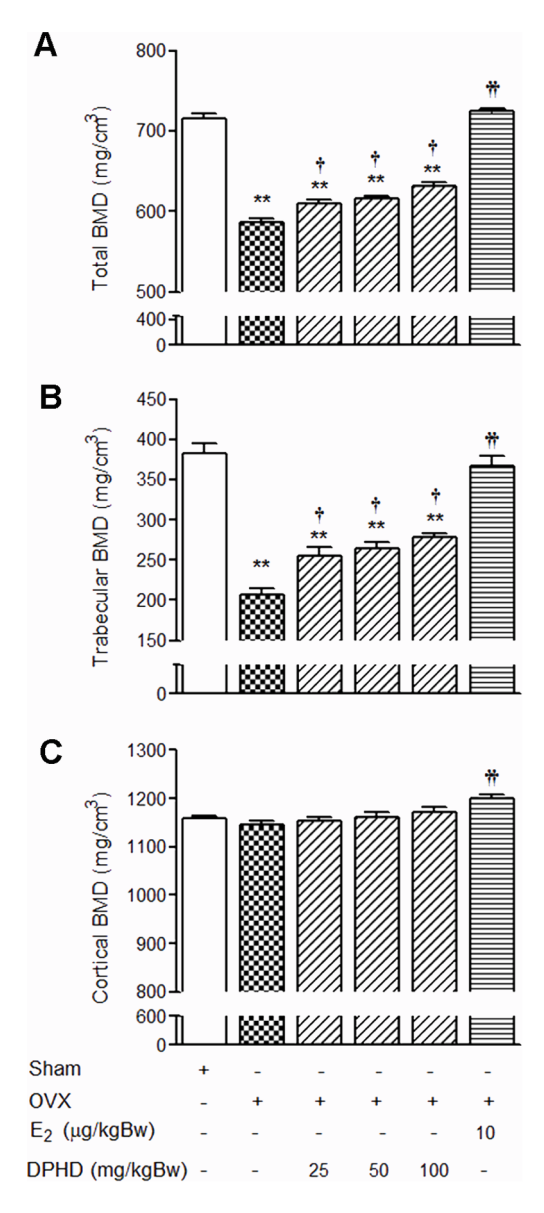


Figure 2. DPHD increases ex vivo bone mineral density (BMD), as measured by pQCT. Total (A), trabecular (B), and cortical (C) BMD of tibial metaphysis from sham-operated and ovariectomized (OVX) rats receiving vehicle, DPHD (25, 50 and 100 mg/kg Bw) or 17β-estradiol (E₂, 10 μg/kg Bw) for 12 weeks. Results are expressed as mean \pm SEM, n=6-8. **p<0.01, significantly different from sham rats. † p<0.05 and †† p<0.01, significantly different from OVX rats. doi:10.1371/journal.pone.0078739.g002

determined by the distance between two fluorochrome markers given at different days and divided by the number of days between administrations. This index reflects the activity of osteoblasts. Compared to sham animals, MAR in OVX rats was significantly increased from 2.89 ± 0.2 to 3.98 ± 0.1 , indicating that ovariectomy caused an increase in new bone formation leading to increase bone turnover (Figure 3G).

Treatments with E₂ or DPHD at doses of 50, and 100 mg/kg BW significantly decreased MAR to levels seen in the sham controls. Bone formation rate (BFR), an index of bone turnover provides the best correlation with the serum bone turnover markers [24], and the bone formation rate per total volume (BFR/TV) was significantly increased after ovariectomy (Figure 3H).

Table 1. Effect of DPHD on bone area and thickness of OVX rats.

Groups/Parameters	Total CSA (mm²)	Trebecular CSA (mm²)	Cortical CSA (mm ²)	Cortical thickness (mm)
Sham	14.61±0.38	7.89±0.30	6.21±0.14	0.68±0.011
OVX + Vehicle	16.50±0.50*	9.51±0.49*	6.41 ± 0.11	0.70 ± 0.010
OVX + DPHD (25 mg/kg)	16.15±0.42*	9.03±0.40*	6.45±0.12	0.70±0.005
OVX + DPHD (50 mg/kg)	$14.99 \pm 0.39^{\dagger}$	$8.36 \pm 0.15^{\dagger}$	6.02±0.12	0.69 ± 0.006
OVX + DPHD (100 mg/kg)	$14.72 \pm 0.44^{\dagger}$	8.12±0.39 [†]	5.91±0.13	0.69±0.005
OVX + E ₂ (10 μg/kg)	$14.73\!\pm\!0.48^{\dagger}$	$7.82 \pm 0.51^{\dagger}$	5.97 ± 0.10	0.68 ± 0.007

Total, trabecular, and cortical cross sectional area (CSA) and cortical thickness were measured from sham-operated and ovariectomized (OVX) rats receiving vehicle, DPHD (25, 50 and 100 mg/kg Bw) or 17β -estradiol (E₂, $10 \mu g/kg$ Bw) for 12 weeks. Data are expressed as mean \pm SEM, n=6-8.

Similar to MAR, the increase in BFR/TV in OVX animals was effectively prevented by treatment with either E_2 or DPHD. The reduction of MAR and BFR in DPHD treated rats indicated that DPHD was capable of decreasing bone turnover rate in a similar manner as E_2 .

Effects of DPHD Treatment on Biochemical Bone Turnover Markers

To evaluate the effect of E₂ and DPHD treatments on bone turnover in OVX rats, we measured the serum osteocalcin concentration and tartrate-resistant acid phosphatase activity. As shown in Figure 4A, the serum osteocalcin concentration in OVX rats was significantly higher than that in sham animals and DPHD treatment of OVX rats significantly reduced the serum osteocalcin concentration. These results indicate that DPHD prevents the ovariectomy-induced increase of bone turnover in rats. The TRAP activity of osteoclast, an index of bone resorption, was 25% higher in OVX rats compared to the sham group and DPHD treatment restored TRAP activity to level similar to those of Sham and E₂-treated groups (Figure 4B). Since the decreases in bone turnover and resorption markers are related to the suppression of bone formation rate, these results suggest that DPHD decreased the bone turnover rate by suppressing osteoclast activity in OVX rats.

Discussion

The present study has demonstrated for the first time of the bone sparing effect of a novel diarylheptanoid phytoestrogen (DPHD) isolated from *C. comosa*. In ovariectomy-induced osteopenia (OVX), a deterioration in trabecular bone microarchitecture (12 weeks after ovariectomy) clearly led to the loss of bone mass in rats. Treatments with DPHD effectively prevented the trabecular bone loss and improved bone microstructure. Moreover, markers of bone turnover, including osteocalcin and TRAP activity, were decreased in DPHD treated animals. These results suggest that DPHD provides a protective effect against OVX-induced bone loss that is associated with decreased bone turnover through suppressing bone resorption.

The integrity of skeletal is maintained through a bone remodeling process that balances bone formation and bone resorption [4] and estrogen plays an important role in the maintenance of bone mass [27]. The rapid decline of estrogens in postmenopausal women results in an imbalance in the bone remodeling process leading to osteoporosis [28]. Mornitoring of BMD is important for diagnosis and the treatment of osteoporosis as decreased bone mass is a major characteristic of this disease. In

this study, decreased BMD in OVX rats, determined using pQCT was observed only in the metaphysic of the tibia, which has a greater proportion of trabecular bone in the proximal end. Trabecular bone, a sponge-like bone found at the ends of long bones and vertebrae, contains osteoblasts and osteoclast on its surface and is more active in bone turnover and bone remodeling compared to cortical bone [29,30]. Indeed, our analysis of OVX rats showed only loss of trabecular BMD. This finding is consistent with previous studies that report the loss of bone in adult OVX rats was more prominent in trabecular than cortical bone [31]. However the loss of trabecular BMD in OVX rats was attenuated by DPHD treatment. Consistent with reports that estrogen decreases periosteal bone formation and radial growth [32], OVX rats displayed an increase in cross sectional bone area indicating that radial growth was increased. Similar to estrogen, treatment with DPHD prevent the increase in bone area in OVX animals. The improvement in bone measurements following DPHD treatment may be partly attributed to its estrogenic like activity, as evidenced by increased uterine weight in DPHD exposed animals (Figure 1C) and our earlier study on uterotropic activity of DPHD [17,18].

A rapid reduction in trabecular bone volume is known to occur following ovariectomy and is associated with an increase in bone turnover rate resulting from an excessive osteoclast activity [33]. Our analysis of the destruction of bone microarchitecture, another important characteristic of osteoporosis, evaluated using bone histomorphometry is consistent with an increased rate of bone turnover in OVX rats. Ovariectomy also markedly decreased static indices, including trabecular bone volume, thickness, and number with an increase in trabecular separation. In addition to direct effects on bone morphology, monitoring changes in circulating bone biochemical markers can also reveal the status of bone remodeling process [34]. These markers include osteocalcin, an osteoblast-specific bone formation marker, and tartrate-resistant acid phosphatase (TRAP) activity, an osteoclastspecific bone resorption marker [34,35]. A dramatic increase in serum osteocalcin and TRAP activity was observed 12 weeks following ovariectomy, confirming that bone loss was due to an increase in bone turnover rate. DPHD reduced these markers of bone turnover in OVX rats suggesting that DPHD prevented trabecular bone loss and micro-architecture deterioration by suppressing the rate of bone turnover either by decreasing bone resorption or increasing bone formation.

DPHD at doses of 25 and 50 mg/kg BW preserved bone mass in OVX rats without showing an uterotrophic effect. These results indicate that the beneficial effect of DPHD on bone is not limited

^{*}p<0.05, significantly different from sham rats.

 $^{^\}dagger$ p<0.05, significantly different from OVX rats.

doi:10.1371/journal.pone.0078739.t001

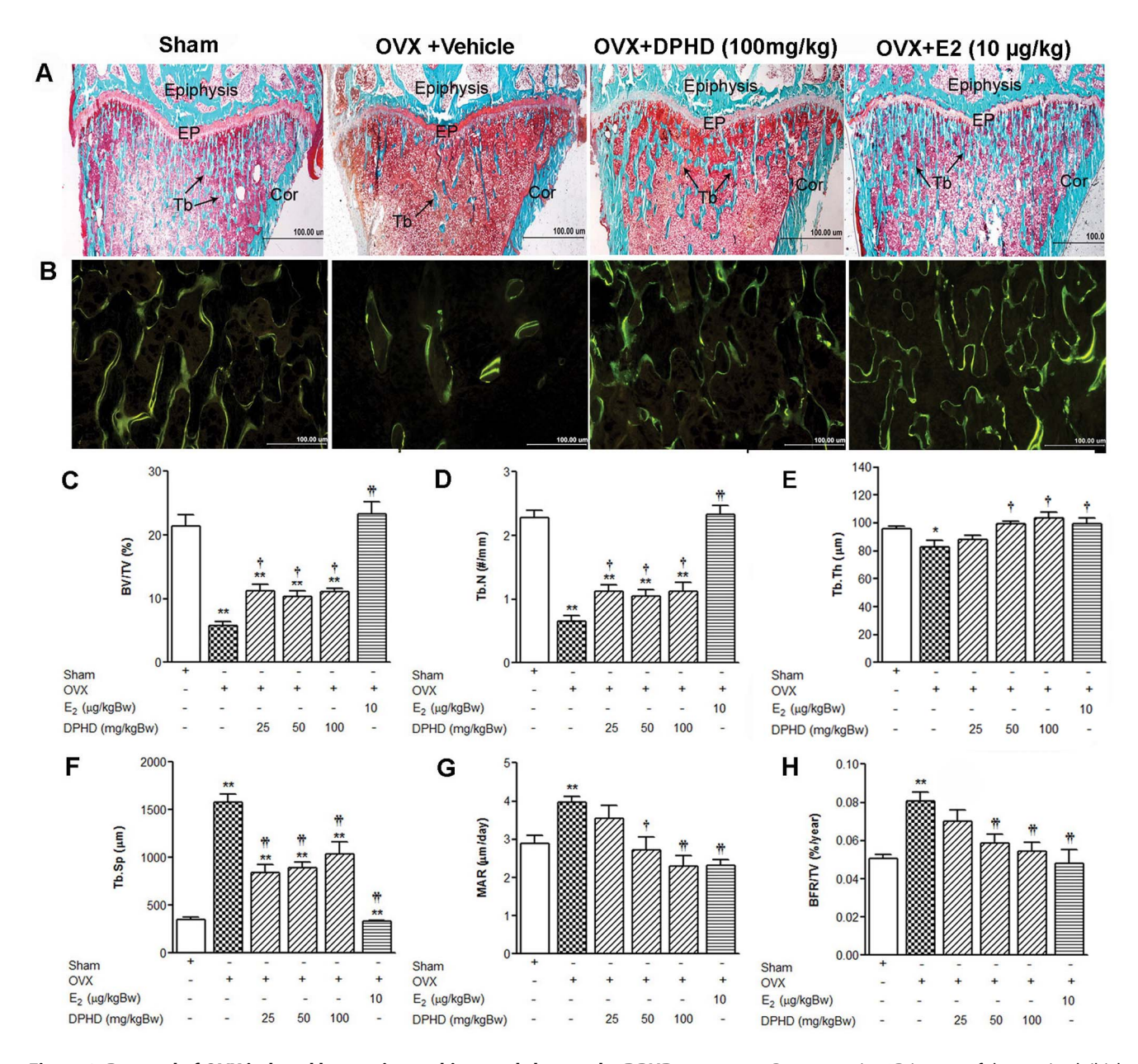


Figure 3. Reversal of OVX induced bone microarchitectural changes by DPHD treatment. Representative 2D images of the proximal tibial metaphysic (trabecular structure) of sham operated and OVX rats receiving vehicle, DPHD (DPHD 100 mg/kg Bw and 17β-estradiol (E₂, 10 μg/kg Bw) for 12 weeks. Samples were stained with Goldner's trichrome for bright-field microscopy at a magnification of 2X showing the following: epiphysis, epiphyseal plate (EP), trabecular bone (Tb), and cortical bone (Cor) (A). Fluorescence micrographs (calcein labeling) (B). Static parameters: trabecular bone volume normalized by tissue volume (BV/TV, %) (C), trabecular number (Tb.N, mm $^{-1}$) (D), trabecular thickness (Tb.Th, μm) (E), and trabecular separation (Tb.Sp, μm) (F). Dynamic parameters: mineral apposition rate (MAR) (G) and bone formation rate (BFR) (H). Data are expressed as the mean \pm SEM, n = 6 - 8. **p<0.01 significantly different from sham rats and † p<0.05 and †† p<0.01, significantly different from OVX rats. doi:10.1371/journal.pone.0078739.g003

to its estrogenic property but also mediate through other biological effects of DPHD, such as an anti-inflammatory activity [19]. Inflammation is one of the causal factors of osteoporosis and several cytokines, such as IL-1, M-CSF and RANKL, are involved in the pathogenesis of osteoporosis. The role of these cytokines is to activate osteoclast differentiation and bone resorption [36]. RANKL, a TNF family member, is synthesized by the osteoblast and is an essential cytokines for activation of osteoclast formation, function, and survival [37]. The interaction of RANKL and RANK stimulates the osteoclastogenesis, the coupling process between the osteoblast and osteoclast to control bone remodeling

[38]. Inhibiting the interaction of RANKL and RANK may have benefits in the treatment of osteoporosis and DPHD treatment reduces mRNA level of RANKL produced by osteoblast cells during differentiation [21]. The inhibitory effect of DPHD on RANKL may in turn attenuate the interaction of RANKL and RANK and subsequently reduce the downstream inflammatory cytokine induced osteoclastogenesis and bone resorption. Estrogen deficiency in OVX rats is associated with the local disturbance of cytokines in bone marrow, leading to an increase in osteoclast numbers that ultimately penetrate trabecular bone and cause deep resorption cavities [39]. Consequentially, trabecular bones are lost

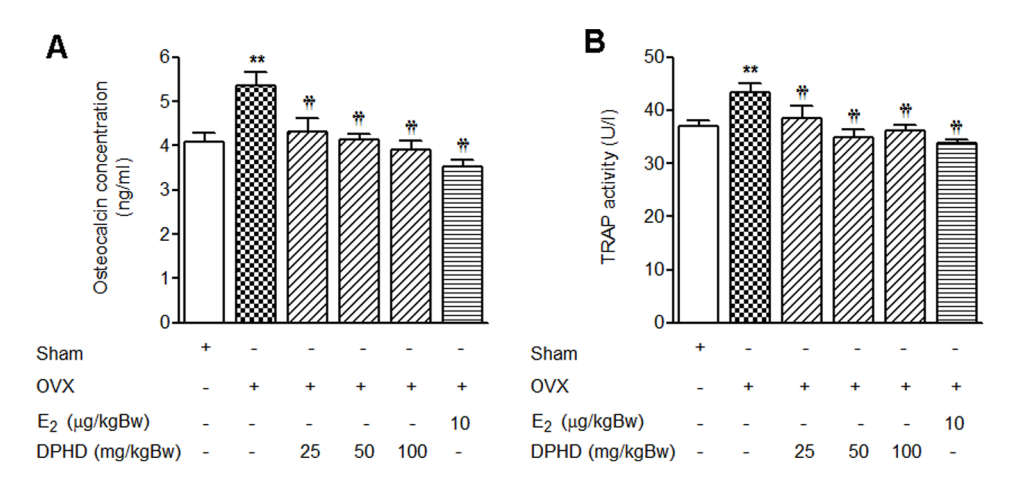


Figure 4. Effects of DPHD on biochemical bone turnover markers. Serum osteocalcin levels (A) and TRAP activity (B) of sham-operated and ovariectomized (OVX) rats receiving the indicated doses of DPHD (25, 50 and 100 mg/kg Bw) or 17β-estradiol (E_2 , 10 μg/kg Bw) for 12 weeks. Results are expressed as the mean \pm SEM, n=6-8. **p<0.01 significantly different from sham rats and †p<0.05 and ††p<0.01, significantly different from OVX rats.

doi:10.1371/journal.pone.0078739.g004

and the remaining bones are less dense, thinner, and widely separated [40]. Changes in cytokine levels in OVX rats may be attenuated by DPHD treatment. If this is the case, then it suggests that DPHD may suppress osteoclast activity. The inhibitory effect of DPHD on both RANKL mRNA expression and interaction of RANKL and RANK in osteoblast cells may in part account for attenuation of bone turnover and preserving bone mass after ovariectomy [21]. Pharmacokinetic analysis indicates that the amount of DPHD used in treatment of OVX rats in the present study would provide an effective concentration in the range similar to that reported in the *in vitro* study [21,40]. However, the response of cytokines to DPHD treatment in OVX rats has not been investigated and any effect of DPHD on osteoclast cells and the inflammatory system remains to be elucidated.

In conclusion, this is the first report on the effect of DPHD on bone turnover and protection of trabecular bone loss in OVX rats. Our results indicate that the novel phytoestrogen, DPHD, exhibits low uterotrophic activity and has potential in clinical applications for preserving bone mass and structure in postmenopausal osteoporosis.

Acknowledgments

We thank Prof. Chumpol Pholpramool and Assoc. Prof. Dr. L. T. Jensen for their critical reading of the manuscript. We also thank Prof. Suchinda Malaivijitnond, Primate Research Unit, Department of Biology, Faculty of Science, Chulalongkorn University and Prof. Yuzuru Hamada, Primate Research Institute, Kyoto University, for allowing the use of peripheral quantitative computed tomography (pQCT). We are also grateful to COCAB for allowing the use of facilities for bone microstructure study.

Author Contributions

Conceived and designed the experiments: DT PP. Performed the experiments: DT PW A. Chuncharunee. Analyzed the data: DT JW A. Chairoungdua. Contributed reagents/materials/analysis tools: AS PP A. Chuncharunee. Wrote the paper: DT PP JW.

References

- Cummings SR, Melton I.J (2002) Epidemiology and outcomes of osteoporotic fractures. Lancet 359: 1761–1767.
- Cauley JA, Thompson DE, Ensrud KC, Scott JC, Black D (2000) Risk of mortality following clinical fractures. Osteoporos Int 11: 556–561.
- Raisz LG (2005) Pathogenesis of osteoporosis: concepts, conflicts, and prospects. J Clin Invest 115: 3318–3325.
- Lerner UH (2006) Bone Remodeling in Post-menopausal Osteoporosis. Journal of Dental Research 85: 584–595.
- Downey PA, Siegel MI (2006) Bone Biology and the Clinical Implications for Osteoporosis. Physical Therapy 86: 77–91.
- Stevenson M, Jones ML, Nigris ED, Brewer N, Davis S, et al. (2005) A systematic review and economic evaluation of alendronate, etidronate, risedronate, raloxifene and teriparatide for the prevention and treatment of postmenopausal osteoporosis. Health Technology Assessment 9: 1–160.
- Felson DT, Zhang Y, Hannan MT, Kiel DP, Wilson P, et al. (1993) The Effect of Postmenopausal Estrogen Therapy on Bone Density in Elderly Women. New England Journal of Medicine 329: 1141–1146.
- Tham DM, Gardner CD, Haskell WL (1998) Potential Health Benefits of Dietary Phytoestrogens: A Review of the Clinical, Epidemiological, and Mechanistic Evidence. Journal of Clinical Endocrinology & Metabolism 83: 2223–2235.
- Messina MJ, Wood CE (2008) Soy isoflavones, estrogen therapy, and breast cancer risk; analysis and commentary. Nutr J 7: 17.
- Blair HC, Jordan SE, Peterson TG, Barnes S (1996) Variable effects of tyrosine kinase inhibitors on avian osteoclastic activity and reduction of bone loss in ovariectomized rats. J Cell Biochem 61: 629–637.

- Sugimoto E, Yamaguchi M (2000) Stimulatory effect of Daidzein in osteoblastic MC3T3-E1 cells. Biochem Pharmacol 59: 471–475.
- Dang ZC, Lowik C (2005) Dose-dependent effects of phytoestrogens on bone. Trends Endocrinol Metab 16: 207–213.
- Ren P, Ji H, Shao Q, Chen X, Han J, et al. (2007) Protective effects of sodium daidzein sulfonate on trabecular bone in ovariectomized rats. Pharmacology 79: 129–136.
- Piyachaturawat P, Ercharuporn S, Suksamrarn A (1995) Uterotrophic Effect of Curcuma comosa in Rats. Pharmaceutical Biology 33: 334–338.
- Weerachayaphorn J, Chuncharunee A, Mahagita C, Lewchalermwongse B, Suksamrarn A, et al. (2011) A protective effect of *Curcuma comosa* Roxb. on bone loss in estrogen deficient mice. J Ethnopharmacol 137: 956–962.
- Suksamrarn A, Ponglikitmongkol M, Wongkrajang K, Chindaduang A, Kittidanairak S, et al. (2008) Diarylheptanoids, new phytoestrogens from the rhizomes of *Curcuma comosa*: Isolation, chemical modification and estrogenic activity evaluation. Bioorg Med Chem 16: 6891–6902.
- Winuthayanon W, Suksen K, Boonchird C, Chuncharunee A, Ponglikitmongkol M, et al. (2009) Estrogenic activity of diarylheptanoids from *Curcuma comosa* Roxb. Requires metabolic activation. J Agric Food Chem 57: 840–845.
- Winuthayanon W, Piyachaturawat P, Suksamrarn A, Ponglikitmongkol M, Arao Y, et al. (2009) Diarylheptanoid phytoestrogens isolated from the medicinal plant Curcuma comosa: biologic actions in vitro and in vivo indicate estrogen receptordependent mechanisms. Environ Health Perspect 117: 1155–1161.
- Thampithak A, Jaisin Y, Meesarapee B, Chongthammakun S, Piyachaturawat P, et al. (2009) Transcriptional regulation of iNOS and COX-2 by a novel compound from *Curcuma comosa* in lipopolysaccharide-induced microglial activation. Neurosci Lett 462: 171–175.

- Bhukhai K, Suksen K, Bhummaphan N, Janjorn K, Thongon N, et al. (2012) A
 phytoestrogen diarylheptanoid mediates estrogen receptor/Akt/glycogen synthase kinase 3beta protein-dependent activation of the Wnt/beta-catenin
 signaling pathway. J Biol Chem 287: 36168–36178.
- Tantikanlayaporn D, Robinson LJ, Suksamrarn A, Piyachaturawat P, Blair HC (2013) A diarylheptanoid phytoestrogen from *Curcuma comosa*, 1,7-diphenyl-4,6-heptadien-3-ol, accelerates human osteoblast proliferation and differentiation. Phytomedicine 20: 676–682.
- Urasopon N, Hamada Y, Asaoka K, Cherdshewasart W, Malaivijitnond S (2007) Pueraria mirifica, a phytoestrogen-rich herb, prevents bone loss in orchidectomized rats. Maturitas 56: 322–331.
- Suntornsaratoon P, Wongdee K, Goswami S, Krishnamra N, Charoenphandhu N (2010) Bone modeling in bromocriptine-treated pregnant and lactating rats: possible osteoregulatory role of prolactin in lactation. Am J Physiol Endocrinol Metab 299: E426–436.
- 24. Ott SM (2008) Histomorphometric measurements of bone turnover, mineralization, and volume. Clin J Am Soc Nephrol 3 Suppl 3: S151–156.
- Parfitt AM, Mathews CH, Villanueva AR, Kleerekoper M, Frame B, et al. (1983) Relationships between surface, volume, and thickness of iliac trabecular bone in aging and in osteoporosis. Implications for the microanatomic and cellular mechanisms of bone loss. J Clin Invest 72: 1396–1409.
- Lau KH, Onishi T, Wergedal JE, Singer FR, Baylink DJ (1987) Characterization and assay of tartrate-resistant acid phosphatase activity in serum: potential use to assess bone resorption. Clinical Chemistry 33: 458–462.
- Manolagas SC (2000) Birth and death of bone cells: basic regulatory mechanisms and implications for the pathogenesis and treatment of osteoporosis. Endocr Rev 21: 115–137.
- 28. Sample SJ, Racette MA, Hao Z, Thomas CF, Behan M, et al. (2012) Functional adaptation in female rats: the role of estrogen signaling. PLoS ONE 7: e43215.
- 29. Gasser JA (1995) Assessing bone quantity by pQCT. Bone 17: S145–S154.

- Khosla S, Westendorf J, Oursler M (2008) Building bone to reverse osteoporosis and repair fractures. J Clin Invest;118(2): 421–8 118: 421–428.
- Breen SA, Millest AJ, Loveday BE, Johnstone D, Waterton JC (1996) Regional
 analysis of bone mineral density in the distal femur and proximal tibia using
 peripheral quantitative computed tomography in the rat In vivo. Calcified
 Tissue International 58: 449–453.
- 32. Vanderschueren D, Vandenput L, Boonen S, Lindberg MK, Bouillon R, et al. (2004) Androgens and Bone. Endocrine Reviews 25: 389–425.
- Wronski TJ, Cintron M, Doherty AL, Dann LM (1988) Estrogen treatment prevents osteopenia and depresses bone turnover in ovariectomized rats. Endocrinology 123: 681–686.
- Lelovas PP, Xanthos TT, Thoma SE, Lyritis GP, Dontas IA (2008) The laboratory rat as an animal model for osteoporosis research. Comp Med 58: 424–430.
- Habermann B, Eberhardt C, Feld M, Zichner L, Kurth AA (2007) Tartrateresistant acid phosphatase 5b (TRAP 5b) as a marker of osteoclast activity in the early phase after cementless total hip replacement. Acta Orthop 78: 221–225.
- Redlich K, Smolen JS (2012) Inflammatory bone loss: pathogenesis and therapeutic intervention. Nat Rev Drug Discov 11: 234–250.
- Peng X, Guo W, Ren T, Lou Z, Lu X, et al. (2013) Differential Expression of the RANKL/RANK/OPG System Is Associated with Bone Metastasis in Human Non-Small Cell Lung Cancer. PLoS ONE 8: e58361.
- Boyle WJ, Simonet WS, Lacey DL (2003) Osteoclast differentiation and activation. Nature 423: 337–342.
- Wronski TJ, Cintron M, Dann LM (1988) Temporal relationship between bone loss and increased bone turnover in ovariectomized rats. Calcif Tissue Int 43: 179–183.
- Weinstein RS, Majumdar S (1994) Fractal geometry and vertebral compression fractures. J Bone Miner Res 9: 1797–1802.

ELSEVIER

Contents lists available at ScienceDirect

Bioorganic & Medicinal Chemistry Letters

journal homepage: www.elsevier.com/locate/bmcl



Synthesis, cytotoxicity against human oral cancer KB cells and structure–activity relationship studies of trienone analogues of curcuminoids



Thipphawan Chuprajob ^a, Chatchawan Changtam ^b, Ratchanaporn Chokchaisiri ^c, Warangkana Chunglok ^d, Nilubon Sornkaew ^a, Apichart Suksamrarn ^{a,*}

- a Department of Chemistry and Center of Excellence for Innovation in Chemistry, Faculty of Science, Ramkhamhaeng University, Bangkok 10240, Thailand
- ^b Division of Physical Science, Faculty of Science and Technology, Huachiew Chalermprakiet University, Samutprakarn 10540, Thailand
- ^c Department of Chemistry, School of Science, University of Phayao, Phayao 56000, Thailand
- ^d School of Allied Health Sciences and Public Health, Walailak University, Nakhon Si Thammarat 80160, Thailand

ARTICLE INFO

Article history: Received 25 January 2014 Revised 15 April 2014 Accepted 25 April 2014 Available online 5 May 2014

Keywords: Curcuminoid Trienone analogue Synthesis Cytotoxicity KB

ABSTRACT

A general method for the synthesis of substituted (1*E*,4*E*,6*E*)-1,7-diphenylhepta-1,4,6-trien-3-ones, based on the aldol condensations of substituted 4-phenylbut-3-en-2-ones and substituted 3-phenylacrylaldehydes, was achieved. The natural trienones **4** and **5** have been synthesized by this method, together with the trienone analogues **9–20**. These analogues were evaluated for their cytotoxic activity against human oral cancer KB cell line. The structure–activity relationship study has indicated that the analogues with the 1,4,6-trien-3-one function are more potent than the curcuminoid-type function. Analogues with *meta*-oxygen function on the aromatic rings are more potent than those in the *ortho*- and *para*-positions. Free phenolic hydroxy group is more potent than the corresponding methyl ether analogues. Among the potent trienones, compounds **11**, **18** and **20** were more active than the anticancer drug ellipticine. All compounds were also evaluated against the non-cancerous Vero cells and it was found that compounds **11**, **12** and **17** were much less toxic than curcumin (1); they showed high selectivity indices of 35.46, 33.46 and 31.68, respectively. These analogues are regarded as the potent trienones for anti-oral cancer study.

© 2014 Elsevier Ltd. All rights reserved.

Curcuminoids are the major constituents of turmeric (*Curcuma longa* L., Zingiberaceae) and have been used for centuries as a dietary pigment, spice and traditional medicine in India and China. The major curcuminoid isolated from this plant species is curcumin (1), with demethoxycurcumin (2) and bisdemethoxycurcumin (3) as the minor constituents. Curcuminoids exhibited many interesting biological activities, for example, antioxidant activity, anti-inflammatory activity, anticancer activity, anti-protozoal activity and anti-HIV activity. In clinical report, curcuminoids could be orally taken up to 12 g/day without toxic effect in humans. Therefore, many researchers have used this class of compounds to study different biological activities. Some of these studies investigated the role of α , β -unsaturated β -diketo moiety and it was concluded that this functional group is necessary for the biological activities. $\frac{11,12}{1}$ Recently, a new curcuminoid

analogue, 1,7-bis(4-hydroxyphenyl)-1,4,6-heptatrien-3-one (**4**) (see Fig. 1), which is structurally related to the curcuminoid **3**, has been isolated as a minor component of *C. longa.*¹³ This compound inhibited the production of TNF-α in lipopolysaccharide-activated macrophages.¹⁴ Another new curcuminoid analogue, 1,7-bis(4-hydroxy-3-methoxyphenyl)-1,4,6-heptatrien-3-one (**5**), which is structurally related to the curcuminoid **1**, has later been isolated.¹⁵ It is interesting to note that these two compounds possess a 1E,4E,6E-heptatrien-3-one functionality, which is a rare group of naturally occurring curcuminoid analogue and has not much been studied, especially the biological activities of this type of compounds.

The structural diversity of the trienones **4** and **5** has prompted us to investigate their biological activities. However, the scarcity of these compounds in natural sources has prevented us from obtaining them for biological activity evaluations. In order to see whether this group of curcuminoid analogues exhibited more interesting biological activities than those of the curcuminoids **1–3**, we decided to synthesize the natural trienones **4** and **5**. Within

^{*} Corresponding author. Tel.: +66 2 319 0931; fax: +66 2 319 1900.

E-mail addresses: s_apichart@ru.ac.th, asuksamrarn@yahoo.com

(A. Suksamrarn).

1:
$$R^1 = R^2 = OMe$$

2: $R^1 = OMe$, $R^2 = H$
2: $R^1 = OMe$, $R^2 = H$
3. $R^2 = OMe$
2: $R^1 = OMe$, $R^2 = H$
5: $R^1 = R^2 = OMe$

Figure 1. Structures of the natural curcuminoids, curcumin (1), demethoxycurcumin (2) and bisdemethoxycurcumin (3), and the natural trienones 4 and 5.

the heptatrien-3-one framework, the analogues containing different hydroxy and methoxy substituents on the aromatic moieties would then be synthesized if the trienones **4** and **5** showed higher biological activity than the corresponding curcuminoids **3** and **1**.

Oral cancer is a major health problem in the economically developing countries. According to GLOBOCAN 2012, oral cancer was estimated to account for 2.1% of all cancers. 16 There were about 300,000 oral cancer cases in 2012 worldwide and about 50% of patients died from this type of cancer. The five-year relative survival rate of oral cancer patients is less than 35% in advanced stage of disease at initial diagnosis. 17 Late diagnosis, disease recurrence, metastasis and resistant to therapy may attribute to this poor survival rate. Conventional treatments, including surgical treatment combined with radiotherapy and chemotherapy or concomitant chemo-radiotherapy, have limited efficacy and result in adverse systemic and cytotoxic effects on normal cells. Chemoprevention is a promising treatment strategy for oral cancer. Appropriate chemopreventive agents should be inexpensive, nontoxic, and target important pathways involved in the development of this cancer. Combining chemopreventive agents and conventional therapeutic approaches may reduce toxicities and improving treatment outcomes. The addition of cetuximab, epidermal growth factor receptor (EGFR) targeted chemopreventive agent, to current conventional chemotherapeutic agents (cisplatin and 5-fluorouracil) represents a standard systemic treatment for recurrent or metastatic cancer. 18,19 However, the concurrent therapy also leads to substantial toxicities and the overall survival remains short. To date, various molecular targeted chemopreventive agents are actively under investigation, but the only pharmacologic strategy targeting the EGFR has been approved by regulatory agencies worldwide to treat this oral cancer.²⁰

The synthesis of the trienone **4** has been reported in seven steps in good yield.²¹ Compound **5** has previously been prepared by a multi-step chemical modification of compound **1**.²² However, we would like to have a general method for the synthesis of substituted trienones, so that a wide variety of this group of compounds could be prepared in case the trienones **4** and **5** exhibited better cytotoxic activity than the respective curcuminoids **3** and **1**. The

retrosynthetic analysis of (1*E*,4*E*,6*E*)-1,7-diarylhepta-1,4,6-trien-3-ones by cross aldol condensation reaction has been proposed as shown in Scheme 1. Despite the fact that this type of condensation sometimes gives low yield of products, ²³ it was nevertheless is a convenient and concise procedure for the synthesis of a large number of analogues for biological evaluation and structure-activity relationship study. Disconnection of the C4–C5 bond of the seven-carbon linker gave two key fragments, substituted 4-phenylbut-3-en-2-ones (substituted cinnamones) and substituted 3-phenylacrylaldehydes (substituted cinnamaldehydes). The resulting substituted 4-phenylbut-3-en-2-ones and substituted 3-phenylacrylaldehydes would then be further disconnected to the substituted benzaldehydes (Scheme 1).

The key fragment substituted 4-phenylbut-3-en-2-ones and 3phenylacrylaldehydes used for synthesis of the natural trienones (4, 5) and analogues (9-15 and 17-20) were prepared as shown in Scheme 2. Condensation of the substituted benzaldehydes (6a1-d1, 6e and 6f) with excess acetone under basic aldol condensations at room temperature gave the substituted 4-phenylbut-3en-2-one analogues 7a1-d1, 7e and 7f. The analogue 7c3 was obtained by methylation of 7c1 using methyl iodide in the presence of potassium carbonate in acetone. The synthesis of substituted 3-phenylacrylaldehydes 8a1-d1 were planned by coupling of the substituted benzaldehydes **6a1-d1** with acetaldehyde, using aldol condensation in the same method as that of substituted 4phenylbut-3-en-2-one analogues. In this method, we were able to successfully generate only the meta-hydroxy-3-phenylacrylaldehyde analogue 8c1. However, we failed to generate the orthoand para-3-phenylacrylaldehydes 8a1, 8b1 and 8d1. In view of these results, the ortho- and para-hydroxy groups of benzaldehydes 6a1, 6b1 and 6d1 were therefore protected as its tetrahydropyranyl (THP) ethers²⁴ **6a2**, **6b2** and **6d2**, which were then condensed with acetaldehyde to yield the intermediates 8a2, 8b2 and 8d2. Removal of the THP protecting group gave the corresponding 3-phenylacrylaldehydes 8a1, 8b1 and 8d1, respectively. Methylation of **8c1** yielded the analogue **8c3**.

The trienones **4**, **5** and the analogues were synthesized as shown in Scheme 3. Compound **4** was synthesized by the following

Scheme 1. Retrosynthesis of (1E,4E,6E)-1,7-diphenylhepta-1,4,6-trien-3-one analogues.

Scheme 2. Synthesis of the substituted 4-phenylbut-3-en-2-ones **7a**-**f** and the substituted 3-phenylacrylaldehydes **8a**-**d** from the aldehydes **6a**-**f**. Reagents and conditions: (i) excess acetone, 20% aq NaOH, EtOH; (ii) 3,4-dihydro-2*H*-pyran, *p*-TsOH, THF; (iii) Mel, K₂CO₃, acetone, rt; (iv) excess acetaldehyde, 20% aq NaOH, EtOH, 0–10 °C; (v) *p*-TsOH, MeOH–H₂O.

7a1 + 8a1
$$\rightarrow$$
 4: $R^1 = R^2 = R^4 = R^5 = H$, $R^3 = R^6 = OH$, 29% , 32% from $8a2$

7a1 + 8a2 \rightarrow 4a: $R^1 = R^2 = R^4 = R^5 = H$, $R^3 = OH$, $R^6 = OTHP$

7b1 + 8b1 \rightarrow 5: $R^1 = R^4 = H$, $R^2 = R^5 = OMe$, $R^3 = R^6 = OH$, 12% , 14% from $8b2 \rightarrow 0$ (ii)

7b1 + 8b2 \rightarrow 5a: $R^1 = R^4 = H$, $R^2 = R^5 = OMe$, $R^3 = OH$, $R^6 = OTHP$

7a1 + 8c1 \rightarrow 9: $R^1 = R^2 = R^4 = R^6 = H$, $R^3 = R^6 = OH$, 12% , 14% from 12% (iii)

7a1 + 8d2 \rightarrow 10a: 12% 12% 12% 13%

Scheme 3. Synthesis of the trienones 4, 5, 9–15 and 17–20 from aldol condensation of the substituted 4-phenylbut-3-en-2-ones 7a–f and the substituted 3-phenylacrylaldehydes 8a–d, and methylation of the trienone 11 to 16. Reagents and conditions: (i) 20% aq NaOH, EtOH, 0 °C–rt; (ii) 3 M HCl; (iii) Mel, K₂CO₃, acetone, rt.

two different approaches. Condensation of 7a1 with 8a1 under aldol condition gave the trienone 4 in 29% yield. Alternatively, condensation of 7a1 with the intermediate 3-phenylacrylaldehyde 8a2 gave 4a and subsequent THP deprotection with 3 M HCl yielded the trienone **4**. The trienone **5** was similarly synthesized in 12% yield from 7b1 and 8b1, or in 14% from 7b1 and 3-phenylacrylaldehyde **8b2** to yield the intermediate **5a** followed by deprotection of the THP group. All other trienone analogues, 9-15 and 17-20, were similarly obtained from direct coupling of substituted hydroxy and/or methoxy 4-phenylbut-3-en-2-ones (7a1-d1, 7e, **7f** and **7c3**) with substituted hydroxy or methoxy 3-phenylacrylaldehydes (8a1, 8c1, 8d1 and 8c3) (Scheme 3). The trienone 16 was obtained by methylation of compound 11. All synthesized analogues were purified by crystallization or column chromatography and characterized by NMR (1H and 13C NMR, and 2D COSY, HMQC and HMBC) and mass spectroscopy (see Supplementary data).

The natural curcuminoids 1–3, the trienone analogues 4 and 5, and analogues 9-20 were subjected to cytotoxic activity evaluation against the KB cells using resazurin microplate assay for cancer cell growth inhibition²⁵ and the results are presented in Table 1. Compounds 1-3 exhibited weak cytotoxicity against this cancer cell line, with the IC_{50} values of 21.36, 26.45 and 21.44 μM , respectively, which was much less active than ellipticine, the reference anticancer drug, which exhibited cytotoxicity against KB cells at IC_{50} of 2.25 μ M. The trienone analogues **4** and **5**, however, showed strong and moderate cytotoxic effects at IC_{50} of 5.75 and 12.23 μ M, respectively. An increase in cytotoxicity of 1.7-fold from the curcuminoid 1 to the trienone 5, and 3.7-fold from the curcuminoid 3 to the trienone 4 was very significant; it implied that the 1,4,6trien-3-one moiety contributed to higher cytotoxicity against the KB cells than the 1,6-dien-3,5-dione moiety of the curcuminoids. This finding has prompted us to further investigate cytotoxicity

Table 1
The structure and cytotoxicity of trienones against KB and Vero cells and selectivity index

Compound/structure		Cytotoxicity (IC ₅₀ , μM)		SI ^c	
		KB ^a Vero ^b			
1	MeO O O O O O O O O O O O O O O O O O O	21.36	35.05	1.64	
2	MeO OH	26.45	CD^d	_	
3	но	21.44	CD^{d}	_	
4	но	5.75	9.65	1.68	
5	MeO OMe	12.23	6.78	0.55	
9	но	2.98	10.81	3.63	
10	но	8.16	12.18	1.49	
11	HO OH O	1.72	60.99	35.46	
12	ОН О ОН	2.35	78.64	33.46	
13		11.19	19.60	1.75	
14	MeO OH OMO	4.47	8.00	1.79	
15	O	19.06	5.68	0.30	
16	MeO OMe	20.10	54.37	2.70	
17	HO OH MeO	2.90	91.86	31.68	
18	MeO OH	1.70	10.49	6.17	
19	MeO OH	7.57	14.36	1.90	

Table 1 (continued)

Compound/structure		Cytotoxicity (IC ₅₀ , μM)		SI ^c
		KB ^a	Vero ^b	
20	но	1.36	6.97	5.13
Ellipticine	НО	2.25	6.48	2.88

- ^a Cancer of the oral cavity.
- ^b Green African monkey kidney cells.
- ^c Selectivity index = IC_{50} for normal cell line/ IC_{50} for cancerous cell line.
- ^d Could not be determined due to fluorescence behavior of the compound.

of other trienone analogues. The strategy was to modify the trienone structure by varying number and position of the oxygen functions (hydroxy/methoxy groups). As the trienone 4 was about 2-fold more potent than the trienone 5, it was used as the structure lead for analogues with higher cytotoxic activity. In order to see whether substitution pattern of the oxygen function on the aromatic rings affected the cytotoxicity of the trienone structure, compound 9, the B-ring meta-hydroxy analogue of the trienone 4, was synthesized and it was found that this analogue was approximately 2-fold more active than **4**, with the IC₅₀ of 2.98 μ M. In order to see the effect of oxygenation patterns on ring B compared to the para- and meta-hydroxy analogues 4 and 9, the ortho-hydroxy analogue 10 was synthesized and it was found that its cytotoxicity $(IC_{50}~8.16~\mu M)$ was lower than both the analogues 4 and 9. The oxygen function at the meta-position of the B-ring is therefore essential for high cytotoxicity against KB cells. In order to see the effect of oxygenation patterns on ring A, the high cytotoxic compound 9 was further modified by moving the hydroxy group at the para-position on the A ring to the meta-position to give the trienone 11 and this analogue was found to be highly toxic against the KB cells; the IC₅₀ of this compound was 1.72 μ M, or 3.3-fold more active than the trienone 4. It is worth noting that the trienone 11 was 1.3-fold more active than ellipticine. In order to see the effect of replacement of the meta-hydroxy group on the A-ring of compound 11 by the ortho-hydroxy group, compound 12 was synthesized and its cytotoxic activity was 1.4-fold less active than 11; its IC₅₀ value was 2.35 µM, which was almost as active as ellipticine. As expected, placement of the hydroxy groups at the orthopositions on the A- and B-rings in analogue 13 resulted in decrease in activity compared with the meta- or para-dihydroxy analogue; it exhibited moderate cytotoxicity with IC_{50} of 11.19 μM , that is 6.5and 2-fold less active than compounds 11 and 4, respectively. The results have indicated that the presence of hydroxy group at the meta-position of the A-ring was also responsible for the increase in cytotoxicity against KB cells. The contribution of free hydroxy group on cytotoxic activity was demonstrated by the methyl ether 14 that showed 2.6-fold decrease in activity when compared with compound 11. Sharp decrease in cytotoxicity was observed in the isomeric B-ring methyl ether 15; it was 11-fold less active than compound 11. As expected, full methylation of 11 resulted in the analogue 16 which showed weak cytotoxic activity.

In order to see the effect of an extra oxygen function on the aromatic ring, the A-ring 3-hydroxy-4-methoxy analogue **17** was evaluated for cytotoxicity and this compound exhibited 1.7-fold less active than compound **11**. The isomeric A-ring 4-hydroxy-3-methoxy analogue **18**, however, exhibited unexpectedly high activity; it showed comparable cytotoxic potency (IC $_{50}$ 1.70 μ M) to that of compound **11**. In order to compare the B-ring *para*-hydroxy analogue of compound **18** and to make a complete set of the trienone analogue of demethoxycurcumin (**2**), the trienone **19** was synthesized and cytotoxicity was evaluated. As expected, it was more

active (IC_{50} 7.57 μ M) than the curcuminoid **2** and was less active than its isomeric B-ring *meta*-hydroxy analogue **18**. Removal of the methyl group from either compound **17** or **18** gave the corresponding trihydroxy analogue **20**. Surprisingly, compound **20** exhibited the most active cytotoxicity among the trienones tested; its IC_{50} was 1.36 μ M, or 1.7-fold more active than ellipticine.

The results have indicated that the analogues with the 1,4,6-trien-3-one function are more potent than the curcuminoids with the 1,6-dien-3,5-dione function. Analogues with *meta*-oxygen function on both aromatic rings are more potent than those in the *ortho*- and *para*-positions. Free phenolic hydroxy group is more potent than the corresponding methyl ether analogues.

To assess whether the cytotoxic activity described above should be attributed to general toxicity, rather than specific cytotoxic activity of compounds to the cancer cells, these analogues were also tested for their effect on the normal cells (Vero cells, the African green monkey kidney cells) using green fluorescent protein (GFP) detection method²⁶ and the results are included in Table 1. The results have indicated that most of the trienones were toxic against Vero cells and were more toxic than curcumin (1), which was regarded as weakly toxic, except compounds 11, 12, 16 and 17, which were approximately 2- to 3-fold less toxic than the curcuminoid 1. The selectivity indices (SIs, Table 1) of the toxic trienones were between 0.30 and 6.17, whereas those of 1 and ellipticine were 1.64 and 2.88, respectively. In contrast, the SIs of the nontoxic or less toxic trienones, 11, 12 and 17, were 35.46, 33.46 and 31.68, which were relatively very high. Among these three highly active trienones with high SIs, the trienone 11 seems to be the most suitable compound for further in-depth study.

In conclusion, we report the general method for the synthesis of the (1E,4E,6E)-1,7-diarylhepta-1,4,6-trien-3-one based on the aldol condensations of substituted 4-phenylbut-3-en-2-ones and substituted 3-phenylacrylaldehydes. The natural trienones 4 and 5 have been synthesized by this method, together with the trienone analogues 9-20. These analogues were evaluated for their cytotoxic effects against KB cell line. The results have indicated that the analogues with the 1,4,6-trien-3-one function are more potent than the curcuminoids. Analogues with meta-oxygen function on the aromatic rings are more potent than those in the ortho- and parapositions. Free phenolic hydroxy group is more potent than the corresponding methyl ether analogues. Among the potent trienones, compounds 11, 18 and 20 were more active than the anticancer drug ellipticine. All compounds were also evaluated against the non-cancerous Vero cells and it was found that compounds 11, 12 and 17 were much less toxic than curcumin (1); they showed high selectivity indices of 35.46, 33.46 and 31.68, respectively.

Acknowledgments

This work was supported by The Thailand Research Fund. Financial support from the Center of Excellence for Innovation in Chemistry (PERCH-CIC), Office of the Higher Education Commission, Ministry of Education is gratefully acknowledged.

Supplementary data

Supplementary data (¹H, ¹³C NMR and DEPT spectra and mass spectroscopic data) associated with this article can be found, in the online version, at http://dx.doi.org/10.1016/j.bmcl.2014.04.

References and notes

- Maheshwari, R. K.; Singh, A. K.; Gaddipatti, J.; Srimal, R. C. Life Sci. 2006, 78, 2081
- Ruby, A. J.; Kuttan, G.; Babu, K. D.; Rajasekharan, K. N.; Kuttan, R. Cancer Lett. 1995, 94, 79.
- Grinberg, L. N.; Shalev, O.; Tønnesen, H. H.; Rachmilewitz, E. A. Int. J. Pharm. 1996, 132, 251.
- 4. Chan, M. M.-Y.; Ho, C.-T.; Huang, H.-I. Cancer Lett. 1995, 96, 23.
- Chan, M. M.-Y.; Huang, H.-I.; Fenton, M. R.; Fong, D. Biochem. Pharmacol. 1998, 55, 1955.
- Inano, H.; Onoda, M.; Inafuku, N.; Kubota, M.; Kamada, Y.; Osawa, T.; Kobayashi, H.; Wakabayashi, K. Carcinogenesis 2000, 21, 1835.
- 7. Thapliyal, R.; Maru, G. B. Food Chem. Toxicol. 2001, 39, 541.
- 8. Araujo, C. A. C.; Alegrio, L. V.; Gomes, D. C. F.; Lima, M. E. F.; Gomes-Cardoso, L.; Leon, L. L. Mem. Inst. Oswaldo Cruz 1999, 94, 791.
- 9. Mazumder, A.; Raghavan, K.; Weinstein, J.; Kohn, K. W.; Pommier, Y. Biochem. Pharmacol. 1995, 49, 1165.
- Liang, G.; Shao, L.; Wang, Y.; Zhao, C.; Chu, Y.; Xiao, J.; Zhao, Y.; Li, X.; Yang, S. Bioorg. Med. Chem. 2009, 17, 2623.

- 11. Pan, M.-H.; Lin-Shiau, S.-Y.; Lin, J.-K. Biochem. Pharmacol. 2000, 60, 1665.
- Ohtsu, H.; Xiao, Z.; Ishida, J.; Nagai, M.; Wang, H.-K.; Itokawa, H.; Su, C.-Y.; Shih, C.; Chiang, T.; Chang, E.; Lee, Y. F.; Tsai, M.-Y.; Chang, C.; Lee, K.-H. J. Med. Chem. 2002, 45, 5037.
- Nakayama, R.; Tamura, Y.; Yamanaka, H.; Kikuzaki, H.; Nakatani, N. Phytochemistry 1993, 33, 501.
- 14. Jang, M. K.; Sohn, D. H.; Ryu, J.-H. Planta Med. 2001, 67, 550.
- 15. Park, S.-Y.; Kim, D. S. H. L. J. Nat. Prod. 2002, 65, 1227.
- Ferlay, J.; Soerjomataram, İ.; Ervik, M.; Dikshit, R.; Eser, S.; Mathers, C.; Rebelo, M.; Parkin, D. M.; Forman, D.; Bray, F. GLOBOCAN 2012 v1.0, Cancer Incidence and Mortality Worldwide: IARC CancerBase No. 11 [Internet]; International Agency for Research on Cancer: Lyon, France, 2013.
- 17. Siegel, R.; Naishadham, D.; Jemal, A. CA Cancer J. Clin. 2012, 62, 10.
- Peyrade, F.; Cupissol, D.; Geoffrois, L.; Rolland, F.; Borel, C.; Ciais, C.; Faivre, S.; Guigay, J. Oral Oncol. 2013, 49, 482.
- Vermorken, J. B.; Licitra, L.; Stöhlmacher-Williams, J.; Dietz, A.; Lopez-Picazo, J. M.; Hamid, O.; Hossain, A. M.; Chang, S. C.; Gauler, T. C. Eur. J. Cancer 2013, 49, 2877.
- 20. Du, Y.; Peyser, N. D.; Grandis, J. R. Pharmacol. Ther. 2014, 142, 88.
- 21. Da, S. J.; Huang, C. S.; Li, X. H.; Li, Y. L. Chin. Chem. Lett. 1997, 8, 291.
- Changtam, C.; De Koning, H. P.; Ibrahim, H.; Sajid, M. S.; Gould, M. K.; Suksamrarn, A. Eur. J. Med. Chem. 2010, 45, 941.
- (a) Shen, L.; Sun, D. Tetrahedron Lett. 2011, 52, 4570; (b) Dhuru, S.; Bhedi, D.; Gophane, D.; Hirbhagat, K.; Nadar, V.; More, D.; Parikh, S.; Dalal, R.; Fonseca, L. C.; Kharas, F.; Vadnal, P. Y.; Vishwakarma, R. A.; Sivaramakrishnan, H. Bioorg. Med. Chem. Lett. 2011, 21, 3784.
- (a) Munro, T. A.; Duncan, K. K.; Xu, W.; Wang, Y.; Liu-Chen, L.-Y.; Carlezon, W. A., Jr.; Cohen, B. M.; Béguin, C. *Bioorg. Med. Chem.* 2008, 16, 1279; (b) Banaszak, E.; Xu, L.-W.; Bardeau, J.-F.; Castanet, A.-S.; Mortier, J. *Tetrahedron* 2009, 65, 3961.
- 25. Brien, J. O.; Wilson, I.; Orton, T.; Pognan, F. Eur. J. Biochem. 2000, 267, 5421.
- 26. Hunt, L.; Jordan, M.; De Jesus, M.; Wurm, F. M. Biotechnol. Bioeng. 1999, 65, 201.



Curcumin analogues inhibit phosphodiesterase-5 and dilate rat pulmonary arteries

Oraya Kruangtip^a, Krongkarn Chootip^b, Prapapan Temkitthawon^a, Kanokwan Changwichit^a, Thipphawan Chuprajob^c, Chatchawan Changtam^d, Apichart Suksamrarn^c, Nantaka Khorana^a, C. Norman Scholfield^a and Kornkanok Ingkaninan^a

^aDepartment of Pharmaceutical Chemistry and Pharmacognosy, Faculty of Pharmaceutical Sciences and Center of Excellence for Innovation in Chemistry, ^bDepartment of Physiology, Faculty of Medical Sciences, Naresuan University, Phitsanulok, ^cDepartment of Chemistry and Center of Excellence for Innovation in Chemistry, Faculty of Science, Ramkhamhaeng University, Bangkok, ^dDivision of Physical Sciences, Faculty of Science and Technology, Huachiew Chalermprakiet University, Samutprakarn, Thailand

Keywords

curcumin analogues; phosphodiesterase-5; pulmonary artery; pulmonary artery hypertension

Correspondence

Kornkanok Ingkaninan, Faculty of Pharmaceutical Sciences and Center of Excellence for Innovation in Chemistry, Naresuan University, Phitsanulok 65000, Thailand.

E-mail: k_ingkaninan@yahoo.com Krongkarn Chootip, Department of Physiology, Faculty of Medical Sciences, Naresuan University, Phitsanulok 65000, Thailand.

E-mail: krongkarnc@gmail.com

Abbreviations

Ach, acetylcholine; BSA, bovine serum albumin; cGMP, guanosine cyclic monophosphate; DMSO, dimethylsulphoxide; EC₄₀, 40% of maximal effective concentration; ESMS, electrospray mass spectrometry; IC₅₀, half maximal inhibitory concentration; NMR, nuclear magnetic resonance; PAH, pulmonary artery hypertension; PDE, phosphodiesterase; PE, phenylephrine; QAE, quaternary aminoethyl anion exchanger; sGC, soluble quanylyl cyclase.

Received April 21, 2014 Accepted July 4, 2014

doi: 10.1111/jphp.12302

Abstract

Objectives Phosphodiesterase (PDE)-5 inhibitors are useful as vasodilators for the treatment of pulmonary arterial hypertension. We aimed to study curcumin analogues for PDE5 inhibitory activity and vasorelaxation of rat pulmonary arteries.

Methods Three natural curcuminoids (1–3) and six synthetic analogues (4–9) were tested for PDE5 and PDE6 inhibitory activities using enzymatic radioassay. Their vasorelaxation was measured using freshly isolated segments of rat pulmonary artery and aorta.

Key findings Curcuminoids (1–3) mildly inhibited PDE5 (half maximal inhibitory concentration (IC₅₀) = 18 μm): the metamethoxyl of curcumin was important for PDE5 inhibition. But hydroxyl rearrangements, removing both methoxyls and one ketomethylene, yielded the potent 7 and 9 (IC₅₀ = 4 μm) (compared with sildenafil, IC₅₀ = 0.03 μm). Only 1, 3 and 4 were PDE5 selective over PDE6. Triazole-carboxylic addition provided water-solubility while preserving potency. All analogues possessed concentration-dependent vasorelaxant activity on pulmonary arteries (40% of maximal effective concentration (EC₄₀) = 29–90 μm, maximum response = 60–90% at 300 μm), while compounds (1–8) were weakly acting in aorta (maximum response <40%). Only demethoxycurcumin (2) and analogues 5, 8, 9 had endothelium-dependent actions. Sildenafil was highly potent (EC₄₀ = 0.04 μm) and highly endothelium dependent in pulmonary artery but weak on intact aorta (EC₄₀ = 1.8 μm). Activity profiles suggest actions through additional cell pathways for promoting vasorelaxation.

Conclusions Curcumin analogues are potential leads for developing efficacious and selective PDE5 inhibitors and other pathologies of pulmonary hypertension.

Introduction

Idiopathic pulmonary arterial hypertension (PAH) is a relatively rare lung disorder (prevalence ~6 cases/million people^[1]) with a poor prognosis. Pulmonary arteries become constricted, thus reducing blood flow to the lungs and increasing pulmonary arterial pressure. This PAH

increases the load on the right ventricle, leading to right heart failure and death. [2] Several mechanisms for the disease have been proposed and shown to produce PAH in animal models, but none appears to reflect the human condition. Because of this unclear aetiology, current drug

Curcumins inhibit PDE5 Oraya Kruangtip et al.

treatments have focused on symptomatic treatment in the form of vasodilators. Of these, sildenafil, tadalafil, vardenafil and similar drugs have received the most widespread application. These compounds are inhibitors phosphodiesterase-5 (PDE5), which is found in many cells including the smooth muscle cells of pulmonary vascular tree expressed as PDE5A.[3] This enzyme is upregulated in pulmonary hypoxia and PAH^[4] making it an attractive drug target for treatment of these pathologies. The target substrate for PDE5 is the inactivation of guanosine cyclic monophosphate (cGMP) via hydrolysis. Cytosolic cGMP constituatively activates in particular, adenosine triphosphate and big potassium current channels^[5] and the resulting increased K-permeability maintains vasorelaxant tone. Thus inhibiting PDE5 favours cGMP accumulation hence promoting vasodilatation.[6,7]

Sildenafil was initially registered as an oral drug for erectile dysfunction, then later approved for PAH treatment^[6] and is now licensed for Raynaud's disease.^[7] There is a growing list of successful clinical trials with PDE5 inhibitors^[8] that may lead to extended licensing by regulatory bodies.^[7] Clearly, these inhibitors also cause vasodilatation in other tissues^[8] and more especially have retinal-related complications most commonly associated with additional PDE6 blockade.^[9] Therefore, the hunt continues for drugs that are specific for diseased targets including the pulmonary arterial circulation and especially erectile dysfunction.

Several *Curcuma* species are known to be vasorelaxant including *Curcuma longa*,^[10] while curcumin reduces pulmonary arterial pressure.^[11] We have shown that extracts of these plants exhibit PDE5 inhibitory activity.^[12] This suggests that curcuminoids might provide leads for the development of a new generation of selective PDE5 inhibitors. Therefore, here we aimed to explore the activities of both natural and synthetic curcumin analogues on the inhibition of PDE5 in cell-free assay and on the vasorelaxation of freshly isolated rat pulmonary arteries *in vitro*.

Materials and Methods

Materials

Krebs' solution (mm): (NaCl 122; KCl 5; (N-(2-hydroxyethyl)piperazine-N'-(2-ethane-sulfonic acid)) 10; KH₂PO₄ 0.5; NaH₂PO₄ 0.5; MgCl₂ 1; glucose 11 and CaCl₂ 1.8; adjusted to pH 7.3 with 1-N NaOH), acetylcholine (ACh), phenylephrine (PE), ingredients in buffer 1 (100-mm Tris-HCl, pH 7.5; 100-mm imidazole; 15-mm MgCl₂; 1.0-mg/ml bovine serum albumin (BSA) and 2.5-mg/ml snake venom from *Crotalus atrox*), ingredients in Buffer 2 (100-mm Tris-HCl, pH 7.5 100-mm imidazole, 15-mm MgCl₂, 1.0-mg/ml BSA and 0.5-mg/ml histone) were obtained from Sigma (St Louis, MO, USA). Pentobarbital sodium solution (Nembutal) was obtained from Ceva

Sante Animale (Libourne, France). Quaternary aminoethyl anion exchanger (QAE) resin (QAE Sephadex A-25) was purchased from GE Healthcare (Upsala, Sweden). The PDE5 and PDE6 were prepared from rat lung tissues and chicken retinas, respectively.

Preparations of compounds

The natural compounds, (1) curcumin, (2) demethoxycurcumin and (3) bisdemethoxycurcumin, were obtained from the rhizomes of C. longa.[13] Compound 4 was synthesised by the demethylation reaction of compound 1 as described previously.[13] Compounds 5-7 were prepared by aldol condensation of substituted cinnamones (10a and 10b) and substituted cinnamaldehydes (11a, 11b and 11c) under a base-catalysed condition, which has recently been reported^[14] (Figure 1). Compounds 8 and 9, the acid groupcontaining analogues of 7, were synthesised by coupling the alkyne analogues 12 and 13 with the azide 14 as shown in Figure 2. Briefly, the cinnamones 10c and 10b were coupled with cinnamaldehydes 11c and 11d by the same method used to synthesise compounds 5-7^[14] to yield compounds 12 (32%) and 13 (34%). Each of compounds 12 and 13 was later reacted with 2-azidoacetic acid (14) under click conditions^[15] to give compounds 8 and 9 in 69% and 38% yields, respectively. Compound 8: ¹H nuclear magnetic resonance (NMR) (400 MHz, acetone- d_6) δ (ppm): 5.36 (s, 2H), 5.38 (s, 2H), 6.62 (d, J = 15.3 Hz, 1H), 6.82 (d, J = 7.8 Hz, 1H), 7.01–7.08 (m, 5H), 7.21 (t, J = 7.8 Hz, 1H), 7.32 (d, J = 7.7 Hz, 1H), 7.36 (d, J = 16.1 Hz, 1H), 7.42 (t, J = 7.7 Hz, 1H), 7.51 (ddd, J = 15.3, 6.6, 3.4 Hz, 1H), 7.73 (d, J = 7.6 Hz, 1H), 7.93 (d, J = 16.1 Hz, 1H), 8.22 (s, 1H). ¹³C NMR (100 MHz, acetone- d_6) δ (ppm): 51.3, 63.0, 114.0, 114.5, 117.1, 119.7, 122.1, 125.0, 126.3, 126.6, 128.3, 130.1, 130.7, 130.8, 132.4, 138.2, 138.8, 142.0, 143.6, 144.0, 158.6, 158.5, 168.5, 189.2. electrospray mass spectrometry (ESMS) (-ve): m/z 430 [M – H]⁻. Compound 9: ¹H NMR (400 MHz, acetone- d_6) δ (ppm): 5.26 (s, 2H), 5.34 (s, 2H), 6.74 (d, J = 15.2 Hz, 1H), 6.90 (t, J = 7.4 Hz, 1H), 6.98 (d, J = 8.1 Hz, 1H), 7.03 (d, J = 8.1 Hz, 1H), 7.09 (d, J = 15.6 Hz, 1H), 7.17–7.33 (m, 6H), 7.54 (dd, J = 15.1, 10.8 Hz, 1H), 7.69 (d, J = 7.7 Hz, 1H), 8.04 (d, J = 16.1 Hz, 1H), 8.15 (s, 1H). 13 C NMR (100 MHz, acetone- d_6) δ (ppm): 51.2, 62.4, 113.8, 116.6, 117.1, 120.8, 121.2, 122.9, 126.0, 126.1, 128.7, 129.4, 130.6, 130.7, 132.4, 138.5, 138.9, 141.5, 143.3, 144.3, 157.7, 159.9, 168.7, 189.2. ESMS (-ve): m/z 430 [M – H]⁻. The purity of all the test compounds was more than 95% as determined by NMR and thin layer chromatography. The samples were stored at -20°C until use.

Determination of phosphodiesterase-5 inhibitory activity

All samples were dissolved in dimethylsulfoxide (DMSO) and diluted with water giving a final DMSO concentration

Oraya Kruangtip et al. Curcumins inhibit PDE5

R¹ O R⁴ R⁵

10a: R¹ = H, R² = OMe, R³ = OH

11b: R⁴ = H, R⁵ = OMe, R⁶ = OH

11b: R⁴ = R⁵ = H, R⁶ = OH

11c: R⁴ = R⁶ = H, R⁵ = OH

(a) 10c: R¹ = OCH₂C
$$\equiv$$
 CH, R² = R³ = H

(b)

R² 2¹ 1 3 5 7 1 2" R⁵

(a) 10a + 11a \rightarrow 5: R¹ = R⁴ = H, R² = R⁵ = OMe, R³ = R⁶ = OH

10a + 11b \rightarrow 6: R¹ = R⁴ = H, R² = R⁵ = OMe, R³ = R⁶ = OH

10b + 11c \rightarrow 7: R¹ = R⁵ = OH, R² = R³ = R⁴ = R⁶ = H

10c + 11c \rightarrow 12: R¹ = OCH₂C \equiv CH, R² = R³ = R⁴ = R⁶ = H, R⁵ = OH

10b + 11d \rightarrow 13: R¹ = OH, R² = R³ = R⁴ = R⁶ = H, R⁵ = OCH₂C \equiv CH

Figure 1 Preparation of compounds 5–7, 12 and 13. Reagents and conditions: (a) propargyl bromide, K_2CO_3 , acetone, room temperature. (b) 20% aq. NaOH, EtOH, 0°C– room temperature.

Figure 2 Preparation of compounds 8 and 9. Reagents and conditions: (a) NaN₃, H_2O , room temperature. (b) CuSO₄, sodium ascorbate, THF: H_2O (9:1).

of 5%. PDE5 was extracted from rat lung tissue as described previously. [16] The PDE5 assay was conducted using the two-step radioactive procedure, which has been modified from Sonnenburg *et al.*, 1998. [17] Twenty microlitres of the following reagents was added to 96-well plates: buffer 1, EGTA, PDE5 solution and test samples or control (5% DMSO in buffer). The reaction was started by adding 20 μl of 5-μM

[3 H]cGMP (\sim 50 000 cpm) to the reaction mixture and incubated at 30°C for 40 min. Then, 100 μl of 50% QAE resin in water was added to the wells to purify the hydrolysate. The plate was shaken for 10 min and left for 20 min to allow the resin to sediment. The supernatants (100 μl) were transferred to new microplate wells containing 100 μl of fresh 50% QAE resin. The plate was again

Curcumins inhibit PDE5 Oraya Kruangtip et al.

shaken and left to permit sedimentation. Then, 100-µl supernatant was mixed and shaken with 200 µl of Microscint (Perkin Elmer, Waltham, MA, USA) 20 for 2 h. The radioactivity was counted by a TopCount NXT (PerkinElmer, Boston, MA, USA), each well for 1 min. The PDE5 activity in the study was standardised to have a hydrolysis activity of 20–25% of the total substrate counts. The calculation of hydrolysis is shown in equation (1). The PDE5 inhibitory activity was calculated using equation (2).

$$\% hydrolysis_{sample} = \left(\frac{\left(CPM_{sample} - CPM_{background}\right)}{\left(CPM_{total\ count} - CPM_{background}\right)}\right) \times 100$$
(1)

where CPM_{sample} is the radioactive count rate of the assay with enzyme and $CPM_{background}$ is the count rate without enzyme. $CPM_{total\ count}$ is the count rate of 20 μ l of substrate plus 100 ml of buffer 1.

$$\%PDE5 inhibition = \left[1 - \left(\frac{\%hydrolysis_{sample}}{\%hydrolysis_{control}}\right)\right] \times 100 \quad (2)$$

where %hydrolysis_{sample} and %hydrolysis_{control} were the enzyme activities of the sample and solvent (1% DMSO) used in the assay, respectively. The IC₅₀ values were determined using the test samples at >80% PDE5 inhibition.

Determination of phosphodiesterase-6 inhibitory activity

PDE6 activity was conducted using the procedure previously reported, [14] which has been modified from Huang et al., 1998. [18] Twenty-five millilitres of the following reagents was added to tube: buffer 2, EGTA, PDE6 solution and test samples or control (5% DMSO in buffer). The reaction was started by adding 25 µl of 5-µм [3H]cGMP and incubated at 30°C for 10 min. Then, the reaction was stopped by placing the tube in boiling water for 1 min and cooled for 5 min. The second step of reaction used 25 µl of 2.5-mg/ml snake venom added to the reaction, incubated at 30°C for 5 min. After that, 250 μl of 20-mm Tris-HCl, pH 6.8 (buffer I) was added. The reaction was transferred to a QAE resin column and eluted four times with 500 ul of buffer I. The eluent was mixed with a scintillation cocktail, and the radioactivity was measured using a β-counter. The %hydrolysis of PDE6 was similarly calculated as for PDE5.

Animals

Male Wistar rats (200–250 g) were obtained from the National Laboratory Animal Center, Mahidol University, Nakhornpathom, Thailand. The study was approved by the Animal Ethics Committee, Naresuan University, Phitsanulok, Thailand (NU-AE540416). Animals were

housed under standard environmental conditions at 25 ± 2 °C, 12-h light and dark cycle, fed with standard rodent diet and tap water in the Center for Animal Research, Naresuan University, Thailand.

Tissue preparation and vascular protocols

Rats were anaesthetised by pentobarbital (65-mg/kg, i.p. injection) and the lungs and aorta were isolated. Intrapulmonary artery was removed from lung and soaked in Krebs' solution to wash off the surrounding loose connective tissue. The vessel was cut into rings 2-3 mm in length and mounted in tissue chambers via a pair of intraluminal wires. The chambers contained Krebs' solution at 37°C and bubbled with air. The rings were incubated for 45-60 min at an optimum tension of 1 g during which the solution was replaced every 15 min. The wires were connected to force transducers to measure isometric tension via a MacLab A/D converter (Chart V5, A.D. Instruments, Castle Hill, NSW, Australia), stored and displayed on personal computer. The arterial contraction and relaxation was tested by sequential application of 10-μM PE and 10-μM ACh. Only vessels showing 80-100% relaxation to ACh were considered as endothelium intact, while in some experiments, the endothelium was predenuded mechanically, and relaxations of <20% were considered as successfully denuded. After washing for 45-60 min, vessels were precontracted by adding 10-µM PE again. When stable contractions were obtained, the samples (containing compounds 1-9) at concentrations of 0.1-100 µm were cumulatively added (Figure 3). The samples were dissolved in DMSO and then diluted with water to obtain the final concentrations of 300, 100, 30, 10, 3, 1, 0.1 μM in 2-ml tissue baths (final solutions contained <0.1% DMSO). Sildenafil was similarly diluted to working concentrations of 0.0001–100 μм.

Statistical analysis

Data were expressed as the mean \pm standard error of the mean. Statistical analysis was conducted using Student's t-test: unpaired and one-way analysis of variance, followed by Tukey's post-hoc test. P-values of < 0.05 were considered significant.

Results

Inhibition of phosphodiesterase-5 and phosphodiesterase-6 by curcumin analogues

Three naturally occurring curcuminoids (1–3) and six synthetic analogues (4–9) were tested using the PDE5 and PDE6 inhibition assays. The highest potency on PDE5 was for compounds 7 and 9 with IC_{50} s of ~4 μ m. Nevertheless, compounds 7 and 9 were ~100-fold less potent than sildenafil, but more effective than the naturally occurring

Oraya Kruangtip et al. Curcumins inhibit PDE5

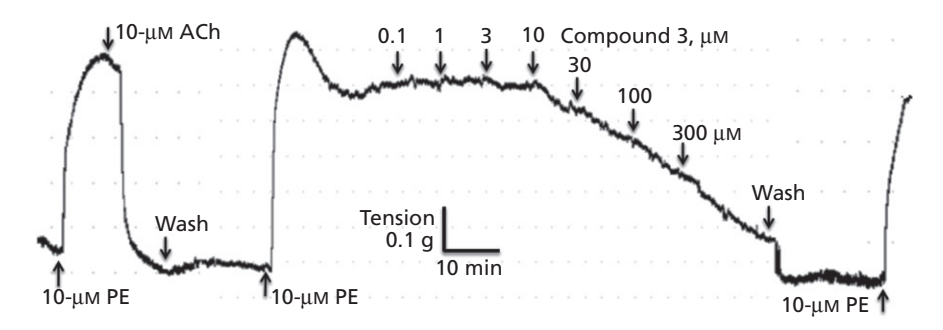


Figure 3 An example time-course showing vasorelaxation of an endothelium-intact pulmonary artery to ACh followed by the relaxant effect of compound 3 at 0.1 to 300 μm. PE, phenylephine, ACh, acetylcholine, K, high potassium solution.

1–3 (Table 1). The other compounds showed IC_{50} values that varied between 10 and 100 μm. For PDE6, the IC_{50} 8 for compounds 2, 5, 6, 7, 8 and 9 were in the range of 3–20 μm. Only 1, 3 and 4 showed IC_{50} 8 >100 μm (Table 1).

Vasorelaxation of pulmonary artery and aorta by curcumin analogues

In isolated pulmonary arteries with intact endothelium, the natural curcuminoids (1-3) and synthetic analogues (4-9) demonstrated concentration-dependent vasodilatation (Figures 3 and 4). Sildenafil achieved a supramaximal relaxation, but limited solubility and lower potency prevented us from determining the supramaximal effect for any of the test analogues while some of maximal responses did not even reach 50% of the maximal sildenafil response. Therefore, all potencies were expressed as an EC_{40} (for sildenafil both EC_{50} and EC_{40} were determined). Every test analogue showed similar potencies (mean EC_{40} s were $58-111 \,\mu\text{M}$) on intact pulmonary arteries (Table 2).

Endothelial denudation of pulmonary arteries showed smaller relaxations with compounds 2, 5, 8 and 9 (Table 2) (Figure 4b, 4e, 4h and 4i). Similarly, sildenafil potency was substantially lower in endothelium-denuded pulmonary arteries (Figure 4j). For the remaining compounds 1, 3, 4, 6 and 7 (Figure 4a, 4c, 4d, 4f and 4g), there was no change in potency with denudation.

In contrast, most of the test compounds produced weaker actions on aorta compared with intact pulmonary artery except compound 9, which was equally potent on both aorta and pulmonary artery (Figure 4i). Sildenafil was ~40-fold less effective on the aorta than intact pulmonary artery; that is, only ~5-fold more potent than denuded pulmonary artery (Figure 4j). This could be a consequence of more PDE5 in pulmonary artery but we are unaware of any direct comparison of PDE5 in vascular smooth muscle on different arteries.

Discussion

Structure-activity relationship of curcumin analogues on phosphodiesterases

Cell-free experiments showed that all curcumin analogues were moderately active PDE5 inhibitors (Table 1). When the metamethoxyl group was missing from 1, the activities of 2 and 3 were reduced suggesting that this group is important for PDE5 inhibitory activity. Demethylation of 1 gave the more polar analogue 4 resulting in a twofold lower inhibitory activity while removing both methoxyl groups yielded compound 3, which produced a fourfold reduction in activity. It might be possible that these metapositions need these bulky substituents for binding to the active site.^[19]

Replacement of the ketomethylene group in 1 giving 5 slightly decreased the inhibitory activity whereas a similar structural modification of 2–6 increased the activity. Taking compound 6 and transposing the two hydroxyl groups from positions 4' to 2' and 4" to 3" and removing the aromatic methoxyl group yielded the highly potent compound 7.

Water solubility was a major challenge for curcumin analogues (1–7) and solubility was improved by adding a triazole carboxylic group to the 2' hydroxyl group in 7 to give 8 but this compromised PDE5 potency. In contrast, a similar substitution on the opposite 3"-hydroxyl group of 7 yielding 9 preserved the inhibitory activity as well as offering superior water solubility.

The inhibitory activity on PDE6 is another concern because it disrupts the cGMP signalling pathway used in retinal transduction and this is avoided in the highly selective PDE5 inhibitor, tadalafil. The inhibition by these compounds on PDE6 suggests that 1, 3 and 4 had weak actions compared with the corresponding actions on PDE5 and accords with the 10-fold selectivity of sildenafil. These results suggest that further modification of curcuminoid analogues could achieve the required specificity and high activity needed to realise clinical usefulness.

Curcumins inhibit PDE5 Oraya Kruangtip et al.

Table 1 The inhibitory effects of curcumin and its analogues on PDE5 and PDE6. Values are means \pm standard error of the mean (n = 3)

		IC ₅₀ against	
Compounds	Chemical structures	PDE5 (µM)	PDE6 (µM)
1	MeO 3' 1 2 3 4 5 6 7 1" 2" OMe 13" OMe 13" OH	18.8 ± 2.1 ^a	113.9 ± 20.9 ^b
2	MeO OH	50.6 ± 3.3°	12.6 ± 2.8 ^a
3	но	94.4 ± 5.2 ^d	>500°
4	HO OH OH	44.5 ± 1.5°	>700 ^d
5	MeO OMe	30.5 ± 5.1 ^b	18.1 ± 9.7°
6	MeO OH	27.6 ± 5.7 ^b	7.6 ± 1.8°
7	OH O OH	4.4 ± 1.6 ^a	4.0 ± 2.1 ^a
8	$HO \longrightarrow N=N$ OH	17.1 ± 2.0°	5.1 ± 2.0ª
9	OH O N=N OH	3.9 ± 0.6^{a}	2.8 ± 2.3^{a}
Sildenafil	O O HN N N	0.03 ± 0.01°	ND
	> ~ ~ ,0, /		

PDE, phosphodiesterase. a-eDifference within columns (samples not connected by the same letter are statistically different at P < 0.05). PDE, phosphodiesterase.

Vasorelaxant effects of curcumin analogues

In these experiments, sildenafil potency on intact pulmonary arteries expressed as EC_{40} was $0.04~\mu \text{M}$ (0.074 \pm 0.016 μM calculated as EC_{50}), which accords with

previous work in rat pulmonary artery^[21] and aorta.^[22] Furthermore, the potency of sildenafil here was similar to the cell-free action on PDE5 protein. Endothelial removal caused a dramatic decrease in sildenafil potency (200-fold less) both here and in previous work on aorta.^[20] This

Oraya Kruangtip et al. Curcumins inhibit PDE5

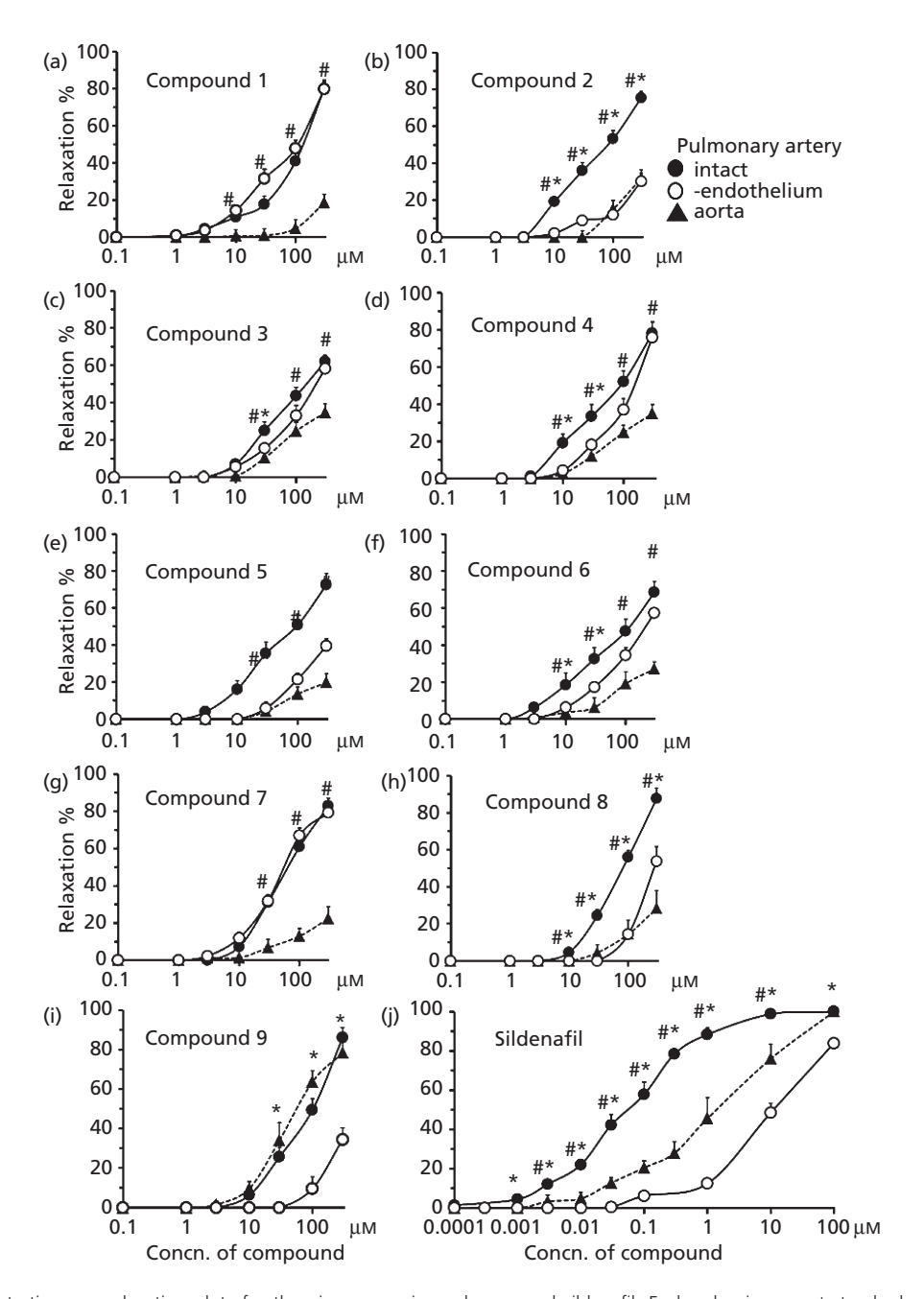


Figure 4 Concentration–vasorelaxation plots for the nine curcumin analogues and sildenafil. Each value is mean \pm standard error of the mean (n = 5-6). *P < 0.05 compared relaxation of pulmonary arteries with and without endothelium, #P < 0.05 comparing endothelium-intact pulmonary arteries with aortas.

confirms that the vascular smooth muscle relaxation was largely mediated through the endothelium-releasing vasodilator factors even though sildenafil is acting on vascular smooth muscle. [22]

All the curcuminoids were vasorelaxant using endothelium-intact pulmonary artery and all had similar potencies (Table 2). Compounds 2, 5, 8, 9 and possibly 4

had actions that indicate that the endothelium was necessary. But, these four compounds had similar potencies that did not reflect those variations seen in the cell-free assays on either PDE5 of PDE6. Thus for compounds 2, 5, 8 and 9, there was clearly endothelium dependency, but the poor potency correlation with the cell-free studies does not clearly indicate that they are acting on PDE5.

Curcumins inhibit PDE5 Oraya Kruangtip et al.

Table 2 Vasorelaxant actions of curcumin and its analogues on rat endothelium-intact and denuded pulmonary arteries and aorta. (n = 5-6), P-values listed are for differences between endothelium-intact versus endothelium-denuded pulmonary arteries.

		EC ₄₀ (μM)	
Compounds	Pulmonary artery intact	Pulmonary artery denuded	Aorta-intact
1	109 ± 23	93 ± 30 (P = 0.82)	>300 ± 0#
2	58 ± 10	>300 ± 0 (P < 0.0001)	>300 ± 0#
3	111 ± 29	$184 \pm 31 \ (P = 0.14)$	$>300 \pm 0^{\#}$
4	58 ± 20	$121 \pm 20 \ (P = 0.058)$	>300 ± 0#
5	76 ± 24	>300 ± 0 (P < 0.0001)	$>300 \pm 0^{\#}$
6	98 ± 28	$147 \pm 21 \ (P = 0.17)$	>300 ± 0#
7	59 ± 8	$52 \pm 6 \ (P = 0.74)$	$>300 \pm 0^{\#}$
8	59 ± 8	208 ± 17 (P < 0.0001)	>300 ± 0#
9	71 ± 15	>300 ± 0 (P < 0.0001)	46 ± 11
Sildenafil	0.042 ± 0.009	8.4 ± 0.8 (<i>P</i> < 0.0001)	1.8 ± 1.0#

 $^{\#}P < 0.0001$ for endothelium-intact pulmonary arteries versus intact aorta.

Compounds 1 and 7 were unaffected by endothelial denudation suggesting that they acted directly on vascular smooth muscle through a mechanism probably not directly on PDE5. These might include actions on soluble guanylyl cyclase $^{[23]}$ on β -receptors, or cytosolic Ca $^{2+}$ handling. $^{[24]}$

There are two important differences between the cell-free and vascular relaxation studies, which might affect potency of our compounds: (1) the compounds have to gain access to the cell interior, and numerous bioavailability studies have shown that the membrane permeability of at least curcumin itself is very poor;^[25] (2) a vast number of cellular effects for curcuminoids have been described.^[26]

However, the very high concentrations needed to have any effect on the aorta suggest that these compounds have some selectivity for the pulmonary artery. This alone indicates that the compounds may form the basis for the development of drugs that selectively target the pulmonary circulation. Finally, the multiple cellular actions of curcuminoids^[26–28] may be an asset in the treatment of PAH where there are multiple pathologies including inflammation, PDE5 upregulation, ionchannelopathies, vasoconstriction, endothelial dysfunction and vascular hyperplasia.

Conclusions

Curcumin analogues showed PDE5 inhibitory activity with varying potencies and some showed selectivity for PDE5 over PDE6. There were clear endothelium-dependent vasorelaxant effects to which the pulmonary artery was more sensitive compared with the aorta. These results suggest that these curcuminoids could underpin the further development of highly selective and potent compounds, which could discriminate the pulmonary arterial circulation by targeting several coincident pathologies of PAH including PDE5 upregulation.

Declarations

Conflict of interest

The Author(s) declare(s) that they have no conflicts of interest to disclose.

Funding

The financial supports from Naresuan University, the Center of Excellence for Innovation in Chemistry (PERCHCIC), Office of the Higher Education Commission, Ministry of Education, Thailand and The Thailand Research Fund are acknowledged.

References

- 1. Ling Y *et al.* Changing demographics, epidemiology, and survival of incident pulmonary arterial hypertension: results from the pulmonary hypertension registry of the United Kingdom and Ireland. *Am J Respir Crit Care Med* 2012; 186: 790–796. doi: 10.1164/rccm.201203-0383OC.
- 2. Barst RJ *et al.* Diagnosis and differential assessment of pulmonary arterial hypertension. *J Am Coll Cardiol* 2004; 43(Suppl. 12 S): 40S–47S. doi: 10.1016/j.jacc.2004.02.032.
- 3. Sebkhi A *et al.* Phosphodiesterase type 5 as a target for the treatment of hypoxia-induced pulmonary hypertension. *Circulation* 2003; 107: 3230–3235. doi: 10.1161/01.CIR .0000074226.20466.B1.
- Scipioni A et al. Immunohistochemical localisation of PDE5 in rat lung during pre- and postnatal development. J Biomed Biotechnol 2009; 2009: 1–7. doi: 10.1155/2009/ 932961.
- 5. Schoeffter P *et al.* Role of cyclic AMPand cyclic GMP-phosphodiesterases in the control of cyclic nucleotide levels

- and smooth muscle tone in rat isolated aorta. A study with selective inhibitors. *Biochem Pharmacol* 1987; 36: 3965–3972.
- Galiè N *et al.* Guidelines on diagnosis and treatment of pulmonary arterial hypertension The Task Force on Diagnosis and Treatment of Pulmonary Arterial Hypertension of the European Society of Cardiology. *Eur Heart J* 2004; 25: 2243–2278. doi: 10.1016/ j.ehj.2004.09.014.
- Chrysant SG. Effectiveness and safety of phosphodiesterase 5 inhibitors in patients with cardiovascular disease

Oraya Kruangtip et al. Curcumins inhibit PDE5

- and hypertension. *Curr Hypertens Rep* 2013; 15: 475–483. doi: 10.1007/s11906-013-0377-9.
- 8. Kukreja RC *et al.* Emerging new uses of phosphodiesterase-5 inhibitors in cardiovascular diseases. *Exp Clin Cardiol* 2011; 16: e30–e35.
- Kerr NM, Danesh-Meyer HV. Phosphodiesterase inhibitors and the eye. Clin Experiment Ophthalmol 2009; 37: 514–523. doi: 10.1111/ j.1442–9071.2009.02070.x.
- 10. Adaramoye OA *et al.* Hypotensive and endothelium-independent vasorelaxant effects of methanolic extract from *Curcuma longa* L. in rats. *J Ethnopharmacol* 2009; 124: 457–462. doi: 10.1016/j.jep.2009.05.021.
- 11. Lin Q *et al.* Effect of curcumin on pulmonary hypertension and wall collagen of pulmonary arterioles of chronic hypoxic hypercapnic rats. *Chin J Appl Physiol* 2006; 22: 257–261.
- 12. Temkitthawon P. Investigation of phosphodiesterase-5 inhibitory activity from Thai medicinal plants. Naresuan University, Thailand: PhD thesis, 2012.
- 13. Changtam C *et al.* Curcuminoid analogues with potent activity against *Trypanosoma* and *Leishmania* species. *Eur J Med Chem* 2010; 45: 941–956.
- 14. Chuprajob T *et al.* Synthesis, cytotoxicity against human oral cancer KB cells and structure–activity relationship studies of trienone analogues of curcuminoids. *Bioorg Med Chem Lett* 2014; 24: 2839–2844.
- 15. Kategaonkar AH *et al.* Synthesis and biological evaluation of new 2-

- chloro-3-((4-phenyl-1*H*-1,2,3-triazol-1-yl)methyl)quinoline derivatives via click chemistry approach. *Eur J Med Chem* 2010; 45: 3142–3146.
- 16. Temkitthawon P *et al. Kaempferia* parviflora, a plant used in traditional medicine to enhance sexual performance contains large amounts of low affinity PDE5 inhibitors. *J Ethnopharmacol* 2011; 137: 1437–1441. doi: 10.1016/j.jep.2011.08.025.
- Sonnenburg WK et al. Identification, quantitation, and cellular localization of PDE1 calmodulin-stimulated cyclic nucleotide phosphodiesterases. Methods 1998; 14: 3–19. doi: 10.1006/ meth.1997.0561.
- Huang D et al. Molecular determinants of cGMP binding to chicken cone photoreceptor phosphodiesterase. J Biol Chem 2004; 279: 48143–48151. doi: 10.1074/jbc.M404338200.
- 19. Cahill KB *et al.* Identification of amino acid residues responsible for the selectivity of tadalafil binding to two closely related phosphodiesterases, PDE5 and PDE6. *J Biol Chem* 2012; 287: 41406–41416. doi: 10.1074/ibc.M112.389189.
- 20. Teixeira CE *et al.* Differential effects of the phosphodiesterase type 5 inhibitors sildenafil, vardenafil, and tadalafil in rat aorta. *J Pharmacol Exp Ther* 2006; 316: 654–661. doi: 10.1124/jpet.105.092544.
- 21. Pauvert O *et al.* Effect of sildenafil on cyclic nucleotide phosphodiesterase activity, vascular tone and calcium signaling in rat pulmonary artery. *Br J*

- *Pharmacol* 2003; 139: 513–522. doi: 10.1038/sj.bjp.0705277.
- 22. Mochida H *et al.* Sildenafil and T-1032, phosphodiesterase type 5 inhibitors, showed a different vasore-laxant property in the isolated rat aorta. *Eur J Pharmacol* 2002; 440: 45–52. doi: 10.1016/S0014-2999(02)01339-0.
- 23. Dash JR, Parija SC. Spasmolytic effect of curcumin on goat ruminal artery is endothelium independent and by activation of sGC. *Res Vet Sci* 2013; 95: 588–593. doi: 10.1016/j.rvsc.2013.04.029.
- 24. Xu P-H *et al.* The relaxant effect of curcumin on porcine coronary arterial ring segments. *Vascul Pharmacol* 2007; 47: 25–30. doi: 10.1016/j.vph.2007.03.003.
- 25. Wahlang B *et al.* Identification of permeability-related hurdles in oral delivery of curcumin using the Caco-2 cell model. *Eur J Pharm Biopharm* 2011; 77: 275–282. doi: 10.1016/j.eipb.2010.12.006.
- 26. Shishodia S. Molecular mechanisms of curcumin action: gene expression. *Biofactors* 2013; 39: 37–55. doi: 10.1002/biof.1041.
- Metzler M et al. Curcumin uptake and metabolism. Bio Factors 2013; 39: 14–20. doi: 10.1002/biof.1042.
- 28. Bronte E *et al.* Role of curcumin in idiopathic pulmonary arterial hypertension treatment: A new therapeutic possibility. *Med Hypotheses* 2013; 81: 923–926. doi: 10.1016/j.mehy.2013.08.016.

Microbiology and Immunology

Microbiol Immunol 2014; 58: 581–589 doi: 10.1111/1348-0421.12194

ORIGINAL ARTICLE

A chalcone with potent inhibiting activity against biofilm formation by nontypeable *Haemophilus influenzae*

Duangkamol Kunthalert^{1,2}, Sudarat Baothong¹, Pichit Khetkam³, Suwadee Chokchaisiri³ and Apichart Suksamrarn³

¹Department of Microbiology and Parasitology, ²Centre of Excellence in Medical Biotechnology, Faculty of Medical Science, Naresuan University, Phitsanulok 65000 and ³Department of Chemistry and Center of Excellence for Innovation in Chemistry, Faculty of Science, Ramkhamhaeng University, Bangkok 10240, Thailand

ABSTRACT

Nontypeable Haemophilus influenzae (NTHi), an important human respiratory pathogen, frequently causes biofilm infections. Currently, resistance of bacteria within the biofilm to conventional antimicrobials poses a major obstacle to effective medical treatment on a global scale. Novel agents that are effective against NTHi biofilm are therefore urgently required. In this study, a series of natural and synthetic chalcones with various chemical substituents were evaluated in vitro for their antibiofilm activities against strong biofilm-forming strains of NTHi. Of the test chalcones, 3-hydroxychalcone (chalcone 8) exhibited the most potent inhibitory activity, its mean minimum biofilm inhibitory concentration (MBIC₅₀) being 16 μg/mL (71.35 μM), or approximately sixfold more active than the reference drug, azithromycin (MBIC₅₀ 419.68 μM). The inhibitory activity of chalcone 8, which is a chemically modified chalcone, appeared to be superior to those of the natural chalcones tested. Significantly, chalcone 8 inhibited biofilm formation by all studied NTHi strains, indicating that the antibiofilm activities of this compound occur across multiple strong-biofilm forming NTHi isolates of different clinical origins. According to antimicrobial and growth curve assays, chalcone 8 at concentrations that decreased biofilm formation did not affect growth of NTHi, suggesting the biofilm inhibitory effect of chalcone 8 is non-antimicrobial. In terms of structureactivity relationship, the possible substituent on the chalcone backbone required for antibiofilm activity is discussed. These findings indicate that 3-hydroxychalcone (chalcone 8) has powerful antibiofilm activity and suggest the potential application of chalcone 8 as a new therapeutic agent for control of NTHi biofilm-associated infections.

Key words biofilm formation, chalcone, nontypeable Haemophilus influenzae, strong-biofilm producing strain.

Nontypeable *Haemophilus influenzae* is one of the commonest human respiratory pathogens that cause a spectrum of mild (otitis media, sinusitis) to severe (bronchitis, chronic obstructive pulmonary disease, septicemia, meningitis) illnesses. Substantial morbidity, mortality and socioeconomic burden caused by this microorganism are of enormous concern globally (1–3). There is both *in vitro* and *in vivo* evidence that NTHi

forms biofilm (4, 5). Biofilm infections are notoriously difficult to eradicate because of their resistance to antibiotics and host immune-mediated clearance (6–8). Communal bacteria in a biofilm are upward of 1000-times more resistant to conventional antibiotic treatment than the same organism growing planktonically (9). Usual clinical dosages of antibiotics may therefore fail to adequately clear infections, allowing bacteria to recover,

Correspondence

Duangkamol Kunthalert, Department of Microbiology and Parasitology, Faculty of Medical Science, Naresuan University, Phitsanulok 65000, Thailand. Tel: +66 5596 4626; fax: +66 5596 4770; email: kunthalertd@yahoo.com, kunthalertd@hotmail.com

Received 30 April 2014; revised 29 July 2014; accepted 30 July 2014.

List of Abbreviations: BFI, biofilm forming index; HTM, haemophilus test medium; MBIC, minimum biofilm inhibitory concentration; MIC, minimum inhibitory concentration; MTT, 3-(4,5-dimethylthiazol-2-yl)-2,5-diphenyltetrazolium bromide; NTHi, nontypeable *Haemophilus influenzae*.

persist and spread (10). Increased concentrations or multiple combinations of antibiotics have been suggested for treating biofilm-related infections (11, 12). However, excessive or improper uses of antibiotics may result in development of resistance (13), leading to even greater difficulties in disease treatment. It is therefore important to discover and develop novel, effective antibiofilm agents to improve treatment of NTHi biofilm-mediated infections.

Chalcones are open-chain flavonoids with common skeleton of 1,3-diaryl-2-propen-1-one. Both naturally occurring and synthetic chalcones show an array of biological activities, including anti-bacterial, anti-viral, anti-cancer, anti-oxidant, anti-inflammatory and immunosuppressive activities (14, 15). Because of the simplicity of their chemical structures and their vast variety of actions, compounds with chalcone-based structures are currently receiving a great deal of attention. Their wide range of biological properties is generally attributed to the α , β -unsaturated keto moiety. Chemical substitutions of the two arvl rings is also a subject of interest because it leads to useful structureactivity relationship conclusions and thus facilitates synthesis of pharmacologically active chalcones (14). In recent years, chemically modified chalcone-based compounds have been shown to reduce formation of marine bacterial biofilm (16). Moreover, synthetic chalcones reportedly have strong inhibitory activities against biofilms of bacteria that are pathogenic to humans (17). This raises the possibility of developing chalcone-based compounds as antibiofilm agents.

To our knowledge, there are no reported experimental data regarding the antibiofilm activity of chalcones against NTHi; we therefore investigated these in this study. We quantitatively and qualitatively explored the activities of a series of naturally occurring and synthetic chalcones against biofilm formation by strong-biofilm producing NTHi isolates of clinical origin.

MATERIALS AND METHODS

Chalcones

Chalcones 1 and 2 (Fig. 1) were isolated from the flowers of *Butea monosperma* as described previously (18). Chalcones 3–13 (Fig. 1) were synthesized by the Claisen–Schmidt condensation reaction (19) of substituted acetophenone (8.3 mmol) with substituted benzaldehyde (8.3 mmol) in the presence of an aqueous solution of 50% KOH (25 mL) in ethanol (25 mL) at room temperature for 6–12 hr. The reaction mixture was then acidified with dilute HCl and the resulting precipitates filtered, washed with water, dried, and further purified by recrystallization from EtOH–H₂O (1:1 v/v) or by silica

gel column chromatography, using *n*-hexane—EtOAc as eluent, to produce a high yield (56–92%) of chalcones (Fig. S1). All structures were confirmed by comparison of spectroscopic data and elemental analysis with those previously reported. Chalcones **4** and **5** have been described previously by Karki *et al.* (20), chalcones **6–8** and **13** have been reported by Yadav *et al.* (21), chalcones **9** and **12** have been synthesized by Tatsuzaki *et al.* (22), and chalcones **3**, **10** and **11** have been synthesized by Watanabe and Imazawa (23), Arty *et al.* (24) and Hasan *et al.* (25), respectively.

Bacterial strains and culture conditions

Nontypeable *Haemophilus influenzae* NU7, NU38 and NU48 were used in this study. These bacteria were isolated from different specimen types (sputum, pus and blood) from patients admitted to Buddhachinaraj Hospital (Phitsanulok, Thailand), identified by standard microbiological and biochemical procedures, and PCR-serotyped as described previously (26). All isolates were grown on BHI agar or broth (Oxoid, Basingstoke, UK) supplemented with nicotinamide adenine dinucleotide (Becton Dickinson, MD, USA; $10 \,\mu\text{g/mL}$) and hemin (Becton Dickinson; $10 \,\mu\text{g/mL}$) at $37 \,^{\circ}\text{C}$ in an atmosphere containing $5\% \, \text{CO}_2$.

Microtiter biofilm formation assay

The formation of biofilm by NTHi was evaluated using a method based on that reported previously (4) with some modifications. Overnight cultures of NTHi were washed, diluted 1:200 in fresh HTM and 200 µL was inoculated into the wells of flat-bottomed 96-well polystyrene microtiter plates (Nunc, Roskilde, Denmark). The plates were incubated at 37 °C under 5% CO₂ for 18 hr. Growth was assessed by measuring the OD at 600 nm using a microplate reader (Labsystems iEM Reader MF; Vantaa, Finland) prior to biofilm quantitation. The biofilms were then quantitated by staining the adherent cells with 1% (w/v) aqueous solution of crystal violet for 15 min at room temperature. The dye incorporated by the adherent cells was solubilized in 200 μL of 95% ethanol and the OD measured at 540 nm. The BFI was used to express the amount of biofilm formed by NTHi. It was calculated using the formula (AB - CW)/G, in which AB is the OD of the stained attached microorganisms, CW is the OD of the stained control wells containing microorganisms-free medium only and G is the OD of the cells growth in suspended culture. Biofilm formation was classified semi-quantitatively (strong, moderate, weak or none) based on the BFI readings (27). All NTHi isolates were tested in two independent experiments, with quadruplicate determinations in each.

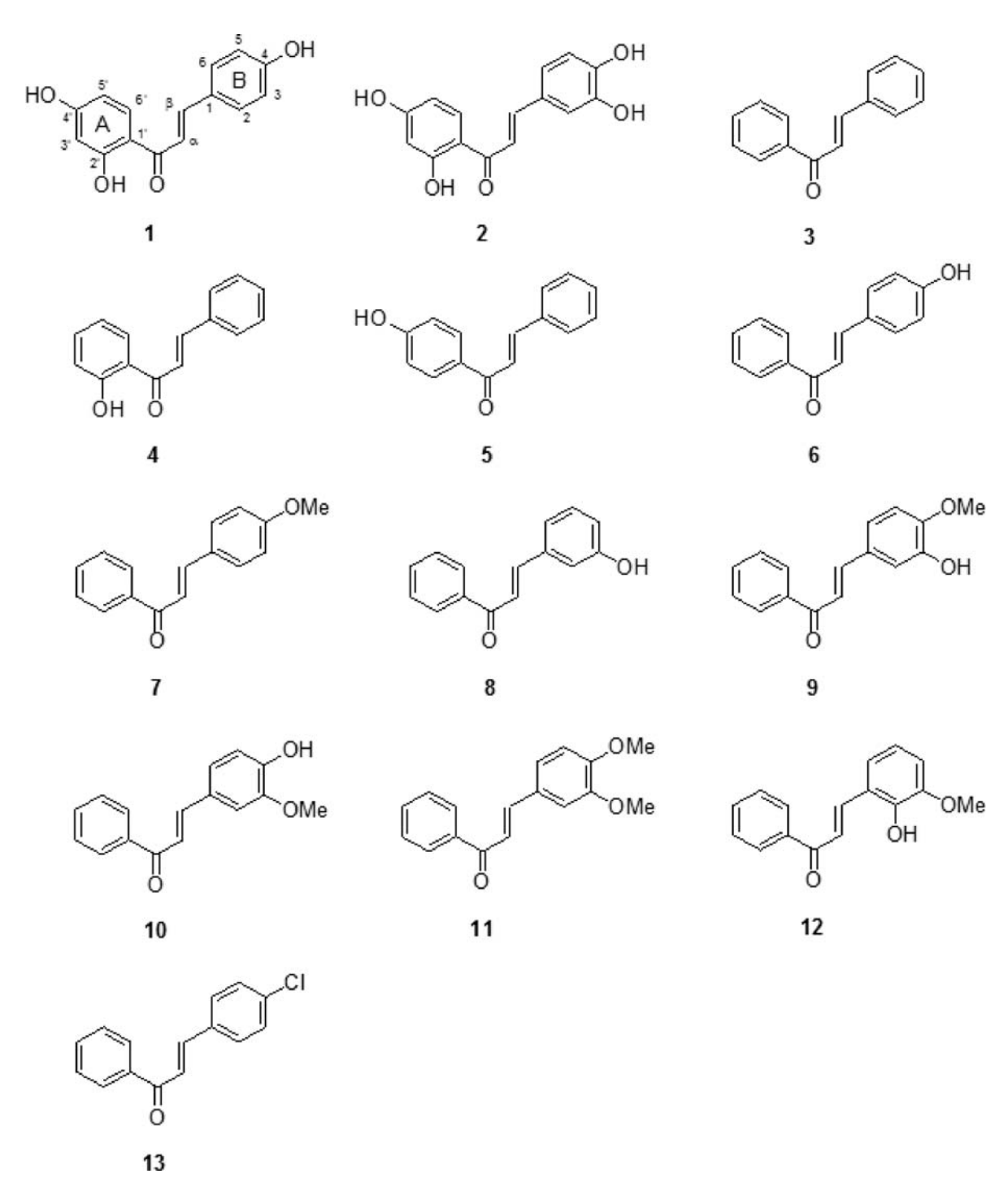


Fig. 1. Chemical structures of the test chalcones.

Biofilm susceptibility assay

The effects of chalcones on NTHi biofilm formation were examined by a microdilution method. Twofold serial dilutions of chalcone were prepared with HTM in the wells of flat-bottomed 96-well microtiter plates

(Nunc). Final concentrations of the test chalcones ranged from 0.25 to 512 μ g/mL. Azithromycin (Fluka, Buchs SG, Switzerland) was included in the assay because this antibiotic reportedly reduces *H. influenzae* biofilms (28, 29). Aliquots of the bacterial suspension at a final concentration of 5×10^5 CFU/mL were added to

the microtiter wells. Culture without the test compound and medium alone were used as non-treated and blank controls, respectively. Following incubation at 37 °C under 5% CO_2 for 18 hr, the medium containing nonadherent cells was decanted and the wells washed with sterile deionized water. Biofilms were quantitated by a microtiter biofilm formation assay as described above. The percentage of inhibition was calculated using the following equation ($[OD_{540}$ of non-treated control $-OD_{540}$ of the test]/ OD_{540} of non-treated control) \times 100. The MBIC₅₀ was defined as the lowest concentration of the test compound that resulted in \geq 50% inhibition of biofilm formation (30).

Time-dependent assay

A time-dependent study was performed using a microdilution method. NTHi strains $(5 \times 10^5 \text{ CFU/mL})$ and chalcone 8 (at the concentration equal to MBIC₅₀) were incubated in HTM at 37 °C under 5% CO₂. At 0, 1, 2, 4, 8, 12, 18 and 24 hr, biofilm formation was quantitated as described above for the biofilm susceptibility assay.

Antimicrobial assay

The antimicrobial effect of chalcone **8** was assessed by determining the MIC by a broth microdilution method. Twofold serial dilutions of the test chalcone at final concentrations ranging from 0.25 to 512 $\mu g/mL$ were prepared in HTM in 96-well microtiter plates (Nunc). Adjusted bacterial inoculum (5 \times 10 5 CFU/mL, final concentration) was then seeded. The medium without the test compound served as a non-treated control. The plates were incubated at 37 $^{\circ}$ C in a 5% CO $_2$ atmosphere for 24 hr and the total bacterial growth determined by OD measurement at 600 nm. The MIC was recorded as the concentration in the first well in which no visible bacterial growth was noted relative to the growth of the non-treated control.

Growth curve assay

The effects of chalcone 8 on planktonic growth of NTHi were examined in 125 mL flasks containing 25 mL of a bacterial culture (5×10^5 CFU/mL, final concentration) and the test chalcone (at the concentration equal to MBIC₅₀). The culture without the test compound was used as a bacterial growth control. The cultures were grown at 37 °C under 5% CO₂ and the OD₆₀₀ nm of 1 mL aliquots recorded at 0, 4, 8, 18 and 24 hr.

Scanning electron microscopy

Scanning electron microscopy was used to visually confirm the effect of chalcone 8 on NTHi biofilm formation. Biofilms grown on glass coverslips for 18 hr

in the presence or absence of the test chalcone (at the concentration equal to MBIC₅₀) were rinsed with PBS (pH 7.2) and fixed with 2.5% glutaraldehyde in PBS (pH 7.2) for 60 min at room temperature. After being carefully washed twice with PBS (pH 7.2), the samples were dehydrated through a graded series of ethanol concentrations (30–100%) and dried with hexamethyl-silazine (Sigma—Aldrich, St Louis, MO, USA). Dried samples were sputtered with palladium/gold and then viewed with a Leo 1455VP scanning electron microscope (LEO Electron Microscopy, Cambridge, UK) in high-vacuum mode at 20 kV.

Cytotoxic evaluation

The cytotoxic effect of chalcone **8** against human cells was evaluated by MTT assay as previously described (31). Briefly, peripheral blood mononuclear cells isolated from healthy adults were cultured under 5% CO₂ and 37 °C in RPMI-1640 medium (PAA, Pasching, Austria) supplemented with 10% (v/v) FBS (Gibco, Gaithersburg, MD, USA), 0.01 M HEPES pH 7.4, 2 mM L-glutamine (PAA), 100 U/mL penicillin and 100 μ g/mL streptomycin (PAA). Cells were plated in 96-well plates and then exposed for 48 hr to chalcone **8** at concentrations ranging from 0.25 to 32 μ g/mL, with untreated cells serving as control. Cell viability was quantified by MTT colorimetric assay. Absorbance was measured at 540 nm and the results expressed as the percentage of cell viability compared with the control.

Statistical analysis

Data are expressed as mean \pm SEM. Statistical significance was assessed using Student's *t*-test. All statistical analyses were performed with SPSS version 11.5 (SPSS, Chicago, IL, USA). Differences were considered to be significant at P < 0.05.

RESULTS

Biofilm formation by NTHi

The ability of clinical NTHi isolates NU7, NU38 and NU48 to form biofilm was determined on the surface of polystyrene wells and expressed as BFI. The BFI values for NU7, NU38 and NU48 were 2.07 ± 0.27 (biofilm OD, 0.782; growth OD, 0.377), 2.54 ± 0.15 (biofilm OD, 0.844; growth OD, 0.333) and 2.01 ± 0.78 (biofilm OD, 0.435; growth OD, 0.217), respectively. According to the semi-quantitative classification of biofilm formation, any bacteria with BFI values ≥ 1.10 are defined as strong biofilm producers (27). Thus, the clinical isolates of NTHi in this study were all strong-biofilm producing strains.

Effects of chalcones on NTHi biofilm formation

Initially, the natural chalcones 1 and 2 were tested for their inhibitory activities against biofilm formed by clinical NTHi isolates NU7, NU38 and NU48. We found that these natural compounds inhibit formation of NTHi biofilm (mean MBIC₅₀ 166.63 and 254.82 μM, respectively) and are more potent inhibitors than azithromycin (mean MBIC₅₀ 419.68 μM), suggesting that chalcones have potential as antibiofilm agents for NTHi (Table 1). Further to these observations, we postulated that chemical modifications of chalcones might strengthen their inhibitory activities. Therefore, compounds with various chemical substituents introduced to the two aryl rings of chalcone backbone were synthesized and their antibiofilm activities assessed. Modification of NTHi biofilm formation to varying degrees was observed in the presence of these synthetic chalcones. Among the synthetic chalcones evaluated, chalcone 8 was the most effective. This compound clearly showed concentration-dependent inhibitory effects on in vitro biofilm formation by all NTHi studied, even with the strongestbiofilm producing strain, NU38 (Fig. 2). Consistent with when there is >50% inhibition of biofilm formation, chalcone 8 demonstrated the most distinct and potent inhibitory effect, the lowest mean MBIC₅₀ value being $16 \mu g/mL$ (71.35 μM ; Table 1). At this concentration, the biofilm inhibitory activity of chalcone 8 was timedependent within 24 hr of incubation. Within this time range, obviously reduced biofilm formation by NU38 was seen as early as 4 hr after beginning incubation, whereas reduction of biofilm produced by NTHi strains NU7 and NU48 was observed 8 and 12 hr, respectively, after exposure (results not shown). Inhibitory activities were less pronounced for chalcones 5, 6 and 9; little or no inhibition was found in the presence of chalcones 3, 4, 7 and 10–13 (Table 1). It is interesting to note that chalcone 8 exerted several-fold stronger antibiofilm activity against NTHi than both the tested natural chalcones and azithromycin. Accordingly, chalcone 8 was chosen for further studies.

Effect of chalcone on growth of NTHi

To determine whether biofilm inhibition by chalcone 8 was attributable to a growth-inhibitory effect, growth of NTHi cultures in the presence or not of such a compound was monitored by measuring turbidity. Growth of all NTHi strains in the presence of chalcone **8** at concentrations ranging from 0.25 to 128 µg/mL was comparable to that of non-treated control cultures, although bacterial growth was decreased at 256 and 512 µg/mL (data not shown). Consistent with the growth curve assay, it was also found that all studied NTHi cultures continued to grow after addition of chalcone 8: the growth curves appeared to be similar to those of the non-treated control cultures after prolonged exposure to the test compound (Fig. 3). Thus, the results of antimicrobial and growth curve assays suggested that NTHi biofilm inhibition by chalcone 8 is not caused by inhibition of growth.

Table 1. Minimum biofilm inhibitory concentrations (MBIC₅₀) of chalcones against nontypeable *H. influenzae* NU7, NU38 and NU48

		MBIC ₅₀ [†]				
		Range		Mean		
Compound	μg/mL	μΜ	μg/mL	μΜ		
1	32–64	124.97–249.93	42.67	166.63		
2	16–128	58.81-470.47	69.33	254.82		
3	128–512	$614.62-2.46 \times 10^3$	298.67	1.43×10^{3}		
4	16–512	$71.35-2.28 \times 10^3$	218.67	975.12		
5	16–128	71.35–570.79	69.33	309.16		
6	16–256	$71.35-1.14 \times 10^3$	101.33	451.86		
7	64 to >512	$268.59 \text{ to } > 2.15 \times 10^3$	>512	$>2.15 \times 10^{3}$		
8	16–16	71.35–71.35	16	71.35		
9	64–128	251.69–503.38	85.33	335.58		
10	32–512	$125.85-2.10 \times 10^3$	202.67	797.03		
11	256–256	954.12–954.12	256	954.12		
12	32–512	$125.85 - 2.01 \times 10^3$	202.67	797.04		
13	512 to >512	$2.11 \times 10^3 \text{ to } > 2.11 \times 10^3$	>512	$>2.11 \times 10^{3}$		
Azithromycin	256–512	341.80–683.60	314.33	419.68		

[†]Minimum biofilm concentration of the chalcone tested that showed >50% inhibition of biofilm formation.

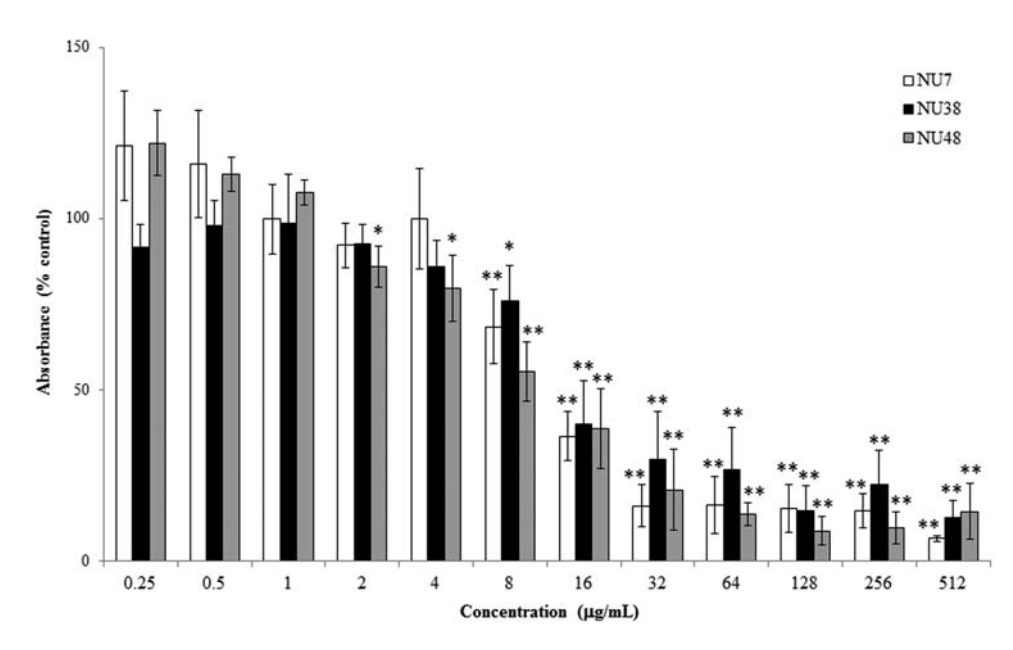


Fig. 2. Effects of chalcone **8** on biofilm formation by nontypeable *H. influenzae*. The bacteria (NU7, NU38 and NU48) were incubated in 96-well microtiter plates with different concentrations of the test compound and without a test compound (non-treated control). After incubation at 37 °C under 5% CO_2 , the adherent bacteria were stained with crystal violet and the OD at 540 nm determined to assess the amount of biofilm formed. The results are expressed as percentages of biofilm formed by the non-treated control. Data represent the mean \pm SEM of four independent experiments. *, P < 0.05; **, P < 0.01 compared with the control without test compound.

Effect of chalcone 8 on NTHi biofilm morphology

Scanning electron microscopy was performed to more closely examine the effect of chalcone 8 on NTHi biofilm morphology; scanning electron photographs are shown in Figure 4. With the non-treated control, thick and

relatively homogenous biofilm was formed on the glass coverslips. Compared to the non-treated control, treatment with chalcone 8 resulted in greatly reduced biofilm formation: only a few scattered bacterial microcolonies were seen. These visual findings confirm the inhibitory activity of chalcone 8 on biofilm formation by NTHi.

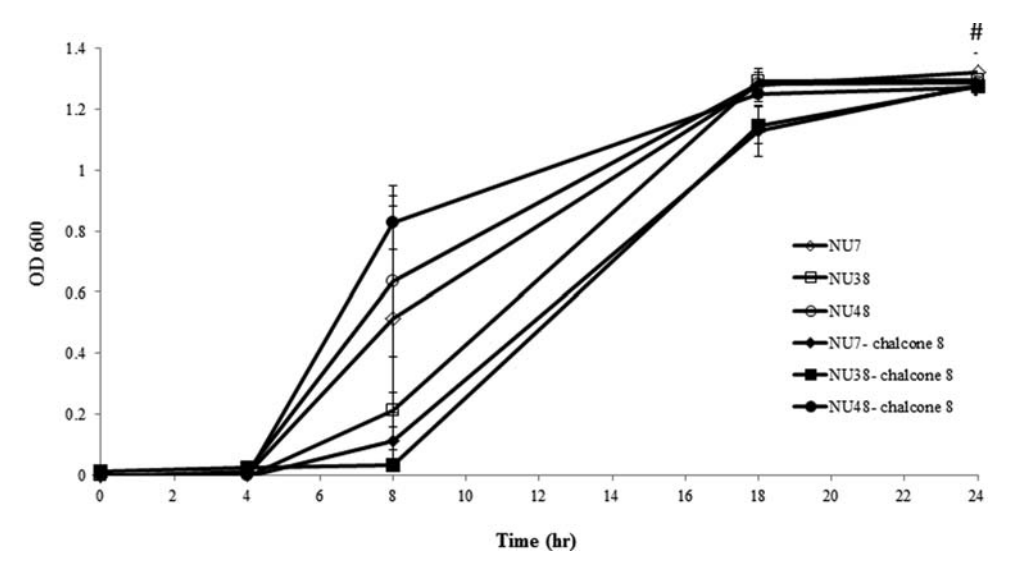
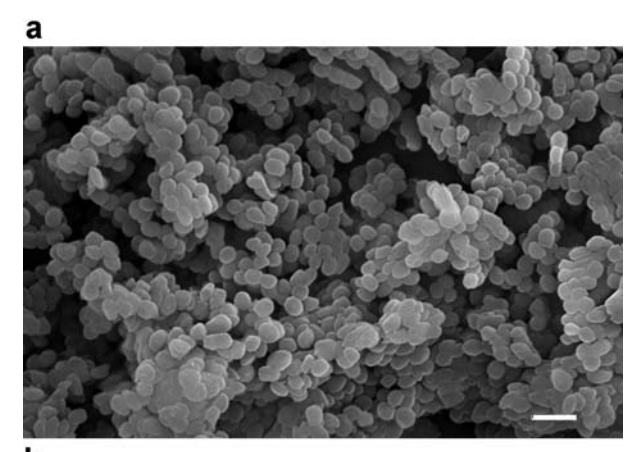


Fig. 3. Effects of chalcone **8** on growth of nontypeable *H. influenzae*. The bacteria (NU7, NU38 and NU48) were grown in HTM with the test chalcone (at the concentration equal to $MBIC_{50}$) at 37 °C, 5% CO_2 . A culture without the test compound was used as a bacterial growth control. Bacterial growth was assessed by measuring OD_{600} at the indicated time points. Data represent the mean \pm SEM of two independent experiments. $^{\#}$, not statistically different to control (P > 0.5).



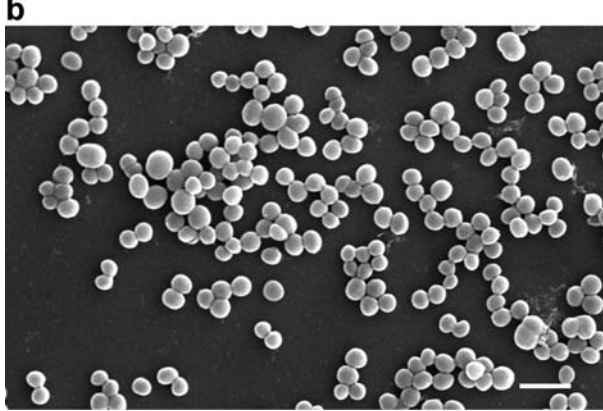


Fig. 4. Effect of chalcone **8** on nontypeable *H. influenzae* biofilm morphology. Biofilm of nontypeable *H. influenzae* was grown on glass coverslips (a) without chalcone or (b) with compound **8** at the concentration equal to $MBIC_{50}$. The images are representative of the results for NU7 (observations for NU38 and NU48 were similar). Magnification, $\times 3000$. Scale bars, 2 μ m.

Cytotoxicity of chalcone 8

Regarding future therapeutic applications of chalcone 8, not only its potent antibiofilm activity, but any toxicity against human cells is very important. Therefore, the cytotoxic effect(s) of chalcone 8 against human peripheral blood mononuclear cells were evaluated. As quantified by MTT assay, chalcone 8 had no effect on the viability of human cells at 48 hr of incubation (Fig. S2). Of particular note, a high percentage (approximately 90%) of cells exposed to chalcone 8 survived at the concentration at which it displayed antibiofilm activity ($16 \,\mu\text{g/mL}$), suggesting that chalcone 8 has little cytotoxic effect.

DISCUSSION

The present study investigated the inhibitory activities of chalcone-based compounds on biofilm formation of NTHi. Significant findings of this study are that (i) chalcone **8** is the most active of the chalcones evaluated; (ii) the antibiofilm activity of chalcone **8**, a chemically modified chalcone, is superior to those of the natural chalcones tested; (iii) its excellent inhibitory action was demonstrated both quantitatively and qualitatively in all studied NTHi strains; (iv) chalcone **8** has stronger antibiofilm activity against NTHi than the previously reported azithromycin, with a considerably lower MBIC $_{50}$ value; and (v) at active concentrations, chalcone **8** has little toxic effect on human cells.

In this study, we found that chemical modification of the chalcone backbone markedly increases inhibitory activity against NTHi biofilms. The NTHi used in this study were clinical isolates collected from various specimen types and were all proven to be strong biofilm producers. Thus, we demonstrated that the antibiofilm activity of the chemically modified chalcone, chalcone 8, occurs across multiple strong biofilm-forming NTHi isolates of different clinical origins. These findings indicate that chalcone 8 has powerful antibiofilm activity and convincingly suggest such a compound has the potential to improve treatment of NTHi biofilm-associated diseases in various clinical settings.

Remarkably, growth of NTHi was unaffected by chalcone 8 at concentrations that decreased biofilm formation, indicating the biofilm inhibitory effect of this compound is non-antimicrobial. In the biofilm susceptibility assay, we added the test compound to polystyrene wells of microtiter plates at the same time as bacterial cells; time-dependent assays showed that biofilm formation decreased as early as 4 hr after incubation. The initial adherence to and accumulation of microorganisms on surfaces is a critical step in both establishment of infection and the subsequent stage of biofilm formation. It is possible that chalcone 8 interferes with the early step of bacterial adhesion and that formation of biofilm is subsequently inhibited. Our findings are of clinical significance because chalcone 8 may serve as an anti-adherent and antibiofilm agent: its presence would undoubtedly prevent establishment of infection and inhibit biofilm formation. With bacteria that can form biofilm, once attached to a surface, they initially continue to grow into a sessile biofilm, later detaching from it and dispersing into the surroundings to colonize new sites. Thus, the presence of chalcone 8 would limit the spread of biofilm diseases by preventing bacterial cells that have detached from a biofilm colony from colonizing new unoccupied tissues. Targeting the virulence determinants involved in bacterial adherence, rather than inhibiting cellular components necessary for growth or viability, thus provides an alternative strategy for limiting or ameliorating infections (32). Though unconventional, this promising new approach has

received attention during the last decade (17, 33). Natural compounds, in particular the flavonoids, have increasingly been documented to interfere with a number of bacterial virulence factors, including quorum-sensing signal receptors, enzymes and toxins (17, 34, 35). In this study, we did not address the mechanisms by which the open chain flavonoid chalcone 8 inhibits NTHi biofilm formation. Whether this compound interferes with virulence factors or other additional mechanisms required for such inhibitory actions requires further investigation. Nevertheless, because its antibiofilm activity does not interfere with bacterial growth, chalcone 8 will probably exert low selection pressure on NTHi and may therefore contribute minimally to development of problematic antibiotic resistance.

Assessment of antibiofilm activities of a series of compounds with different chemical structures would deliver certain correlations between structure and activity, even if such correlations are not specifically being investigated. Both the natural chalcones 1 and 2 possess hydroxyl groups in both the A and B rings. In order to investigate the effects of oxygen functions in the molecule, we synthesized a chalcone with no hydroxyl group (chalcone 3) and evaluated it for antibiofilm activity: we found that this compound was much less active than the natural chalcones 1 and 2 (Table 1). The low activity of chalcone 3 against NTHi biofilms indicates that oxygen function is essential for antibiofilm potential. To determine the effects of hydroxyl groups on the A ring, we synthesized chalcones 4 and 5. Although these two chalcones have stronger antibiofilm activity than the unsubstituted chalcone 3, they have less activity than the natural chalcones 1 and 2 (Table 1). We therefore synthesized chalcone 6, a chalcone with a hydroxyl group at position 4 of the B ring. The assay results indicate that, though chalcone 6 is twofold more active than chalcone 4, it is slightly less active than chalcone 5 and azithromycin (Table 1). Methylation of chalcone 6 to chalcone 7 resulted in sharp decrease in activity. However, chalcone 8, a chalcone with a 3hydroxyl group on the B ring, exhibited very strong antibiofilm activity (mean $MBIC_{50}$ 71.35 μM); it was approximately sixfold more active than azithromycin. Placement of an extra methoxyl group at the 4-position of the chalcone 8 to yield chalcone 9 caused decrease in activity. This implies that the hydroxyl group should be free and that the presence of a methoxyl group results in decrease in activity. This was further evident from the low activity of chalcones 10–12 (Table 1). The 4-chloro analogue 13 is much less active than its hydroxyl analogue 6, which indicates the importance of a free hydroxyl group. Taken together, these observations indicate that a free hydroxyl group at position 3 on the B ring is a crucial structural requirement for anti-NTHi biofilm activity.

In conclusion, the present study has clearly demonstrated, for the first time, that 3-hydroxychalcone (chalcone 8) possesses antibiofilm activity against NTHi. This compound inhibits biofilm formation by clinically strong-biofilm producing isolates of NTHi. Although further studies on the mechanisms of action as well as *in vivo* assessments are still required, our results indicate that chalcone 8 has potential as a novel therapeutic agent that would be of value in treatment of NTHi biofilm-related infections. Future research on eradication of already formed biofilms by chemically modified chalcones is also required. Because flavonoids are often influenced by pH, the effects of pH on stability and antibiofilm activity of the active chalcones should also be further investigated.

ACKNOWLEDGMENTS

This study was supported by the National Research Council of Thailand through the Annual Research Fund of Naresuan University and also supported partially by the Thailand Research Fund.

DISCLOSURE

The authors declare they have no competing interests.

REFERENCES

- Kochanek K.D., Murphy S.L., Anderson R.N., Scott C. (2004)
 Deaths: final data for 2002. Natl Vital Stat Rep 53: 1-115.
- 2. Sullivan S.D., Ramsey S.D., Lee T.A. (2000) The economic burden of COPD. *Chest* 117: 5S–9S.
- Gates G.A. (1996) Cost-effectiveness considerations in otitis media treatment. Otolaryngol Head Neck Surg 114: 525–30.
- 4. Murphy T.F., Kirkham C. (2002) Biofilm formation by nontypeable *Haemophilus influenzae*: strain variability, outer membrane antigen expression and role of pili. *BMC Microbiol* 2: 7
- Hall-Stoodley L., Hu F.Z., Gieseke A., Nistico L., Nguyen D., Hayes J., Forbes M., Greenberg D.P., Dice B., Burrows A., Wackym P.A., Stoodley P., Post J.C., Ehrlich G.D., Kerschner J.E. (2006) Direct detection of bacterial biofilms on the middleear mucosa of children with chronic otitis media. *JAMA* 296: 202-11
- 6. Hüiby N., Ciofu O., Bjarnsholt T. (2010) Antibiotic resistance of bacterial biofilms. *Int J Antimicrob Agents* **35**: 322–32.
- Fux C.A., Costerton J.W., Stewart P.S., Stoodley P. (2005) Survival strategies of infectious biofilms. *Trends Microbiol* 13: 34–40.
- Hong W., Juneau R.A., Pang B., Swords W.E. (2009) Survival of bacterial biofilms within neutrophil extracellular traps promotes nontypeable *Haemophilus influenzae* persistence in the chinchilla model for otitis media. *J Innate Immun* 1: 215–24.

- Fux C.A., Stoodley P., Hall-Stoodley L., Costerton J.W. (2003)
 Bacterial biofilms: a diagnostic and therapeutic challenge. Expert Rev Anti Infect Ther 1: 667–83.
- 10. Bjarnsholt T. (2013) The role of bacterial biofilms in chronic infections. *APMIS Suppl* **136**: 1–51.
- Uemura Y., Qin L., Gotoh K., Ohta K., Nakamura K.I., Watanabe H. (2013) Comparison study of single and concurrent administrations of carbapenem, new quinolone, and macrolide against in vitro nontypeable Haemophilus influenzae mature biofilms. J Infect Chemother 19: 902–8.
- Slinger R., Chan F., Ferris W., Yeung S.-W., St. Denis M., Gaboury I., Aaron S.D. (2006) Multiple combination antibiotic susceptibility testing of nontypeable *Haemophilus influenzae* biofilms. *Diagn Microbiol Infect Dis* 56: 247–53.
- Goossens H. (2005) European status of resistance in nosocomial infections. Chemotherapy 51: 177–81.
- Dimmock J.R., Elias D.W., Beazely M.A., Kandepu N.M. (1999) Bioactivities of chalcones. Curr Med Chem 6: 1125–49.
- Bukhari S.N., Jantan I., Jasamai M. (2013) Anti-inflammatory trends of 1,3-diphenyl-2-propen-1-one derivatives. *Mini Rev Med Chem* 13: 87–94.
- Sivakumar P.M., Prabhawathi V., Doble M. (2010) Antibacterial activity and QSAR of chalcones against biofilm-producing bacteria isolated from marine waters. SAR QSAR Environ Res 21: 247–63.
- 17. de Lima Pimenta A., Chiaradia-Delatorre L.D., Mascarello A., de Oliveira K.A., Leal P.C., Yunes R.A., de Aguiar C.B., Tasca C.I., Nunes R.J., Smânia A.J. (2013) Synthetic organic compounds with potential for bacterial biofilm inhibition, a path for the identification of compounds interfering with quorum sensing. *Int J Antimicrob Agents* 42: 519–23.
- Chokchaisiri R., Suaisom C., Sriphota S., Chindaduang A., Chuprajob T., Suksamrarn A. (2009) Bioactive flavonoids of the flowers of *Butea monosperma*. Chem Pharm Bull 57: 428–32.
- Kohler E.P., Chadwel H.M. (1922) Benzalacetophenone. Org Synth 2: 1–3.
- Karki R., Thapa P., Kang M.J., Jeong T.C., Nam J.M., Kim H.L., Na Y., Cho W.J., Kwon Y., Lee E.S. (2010) Synthesis, topisomerase I and II inhibitory activity, cytotoxicity, and structure–activity relationship study of hydroxylated 2,4diphenyl-6-aryl pyridines. *Bioorg Med Chem* 18: 3066–77.
- Yadav H.L., Gupta P., Pawar R.S., Singour P.K., Patil U.K.
 (2011) Synthesis and biological evaluation of anti-inflammatory activity of 1,3-diphenyl propenone derivatives. *Med Chem Res* 20: 461–5
- Tatsuzaki J., Bastow K.F., Nakagawa-Goto K., Nakamura S., Itokawa H., Lee K.H. (2006) Dehydrozingerone, chalcone, and isoeugenol analogues as *in vitro* anticancer agent. *J Nat Prod* 69: 1445–9.
- Watanabe K., Imazawa A. (1982) Aldol condensations catalyzed by Co(II) complexes of pyridine-containing copolymers. *Bull Chem Soc Jpn* 5: 3208–11.
- Arty I.S., Timmerman H., Samhoedi M., Sastrohamidjojo Sugiyanto, van der Goot H. (2000) Synthesis of benzylideneacetophenones and their inhibition of lipid peroxidation. *Eur J Med Chem* 35: 449–57.
- Hasan A., Khan K.M., Sher M., Maharvi G.M., Nawaz S.A., Choudhary M.I., Rahman A.U., Supuran C.T. (2005) Synthesis and inhibitory potential towards acetylcholinesterase, butyrylcholinesterase and lipoxygenase of some variably

- substituted chalcones. *J Enzyme Inhib Med Chem* **20**: 41–7
- Kunthalert D., Kamklon P. (2007) PCR-based serotyping of the clinical Haemophilus influenzae isolates. J Med Tech Assoc Thailand 35: 1778–92.
- Naves P., del Prado G., Huelves L., Gracia M., Ruiz V., Blanco J., Rodriguez-Cerrato V., Ponte M.C., Soriano F. (2008)
 Measurement of biofilm formation by clinical isolates of *Escherichia coli* is method-dependent. *J Appl Microbiol* 105: 585–90
- Starner T.D., Shrout J.D., Parsek M.R., Appelbaum P.C., Kim G. (2008) Subinhibitory concentrations of azithromycin decrease nontypeable *Haemophilus influenzae* biofilm formation and diminish established biofilms. *Antimicrob Agents Chemother* 52: 137–45.
- 29. Wang D., Wang Y., Liu Y.N. (2009) Activity of ciprofloxacin and azithromycin on biofilms produced *in vitro* by *Haemophilus influenzae*. Chin Med J 122: 1305–10.
- 30. Wei G-X., Campagna A.N., Bobek L.A. (2006) Effect of MUC7 peptides on the growth of bacteria and on *Streptococcus mutans* biofilm. *J Antimicrob Chemother* 57: 1100–9.
- Mosmann T. (1983) Rapid colorimetric assay for cellular growth and survival: application to proliferation and cytotoxicity assays. J Immunol Methods 65: 55–63.
- Klemm P., Vejborg R.M., Hancock V. (2010) Prevention of bacterial adhesion. Appl Microbiol Biotechnol 88: 451–9.
- Kim H.S., Park H.D. (2013) Ginger extract inhibits biofilm formation by *Pseudomonas aeruginosa* PA14. *PLos ONE* 8: e76106.
- Cushnie T.P., Lamb A.J. (2011) Recent advances in understanding the antibacterial properties of flavonoids. *Int J Antimicrob Agents* 38: 99–107.
- Vasavi H.S., Arun A.B., Rekha P.D. (2014) Anti-quorum sensing activity of *Psidium guajava* L. flavonoids against *Chromobacterium violaceum* and *Pseudomonas aeruginosa* PAO1. *Microbiol Immunol* 58: 286–93.

SUPPORTING INFORMATION

Additional supporting information may be found in the online version of this article at the publisher's web-site.

Fig. S1. Synthesis of chalcones 3-13. Chalcones 3-13 were synthesized by the Claisen–Schmidt condensation reaction of substituted acetophenone with substituted benzaldehyde in the presence of an aqueous solution of 50% KOH in ethanol at room temperature for 6-12 hr. Fig. S2. Viability of human peripheral blood mononuclear cells after exposure to chalcone 8. Cells were cultured in the absence or presence of chalcone 8 at varying concentrations for 48 hr at 37 °C in a humidified CO_2 incubator. Cell viability was determined by MTT colorimetric assay. Results are expressed as percentage viability of the control without test compound. Data represent the mean \pm SEM of two independent experiments.

RESEARCH ARTICLE

In vitro and In vivo Antitumor Activity of Tiliacorinine in Human Cholangiocarcinoma

Somkid Janeklang^{1,3}, Archawin Nakaew⁴, Kulthida Vaeteewoottacharn^{1,3,5}, Wunchana Seubwai^{2,3}, Patcharee Boonsiri¹, Gorkem Kismali⁶, Apichart Suksamrarn⁴, Seiji Okada⁵, Sopit Wongkham^{1,3}*

Abstract

Cholangiocarcinoma (CCA) is a fatal cancer with poor prognosis and less than 10% of CCA patients can be offered surgical cure. Conventional chemotherapy results in unfavorable outcomes. At present, plant-derived compounds are gaining interest as potential cancer therapeutics, particularly for treatment-refractory cancers. In this study, antitumor activity of tiliacorinine, the major alkaloid isolated from a tropical plant, on CCA was first demonstrated. Antiproliferative effects of tiliacorinine on human CCA cell lines were investigated using SRB assays. Acridine orange/ethidium bromide staining, flow cytometric analysis and DNA laddering assays were used for apoptotic determination. Apoptosis-related proteins were verified by Western blotting and antitumor activity of tiliacorinine $in\ vivo$ was demonstrated in CCA xenografted mice. Tiliacorinine significantly inhibited proliferation of human CCA cell lines with IC $_{50}$ 4.5-7 μ M by inducing apoptosis through caspase activation, upregulation of BAX, and down-regulation of Bcl $_{xL}$ and XIAP. Tiliacorinine considerably reduced tumor growth in CCA xenografted mice. These results demonstrated antitumor effects of tiliacorinine on human CCA $in\ vitro$ and $in\ vivo$. Tiliacorinine may be an effective agent for CCA treatment.

Keywords: Antitumor activity - apoptosis - growth inhibition - bile duct cancer - alkaloid

Asian Pac J Cancer Prev, 15 (17), 7473-7478

Introduction

Cholangiocarcinoma (CCA), a malignant cancer arising from bile duct epithelium, is a rare liver cancer but a serious public health problem in the northeast of Thailand as it has the highest incidence and mortality rate in the world (Sripa and Pairojkul, 2008). Generally, only 10% of patients present with early-stage disease are considered surgical candidates (Han et al., 2005) and chemotherapy is the option left for these inoperable patients (Chou and Talalay, 1984). However, the outcome of the chemo-drug treatment is unfavorable with the five year survival lesser than 10% (Butthongkomvong et al., 2013; Rizvi and Gores, 2013; Thunyaharn et al., 2013). To reduce the mortality rate of CCA, new effective treatment strategies are needed.

Plant-derived compounds are gaining interest as potential cancer therapeutics (Shukla, 2007; Aras et al., 2014), particularly for treatment-refractory cancers such as CCA (Naus et al., 2007). In this study, tiliacorinine (Figure. 1A), the bisbenzylisoquinoline alkaloid isolated

from a tropical medicinal plant, Tiliacora triandra (Colebr.) Diels, was investigated for antitumor activity in CCA cell lines *in vitro* and *in vivo*. The molecular mechanism by which tiliacorinine induces apoptosis of CCA was also determined. Our findings suggested tiliacorinine to be a new promising compound for effective treatment against human CCA.

Materials and Methods

Chemicals and reagents

Cell culture reagents were purchased from Gibco/ Invitrogen (Carlsbad, CA). Antibodies were obtained from companies as indicated: Bcl-2-associated X protein (BAX), B-cell leukemia protein xL (Bcl_{xL}), X-linked inhibitor of apoptosis protein (XIAP), and poly-adenosine diphosphate ribose polymerase (PARP) from Santa Cruz Biotechnology (Santa Cruz, CA); anti-caspase-3 and-9, goat anti-rabbit IgG- and goat anti-mouse IgG-conjugated to horseradish peroxidase (HRP) from Cell Signaling Technology (Beverly, MA), and β-actin antibody from

¹Department of Biochemistry, ²Department of Forensic Medicine, ³Liver fluke and Cholangiocarcinoma Research Center, Faculty of Medicine, Khon Kaen University, Khon Kaen, ⁴Department of Chemistry and Center of Excellence for Innovation in Chemistry, Faculty of Science, Ramkhamhaeng University, Bangkok, Thailand, ⁵Division of Hematopoiesis, Center of AIDS Research, Kumamoto University, Honjo, Kumamoto, Japan, ⁶Department of Biochemistry, Faculty of Veterinary Medicine, Ankara University, Ankara, Turkey *For correspondence: sopit@kku.ac.th

Sigma Chemical Co (St Louis, MO).

Cell lines and cell culture

Four human CCA cell lines-KKU-M055, KKU-100-KKU-M213 and KKU-M214-were established from primary tumors of CCA patients as described previously (Sripa et al., 2005; Seubwai et al., 2010). All cells were cultured at 37°C with 5% $\rm CO_2$ in Ham's F-12 containing 1% antibiotics-antimycotics solution and 10% FBS.

Isolation of tiliacorinine

Tiliacorinine was isolated from Tiliacora triandra as described previously (Pachaly and Khosravian, 1988) with modification. Briefly, 10.0 kg of pulverized dried roots and stems were macerated successively with n-hexane and ethyl acetate to give the hexane (535.20 g) and ethyl acetate (519.86 g) extracts. The plant material was then extracted with methanol-chloroform-ammonium hydroxide (15:5:1). After solvent evaporation, glacial acetic acid was added followed by ammonium hydroxide. The insoluble polymeric material was removed from the aqueous suspension and the latter was extracted with chloroform. The crude alkaloid extract was chromatographed to give tiliacorinine (1.053 g) and a mixture of minor alkaloids (300 mg). More tiliacorinine (96mg) was obtained from the ethyl acetate extract by column chromatographic separation. The spectroscopic (proton and carbon-13 NMR, and mass spectra) data were consistent with the literature values (Wiriyachitra, 1981; Pachaly and Khosravian, 1988). Tiliacorinine was dissolved in DMSO and diluted with completed media to the indicated concentrations.

In vitro cytotoxicity test

The effects of tiliacorinine on the proliferation of CCA cells were determined using SRB assay (Skehan et al., 1990). Briefly, CCA cells (3,000 cells/well) were incubated with tiliacorinine in a 96-well plate. At indicated time points, cells were treated with 10% ice-cold trichloroacetic acid and stained with 0.4% SRB in 1% acetic acid. The stained proteins were solubilized and the absorbance at 540nm was measured (Vichai and Kirtikara, 2006). Dose-response curves were plotted, and the concentration of drug required to inhibit cell proliferation by 50% (IC $_{50}$) was calculated using the Calcusyn software (Biosoft, Oxford, UK).

DNA fragmentation assay

The isolation of fragmented DNA was carried out as previously described (Herrmann et al., 1994). Briefly, 5×10^5 cells were lyzed in 100 μ L of 10 mM Tris-HCl buffer (pH 7.4), 10 mM EDTA and 0.5% Triton X-100. Final samples were dissolved in 40 μ L of Tris-EDTA buffer, pH 8.0, subjected to agarose gel electrophoresis and stained with ethidium bromide.

Acridine orange/ethidium bromide double staining

Cells (3,000 cells/100 μ L) were treated with 0.01% DMSO or various concentrations of tiliacorinine for 72h and subjected to acridine orange/ethidium bromide (AO/EB) staining as previously described (Petit et al., 1995).

The stained cells were visualized under a fluorescent microscope (Nikon Eclipse TS100, Nikon Corporation, Tokyo, Japan). Multiple photos (9 fields/sample) were taken at randomly-selected areas and apoptotic cells were count using Image ProPlus 7.0 (Media Cybernetics, Inc., Bethesda, MD). A minimum of 100 total cells were count and expressed as a percentage. Tests were done in triplicate.

Western blotting

Cells were lyzed with RIPA buffer (50 mM Tris-HCl, pH 7.4, 150 mM NaCl, 1% NP-40) supplemented with cocktail proteinase inhibitors (Roche, Mannheim, Germany). Proteins in cell lysates were separated by a 10% SDS-polyacrylamide gel electrophoresis according to Laemmli (Laemmli, 1970) and electro-transferred onto a polyvinylidene difluoride membrane according to Bolt and Mahoney (Bolt and Mahoney, 1997). The membrane was blocked with 1% (w/v) skim milk, 0.1% tween (v/v) in Tris-buffered saline, pH 7.4 for 30 min and incubated with specific primary antibodies at 4°C overnight and secondary antibody conjugated-HRP at room temperature for 2h. The expression level of proteins were detected using Amersham ECL Plus Western blotting detection reagents (GE Health care, Piscataway, NJ) and captured with ImageQuantTM 400 and analyzed with ImageQuantTM TL software.

Flow cytometric analysis of apoptotic cells

Flow cytometric analysis of cell cycle distribution was performed using a FACSCalibur flow cytometer (BD-Biosciences, San Jose, CA) as previously described (Seubwai et al., 2010). Briefly, cells were fixed with 70% ethanol at -20°C overnight and stained with 10 μ g/mL propidium iodine (PI; Sigma, St Louis, MO) in phosphate buffer saline for 30 min in the dark. A total of 10,000 cells were analyzed by flow cytometry. Sub-G1 peak was analyzed using BD FACSDiva software (BD Biosciences, San Jose, CA).

In vivo assay

Bulb/c Rag-2 Jak3 double knock-out mice (Ono et al., 2011) aged 8-10 week old were housed and monitored in the animal research facility according to the institutional guidelines. All experimental protocols were approved by the Institutional Animal Care and Use Committee, Kumamoto University (Kumamoto, Japan). Mice were subcutaneously injected with 4×10⁶ of KKU-M213 cells at both flank sides. Three days after CCA cell-injection, mice were intraperitoneally injected with 0.01% DMSO (control group; n=5) or tiliacorinine (10mg/kg body weight; n=5) once daily for 3 consecutive days. Body weights and tumor volumes were measured every 3 days. Tumors were removed and weighed 9 days after inoculation.

Statistical analysis

Experimental data were analyzed using SPSS 16.0 Windows Evaluation software (SPSS Inc., Chicago, IL). The results are presented as the mean±standard deviation of at least 3 separated experiments. Statistical significance

was determined with the Student t test. p values <0.05 were considered significant.

Results

Tiliacorinine inhibits growth of human CCA cells

In order to determine the growth inhibitory effect of tiliacorinine on human CCA cells-KKU-M055, KKU-100, KKU-M213, and KKU-M214-cells were treated with various concentrations of tiliacorinine for 72h and investigated by SRB assay. Growth inhibitory effects of tiliacorinine on the tested cells were KKU-M055>KKU-M213>KKU-M214>KKU-100 with IC₅₀ values of 4.5±0.3, 5.7±0.2, 6.1±0.3, and 7.0±0.6 respectively (Figure 1B). Treated cells exhibited dosedependent sensitivity to tiliacorinine from 1.7-8.7 μ M. As KKU-M214 and KKU-100 were less sensitive to tiliacorinine, they were selected as representative of CCA cells for the subsequent studies.

Tiliacorinine suppresses growth of human CCA cells by inducing apoptosis

We further investigated whether tiliacorinine inhibited growth of human CCA cells by induction of apoptosis. Apoptotic indices were determined by 3 different approaches. AO/EB double staining was applied to discriminate the live, apoptotic and necrotic cells. Exposure of KKU-M214 and KKU-100 cells to 4-7 μ M of tiliacorinine significantly induced apoptotic cells with typical apoptotic features e.g., cell shrinkage, membrane

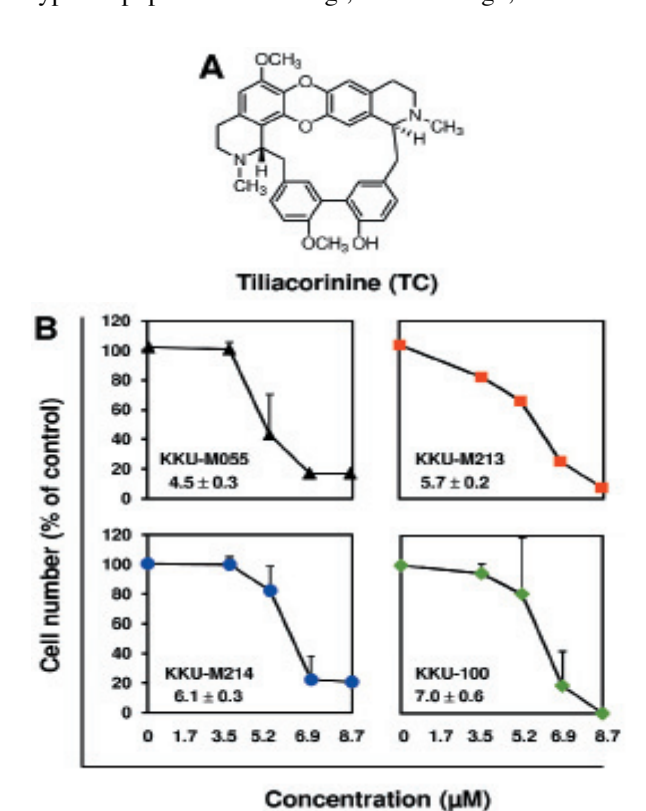


Figure 1. Chemical Structure and Antiproliferative Effect of Tiliacorinine. (A) The chemical structure of tiliacorinine ($C_{36}H_{36}N_2O_5$) with molecular weight of 576.26. (B) Tiliacorinine suppressed proliferation of CCA cell lines. Cells were treated with the indicated concentrations of tiliacorinine for 72h. The numbers indicate IC_{50} of tiliacorinine

blebbing, and chromatin condensation (Figure 2A; left panel) in a dose-dependent manner (Figure 2A; right panel). Number of dead cells stimulated by tiliacorinine was next validated using flow cytometric analysis with PI staining. Cells treated with tiliacorinine for 48-72h exhibited 45-60% apoptotic cells in the sub G1 peaks which were significantly higher than the controls (p<0.05; Figure 2B). Degradation of nuclear DNA, the hallmark of apoptotic cells, was determined by DNA fragmentation assay. Cells treated with various concentrations of tiliacorinine for 24, 48, and 72h showed a gradual increase of DNA ladders, in both dose-and time-dependent manners (Figure 2C).

Tiliacorinine induces apoptosis through caspase activation

To determine whether tiliacorinine induced apoptosis via caspase activation, KKU-M214 was treated with IC $_{50}$ (6 μ M) of tiliacorinine for 24, 48, and 72h and whole cell

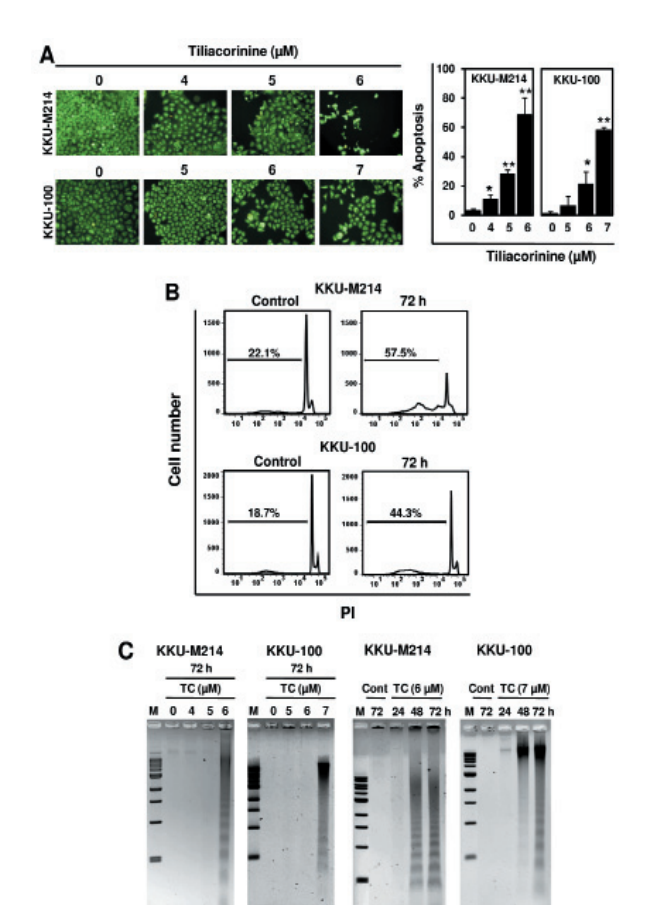


Figure 2. Tiliacorinine Induced Apoptosis in Human CCA Cells. (A) Left panel: Apoptotic cells were determined using orange/ethidium bromide staining. KKU-M214 and KKU-100 cells were treated with 0.01% DMSO or tiliacorinine at the indicated concentrations for 72h. Cells were captured at 200x magnification; right panel: apoptotic cells expressed as a percentage from each treatment were compared. Results are mean±SE and *p<0.05, **p<0.01. (B) The degree of apoptosis induced by tiliacorinine was quantified by a flow cytometry with PI staining. Sub-G1 DNA content represented the fractions undergone apoptotic DNA degradation, was evaluated. (C) DNA fragmentations of tiliacorinine treated cells were shown as time and dose dependent manners. M = 1Kb DNA ladder marker. The figures are representative results of three independent experiments

lysates were subjected to western blotting. Tiliacorinine activated caspase-3, -9 and PARP cleavages in a time-dependent fashion (Figure 3A). In addition, tiliacorinine significantly increased expression of a proapoptotic protein, BAX, and decreased expression of antiapoptotic proteins, XIAP and Bcl_{xL}, in a time-dependent manner (Figure 3B).

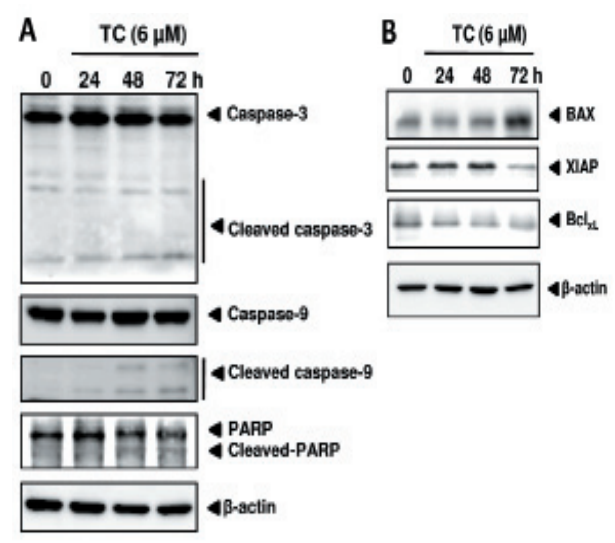


Figure 3. Tiliacorinine Induced Apoptosis Via Caspase Activation. Western blot analysis of tiliacorinine treated KKU-M214 cells at indicated time points were determined. β-actin was used as an internal control. (A) Expression of proteins in the caspase related pathway; (B) Proapoptotic and antiapoptotic proteins. TC= tiliacorinine

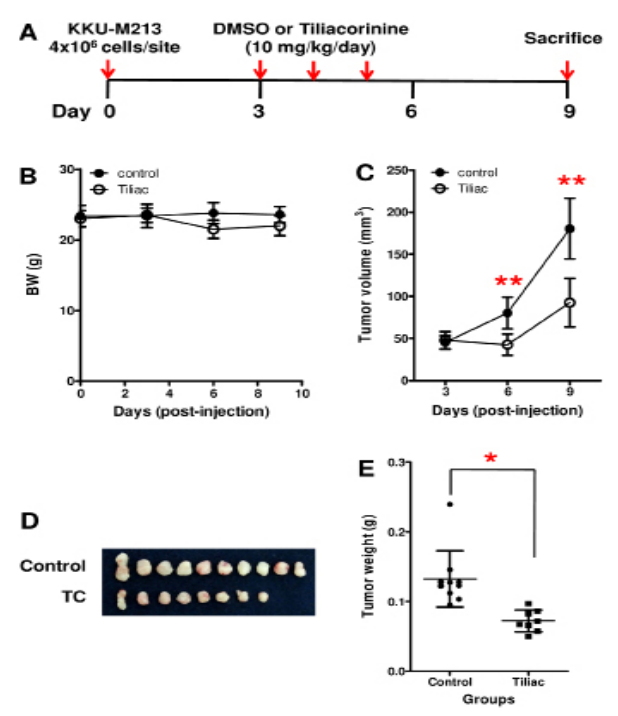


Figure 4. Antitumor Activity of Tiliacorinine in CCA Xenografted Mice. (A) Treatment protocol. Mice were subcutaneously injected with KKU-M213 in both flanks and intraperitoneally injected with DMSO or tiliacorinine once daily for 3 consecutive days (red arrows). (B) Average body weights and (C) tumor volumes of mice in each group were evaluated. (D) Tumor tissues and (E) tumor weights from DMSO and tiliacorinine-treated mice were compared. *p<0.05, **p<0.001

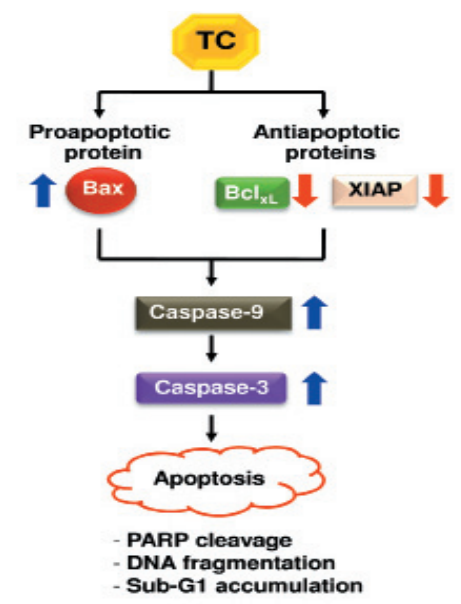


Figure 5. Proposed Mechanism of Tiliacorinine on Apoptotic Induction in Human CCA Cells

Tiliacorinine reduced tumor growth in CCA xenografted mice

To investigate the antitumor activity of tiliacorinine in animal model, KKU-M213 cells were subcutaneously injected into both flanks of mice and tiliacorinine or DMSO (control group) was intraperitoneally injected once daily for 3 consecutive days, 3 days post-CCA cell-injection (Figure 4A). Body weights of mice from both groups were not significantly different (Figure 4B). One mouse in tiliacorinine treated group died on day 8 and hence all mice were sacrificed on day 9. Mean tumor volumes from tiliacorinine treated group (45.16±12.52 mm³) was significantly lower than those of the control group (80.22±18.75 mm³) instantly on day 3 of treatment (Figure. 4C; p<0.001). On day 9, mean tumor weights from tiliacorinine treated group (0.07±0.02 g) was significantly lower than those of the control group $(0.13\pm0.04 \text{ g})$ (Figure 4E; p<0.05).

Discussion

Tiliacorinine, the major alkaloid isolated from the medicinal plant-Tiliacora triandra has been proved for anti-malarial activity (Dechatiwongse et al., 1987) and antimycobacterial activity (Sureram et al., 2012). In this study, the anticancer activity of tiliacorinine was first demonstrated *in vitro* and *in vivo*. Tiliacorinine effectively inhibited proliferation of CCA cells via induction of apoptosis and significantly reduced tumor growth in CCA xenografted mice model. These results indicate the therapeutic potential of tiliacorinine against human CCA.

Tiliacorinine inhibited growth of four human CCA cell lines with IC $_{50}$ ranging from 4.5-7.0 μ M. Comparing to other natural compounds, tiliacorinine seems to be more potent than tannic acid and sesquiterpene but less effective when compared to caged xanthones. Tannic acid, a natural polyphenolic compound, inhibited proliferation of malignant human cholangiocytes with IC $_{50}$ of 60 μ M (Marienfeld et al., 2003) while sesquiterpene-the

derivative of zerumbone-showed antiproliferative activity against KKU-100 cell line with an IC $_{50}$ of 16.44 μ M (Songsiang et al., 2010). The growth inhibitory effect of four caged xanthones-isomorellin, isomorellinol, forbesione and gambogic acid-on KKU-100 showed IC $_{50}$ ranging from 0.11-2.64 μ M (Hahnvajanawong et al., 2010).

Tiliacorinine exhibited antiproliferative activity on CCA cell lines as time-and dose-dependent manners, with a narrow range of 4.0-7.5 μ M at 72h. Comparing to other CCA cell lines, KKU-100 was the less sensitive cell line toward most of conventional chemotherapeutic agent tested (Tepsiri et al., 2005). KKU-100 exhibited the IC₅₀ of 5-fluorouracil, mitomycin-C, paclitaxel and cisplatin = 1,018 μ M, 45 μ M, 39 μ M and 37 μ M, respectively. KKU-100, however, was sensitive to tiliacorinine with the IC₅₀ of 7 μ M which was similar to other CCA cell lines. This highlights tiliacorinine as a potent agent for CCA treatment.

Tiliacorinine inhibited CCA cell growth by inducing apoptosis as evidenced by the results from three different assays. First, tiliacorinine treatment increased number of apoptotic cells as determined by AO/EB staining. Second, DNA ladder, the hallmark of apoptosis revealed by DNA fragmentation assay was clearly demonstrated in cells treated with tiliacorinine. Third, tiliacorinine treated cells significantly increased apoptotic cells in sub G1 peak as demonstrated by flow cytometry. Induction of apoptosis has been considered to be the major mechanism of anticancer drug discovery (Reed, 2001).

The molecular mechanism by which tiliacorinine induced apoptosis was shown to be via activation of caspase-3, -9, and consequently PARP cleavage. Tiliacorinine also up-regulated BAX, a proapoptotic protein, and down-regulated XIAP and Bcl_{xL} in human CCA cells. Induction of apoptosis via caspase-activation pathways seems to be the general mechanisms of anticancer agents from natural compounds, such as cepharanthine, a biscoclaurine alkaloid from roots of *Stephania cepharantha* Hayata (Wu et al., 2001; Seubwai et al., 2010), emodin, an anthraquinone derivative (Yaoxian et al., 2013) and berberine, an isoquinoline alkaloid (Yip and Ho, 2013).

Several attempts have been made to find new agents that effectively inhibited growth and metastatsis of CCA, however, most of them demostrated the effects in vitro, e.g., diethyldithiocarbamate (Srikoon et al., 2013), histone deacetylase inhibitors (Sriraksa and Limpaiboon, 2013). The antitumor activity of tiliacorinine was obviously demonstrated in CCA cell lines and CCA xenografted mice. Tumor volumes and tumor weights of tiliacorinine treated group were 2 folds reduced compared to the control group. Tiliacorinine appeared to have a rapid antitumor activity as it was administrated only 3 consecutive days after CCA cell-injection and the tumor volume was significantly reduced instantly. As this study was the first report on the antitumor activity of tiliacorinine in the xenografted mouse model, the pharmaco-kinetic, drug safety and efficacy of tiliacorinine have to be investigated cautiously.

The abundance of literature suggests that defects along

apoptotic pathways play a crucial role in carcinogenesis and that many new treatment strategies targeting apoptosis are feasible for the treatment of various cancers (Wong, 2011; Sankari et al., 2012). Additionally, almost clinically used anticancer drugs are aimed to activate apoptosis of tumor cells (Hadi et al., 2000). In this study, tiliacorinine showed apoptotic effect on human CCA cells and suppressed tumor growth in CCA xenografted mice, suggesting this auspicious alkaloid an effective agent for CCA treatment. Nevertheless, further intensive study in safety and efficacy of tiliacorinine is highly recommended. Furthermore, to overcome cancer by achieving synergistic therapeutic effect, reducing toxicity, and minimizing the drug resistance (Chou, 2010), further study on drug combination between tiliacorinine and the conventional chemotherapeutic drugs is encouraged.

Acknowledgements

This study was supported by Research grants from Khon Kaen University and the Higher Education Research Promotion and National Research University Project of Thailand, Office of the Higher Education Commission, through the Health cluster (SHeP-GMS) to S. Wongkham. S. Janeklang is supported by the Royal Golden Jubilee-Commission on Higher Education PhD Program (PHD/0133/2550). A. Suksamrarn and A. Nakaew acknowledge supports from The Thailand Research Fund and Center of Excellence for Innovation in Chemistry. We would like to thank Prof. James A. Will for the English presentation of this manuscript via the Faculty of Medicine Publication Clinic, and the Research Instrument Center, Khon Kaen University, for the service support of flow cytometer.

References

- Aras A, Khokhar AR, Qureshi MZ, et al (2014). Targeting cancer with nano-bullets: curcumin, EGCG, resveratrol and quercetin on flying carpets. *Asian Pac J Cancer Prev*, **15**, 3865-71.
- Bolt MW, Mahoney PA (1997). High-efficiency blotting of proteins of diverse sizes following sodium dodecyl sulfate-polyacrylamide gel electrophoresis. *Anal Biochem*, **247**, 185, 92
- Butthongkomvong K, Sirachainan E, Jhankumpha S, et al (2013). Treatment outcome of palliative chemotherapy in inoperable cholangiocarcinoma in Thailand. Asian Pac J Cancer Prev, 14, 3565-8.
- Chou TC (2010). Drug combination studies and their synergy quantification using the chou-talalay method. *Cancer Res*, 70, 440-6.
- Chou TC, Talalay P (1984). Quantitative analysis of dose-effect relationships: the combined effects of multiple drugs or enzyme inhibitors. *Adv Enzyme Regul*, **22**, 27-55.
- Dechatiwongse T, Chavalittumrong P, Nutakul W (1987). Isolation of the *in vitro* antimalarial principles from tiliacora triandra diels. bull. Dept. *Med Sci*, **29**, 6.
- Hadi SM, Asad SF, Singh S, et al (2000). Putative mechanism for anticancer and apoptosis-inducing properties of plantderived polyphenolic compounds. *IUBMB Life*, 50, 167-71.
- Hahnvajanawong C, Boonyanugomol W, Nasomyon T, et al (2010). Apoptotic activity of caged xanthones from Garcinia hanburyi in cholangiocarcinoma cell lines. World

- J Gastroenterol, 16, 2235-43.
- Han SL, Zhu GB, Yao JG, et al (2005). Diagnosis and surgical treatment of primary hepatic cholangiocarcinoma. *Hepatogastroenterology*, **52**, 348-51.
- Herrmann M, Lorenz HM, Voll R, et al (1994). A rapid and simple method for the isolation of apoptotic DNA fragments. *Nucleic Acids Res*, **22**, 5506-7.
- Laemmli UK (1970). Cleavage of structural proteins during the assembly of the head of bacteriophage T4. *Nature*, **227**, 680-5
- Marienfeld C, Tadlock L, Yamagiwa Y, et al (2003). Inhibition of cholangiocarcinoma growth by tannic acid. *Hepatology*, **37**, 1097-104.
- Naus PJ, Henson R, Bleeker G, et al (2007). Tannic acid synergizes the cytotoxicity of chemotherapeutic drugs in human cholangiocarcinoma by modulating drug efflux pathways. *J Hepatol*, **46**, 222-9.
- Ono A, Hattori S, Kariya R, et al (2011). Comparative study of human hematopoietic cell engraftment into BALB/c and C57BL/6 strain of rag-2/jak3 double-deficient mice. *J Biomed Biotechnol*, **2011**, 539748.
- Pachaly P, Khosravian H (1988). New bisbenzylisoquinoline alkaloids from Tiliacora triandra. *Planta Med*, **54**, 433-7.
- Petit PX, Lecoeur H, Zorn E, et al (1995). Alterations in mitochondrial structure and function are early events of dexamethasone-induced thymocyte apoptosis. *J Cell Biol*, **130**, 157-67.
- Reed JC (2001). Apoptosis-regulating proteins as targets for drug discovery. *Trends Mol Med*, **7**, 314-9.
- Rizvi S, Gores GJ (2013). Pathogenesis, diagnosis, and management of cholangiocarcinoma. *Gastroenterology*, 145, 1215-29.
- Sankari SL, Masthan KM, Babu NA, et al (2012). Apoptosis in cancer an update. *Asian Pac J Cancer Prev*, **13**, 4873-8.
- Seubwai W, Vaeteewoottacharn K, Hiyoshi M, et al (2010). Cepharanthine exerts antitumor activity on cholangiocarcinoma by inhibiting NF-kappaB. *Cancer Sci*, **101**, 1590-5.
- Shukla Y (2007). Tea and cancer chemoprevention: a comprehensive review. Asian Pac J Cancer Prev, 8, 155-66.
- Skehan P, Storeng R, Scudiero D, et al (1990). New colorimetric cytotoxicity assay for anticancer-drug screening. *J Natl Cancer Inst*, **82**, 1107-12.
- Songsiang U, Pitchuanchom S, Boonyarat C, et al (2010). Cytotoxicity against cholangiocarcinoma cell lines of zerumbone derivatives. *Eur J Med Chem*, **45**, 3794-802.
- Srikoon P, Kariya R, Kudo E, et al (2013). Diethyldithiocarbamate suppresses an NF-kappaB dependent metastatic pathway in cholangiocarcinoma cells. *Asian Pac J Cancer Prev*, **14**, 4441-6.
- Sripa B, Leungwattanawanit S, Nitta T, et al (2005). Establishment and characterization of an opisthorchiasisassociated cholangiocarcinoma cell line (KKU-100). World J Gastroenterol, 11, 3392-7.
- Sripa B, Pairojkul C (2008). Cholangiocarcinoma: lessons from Thailand. *Curr Opin Gastroenterol*, **24**, 349-56.
- Sriraksa R, Limpaiboon T (2013). Histone deacetylases and their inhibitors as potential therapeutic drugs for cholangiocarcinoma cell line findings. *Asian Pac J Cancer Prev*, **14**, 2503-8.
- Sureram S, Senadeera SP, Hongmanee P, et al (2012). Antimycobacterial activity of bisbenzylisoquinoline alkaloids from tiliacora triandra against multidrug-resistant isolates of mycobacterium tuberculosis. *Bioorg Med Chem Lett*, **22**, 2902-5.
- Tepsiri N, Chaturat L, Sripa B, et al (2005). Drug sensitivity and drug resistance profiles of human intrahepatic

- cholangiocarcinoma cell lines. World J Gastroenterol, 11, 2748-53.
- Thunyaharn N, Promthet S, Wiangnon S, et al (2013). Survival of cholangiocarcinoma patients in northeastern Thailand after supportive treatment. *Asian Pac J Cancer Prev*, **14**, 7029-32.
- Vichai V, Kirtikara K (2006). Sulforhodamine B colorimetric assay for cytotoxicity screening. Nat Protoc, 1, 1112-6.
- Wiriyachitra PP, B (1981). Alkaloids of Tiliacora triandra. *Aust. J Chem*, **34**, 2001-4.
- Wong RS (2011). Apoptosis in cancer: from pathogenesis to treatment. *J Exp Clin Cancer Res*, **30**, 87.
- Wu J, Suzuki H, Zhou YW, et al (2001). Cepharanthine activates caspases and induces apoptosis in jurkat and K562 human leukemia cell lines. *J Cell Biochem*, **82**, 200-14.
- Yaoxian W, Hui Y, Yunyan Z, et al (2013). Emodin induces apoptosis of human cervical cancer hela cells via intrinsic mitochondrial and extrinsic death receptor pathway. *Cancer Cell Int*, 13, 71.
- Yip NK, Ho WS (2013). Berberine induces apoptosis via the mitochondrial pathway in liver cancer cells. *Oncol Rep*, 30, 1107-12.

FISEVIER

Contents lists available at ScienceDirect

Bioorganic & Medicinal Chemistry Letters

journal homepage: www.elsevier.com/locate/bmcl



Curcuminoid derivatives enhance telomerase activity in an in vitro TRAP assay



Thanachai Taka ^a, Chatchawan Changtam ^b, Pak Thaichana ^a, Navakoon Kaewtunjai ^a, Apichart Suksamrarn ^c, T. Randall Lee ^d, Wirote Tuntiwechapikul ^{a,*}

- ^a Department of Biochemistry, Faculty of Medicine, Chiang Mai University, Chiang Mai 50200, Thailand
- ^b Division of Physical Science, Faculty of Science and Technology, Huachiew Chalermprakiet University, Samutprakarn 10540, Thailand
- ^c Department of Chemistry, Faculty of Science, Ramkhamhaeng University, Bangkok 10240, Thailand
- d Department of Chemistry and the Texas Center for Superconductivity, University of Houston, Houston, TX 77204-5003, USA

ARTICLE INFO

Article history: Received 4 May 2014 Revised 1 September 2014 Accepted 20 September 2014 Available online 28 September 2014

Keywords:
Telomerase
Telomerase activator
Cell senescence
Curcuminoid derivatives

ABSTRACT

The length of telomeres controls the life span of eukaryotic cells. Telomerase maintains the length of telomeres in certain eukaryotic cells, such as germline cells and stem cells, and allows these cells to evade replicative senescence. Here, we report for the first time a number of curcuminoid derivatives that enhance telomerase activity in an in vitro TRAP assay. A preliminary analysis of structure–activity relationships found that the minimal requirement for this enhanced telomerase activity is a curcuminoid core with at least one n-pentylpyridine side chain, while curcuminoids with two such side chains exhibit even greater activity. The finding here might lead to a new class of telomerase activators that act directly or indirectly on telomerase, rather than through the reactivation of the telomerase reverse transcriptase (TERT) gene associated with other telomerase activators found in the literature.

© 2014 Elsevier Ltd. All rights reserved.

Telomerase expression is associated with cell immortalization and tumorigenesis. Most human somatic cells do not express telomerase; and therefore, their telomeres are gradually shortened with each cell division due to the 'end-replication' problem. Once a few telomeres are shortened to a critical length, they signal the cell to enter growth arrest known as replicative senescence. Cancer cells evade replicative senescence by maintaining their telomeres, mostly by reactivating telomerase reverse transcriptase (TERT) expression. Inhibition of telomerase is thus a selective cancer therapy with the capacity to render cancer cells to replicative senescence.

Telomerase is a multi-subunit ribonucleoprotein enzyme comprised of the telomerase reverse transcriptase (TERT), the telomerase RNA (TR), and species-specific accessory proteins. TERT catalyzes the addition of a short repetitive telomeric sequence onto the 3'-end of telomeres using a section of TR as the template in a process known as repeat addition processivity. This elongation mechanism requires a translocation step of the previous round of telomerase-extended product to the original position on the RNA template before the new round of telomeric repeat can be reverse transcribed onto the telomeric end. The activity and processivity

of telomerase depends on several factors, including both TR and TERT, as well as some telomerase-associated proteins, notably POT1–TPP1 heterodimer, which enhances telomerase processivity by slowing primer dissociation and aiding translocation.⁸

Many small molecules have been shown to inhibit telomerase activity. Some G-quadruplex ligands were also found to inhibit telomerase processivity. Until now, however, there have been no reports of small molecules that directly enhance telomerase activity in a cell-free system. Here, we report for the first time a series of curcuminoid derivatives that enhance telomerase activity in an in vitro telomerase assay. The structures of these compounds are shown in Figure 1. The strategies used to synthesize these compounds followed the general procedures outlined in two previous publications and are described in detail in Supplementary data \$1.11

In our search for telomerase inhibitors, we employed a modified telomerase repeat amplification protocol (TRAP) assay introduced by Szatmari and Aradi as our standard protocol because this method can retain the original length of telomerase products, and thus the processivity of telomerase can be analyzed. To detect the amplified telomerase products, we modified the method by using a fluorescent-tagged primer instead of using radioactive nucleotides. The crude cell lysate from HEK293T cells transfected with hTERT and hTR plasmids was used as the source of telomerase

st Corresponding author.

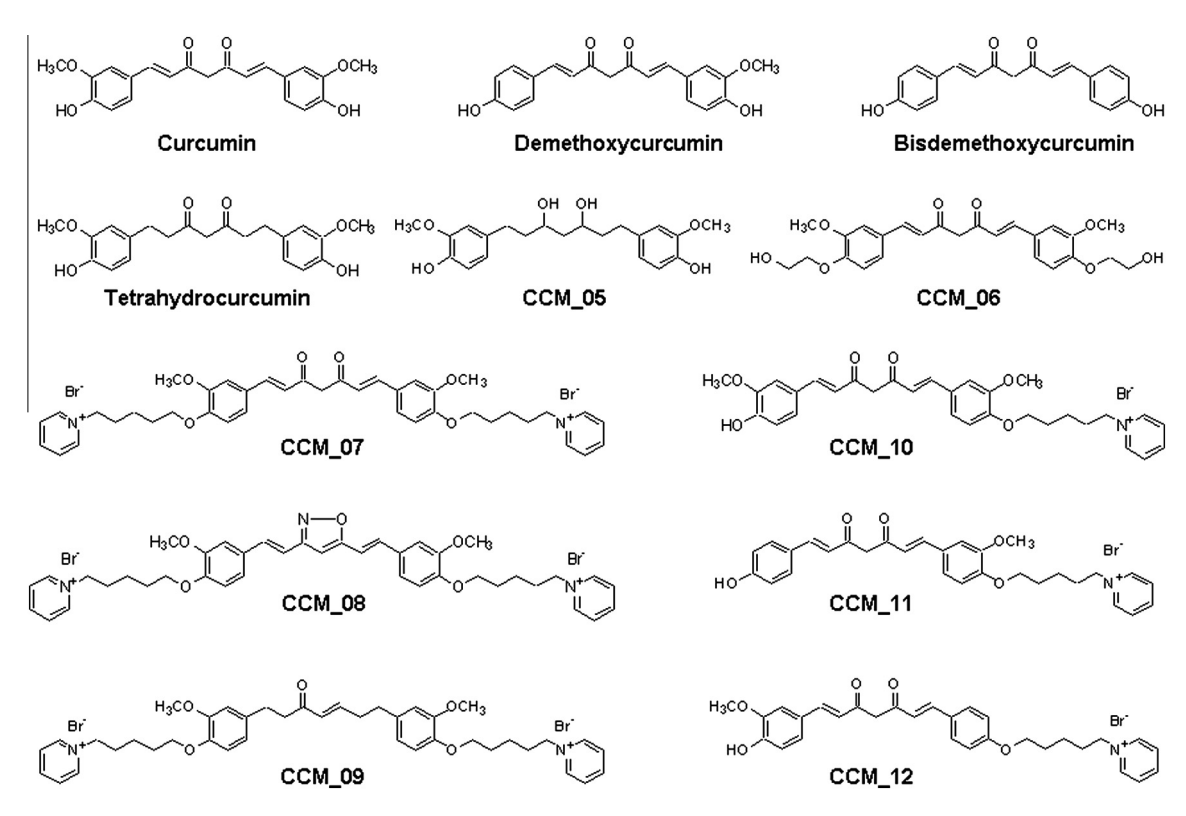


Figure 1. Structures of curcumin and curcuminoid derivatives evaluated in the present study.

according to a published protocol.¹³ In all assays, the test compound was removed from telomerase products by phenol–chloroform extraction and ethanol precipitation before the amplification step to prevent any false negative result due to the inhibition of *Taq* DNA polymerase. The details of each TRAP assay are described in the figure captions. The DNA sequences of oligonucleotides used in the TRAP assay are listed in Table 1.

We first tested the first seven curcuminoid derivatives shown in Figure 1 (curcumin to CCM_07) using our modified TRAP assay. We found that most curcuminoids had no effect on telomerase activity (see Supplementary data Fig. S1), except for CCM_07, which was found to enhance telomerase activity in a concentration-dependent manner. As shown in Figure 2A, the telomerase products increase in intensity and length with increasing amounts of CCM_07, while the intensity of the internal control (IC) remains unchanged. Note that our TRAP system does not generate DNA ladders from a single telomeric DNA template as often seen with conventional TRAP assay. 12a As shown in lanes 0.25R6 and 0.125R6, where the artificial telomerase product with 6 repeats (MTS-R6 at 0.25 and 0.125 amol) was used as the template for the amplification step, only one single amplified product was observed. The intensity of the amplified MTS-R6 correlates well with the input

Table 1 Oligonucleotides employed in our modified TRAP assay

Name	Sequence
MTS	AGCATCCGTCGAGCAGAGTT
RPc3g	TAGAGCACAGCCTGTCCGTG(CTAACC)₃GG
RP*	TAGAGCACAGCCTGTCCGTG
IC	TAGAGCACAGCCTGTCCGTGAAAAGGCCGAGAAGCGATCG
NT	CGATCGCTTCTCGGCCTTTT
RC(+)*	AAGCTTTAATACGACTCACTATACGGACGTCC
RC(-)	GGACGTCCGTATAGTGAGTCGTATTAAAGCTT
MTS-R6	AGCATCCGTCGAGCAGAGTTAG(GGTTAG) ₆

^{*} FAM-tagged strand.

template, which implies that the PCR cycle used in our TRAP assay does not reach the plateau stage; and therefore, the amplified products reflect the amount of telomerase products in the reaction. We repeated this experiment three times, and the intensity of the telomerase products was quantified using Image J software. The average accumulated intensity was then plotted against the concentration and shown as a bar graph in Figure 2B. The graph demonstrates that CCM_07 enhances telomerase activity in the concentration-dependent manner, up to 5 fold at 60 μM of CCM_07.

The ability of CCM_07 to enhance telomerase activity is also evident from the time-course experiment, where we examined telomerase activity in the absence and presence of 40 μ M CCM_07 at various incubation times. Figure 2C shows the phosphorimage of the time-course experiment, and Figure 2D shows the line graph plotted between the accumulated intensity of telomerase products and time. As shown in Figure 2C, the telomerase products, both length and intensity, increase with the incubation time in both the experimental and the control sets. However, as shown in Figure 2D, when compared with the control set, the intensity and length of telomerase products appear to increase in the presence of 40 μ M CCM_07 at every time interval.

As mentioned above, the test compound was removed from telomerase products by phenol–chloroform extraction and ethanol precipitation before the amplification step in our TRAP protocol; therefore, the increase of amplified telomerase products by CCM_07 shown in Figure 2 does not occur in the amplification step. In fact, without compound removal, the gel data appear as if CCM_07 were a telomerase inhibitor (see Supplementary data Fig. S2A). We found out later, in a separate experiment using ordinary PCR, that CCM_07 strongly inhibited Taq DNA polymerase at concentrations as low as 5 μ M (see Supplementary data Fig. S2B). Therefore, the increase in intensity of telomerase products observed in Figure 2 likely arises solely from an increase in telomerase activity. The recovery control (RC), which was added to each

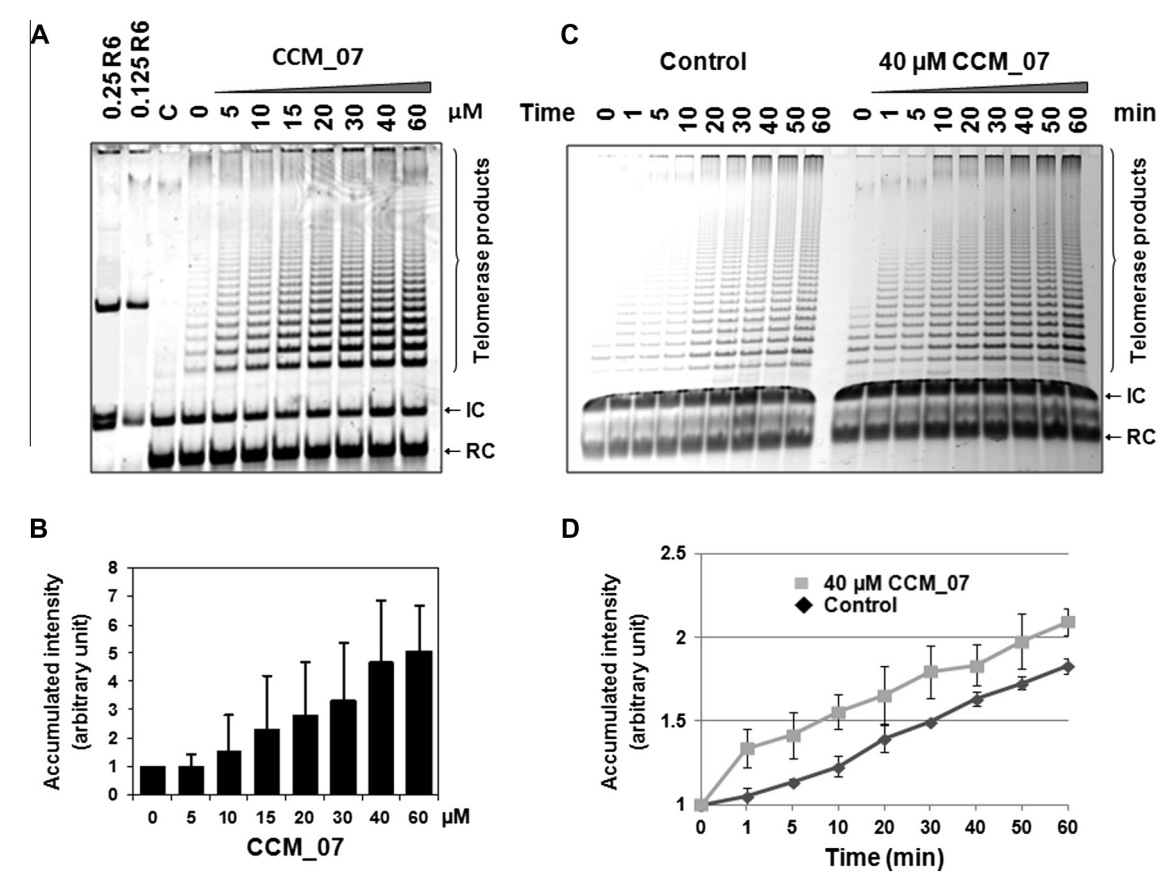


Figure 2. CCM_07 enhances telomerase activity in a concentration-dependent and time-dependent manner. (A) Phosphorimage from the concentration-dependent experiment. The MTS primer and the indicated concentration of CCM_07 were incubated in the 100 μl telomerase reaction buffer at 30 °C for 30 min. The compound was then extracted by two rounds of phenol-chloroform extraction, and the telomerase products were then ethanol precipitated and amplified by PCR. The amplification products were electrophoretically separated in 8% non-denaturing acrylamide gel and visualized with a phosphorimaging system (Typhoon; Molecular Dynamics). The lanes labeled as 0.25R6 and 0.125R6 are assay controls, when 0.25 amol and 0.125 amol of MTS-R6 (the artificial telomerase product with 6 repeats) were used as template in our TRAP assay. Notice that MTS-R6 only generated one amplified product, and not DNA ladders associated with conventional TRAP assay. (B) Phosphorimage from the time-course experiment. First, a 2-ml master mix of telomerase reaction mixture was prepared on ice to prevent any telomerase activity. Then, 990 μl of this master mix was dispensed into a tube containing 110 μl of 400 μM CCM_07 in 25% DMSO, and a tube containing 110 μl of 25% DMSO (the control set). The reaction mixture was mixed and incubated in a water bath at 30 °C. At the indicated times, 100 μl from this reaction mixture was drawn from both sets, and the enzyme activity was terminated by heating at 95 °C for 10 min. DNA purification, PCR amplification, and electrophoresis of the telomerase products were performed in the same manner as described above. IC represents the internal control, and RC represents the recovery control. (C and D) Graphs represent the accumulated intensity of telomerase products from three independent experiments of (A) and (B), respectively. The telomerase products were quantified using Image] software.

sample before the phenol–chloroform extraction and ethanol precipitation, also ensured that all the primer-extended products were fully recovered during the procedure. The internal control (IC) was used in the reaction to ensure that there was no inhibition or enhancement in the amplification step.

Since the existence of a telomerase activator of this kind had, to our knowledge, never been reported, we questioned whether the enhanced telomerase activity was specific to CCM_07, or would structurally related derivatives yield similar results. To this end, we synthesized five new *n*-pentylpyridine curcuminoid derivatives, CCM_08-CCM_12 (Fig. 1). In CCM_08, the double carbonyl groups in the curcumin core of CCM_07 are replaced with an isoxazole ring. CCM 09 possesses only one carbonyl group and one double bond in the center of the curcumin core. CCM_10 possesses only one *n*-pentylpyridine side chain on the curcumin core. CCM_11 and CCM_12 are isomers of the demethoxycurcumin core with one *n*-pentylpyridine side chain located in two distinct positions. We then tested these compounds for their effect on telomerase activity using the same TRAP assay. Figure 3A shows the gel data, and Figure 3B shows graphs representing the accumulated intensity of telomerase products enhanced by each curcuminoid derivative at various concentrations, averaged from three independent experiments. As shown in Figure 3B, CCM_08 and CCM_10, CCM_11, and CCM_12 enhance telomerase activity roughly three-fold at 60 μM , compared to roughly fivefold for CCM_07. In contrast, CCM_09 had little or no effect on telomerase activity within the concentration range tested.

Based on the results obtained from the 12 compounds studies here, we can conclude that the minimal requirement for enhanced telomerase activity is a curcuminoid core having at least one *n*-pentylpyridine side chain, but the activity is greater when there are two such side chains. The curcuminoid core can be curcumin or demethoxycurcumin, and the existence or position of the methoxy group on the benzene ring is seemingly unimportant. The double carbonyl group in the heptyl-linker chain of the curcuminoid core can be replaced by an isoxazole ring, but the mono-oxygenated analog loses activity. It is likely that the conjugated double bonds, which keep the molecules in an extended planar configuration, are important for this activity. It should be noted, however, that these conclusions are based on a limited set of compounds; a larger library of compounds is needed for a full assessment.

Furthermore, we have observed this enhanced telomerase activity only in an in vitro TRAP assay. We do not know whether these compounds can enhance telomerase activity inside cells. To date, there have been few reports of telomerase activators; namely, an extract from *Astragalus membranaceus* root (TA-65) or from its

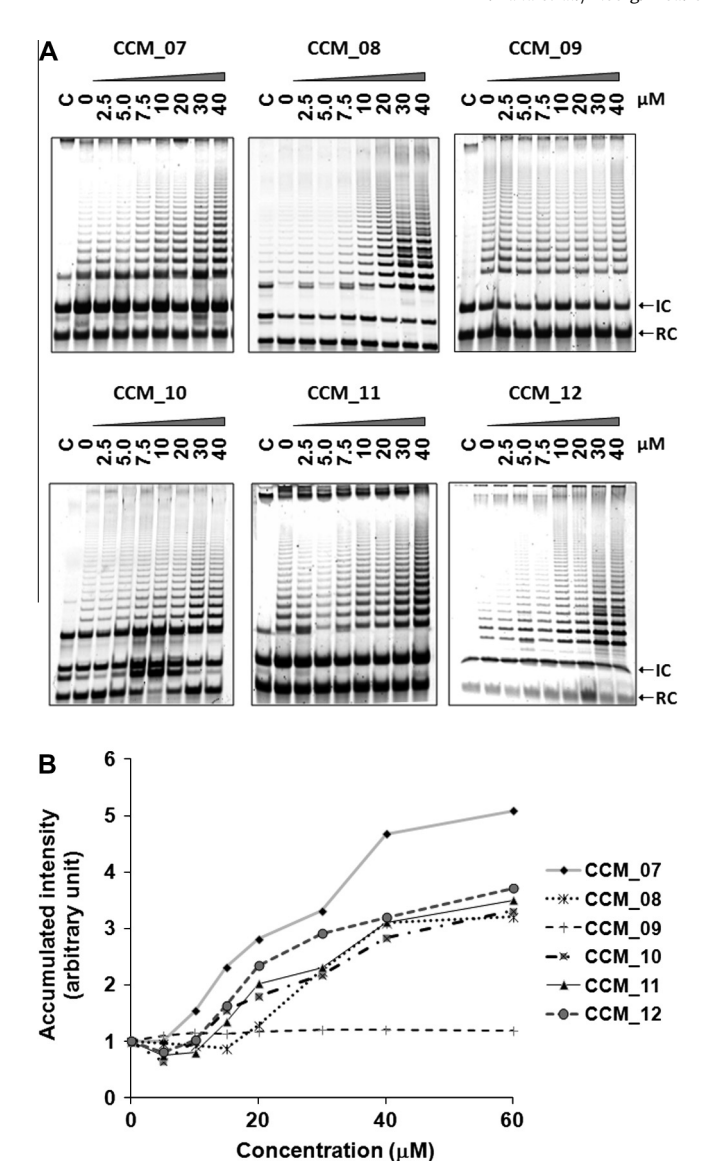


Figure 3. The effect of CCM_07-CCM_12 on telomerase activity. (A) Phosphorimages from the concentration-dependent experiment. The experiments were performed in the same manner as described in Figure 2. IC represents the internal control, and RC represents the recovery control. Lane C represents the negative control experiment in which telomerase was heat-denatured. (B) Graphs represent the accumulated intensity of telomerase products enhanced by each curcuminoid derivative at various concentrations, averaged from three independent experiments. The standard deviations are omitted from this figure for clarity of the data. Bar graphs with standard deviation are available in Supplemental data Figure S10.

active compound cycloastragenol (GRN665 or TAT2) and its derivative (GRN510). However, the plant extract or its active compounds exert their activity through the enhancement of TERT expression, leading to an increase in telomerase activity and telomere lengthening inside the cells or in in vivo murine models. However, our curcuminoid derivatives exert their telomerase enhancement via a completely different mechanism that involves no cellular activity. We believe that these agents might augment the binding of the telomeric end to the enzyme since the activity seems to increase immediately after the compound is added to the reaction mixture (Fig. 2C). However, further investigation into the mechanism of action is needed. Also, it would be interesting to investigate these compounds further at the cellular level or in in vivo models.

Most human somatic cells lack sufficient telomerase to maintain their telomeres, which leads to their limited life span.^{2,3}

Reactivation of telomerase by transfecting hTERT, the catalytic subunit of telomerase, into various human cell types has been shown to increase the cellular life span. 15 Moreover, restoration of telomerase in mice models has been shown to rescue critically short telomeres, to prevent or reverse tissue defects associated with cellular aging, and to increase life span. 16 Recent studies of telomerase activators TA-65 and GRN510 in mice have shown that small molecules can increase cellular telomerase activity in some tissues and rescue critically short telomeres, which leads to a longer life span, or in the case of GRN510, suppression of lung damage from bleomycin-induced fibrosis. 14b,c The reports from humans taking TA-65 in a commercial health maintenance program, PattonProtocol-1, show an improvement in markers of immune, metabolic, bone, and cardiovascular health. 14a,d These findings support the notion that activating telomerase might limit premature aging and increase organismal life span. Further, the findings in this Letter might lead to development of new telomerase activators that act directly on telomerase.

Acknowledgments

This work was supported by Grants from: (i) The Thailand Research Fund, Thailand (DBG5080015 and DBG5680006), (ii) Faculty of Medicine Research Fund, Chiang Mai University, Chiang Mai, Thailand, (iii) the Robert A. Welch Foundation (Grant No. E-1320), and (iv) Faculty of Science and Technology, Huachiew Chalermprakiet University (CC). We thank Professor Joachim Lingner (ISREC, Lausanne, Switzerland) for generously donating plasmids containing hTERT gene and hTR gene.

Supplementary data

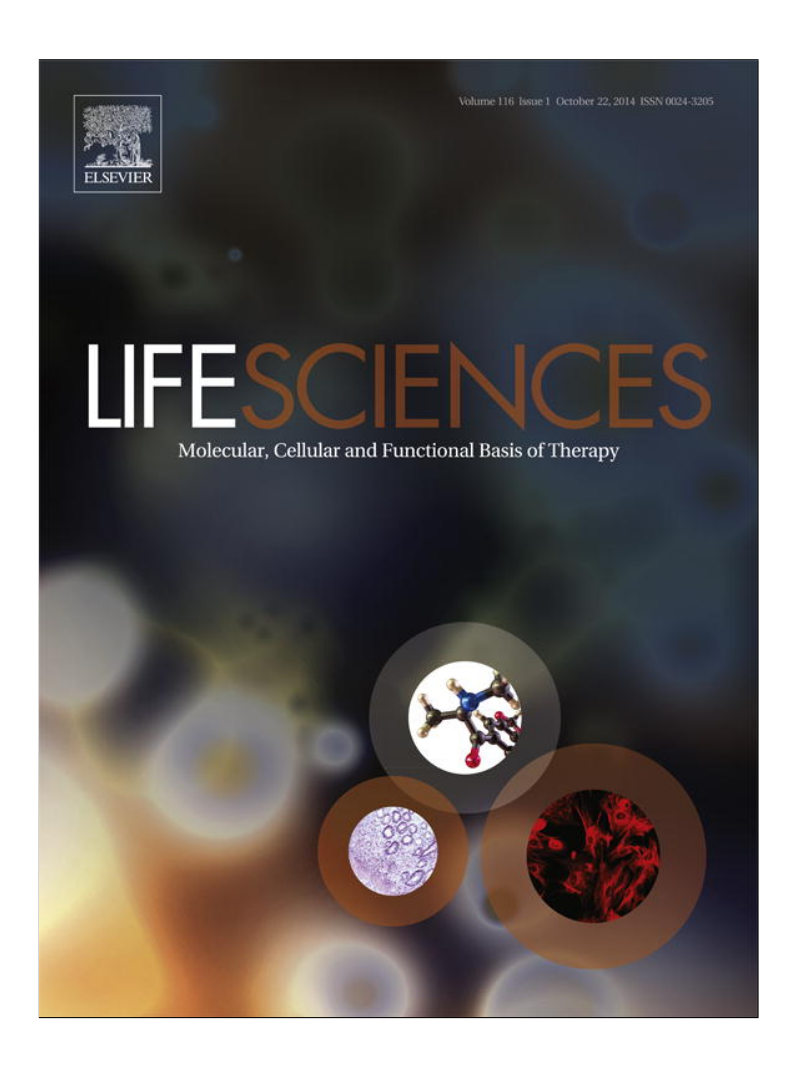
Supplementary data associated with this article can be found, in the online version, at http://dx.doi.org/10.1016/j.bmcl.2014.09.059. These data include MOL files and InChiKeys of the most important compounds described in this article.

References and notes

- (a) Shay, J. W.; Wright, W. E. Semin. Cancer Biol. 2011, 21, 349; (b) Autexier, C.; Greider, C. W. Trends Biochem. Sci. 1996, 21, 387.
- 2. Olovnikov, A. M. Exp. Gerontol. 1996, 31, 443.
- 3. Shay, J. W.; Wright, W. E. Carcinogenesis 2005, 26, 867.
- (a) Deng, Y.; Chan, S. S.; Chang, S. Nat. Rev. Carcer 2008, 8, 450; (b) Kim, N. W.; Piatyszek, M. A.; Prowse, K. R.; Harley, C. B.; West, M. D.; Ho, P. L. C.; Oviello, G. M.; Wright, W. E.; Weinrich, S. L.; Shay, J. W. Science 1994, 266, 2011.
- 5. Ouellette, M. M.; Wright, W. E.; Shay, J. W. J. Cell. Mol. Med. 2011, 15, 1433.
- 6. Wyatt, H. D.; West, S. C.; Beattie, T. L. Nucleic Acids Res. **2010**, 38, 5609.
- (a) Greider, C. W. Mol. Cell. Biol. 1991, 11, 4572; (b) Hardy, C. D.; Schultz, C. S.;
 Collins, K. J. Biol. Chem. 2001, 276, 4863; (c) Moriarty, T. J.; Marie-Egyptienne, D. T.; Autexier, C. Mol. Cell. Biol. 2004, 24, 3720.
- 8. Latrick, C. M.; Cech, T. R. EMBO J. 2010, 29, 924.
- (a) Neidle, S. FEBS J. 2010, 277, 1118; (b) Kelland, L. R. Eur. J. Cancer 2005, 41, 971; (c) Rankin, A. M.; Faller, D. V.; Spanjaard, R. A. Anticancer Drugs 2008, 19, 329
- D'Ambrosio, D.; Reichenbach, P.; Micheli, E.; Alvino, A.; Franceschin, M.; Savino, M.; Lingner, J. Biochimie 2012, 94, 854.
- (a) Changtam, C.; De Koning, H. P.; Ibrahim, H.; Sajid, S.; Gould, M. K.; Suksamrarn, A. Eur. J. Med. Chem. 2010, 45, 941; (b) Changtam, C.; Hongmanee, P.; Suksamrarn, A. Eur. J. Med. Chem. 2010, 45, 4446.
- (a) Szatmari, I.; Aradi, J. Nucleic Acids Res. 2001, 29, e3; (b) Taka, T.; Huang, L.; Wongnoppavich, A.; Tam-Chang, S. W.; Lee, T. R.; Tuntiwechapikul, W. Bioorg. Med. Chem. 2013, 21, 883.
- (a) Cristofari, G.; Lingner, J. EMBO J. 2006, 25, 565; (b) Cristofari, G.; Reichenbach, P.; Regamey, P. O.; Banfi, D.; Chambon, M.; Turcatti, G.; Lingner, J. Nat. Methods 2007, 4, 851.
- (a) Harley, C. B.; Liu, W.; Flom, P. L.; Raffaele, J. M. Rejuvenation Res. 2013, 16, 386; (b) Le Saux, C. J.; Davy, P.; Brampton, C.; Ahuja, S. S.; Fauce, S.; Shivshankar, P.; Nguyen, H.; Ramaseshan, M.; Tressler, R.; Pirot, Z.; Harley, C. B.; Allsopp, R. PLoS One 2013, 8, e58423; (c) Bernardes de Jesus, B.; Schneeberger, K.; Vera, E.; Tejera, A.; Harley, C. B.; Blasco, M. A. Aging Cell 2011, 10, 604; (d) Harley, C. B.; Liu, W.; Blasco, M. A.; Vera, E.; Andrews, W. H.; Briggs, L. A.; Raffaele, J. M. Rejuvenation Res. 2011, 14, 45; (e) Fauce, S. R.;

- Jamieson, B. D.; Chin, A. C.; Mitsuyasu, R. T.; Parish, S. T.; Ng, H. L.; Kitchen, C. M.; Yang, O. O.; Harley, C. B.; Effros, R. B. J. Immunol. 2008, 181, 7400.
 15. (a) Bodnar, A. G.; Ouellette, M.; Frolkis, M.; Holt, S. E.; Chiu, C. P.; Morin, G. B.;
- (a) Bodnar, A. G.; Ouellette, M.; Frolkis, M.; Holt, S. E.; Chiu, C. P.; Morin, G. B.; Harley, C. B.; Shay, J. W.; Lichtsteiner, S.; Wright, W. E. Science 1998, 279, 349; (b) Yang, J.; Chang, E.; Cherry, A. M.; Bangs, C. D.; Oei, Y.; Bodnar, A.; Bronstein, A.; Chiu, C. P.; Herron, G. S. J. Biol. Chem. 1999, 274, 26141; (c) Rufer, N.; Migliaccio, M.; Antonchuk, J.; Humphries, R. K.; Roosnek, E.; Lansdorp, P. M. Blood 2001, 98, 597; (d) Terai, M.; Uyama, T.; Sugiki, T.; Li, X. K.; Umezawa, A.; Kiyono, T. Mol. Biol. Cell 2005, 16, 1491.
- 16. (a) Jaskelioff, M.; Muller, F. L.; Paik, J. H.; Thomas, E.; Jiang, S.; Adams, A. C.; Sahin, E.; Kost-Alimova, M.; Protopopov, A.; Cadiñanos, J.; Horner, J. W.; Maratos-Flier, E.; Depinho, R. A. Nature 2011, 469, 102; (b) Tomás-Loba, A.; Flores, I.; Fernández-Marcos, P. J.; Cayuela, M. L.; Maraver, A.; Tejera, A.; Borrás, C.; Matheu, A.; Klatt, P.; Flores, J. M.; Viña, J.; Serrano, M.; Blasco, M. A. Cell 2008, 135, 609; (c) Siegl-Cachedenier, I.; Flores, I.; Klatt, P.; Blasco, M. A. J. Cell Biol. 2007, 179, 277; (d) Samper, E.; Flores, J. M.; Blasco, M. A. EMBO Rep. 2001, 2, 800

Provided for non-commercial research and education use. Not for reproduction, distribution or commercial use.



This article appeared in a journal published by Elsevier. The attached copy is furnished to the author for internal non-commercial research and education use, including for instruction at the authors institution and sharing with colleagues.

Other uses, including reproduction and distribution, or selling or licensing copies, or posting to personal, institutional or third party websites are prohibited.

In most cases authors are permitted to post their version of the article (e.g. in Word or Tex form) to their personal website or institutional repository. Authors requiring further information regarding Elsevier's archiving and manuscript policies are encouraged to visit:

http://www.elsevier.com/authorsrights

Author's personal copy

Life Sciences 116 (2014) 31-36



Contents lists available at ScienceDirect

Life Sciences

journal homepage: www.elsevier.com/locate/lifescie



Endothelium-independent vasorelaxation effects of 16-O-acetyldihydroisosteviol on isolated rat thoracic aorta



Rungusa Pantan ^a, Amnart Onsa-ard ^b, Jiraporn Tocharus ^c, Orawan Wonganan ^d, Apichart Suksamrarn ^d, Chainarong Tocharus ^{a,*}

- ^a Department of Anatomy, Faculty of Medicine, Chiang Mai University, Chiang Mai 50200, Thailand
- ^b Department of Biochemistry, Faculty of Medical Science, Phayao University, Phayao 56000, Thailand
- ^c Department of Physiology, Faculty of Medicine, Chiang Mai University, Chiang Mai 50200, Thailand
- d Department of Chemistry and Center of Excellence for Innovation in Chemistry, Faculty of Science, Ramkhamhaeng University, Bangkok 10240, Thailand

ARTICLE INFO

Article history:
Received 24 March 2014
Accepted 11 August 2014
Available online 21 August 2014

Keywords: 16-O-Acetyldihydroisosteviol Vasorelaxation Endothelium-independent Aorta

ABSTRACT

Aims: The aim of this study is to investigate the vasorelaxant effect of 16-*O*-acetyldihydroisosteviol (ADIS) and its underlying mechanisms in isolated rat aorta.

Main methods: Rat aortic rings were isolated, suspended in organ baths containing Kreb's solution, maintained at $37\,^{\circ}$ C, and mounted on tungsten wire and continuously bubbled with a mixture of $95\%\,O_2$ and $5\%\,CO_2$ under a resting tension of 1 g. The vasorelaxant effects of ADIS were investigated by means of isometric tension recording experiment.

Key findings: ADIS (0.1 μM–3 mM) induced relaxation of aortic rings pre-contracted by phenylephrine (PE, 10 μM) and KCl (80 mM) with intact-endothelium ($E_{max}=79.26\pm3.74$ and 79.88 ± 3.79 , respectively) or denuded-endothelium ($E_{max}=88.05\pm3.69$ and 78.22 ± 6.86 , respectively). In depolarization Ca^{2+} -free solution, ADIS inhibits calcium chloride ($CaCl_2$)-induced contraction in endothelium-denuded rings in a concentration-dependent manner. In addition, ADIS attenuates transient contractions in Ca^{2+} -free medium containing EGTA (1 mM) induced by PE (10 μM) and caffeine (20 mM). By contrast, relaxation was not affected by tetraethylammonium (TEA, 5 mM), 4-aminopyridine (4-AP, 1 mM), glibenclamide (10 μM), barium chloride (BaCl₂, 1 mM), and 1H-[1,2,3]oxadiazolo[4,3-α]quinoxalin-1-one (ODQ, 1 μM). Significance: These findings reveal the vasorelaxant effect of ADIS, through endothelium-independent pathway. It acts as a Ca^{2+} channel blocker through both intracellular and extracellular Ca^{2+} release.

 $\hbox{@ 2014 Elsevier Inc. All rights reserved.}$

Introduction

Stevioside is a diterpene glycoside isolated from the leaves of the plant *Stevia rebaudiana* (Bertoni) Bertoni, and it has been popularly used as an artificial sweetener worldwide (Geuns, 2003; Chatsudthipong and Muanprasat, 2009; Goyal et al., 2010). Stevioside is the main component of *S. rebaudiana* extract and has shown the effects similar to calcium antagonists were shown on arterial pressure and renal function (Melis, 1992) and it lowered arterial pressure in the form of an intravenous injection in anesthetized spontaneously hypertensive rats (SHRs) (Chan et al., 1998). Additionally, studies in humans demonstrated that stevioside cause bradycardia

and hypotension (Humboldt and Boech, 1977) and continuous oral administration tea prepared from *S. rebaudiana* daily for 30 days also showed a slight hypotensive effect (Boeckh and Humboldt, 1981). Furthermore, isosteviol (*ent*-16-oxobeyeran-19-oic acid), a tetracyclic diterpenoid obtained by acid hydrolysis of stevioside, has been reported as exhibiting pharmacological activity. Isosteviol attenuates myocardial damage induced by ischemia-reperfusion in isolated perfused guinea pig heart (Xu et al., 2007a), rat heart in vivo (Xu et al., 2007b), and rat brain in vivo (Xu et al., 2008). Moreover, isosteviol also shows the vasorelaxant effect via opening the K⁺ channels in rat aorta (Wong et al., 2004). Recently, the chemical modification of isosteviol was performed by sodium borohydride reduction of isosteviol, followed by acetylation to give 16-0-acetyldihydroisosteviol (ADIS) (Fig. 1). The vasorelaxant effect in rat aortic rings was found to be greater in the case of ADIS than in the case of isosteviol about 12-fold (Wonganan

^{*} Corresponding author. Tel.: +66 53 945312; fax: +66 53 945304. E-mail address: chainarongt@hotmail.com (C. Tocharus).

Fig. 1. The chemical structure of 16-O-acetyldihydroisosteviol (ADIS).

et al., 2013). This is of special interest as far as evaluating the mechanism of ADIS on the vasorelaxant effect is concerned. Thus, the purpose of this study is to investigate the mechanism of ADIS as regarding vasorelaxant activity, as it would be beneficial in evaluating natural products, which may be considered as an alternative modality for hypertensive patients.

Materials and methods

Drugs and chemicals

Phenylephrine (PE), acetylcholine (ACh), ethylene glycol-bis(β-aminoethyl ether)-N,N,N',N'-tetraacetic acid (EGTA), glibenclamide, tetraethylammonium, 4-aminopyridine (4-AP), 1H-[1,2,4]oxadiazolo [4,3-a]quinoxalin-1-one (ODQ), and caffeine were purchased from Sigma (St. Louis, MO, USA).

Preparation of ADIS

The pulverized, dry *S. rebaudina* leaves were successively extracted with n-hexane, ethyl acetate, and methanol. The methanol extract was subjected to silica column chromatography to yield stevioside. ADIS was obtained from stevioside as described previously (Wonganan et al., 2013). Briefly, stevioside was dissolved in 20% sulfuric acid solution and then heated at 60–70 °C for 6 h with stirring. The mixture was extracted with ethyl acetate. The solvent was evaporated and the product was purified by column chromatography to give isosteviol. Sodium borohydride reduction of isosteviol in tetrahydrofuran produced dihydroisosteviol, which upon acetylation with acetic anhydride in pyridine yielded ADIS. The spectroscopic data (1 H-NMR and mass spectra) of the synthesized ADIS were identical to those reported previously (Wonganan et al., 2013).

Animals

Male Wistar rats (200–250 g) were obtained from the National Laboratory Animal Center, Mahidol University, Salaya, Nakornpathom, Thailand. All the animals were housed under a 12:12 h light–dark cycle condition, with a steady temperature maintained (24 \pm 1 $^{\circ}$ C). The animals were allowed free access to rodent diet and tap water. The experimental protocol was approved by the Animal Ethics Committee in accordance with the guidelines for the care and use of laboratory animals, as prepared by Chiang Mai University.

Preparation of isolated rat thoracic aortic rings

Rats were anesthetized by intraperitoneal injection using sodium pentobarbital (60 mg/kg BW). After they attained complete unconsciousness, the rats were sacrificed and the thoracic aorta was immediately removed to be cleaned of the adhering connective tissue and fat. The vessels were cut into rings approximately 3 mm in length. For the endothelium-denuded rings, the endothelial layer was removed by gently rubbing the internal surface of the vascular lumen. The aortic

rings were immersed in a 2 ml chamber bath which contained Krebs solution (composition, mM: NaCl, 122; KCl, 4.9; HEPES, 10; KH₂PO₄, 0.5; NaH₂PO₄, 0.5; MgCl₂, 1.0; glucose, 11.0; CaCl₂, 1.8, pH 7.3), maintained at a 37 °C temperature, mounted on tungsten wire and continuously bubbled with oxygen. A resting tension of 1 g was applied to each tissue and equilibrated at least 1 h. During the equilibrium period, the Krebs solution was changed every 15 min. After equilibration, the endothelial integrity was verified with a sub-maximal pre-contraction of PE (10 μM). After the tension was stabilized, ACh (10 μM) was directly added into the chamber bath in order to detect and evaluate the presence or absence of the endothelial cell layer; more than 90% relaxation of the rings was considered to be an endothelium-intact ring, whereas less than 10% relaxation was considered to be endothelium-denuded ring. Relaxation was calculated as a percentage of the maximal contraction induced by PE. Before each experimental protocol was performed, the presence or absence of the endothelial cell layer was tested and washed out with the Krebs solution for at least 30 min. Changes in tension were detected using FT-104 isometric force transducers (Iworx System, Inc., NH, USA) coupled with Power Lab data acquisition system (ADIntruments, Sydney, Australia), and then connected to a computer equipped with Lab Chart 7 Software program (ADIntruments, Sydney, Australia).

Aorta ring contraction assay

The vasorelaxant effects of ADIS were investigated in both endothelium-intact and endothelium-denuded aortic rings. After the rings were pre-equilibrated, they were pre-contracted with PE (10 μ M) until the stability of tension was established, which was followed by cumulative exposure to ADIS (0.1 μ M–3 mM).

Role of K⁺ *channels on ADIS-induced relaxation*

The role of the K $^+$ channels was elucidated by the vasorelaxation response upon pre-incubating the endothelium-denuded aortic rings with one of the following specific K $^+$ channel blockers: TEA (5 mM), 4-AP (1 mM), glibenclamide (10 μ M), and BaCl₂ (1 mM) for 30 min before PE (10 μ M) pre-contraction. Then, ADIS (0.1 μ M-3 mM) was added cumulatively.

Role of soluble guanylyl cyclase (sGC) in ADIS-induced relaxation

The mechanism of vasorelaxation induced by ADIS (0.1 μ M–3 mM) was further tested by using ODQ, a selective inhibitor of sGC, to focus on the role of soluble guanylyl cyclase (sGC) in the relaxant activity. The procedure was conducted by pre-incubating the endothelium-denuded aortic ring with ODQ (1 μ M) for 30 min before PE (10 μ M) induced contraction was performed. After the pre-contraction stabilized, ADIS (0.1 μ M–3 mM) was added. The vasorelaxation abilities of ADIS in the presence and absence of ODQ were compared.

Endothelium denudation effect of ADIS contraction induced by PE and KCl After the equilibration period, the aortic rings were pre-contracted with PE (10 μM) or KCl (80 mM). Then, the tension was allowed to stabilize, which was followed by exposure to ADIS (0.1 μM–3 mM) cumulatively. The extent of relaxation was expressed as the percentage of PE-induced or KCl-induced contraction.

Role of α_1 -receptor in inhibitory vasoconstriction effect of ADIS. Endothelium-denuded rings were tested in normal Krebs solution. ADIS was added in concentrations of 1 μ M, 10 μ M, and 100 μ M to the aortic rings for 20 min before vasoconstriction was performed. The contractions of the aortic rings were induced by PE (0.1 nM–10 μ M) which was added cumulatively. The obtained results were shown as percentages of contraction compared with the absence of ADIS (control).

Effect of ADIS on extracellular Ca^{2+} influx to SMC. Further to examine the mechanism of ADIS-induced vasorelaxation on Ca^{2+} channel, the endothelium-denuded rings were used to investigate the $CaCl_2$ concentration–response curve. Briefly, after the aortic rings stabilized under the Ca^{2+} free Krebs solution containing EGTA (1 mM) for 20 min, the rings were allowed in Ca^{2+} free solution containing 80 mM Ca^{2+} free produce depolarization in the smooth muscle cell for the opening up of the voltage-operated calcium channels (VOCCs). Then, $CaCl_2$ (0.01–10 mM) was added cumulatively. After the maximal response was obtained, the rings were washed out with Ca^{2+} free Krebs solution for 20 min. Next, Ca^{2+} free KCl (80 mM) was re–exposed after preincubating with ADIS (1 μ M, 10 μ M, and 100 μ M) and nifedipine (1 μ M). The percentages of contraction induced by $CaCl_2$ in the absence and presence of ADIS were compared.

Role of ADIS on intracellular Ca^{2+} release. To determine whether ADIS could attenuate the release of Ca^{2+} from sarcoplasmic reticulum (SR), the endothelium-denuded rings were used in this experiment. The rings were pre-contracted with KCl (80 mM) to provide Ca^{2+} loading into SR. Then, the aortic rings were washed and exposed to Ca^{2+} free Krebs solution containing EGTA (1 mM), followed by activating transient contraction by PE (10 μ M) or caffeine (20 mM) in Ca^{2+} free solution before and after the pre-incubation with ADIS (1 μ M, 10 μ M, and 100 μ M). The percentages of contraction in the absence of ADIS and in the presence of ADIS, both activated by PE and caffeine, were compared.

Statistical analysis

All the data were expressed as mean \pm SEM. The statistical analysis was performed using unpaired Student's t-test between two groups and one-way-analysis of variance (ANOVA) by following Dunnett's post hoc test for the comparison between multiple groups by SPSS. A value of p < 0.05 was considered to be having significance. Concentration-response curves were plotted and experimental data obtained by using a nonlinear curve-fit program (GraphPad Prism 5).

Results

Role of endothelium in ADIS-induced relaxation in rat aortic rings

In the rat aortic rings with or without endothelium, PE (10 $\mu M)$ induced a steady contraction. ADIS caused concentration-dependent vasorelaxant effect on PE-induced contraction in both endothelium-intact and endothelium-denuded arteries, with E_{max} values of 79.26 \pm 3.74 and 88.05 \pm 3.31%, respectively (vs. control group E_{max} value of 11.98 \pm 4.19%, p < 0.01). The EC50 values of the relaxing effect of ADIS for the endothelium-intact arteries and the endothelium-denuded arteries were 41.99 \pm 7.14 μM and 54.5 \pm 1.76 μM , respectively. These two values were not significantly different (Fig. 2).

Role of K^+ channels on ADIS-induced relaxation

To define the role of K $^+$ channels on vasorelaxation induced by ADIS, the endothelium-denuded rings were pre-incubated with four different K $^+$ channel blockers such as TEA (5 mM), 4-AP (1 mM), glibenclamide (10 mM), and BaCl $_2$ (1 mM). The vasorelaxant effect of ADIS on PE (10 μ M) pre-contracted aortic rings was not altered by the pre-incubation of the rings with four types of K $^+$ channel blockers (Table 1 and Fig. 3A).

Role of soluble guanylyl cyclase (sGC) in ADIS-induced relaxation

To investigate the effect of ADIS on the NO-cyclic guanosine monophosphate (cGMP) pathway, the aortic rings were pre-incubated with ODQ (1 μ M). As is evident from Fig. 3B, ODQ did not alter the

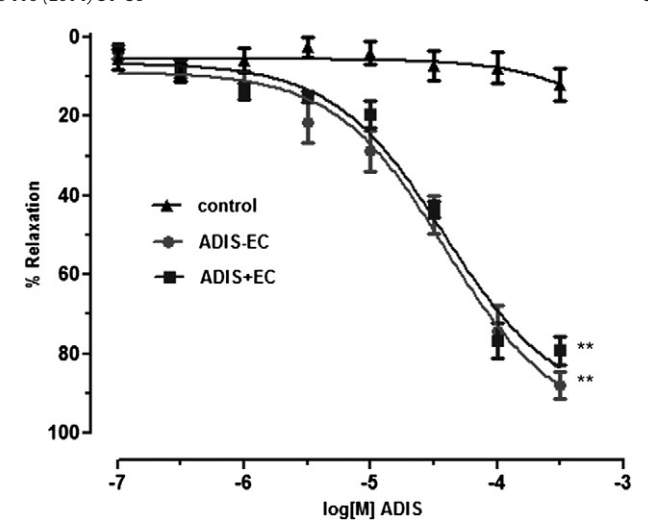


Fig. 2. The cumulative concentration–response curve of ADIS (0.1 μ M–3 mM) on endothelium–intact (+EC) and endothelium–denuded (–EC) aortic rings precontracted with PE (10 μ M). Data are analyzed by one way ANOVA followed by Dunnett's multiple comparison test and expressed as mean \pm SEM of six rats. **p < 0.01 vs. control group (0.01% DMSO).

relaxation induced by ADIS, which had an E_{max} value of $78.25 \pm 7.22\%$ (vs. control group E_{max} value of $88.05 \pm 3.31\%$).

ADIS relaxation in PE and KCl contracted endothelium denuded rings

In endothelium-denuded aortic rings, ADIS (0.1 $\mu\text{M}{-}3$ mM) significantly relaxed PE (10 $\mu\text{M})$ and KCl (80 mM) pre-contracted aortic rings in a concentration-dependent manner (Fig. 4). The EC₅₀ values amounted to 41.99 \pm 7.14 μM and 51.89 \pm 1.42 μM for PE and KCl induced contractions, respectively. The E_{max} value of PE was at 79.26 \pm 3.74% of the control and the E_{max} value of KCl was at 82.12 \pm 2.61% of the control.

Role of α_1 -receptor in inhibitory vasoconstriction effect of ADIS

To verify the ability of ADIS to prevent contractile effect conveyed through the α_1 -receptor, the aortic rings were pre-incubated with ADIS (1 μ M, 10 μ M, and 100 μ M) before exposing them to PE (0.1 nM–10 μ M), which was added cumulatively. The results revealed that all the three concentrations of ADIS attenuated the maximal contraction of PE to 83.70 \pm 3.20%, 70.01 \pm 5.67%, and 64.20 \pm 3.53%, respectively (vs. control group 89.86 \pm 10.02%), as demonstrated in Fig. 5.

Effect of ADIS on extracellular Ca²⁺-induced contraction

To investigate the effect of ADIS on the voltage-dependent calcium channels (VOCCs) pathway, Ca^{2+} -free high KCl (80 mM) solution was applied to induce stable contraction. $CaCl_2$ (0.01–10 mM) was then added cumulatively to induce a progressive increase in the contraction of the aortic rings. ADIS (1 μ M, 10 μ M, and 100 μ M) pre-incubation

Table 1 Effect of various K^+ channel inhibitors on the negative logarithm of EC_{50} (pD₂) and maximal vasorelaxation (E_{max}) induced by ADIS on endothelium-denuded, pre-contracted with PE (10 μ M).

	pD2 (M)	E _{max} (%)
Control	4.07 ± 0.12	87.53 ± 3.10
4-AP	4.16 ± 0.16	62.60 ± 7.23
TEA	4.14 ± 0.08	78.84 ± 5.48
Glibenclamide	4.45 ± 0.20	75.69 ± 12.09
BaCl ₂	4.37 ± 0.11	89.65 ± 6.99

The data are expressed as mean \pm SEM (n=6).

R. Pantan et al. / Life Sciences 116 (2014) 31-36

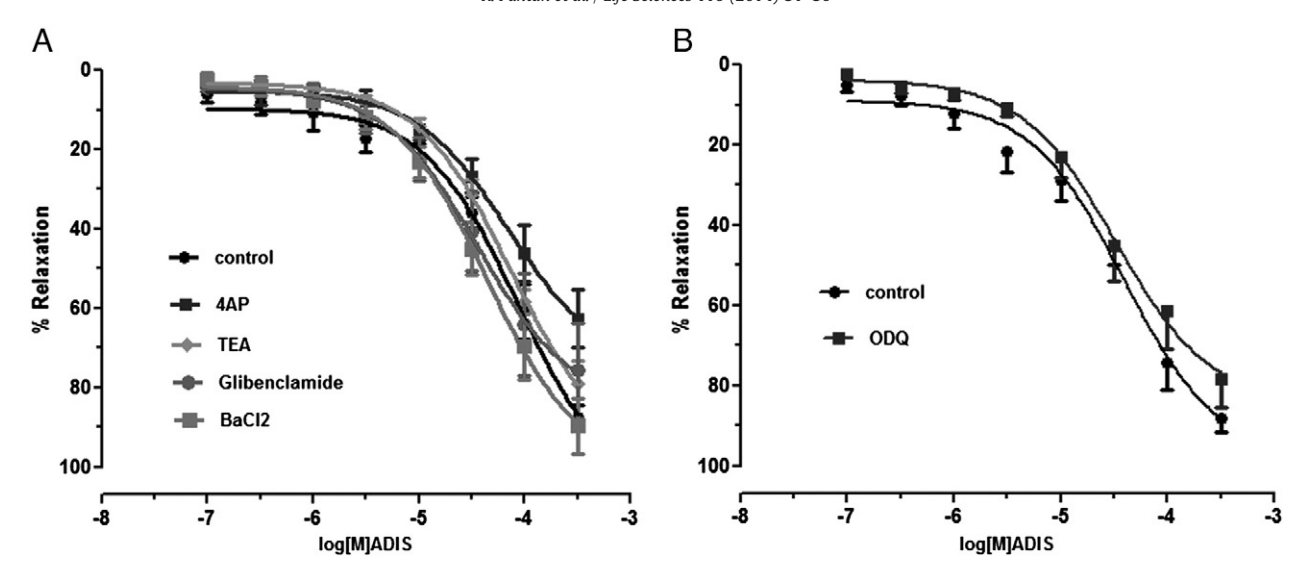


Fig. 3. The effects of K^+ channel blockers: 4-aminopyridine (4-AP, 1 mM), tetraethylammonium (TEA, 5 mM), glibenclamide (10 μ M), and barium chloride (BaCl₂, 1 mM) (A) and soluble guanylyl cyclase; ODQ (1 μ M) (B) on ADIS (0.1 μ M-3 mM) induced relaxation in endothelium-denuded aortic rings pre-contracted with PE (10 μ M). Data are analyzed by one way ANOVA followed by Dunnett's multiple comparison test and expressed as mean \pm SEM, where n=6 rats.

significantly inhibited the contraction induced by extracellular Ca $^{2+}$ to 92.87 \pm 8.52%, 87.28 \pm 8.12%, and 70.63 \pm 6.16%, respectively (vs. control group 103.80 \pm 5.80%). In addition, pretreatment with nifedipine (1 μ M), the Ca $^{2+}$ channel blocker, also inhibited the contraction induced by the extracellular Ca $^{2+}$ (E $_{max}=30.69\pm4.04\%$), as presented in Fig. 6A.

Role of ADIS in sarcoplasmic reticulum calcium release induced by PE or caffeine

The inhibitory effect of ADIS on a transient contraction due to Ca²⁺ release from intracellular stores was carried out in a Ca²⁺ free solution by using endothelium-denuded rings which were activated by PE (10 μ M) and caffeine (20 mM). As shown in Fig. 6B, pretreatment with ADIS (1 μ M, 10 μ M, and 100 μ M) reduced the percentage of PE-induced transient contraction to 66.44 \pm 3.42, 64.86 \pm 3.36, and 41.09 \pm 3.45, respectively (vs. control group 93.26 \pm 2.61). In addition, ADIS also decreased the percentage of caffeine-induced transient

contraction to 79.58 \pm 3.59, 79.18 \pm 3.12, and 64.61 \pm 3.20, respectively (vs. control group 91.19 \pm 3.06).

Discussion

ADIS has been studied for its efficiency in vasorelaxation and has been found to have more potential than isosteviol, which is the parent compound, by approximately 12-fold (Wonganan et al., 2013). This study is intended to verify the underlying mechanism of ADIS on the vasorelaxation response. Vasorelaxation is the response of the vascular smooth muscle cell which is regulated via the endothelium-dependent and the endothelium-independent signaling pathways. In the present study, ADIS showed relaxant effects on PE pre-contracted endothelium-intact as well as endothelium-denuded aortic rings. These findings suggest that the vasorelaxant effect caused by ADIS was endothelium-independent. To reduce experimental complexity we investigated the relaxing effect of ADIS on endothelium denuded rings. The opening of K^+ channels in the vascular smooth muscle cell is one of the mechanisms involved in the regulation of muscle contractility (Nelson and Quayle,

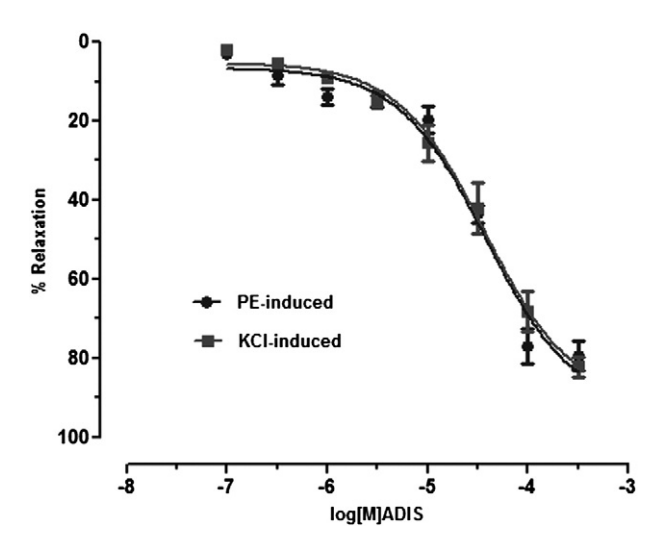


Fig. 4. The effect of ADIS (0.1 μ M–3 mM) on PE (10 μ M) and KCI (80 mM) pre-contracted endothelium-denuded aortic rings. Data are analyzed with Student's t-test and expressed as mean \pm SEM of six rats.

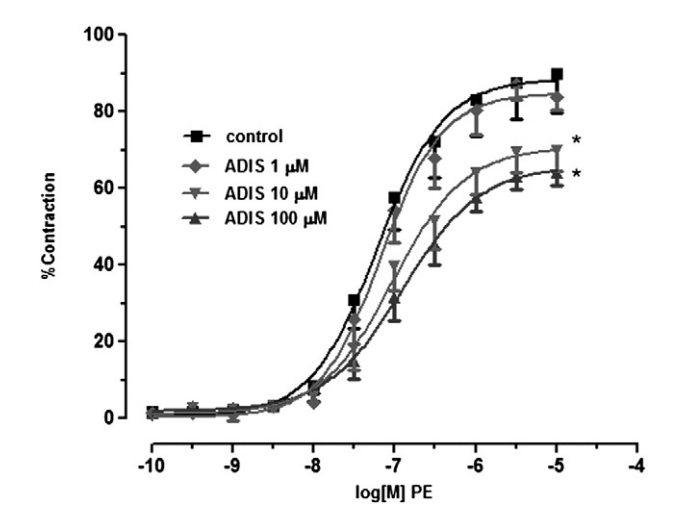


Fig. 5. The inhibitory effects of ADIS (1 μ M, 10 μ M, and 100 μ M) on the contraction induced by PE (0.1 nM–10 μ M) in endothelium-intact rat aortic rings. Data are analyzed by one way ANOVA followed by Dunnett's multiple comparison test and expressed as mean \pm SEM of six rats. *p < 0.05 vs. control group (0.01% DMSO).

R. Pantan et al. / Life Sciences 116 (2014) 31-36

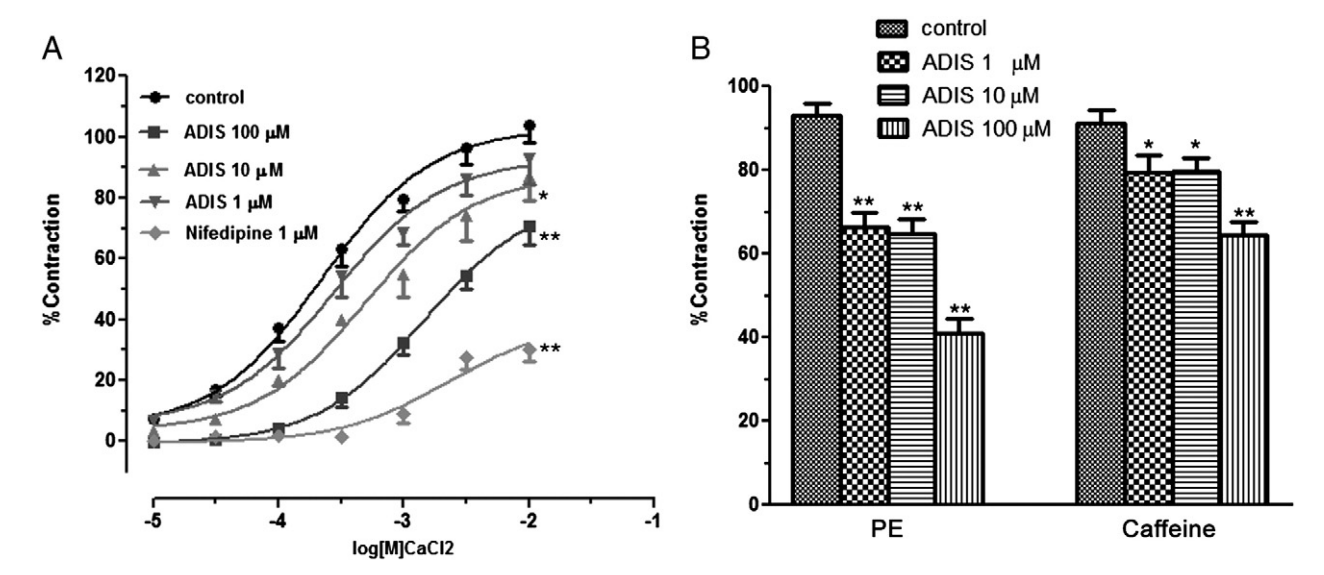


Fig. 6. The effect of ADIS ($1 \mu M$, $10 \mu M$, and $100 \mu M$) and nifedipine ($1 \mu M$) on the cumulative-concentration curve induced by extracellular Ca^{2+} in endothelium-denuded rings pre-challenged with KCI ($80 \mu M$), in Ca^{2+} free solution (A) and inhibitory effect of ADIS on PE ($10 \mu M$) and caffeine ($20 \mu M$) induced transient contractions in Ca^{2+} free Krebs solution in endothelium-denuded aortic rings (B). Data are analyzed by one way ANOVA followed by Dunnett's multiple comparison test and expressed as mean \pm SEM of six rats. *p < 0.05 and **p < 0.01 vs. control group (0.01% DMSO).

1995; Quayle et al., 1997; Jackson, 2000; Brayden, 2002). TEA (5 mM), glibenclamide (10 μ M), 4-AP (1 mM), and BaCl₂ (1 mM) are the K⁺ channel blockers used to investigate potential K⁺ channel-related vasorelaxant effects of various agents. The vasorelaxant effects of ADIS were not affected by pre-treatment with these K⁺ blockers. Our study indicated that the relaxant effect of ADIS is not related to the opening of the K⁺ channels. Moreover, we have tested the role of soluble guanylyl cyclase (sGC) which effects an increase in the amount of cGMP in the smooth muscle cell and causes vasorelaxation (Waldman and Murad, 1987; Warner et al., 1994; Lucas et al., 2000). The result revealed that inhibition of the sGC activity by using ODQ did not have any effect on the relaxation of the aortic ring induced by ADIS. Therefore, this is a clear indication that the action of ADIS on the K⁺ channels and the sGC activities in the aortic ring can be ruled out.

The vascular smooth muscle contraction in also regulated by the inhibition of extracellular Ca²⁺ influx via voltage and/or receptoroperated calcium channels (VOCCs and/or ROCCs) and the release of Ca²⁺ from intracellular stores (Hurwitz, 1986; Van Breemen and Saida, 1989; Hori et al., 1993; Nelson and Quayle, 1995; Horowitz et al., 1996). In addition, the binding of alpha adrenergic agonist molecule such as phenylephrine (PE) to its receptor activates IP₃ and induces release of calcium from intracellular stores. However, elevated intracellular calcium might activate voltage dependent calcium channels through the PKC pathway (Chen et al., 2009; Lee et al., 2013). Moreover. it is widely known that KCl induces smooth muscle contraction through the activation of VOCCs and the subsequent release of calcium from SR, whereas PE-induced vasoconstriction is mediated by extracellular Ca²influx through ROCCs and by internal calcium release from the specific IP3 receptor (IP3R) channels in the SR membrane (Ruzycky and Morgan, 1989; Van Breemen and Saida, 1989; Meissner, 1994). Thus, both the contractile agents produce a significant increase in the intracellular calcium concentration through calcium influx. It should be noted that ADIS possesses vasorelaxation via both VOCCs and ROCCs which respond to KCl and PE, respectively. The blocking activity of the VOCC and the ROCC effect are result in a decrease of intracellular calcium, which is followed by the relaxation of the vascular smooth muscle (Ehrlich and Watras, 1988). In addition, this study clearly demonstrated that preincubation with ADIS reduces the aortic tension induced by PE cumulatively in a concentration-dependent manner. It is well known that PE regulates vasoconstriction through α_1 -adrenergic receptors and also affects the ROCCs (Ferris and Snyder, 1992; Hori et al., 1993). As it

was expected, the ADIS' relaxation effects could be observed in contraction induced by the alpha adrenergic agonist. To determine the role of the VOCCs, we further evaluated the concentration–response curve of CaCl₂ in a Ca²⁺ free medium containing 80 mM KCl which affects the influx of Ca²⁺ into cytoplasm. The results show that ADIS significantly reduced the KCl-induced vascular smooth muscle contraction in the endothelium–denuded rings, in a concentration–dependent manner, and clearly reduced the Ca²⁺-induced contraction in the aortic rings exposed to KCl. In addition, the contraction was reduced by nifedipine, a typical L-type voltage–operated calcium channel blocker, confirming the involvement of L-type voltage–operated calcium channels in the contraction response (Hockerman et al., 1997). These results demonstrate that ADIS acts by inhibiting the Ca²⁺ influx through the membrane of the smooth muscle, through interference with the VOCCs.

Next, we investigated whether ADIS could exert its vasorelaxant effects by interfering with the Ca²⁺ released from intracellular stores by phosphoinositide production, following the receptor activation. PE and caffeine were used as the contractile agents; PE induces mobility of Ca²⁺ from SR by IP₃R activity, whereas caffeine induces Ca²⁺ release from the SR by ryanodine receptor activity (Ferris and Snyder, 1992; Meissner, 1994). ADIS significantly inhibited the transient contraction induced by both PE and caffeine. Thus, it seems likely that the vascular effects of ADIS involved the reduction of IP₃-dependent Ca²⁺ releases from SR sensitive to PE.

Conclusion

Taken together, our results suggest that ADIS induces relaxation in aortic rings through an endothelium-independent pathway, involving both blockage of voltage dependent cytoplasma membrane calcium channels and calcium release from intracellular stores in vascular smooth muscle cells.

Conflict of interest

The authors have declared no conflict of interest.

Acknowledgments

This work was supported by the Higher Education Research Promotion (HERP) Program, the Office of the Higher Education Commission,

Thailand, the Faculty of Medicine Research Fund, Chiang Mai University, and the Graduate School, Chiang Mai University, Chiang Mai, Thailand. Parted supports from The Thailand Research Fund and the Center of Excellence for Innovation in Chemistry are gratefully acknowledged.

References

- Boeckh E, Humboldt G. Cardiocirculatory effects of total aqueous extract in normal
- subjects and stevioside in rats. Cienc Cult 1981;32:208–10.

 Brayden JE. Functional roles of K_{ATP} channels in vascular smooth muscle. Clin Exp Pharmacol Physiol 2002;29:312–6.
- Chan P, Xu DY, Liu JC, Chen YJ, Tomlinson B, Huang WP, et al. The effect of stevioside on blood pressure and plasma catecholamines in spontaneously hypertensive rats. Life Sci 1998;63:1679-84.
- Chatsudthipong V, Muanprasat C. Stevioside and related compounds: therapeutic benefits beyond sweetness. Pharmacol Ther 2009:121:41-54
- Chen GP, Ye Y, Li L, Yang Y, Qian AB, Hu SJ. Endothelium-independent vasorelaxant effect of sodium ferulate on rat thoracic aorta. Life Sci 2009;84:81-8.
- Ehrlich BE, Watras J. Inositol 1,4,5-trisphosphate activates a channel from smooth muscle sarcoplasmic reticulum. Nature 1988;336:583-6.
- Ferris CD, Snyder SH. Inositol 1,4,5-trisphosphate-activated calcium channels. Annu Rev Physiol 1992;54:469-88.
- Geuns JM. Stevioside. Phytochemistry 2003;64:913-21.
- Goyal SK, Samsher, Goyal RK. Stevia (Stevia rebaudiana) a bio-sweetener: a review. Int J Food Sci Nutr 2010;61:1-10.
- Hockerman GH, Peterson BZ, Johnson BD, Catterall WA. Molecular determinants of drug binding and action on L-type calcium channels. Annu Rev Pharmacol Toxicol 1997;
- Hori M, Sato K, Miyamoto S, Ozaki H, Karaki H. Different pathways of calcium sensitization activated by receptor agonists and phorbol esters in vascular smooth muscle. Br J Pharmacol 1993;110:1527-31.
- Horowitz A, Menice CB, Laporte R, Morgan KG. Mechanisms of smooth muscle contraction. Physiol Rev 1996;76:967-1003.
- Humboldt G, Boech E. Efeito do edulcorante natural (stevioside) e sinte'tico (sacarina) sobre o ritmo cardiaco em ratos. Arq Bras Cardiol 1977;30:257-77.
- Hurwitz L. Pharmacology of calcium channels and smooth muscle. Annu Rev Pharmacol Toxicol 1986;26:225-56.

- Jackson WF. Ion channels and vascular tone. Hypertension 2000;35:173-8.
- Lee K, Jung J, Yang G, Ham I, Bu Y, Kim H, et al. Endothelium-independent vasorelaxation effects of sigesbeckia glabrescens (Makino) Makino on isolated rat thoracic aorta. Phytother Res 2013;27:1308-12.
- Lucas KA, Pitari GM, Kazerounian S, Ruiz-Stewart I, Park J, Schulz S, et al. Guanylyl cyclases and signaling by cyclic GMP. Pharmacol Rev 2000;52:375-414
- Meissner G. Ryanodine receptor/Ca2+ release channels and their regulation by endogenous effectors. Annu Rev Physiol 1994;56:485–508.
- Melis MS. Influence of calcium on the blood pressure and renal effects of stevioside. Braz J Med Biol Res 1992;25:943-9.
- Nelson MT, Quayle JM. Physiological roles and properties of potassium channels in arterial smooth muscle. Am J Physiol Endocrinol Metab 1995;268:C799-822
- Quayle JM, Nelson MT, Standen NB. ATP-sensitive and inwardly rectifying potassium channels in smooth muscle. Physiol Rev 1997;77:1165-232
- Ruzycky AL, Morgan KG. Involvement of the protein kinase C system in calcium-force relationships in ferret aorta. Br J Pharmacol 1989;97:391-400.
- Van Breemen C, Saida K. Cellular mechanisms regulating [Ca²⁺]i smooth muscle. Annu Rev Physiol 1989;51:315-29.
- Waldman SA, Murad F. Cyclic GMP synthesis and function. Pharmacol Rev 1987;39: 163-96
- Warner TD, Mitchell JA, Sheng H, Murad F. Effects of cyclic GMP on smooth muscle relaxation. Adv Pharmacol 1994;26:171-94.
- Wong KL, Chan P, Yang HY, Hsu FL, Liu IM, Cheng YW, et al. Isosteviol acts on potassium channels to relax isolated aortic strips of Wistar rat. Life Sci 2004;74:2379-87.
- Wonganan O, Tocharus C, Puedsing C, Homvisasevongsa S, Sukcharoen O, Suksamrarn A. Potent vasorelaxant analogs from chemical modification and biotransformation of isosteviol, Eur I Med Chem 2013:62:771-6.
- Xu D, Du W, Zhao L, Davey AK, Wang J. The neuroprotective effects of isosteviol against focal cerebral ischemia injury induced by middle cerebral artery occlusion in rats. Planta Med 2008;74:816-21.
- Xu D, Li Y, Wang J, Davey AK, Zhang S, Evans AM. The cardioprotective effect of isosteviol on rats with heart ischemia-reperfusion injury. Life Sci 2007a;80:269-74.
- Xu D, Zhang S, Foster D, Wang J. The effects of isosteviol against myocardium injury induced by ischaemia-reperfusion in the isolated guinea pig heart. Clin Exp Pharmacol Physiol 2007b;34:488-93.

Synergistic Effect of Cationic Lipids with Different Polarheads, Central Core Structures and Hydrophobic Tails on Gene Transfection Efficiency

Nattisa Niyomtham, Nuttapon Apiratikul, Kanyarat Chanchang, Praneet Opanasopit, and Boon-ek Yingyongnarongkul*

^a Department of Chemistry and Center of Excellence for Innovation in Chemistry, Faculty of Science, Ramkhamhaeng University; Bangkapi, Bangkok 10240, Thailand: ^b Department of Chemistry, Faculty of Science, Siam University; Phasi-Charoen, Bangkok 10160, Thailand: and ^c Pharmaceutical Development of Green Innovations Group (PDGIG), Faculty of Pharmacy, Silpakorn University; Nakhon Pathom 73000, Thailand.

Received May 5, 2014; accepted June 17, 2014

Lipid-mediated delivery of DNA into cells holds great promise both for gene therapy and basic research applications. The primary approach to improving transfection efficiency is the design and synthesis of novel cationic lipids. Alternatively, using the synergistic effect of different cationic mixtures can provide another approach to increasing transfection efficiency. This paper describes the synergistic effect of lipids with different polarheads, central core structures and hydrophobic tails. The enhancement of cellular transfection into HEK293 cells was observed by combining two lipids having aminoglycerol and di(hydroxylethyl)amino core structures at a 1:1 weight ratio. Additionally, the liposome formation of these lipids with the helper lipid, 1,2-dioleoyl-propyl-3-phosphatidylethanolamine (DOPE), at the weight ratio of 1:1 can provide higher transfection efficiency into HEK293, MCF-7 and HeLa cells than LipofectamineTM 2000. Our finding indicated that cationic liposomes comprised of a mixture of lipids with different polarheads, central core structures and hydrophobic tails should be very promising in liposome-mediated gene delivery in vitro and in vivo.

Key words cationic liposome; synergistic effect; DNA delivery; non-viral vector.

Gene therapy has gained significant attention over past two decades as an alternative method to treat genetic disorders^{1,2)} as well as cancers.3) One fundamental of gene therapy is the delivery system that can introduce and stabilize genetic material. Since free oligonucleotides and DNA are rapidly degraded by serum nucleases.4) many efforts are focused on developing the carriers to protect and deliver these materials into targeted cells. Two delivery systems namely viral and non-viral vectors are currently developed to solve the problems. Viral carriers have known to be one of the most effective gene delivery methods for in vivo application. 5-8) Over one thousand gene therapy clinical trials have been completed or approved; two-thirds of which performed by viral vectors.⁸⁾ However, the limitation of viral vectors concerning toxicity, immunogenicity, scale-up procedures and their relatively small capacity for therapeutic DNA has prompted the development non-viral vectors. Delivery systems based on non-viral vectors, for example cationic lipids, dendrimers or cationic polymers, have been the focus of much recent research.9 Non-viral systems have proved to be generally less toxic or immunogenic, more easily to produce and a greater stability.

Cationic liposomes are one of the most extensively studied of non-viral vectors because of their lesser immunogenic nature, ease of production and handle, and ability to deliver large pieces of DNA. Cationic liposomes, like other non-viral vectors bearing positive charge, interact with the negatively charged phosphate backbone of nucleic acids to form a compact structure and facilitate cellular uptake by endocytic routes. 10–131 Since the first application of cationic lipid in DNA delivery, 141 numerous cationic lipids have been synthesized and demonstrated the capability of delivering genetic materials into various cells. 91 Some of cationic liposomes-mediated gene transfers have been used in gene therapy clinical trials. 81

However, significant limitations of cationic liposomes are low transfection efficiency and much research activity has been focused on increase efficiency. The main approach to improving the transfection properties was to synthesize new kinds of cationic lipids. The alternative strategy, apart from employing the helper lipids such as 1,2-dioleoyl-propyl-3-phosphatidyl-ethanolamine (DOPE) or cholesterol, to improve tansfection efficiency is the use of mixture cationic lipids.

Previous studies have shown that the use of a mixture of cationic lipids with the same head group but with different chain lengths dramatically enhances the transfection of human umbilical artery endothelial cells (HUAEC).¹⁵⁾ The synergistic effect was not only limited to the homologous, but it also exhibited to cationic lipids with different polarhead and hydrophobic tails. 16) Mixture of multi-components to form lipoplexes has also been reported.¹⁷⁾ Asymmetric vesicles formulated with lipids having very different headgroups have been prepared. This vesicle is expected to be a delivery system with increase in biocompatibility and flexibility.¹⁸⁾ Recently, we described the cationic lipids 1191 and 220,211 (Fig. 1) which exhibited transfection efficiency higher than and comparable to the commercially available transfection reagents. These lipids contain different polarheads, central core structure, and hydrophobic tails; 1 comprise of the commonly used template, aminoglycerol, primary amino headgroup and dodecanoyl tails whereas 2 has di(hydroxyethyl)amino core structure, polyamine polarhead and myristoyl tails. Therefore, to investigate how transfection changes with the liposome comprised of cationic lipids with different polarheads, central core structures and hydrophobic tails, cationic liposome consisting of 1 and 2 was prepared and tested for transfection efficiency in mammalian cells. The size and zeta potential of the prepared liposome were also evaluated.

The authors declare no conflict of interest.

September 2014 1535

Fig. 1. Structures of Cationic Lipids 1 and 2

MATERIALS AND METHODS

General Solvents and reagents were purchased from commercial suppliers and used without further purification. IR spectra were recorded as neat on a Perkin-Elmer FT-IR spectrum 400 spectrometer attenuated total reflectance (ATR). ¹H- and ¹³C-NMR spectra were recorded on a Bruker AVANCE400 spectrometer operating at 400 and 100 MHz. respectively. Chemical shifts are given in ppm relative to residual CHCl₃/CDCl₃ ($\delta_{\rm H}$ 7.24/ $\delta_{\rm C}$ 77.00, central signal of the triplet related to carbon). Mass spectra were obtained using a Finnigan LC-Q mass spectrometer. High resolution mass spectra were performed on a Bruker micrOTOF II mass spectrometer. Unless indicated otherwise, column chromatography and TLC were carried out using Merck silica gel 60 (finer than 0.063 mm) and precoated silica gel 60 F254 plates, respectively. Spots on TLC were detected by spraying with ninhydrin reagent followed by heating.

Synthesis of Cationic Lipid 1 (Chart 1) (i) N-(tert-Butoxycarbonyl)-1.2-diaminoethane (4): A solution of di-tertbutyl dicarbonate (4.0 g. 18.6 mmol) in CH₂Cl₂ (200 mL) was added dropwise to a stirred solution of 1,2-diaminoethane (3) (5.3 g. 93.1 mmol) in CH₂Cl₂ (500 mL) and the mixture was stirred for 24h. The solvent was evaporated and the residue was suspended in H₂O (200 mL). The insoluble white solid was removed by filtration and the product was then extracted using CH₂Cl₂ (3×200 mL). The combined organic phase was dried over anhydrous Na₂SO₄ and concentrated in vacuo. The crude product was purified by column chromatography using CH₂Cl₂ and CH₂Cl₂-MeOH as eluting solvent with gradual increase in concentration of the more polar component to yield the title compound as a white solid (2.5 g, 84%). The spectroscopic data were in agreement with those found in the literature.22)

(ii) N-(1-(2.3-Dihydroxy)propyl)-N'-(2-(N-Boc)aminoethyl)-carbamide (5): To a solution mixture of N-(tert-butoxycarbonyl)-1.2-diaminoethane (1.1 g. 6.8 mmol) and pyridine (0.8 mL. 10.3 mmol) in CH_2Cl_2 (10 mL) was added dropwise a solution of 4-nitrophenyl chloroformate (1.6 g. 8.2 mmol) in CH_2Cl_2 (10 mL) and the mixture was stirred for 8 h. The reaction was work up by removed the solvents under reduced pressure. The crude product was dissolved in CH_2Cl_2 (20 mL) and (\pm)-3-amino-1,2-propanediol (0.6 mL, 8.2 mmol) in MeOH (15 mL) was then added. The resulting mixture was stirred overnight at the room temperature. The solvent was evaporated and the residue was suspended in H_2O (100 mL) and thoroughly extracted with EtOAc (3×50 mL). The combined organic phase was washed with H_2O , dry over

anhydrous Na₂SO₄ and the solvent was evaporated to dryness. The residue was purified by column chromatography using CH₂Cl₂ and CH₂Cl₂-MeOH as eluting solvent with gradual increase in concentration of more polar component to afford compound 5 (1.0 g, 53%) as colorless oil. IR: v_{max} 3348, 1678, 1590, 1157, 1045 cm⁻¹; ¹H-NMR (400 MHz, CDCl₃+10 drops of CD₃OD) δ : 1.36 (9H, s. C(CH₃)₃), 3.09 (2H, m. BocNHCH₂), 3.15 (2H, m, NHCH₂CH), 3.19 (2H, t, J=5.0 Hz, BocNHCH2CH2NHCO), 3.46 (2H, m, CH2OH), 3.60 (1H, m, CHOH); 13 C-NMR (100MHz, CDCl₃+10 drops of CD₃OD) δ : 28.1 (OC(CH₃)₃), 39.1 (NHCH₂CH), 40.7 (BocNHCH₂), 42.3 (BocNHCH2CH2NHCO), 63.4 (CH2OH), 71.3 (CHOH), 79.4 (OC(CH₃)₃), 156.9 (NHCONH), 160.2 (NHCOO'Bu); high resolution-electrospray ionization-mass spectrum (HR-ESI-MS) (+ve) m/z: Calcd for $C_{11}H_{23}N_3NaO_5$ [M+Na]⁺ 300.1529, Found 300.1553.

(iii) N-(1-(2,3-Didodecanoyloxy)propyl)-N'-(2-(N-Boc)aminoethyl)carbamide (6): Dodecanoic acid (1.8g, 9.0 mmol), dicyclohexylcarbodiimide (DCC) (1.9 g, 9.0 mmol) and 4-dimethylaminopyridine (DMAP) were dissolved in dry CH₂Cl₂ (20 mL). The reaction mixture was stirred at room temperature for 30 min, a solution of compound 5 (1.0 g, 3.6 mmol) in dry CH₂Cl₂ (10 mL) was then added and the resulting mixture was stirred overnight at the same temperature. The precipitated dicyclohexyl urea (DCU) was removed by filtration and the filtrate was evaporated under reduced pressure to give crude product. The product 6 (1.9 g, 82%) was obtained as white solid after usual column chromatographic purification. IR: v_{max} 3400, 3284, 2919, 1736, 1652, 1576, 1163 cm⁻¹; ¹H-NMR (400 MHz, CDCl₃) δ : 0.85 (6H, br t, $J=6.6\,\mathrm{Hz}$, 2×CH₃), 1.23 (32H, s, 16×CH₂), 1.41 (9H, s, $OC(CH_3)_3$), 1.58 (4H, br s, 2×CH₂), 2.29 (4H, m, 2×CH₂), 3.21 (2H, br s. CH₂NHBoc), 3.26 (2H, br s, CH₂CH₂NHCO), 3.37 (2H, br t, J=5.1 Hz, NHCH₂CH), 4.14 (1H, dd, J=12.0, 5.8 Hz, NHCH₂CHCH₄H₆O), 4.25 (1H, dd, J=12.0, 3.5 Hz, NHCH₂CHCH₃H_bO), 4.76 (1H, br s, NH), 5.00 (2H, br s, 2×NH), 5.03 (1H, m, NHCH₂CHCH₂O); ¹³C-NMR (100 MHz, CDCl₃) δ : 14.0 (CH₃), 22.6, 24.84, 24.87, 28.3, 29.1, 29.26, 29.29, 29.4, 29.5, 31.8, 34.0, 34.2, 40.1 (CH₂NHBoc), 40.5 (NHCH₂CH), 40.7 (CH₂CH₂NHCO), 62.8 (NHCH₂CHCH₂O), 70.9(NHCH₂CHCH₂O), 79.4 (OC(CH₃)₃), 156.7 (NHCOO'Bu), 158.4 (NHCONH), 173.4 (OCOCH₂), 173.5 (OCOCH₃); HR-ESI-MS (+ve) m/z: Calcd for $C_{35}H_{67}N_3NaO_7$ [M+Na]⁺ 664.4871, Found 664.4898.

(iv) N-(1-(2,3-Didodecanoyloxy)propyl)-N'-(2-aminoethyl)carbamide (1): To a solution of compound 6 (1.9 g, 2.96 mmol) was added 20% trifluoroacetic acid (TFA) in CH₂Cl₂ (20 mL, excess) and the mixture stirred for 1h. The solvent was removed under stream of nitrogen gas and further dried under vacuum for 2h to dryness to obtain lipid 1 as white sticky solid (1.8 g, 100% as TFA salt). IR: $v_{\rm max}$ 3392, 2922, 1727, 1673, 1568, 1176, 1136 cm⁻¹; ¹H-NMR (400 MHz, CDCl₃) δ : 0.81 (6H, t, J=6.1 Hz, $2\times C\underline{H}_3$), 1.19 (32H, br s, $16\times C\underline{H}_2$), 1.52 (4H, br m, $2 \times CH_2$), 2.25 (4H, br m, $2 \times CH_2$), 2.97 (2H, br s, CH₂NH₂), 3.20 (1H, m, NHCH_aH_bCH), 3.32 (1H, m, NHCH_aH_bCH), 3.36 (2H, m, CH₂CH₂NHCO), 4.02 (1H, dd, J=11.9, 6.3 Hz, NHCH₂CHCH₄H_bO), 4.20 (1H, dd, J=11.9, 3.1 Hz, NHCH₂CHCH_aH_bO), 5.06 (1H, br s, NHCH₂CHCH₂O); ¹³C-NMR (100 MHz, CDCl₃) δ : 13.9 (CH₃), 22.5, 24.75, 24.78, 29.01, 29.04, 29.1, 29.2, 29.4, 29.5, 31.8, 34.0, 34.1, 37.5 (CH₂CH₂NHCO), 40.0 (NHCH₂CH), 40.4 (CH₂NH₂),

1536 Vol. 37, No. 9

$$H_2N \longrightarrow NH_2$$
 $A \longrightarrow BocHN \longrightarrow NH_2$
 Reagents and conditions: a) di-tert-butyl dicarbonate, CH_2Cl_2 , 24h; b) 4-nitrophenyl chloroformate, pyridine, CH_2Cl_2 , 8h; c) (\pm) -3-amino-1,2-propanediol, CH_2Cl_2 : MeOH (1:1), 12h; d) dodecanoic acid, DCC, DMAP, CH_2Cl_2 , 16h; e) 20% TFA/ CH_2Cl_2 , 1h.

Chart 1

Reagents and conditions: a) spermine, DMF, 16h; b) Dde-OH, CH₂Cl₂, 16h; c) di-tert-butyl dicarbonate, pyridine, CH₂Cl₂, 16h; d) 2% hydrazine/DMF, 1h; e) 2-bromoethanol, DIPEA, DMF, 16h; f) myristic acid, DIC, DMAP, CH₂Cl₂: DMF (4:1), 16h; g) 20% TFA/CH₂Cl₂, 2h.

Chart 2

62.8 (NHCH₂CH<u>C</u>H₂O), 70.5 (NHCH₂CHCH₂O), 159.5 (NHCONH), 173.9 (OCOCH₂); HR-ESI-MS (+ve) m/z: Calcd for $C_{30}H_{60}N_3O_5$ [M+H] 542.4527, Found 542.4534.

Synthesis of Cationic N^1 , N^1 -Dimyristoyloxyethyl-spermine (2) (Chart 2) The active carbonate resin 7 (562 mg, 1 eq) was added an excess solution of spermine (610 mg, 3.0 mmole) in DMF (10 mL) and the resulting suspension was then shaken overnight. The resin was filtered and washed successively with CH₂Cl₂, N,N-dimethylformamide (DMF), MeOH, DMF and

 ${\rm CH_2Cl_2}$ (3×10 mL for each solvent) and dried under vacuum for 2 h to give the resin **8**. To this resin was added an excess of 2-acetyldimedone (Dde-OH) in ${\rm CH_2Cl_2}$ (10 mL) and the suspension was shaken overnight. The resin was successfully washed with solvents. The result resin was then treated with di-*tert*-butyl dicarbonate (Boc₂O) (6 eq) and pyridine (20 eq) in ${\rm CH_2Cl_2}$ (10 mL) and the suspension was shaken overnight. The resin was filtered and washed successively with suitable solvents and the resulting resin was further reacted with 2%

September 2014 1537

hydrazine (N₂H₄) in DMF (10 mL) for two cycles of 30 min to give the resin 9. To the resin 9 was added an excess of 2-bromoethanol and N.N-diisopropylethylamine (DIPEA) (20 eq) in DMF (10mL) and the suspension was shaken overnight. The resins were filtered and washed successively with CH₂Cl₂, DMF, MeOH, DMF and CH₂Cl₃ (3×10 mL for each solvent) to give diol resin 10. To the diol resin 10 was added a solution of myristic acid (4 eq), N,N-diisopropylcarbodiimide (DIC) (4eq) and 4-dimethylaminopyridine (DMAP) in CH₂Cl₂/DMF (4:1). The suspensions were shaken overnight and washed with CH₂Cl₂, MeOH, DMF, MeOH and CH₂Cl₂ (3×10 mL for each solvent). The resulting resin was treated with a solution of 20% TFA in CH₂Cl₂ (10mL) for 2h. The filtrate was then collected and evaporated under a stream of nitrogen to give the crude lipid 2. The crude product was purified by Sephadex LH20 using MeOH as eluting solvent to give the lipid 2 (278 mg, 53%). The yield of the product was calculated based on the original loading of Merrifield resin (1.34 mmol/g). IR: v_{max} 2918, 2850, 1723, 1665, 1196, 1176, 1128 cm⁻¹; ¹H-NMR (400MHz, CDCl₃) δ : 0.83 (6H, br s, 2×CH₃), 1.21 (40H, br s, $20 \times \text{CH}_2$), 1.56 (4H, br s, $2 \times \text{OCOCH}_2\text{CH}_2$), 1.75 (4H, br s, NHCH₂CH₂CH₂CH₂NH), 1.81 (2H, br s, NHCH₂CH₂CH₂N), 2.04 (2H, br s, NH₂CH₂CH₂CH₂NH), 2.26 (4H, m, 2×OCOCH₂). 2.65 (2H, br s, NHCH₂CH₂CH₂N), 2.76 (4H, br s, N(CH₂CH₂O)₂), 2.97 (8H, br s, NH₂CH₂CH₂CH₂NH, NHCH₂CH₂CH₂CH₂NH and NHCH₂CH₂CH₂N), 3.04 (2H, br s, $NH_2CH_2CH_2CH_2NH$), 4.10 (4H, m, $2\times NCH_2CH_2O$); ¹³C-NMR (100 MHz, CDCl₃) δ : 13.4 (CH₃), 22.2, 22.3, 22.5, 23.2, 23.4, 24.4, 28.7, 28.8, 28.9, 29.0, 29.2, 31.4, 33.8, 36.1, 44.1, 46.0, 46.5, 46.6, 51.4, 52.2 N(CH₂CH₂O)₂, 61.5 2×NCH₂CH₂O, 173.9 and 173.9 (OCOCH₂); HR-ESI-MS (+ve) m/z: Calcd for $C_{38}H_{79}N_4O_4$ [M+H]⁺ 711.6721, Found 711.6717.

Liposome Preparation (i) Preparation of Cationic Liposomes: Stock solution of lipid 1 ($5 \mu g/\mu L$) and 2 ($5 \mu g/\mu L$) were prepared in absolute ethanol. Lipids 1 and 2 were mixed at various weight ratios (4:1, 3:1, 2:1, 1:1, 0.5:1 and 0.25:1) to produce solutions of mixture lipids in an Eppendorf tubes. The organic solvent was evaporated under a stream of nitrogen and further dried under high vacuum (>2 h). The resulting thin film was hydrated with phosphate buffered saline (PBS, pH 7.4) at room temperature for 1 h to give the final liposome concentration of $1 \mu g/\mu L$. The mixture was vortexed for 1 min and sonicated for 20 min in a bath-type sonicator, producing small unilamellar vesicles.^{23,24)} The liposomes were stored at 4°C for 24 h prior to use.

(ii) Preparation of Cationic Liposomes with and without DOPE: Stock solution of lipid 1 ($5 \mu g/\mu L$), lipid 2 ($5 \mu g/\mu L$) and DOPE ($5 \mu g/\mu L$) were made in absolute ethanol. To prepare cationic liposomes with DOPE, stock solutions of lipid and DOPE were mixed at weight ratio of 1:1 in an Eppendorf tubes. The processes to prepare cationic liposome are the same manner as described above. The liposome without DOPE was prepared as the same manner for DOPE-contained liposome excepted DOPE was not included.

DNA Binding Affinity DNA binding affinities of liposomes were measured at liposome/DNA ratios (w/w) of 5, 10, 15, 20, 25 and 30, by gel electrophoresis. The liposome/DNA complexes were prepared by adding the liposome solution to the DNA solution (the amount of DNA was fixed at $0.1 \mu g$). The mixture was gently mixed by pipetting up and down for 2–3 times and the mixture was held at room temperature for

 $30\,\mathrm{min}$. Each complex was added gel loading buffer (13.3% w/v sucrose in water) to get the final volume of $10\,\mu\mathrm{L}$. The complexes solution was inverted to mix and each sample ($10\,\mu\mathrm{L}$) was loaded onto a 1% agarose gel ($0.5\times\mathrm{TBE}$ buffer). The gel was run at $200\,\mathrm{V}$, $400\,\mathrm{mA}$ for 2h. DNA bands were viewed under UV light by ethidium bromide staining.

Particle Sizes and Zeta Potentials The particle size and surface charge of the cationic liposomes or cationic liposomes/DNA complexes were determined by photon correlation spectroscopy using a Zetasizer Nano ZS (Malvern Instruments Ltd., Malvern, U.K.). The cationic liposomes or cationic liposomes/DNA complexes at varying weight ratios were diluted with distilled water that had been filtered through a $0.22 \,\mu m$ membrane filter to obtain the volume required for each measurement. All samples were measured in triplicate at room temperature.

Transfection Procedure Human embryonic kidney (HEK293) and cervical epithelial adenocarcinoma (HeLa) cells were grown in Dulbecco's modified Eagle's medium (DMEM) medium supplemented with 10% fetal calf serum (FCS), penicillin (100 units/mL), streptomycin (100 mg/mL) and L-glutamine (4 mm) at 37°C, 5% CO $_2$. Human breast adenocarcinoma (MCF-7) was also growth as mentioned above except the medium containing 1% of insulin. For transfection, the cells were seeded up to 1×10^4 cells/well in a 96-well plate, to give 50-70% confluence to be used on the next day.

The growth medium was removed and the cells were washed with PBS and replaced with $100\,\mu\text{L}$ of fresh serumfree DMEM medium. DNA (pCMV-encoding β -galactosidase)/cationic liposome complexes (lipoplexes) were prepared as follows. An appropriate volume of each cationic liposome ($1\,\mu\text{g}/\mu\text{L}$) was added to the plasmid DNA ($1\,\mu\text{L}$, $0.1\,\mu\text{g}/\mu\text{L}$) and the complex was incubated at room temperature for 30 min before being diluted with phosphate-buffered saline to make a final DNA concentration of $0.1\,\mu\text{g}/10\,\text{mL}$. The lipoplexes ($10\,\mu\text{L}$) were then added to the cells and left to incubate at 37°C , 5% CO₂ for 4h. The cells were then washed with PBS and fresh growth medium was added and further incubated for 48h. For LipofectamineTM 2000 transfection, the method was carried out according to the manufacturer's instruction.

After transfection, the cells were washed once with Dulbecco's phosphate buffered saline (D-PBS) containing 0.1 g/L calcium and magnesium and then fixed with $100\,\mu\text{L}$ fixative (2% formaldehyde, 0.05% glutaraldehyde in D-PBS) for 5 min at room temperature. The cells were washed and $100\,\mu\text{L}$ of substrate/stain solution (1 mg/mL X-gal in stain solution; 5 mm potassium ferricyanide, 5 mm potassium ferrocyanide, 2 mm MgCl₂) incubated at 37°C for 2h. The cells were washed with D-PBS and the blue cells were then counted under inverted microscope. The number of transfected cells in each well of 96-well plate (0.32 cm²) was calculated to be a number of positive cells per cm².

RESULTS AND DISCUSSION

Synthesis of Cationic Lipids 1 and 2 Combinatorial synthesis provides a library of bioactive compounds to discover the lead. Lipid 1, which was one of the lead components found from a 60-compound library, ¹⁹⁾ exhibited higher transfection efficiency than the commercially available transfection agent, EffeceneTM. To obtain this compound in high purity and quantity, the lipid 1 was synthesized by a conventional method

Fig. 2. Gel Retardation Assay of Liposomes/DNA Complexes

Lane 1, DNA (pCMV-encoding β -galactosidase), lanes 2–7, liposomes /DNA complexes at weight ratios of 5, 10, 15, 20, 25 and 30 for a) liposomes-lipid 1, b) liposomes-lipid 2, and c) liposomes-lipids 1+2 at weight ratio of 1:1.

(Chart 1). The synthesis was started by the preparation of *N*-(*tert*-butoxycarbonyl)-1,2-diaminoethane (4) by high dilution method.²⁵⁾ The reaction of 4 with 4-nitrophenyl chloroformate followed by treatment with (±)-3-amino-1,2-propanediol afforded diol 5 in 53% yield over three steps. The diol 5 was then esterified with dodecanoic acid using DCC as coupling agent to provide compound 6 in 82% yield. Removal of the Boc-protecting group by the standard method yielded the lipid 1 in quantitative yield.

The lipid 2 which consisted of spermine polarhead was synthesized by solid phase chemistry (Chart 2). The protected spermine having one free primary amino group was prepared using the modified literature method.²⁶⁾ Firstly, the active carbonate Wang resin 727) was reacted with an excess of spermine to give the resin 8. The primary amino group was selectively protected over the presence of secondary amine with 2-acetyldimedone (Dde-OH).²⁸⁾ This reaction is highly selective most likely due to the stabilization provided by a strong intramolecular H-bond. The remaining secondary amines were then protected with tert-butyloxycarbonyl (Boc) groups and the Dde protecting group was selectively removed under mild condition with 2% hydrazine hydrate in DMF to obtain the resin 9. The liberated amine was converted to the desired di(hydroxyethyl)amino by treating the resin 9 with excess 2-bromoethanol in the presence of DIPEA to generate the diol resin 10. The assembly of the lipid was accomplished by reacting the alcohols with myristic acid using DIC as coupling agent in the presence of DMAP as a catalyst. The final product was cleaved from the resin by treatment with 20% TFA in CH₂Cl₂. The filtrate was collected and concentrated in vacuo; the resulting lipid was further purified by Sephadex LH20 column chromatography. The structures of the synthesized cationic lipids were confirmed by spectroscopic means (IR. NMR and HR-MS).

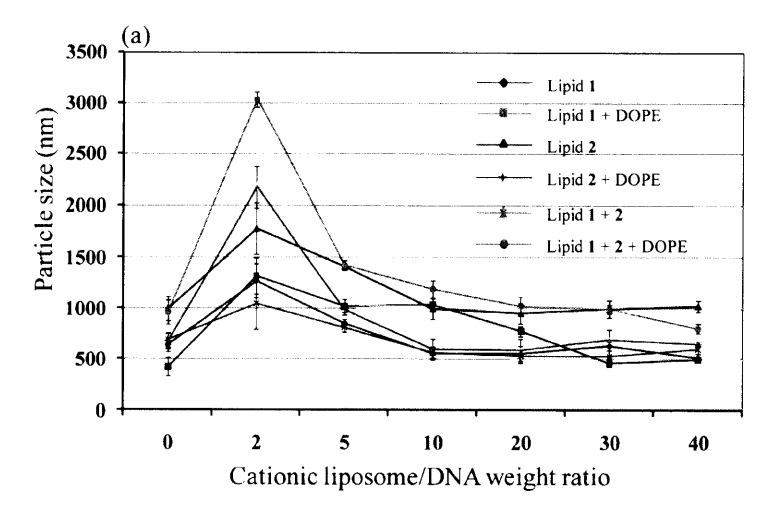
Characterization of the Cationic Liposomes/DNA Complexes The lipoplex formation between the cationic liposome preparing from single lipid and mixture lipids was analyzed by varying the lipid/DNA weight ratio using agarose gel retardation assays (Fig. 2). The results from the agarose gel electrophoresis illustrated that cationic liposomes were able to form lipoplexes. Excess DNA was barely detectable using lipid-to-DNA ratio of 5 in all of the cationic assemblies. The results indicated that liposome in the presence of lipids 1 and 2 did not change the DNA binding property to form the lipoplexes.

Further investigations of the particle size and zeta potentials of the liposomes and liposomes/DNA complexes were performed across the entire weight ratios of 2 to 40. As shown in Fig. 3a, the particle size of the liposome 1 $(636\pm67\,\text{nm})$ was smaller than that of liposome 2 $(997\pm120\,\text{nm})$. The particle sizes of these liposomes consisting of DOPE were smaller than those without DOPE. However, the mixture of lipids 1, 2

and DOPE formed larger liposome (1428±46 nm) than that of the mixture of lipids 1 and 2 alone (810±46 nm). The particle size of the formed lipoplexes with the cationic liposomes/DNA weight ratio varied from 2 to 40 was studied. It was found that most of the liposomes could bind and compact DNA into particles of cationic liposomes/DNA at the weight ratio of 5. The mean diameters of 1/DNA, 1-DOPE/DNA, 2-DOPE/DNA and 1,2/DNA lipoplexes were 500-600 nm, whereas the diameters of 2/DNA and 1.2-DOPE/DNA lipoplexes were 800-1000 nm. The zeta potential, which is a measure of the electrical field of cationic liposomes in an aqueous environment, is one of the important factors that controls their DNA binding ability. High zeta potential is preferred for higher DNA binding ability. From Fig. 3b, it was found that the liposomes of the lipids 1 and 2 have a zeta potential of 53.7 ± 1.7 and 47.5 ± 1.4 mV, respectively. The inclusion of DOPE as the helper lipid in the lipids 1 and 2 leads to an decrease in the zeta potential which is observed to be 39.2 ± 0.8 and 43.3 ± 0.8 mV, respectively. The zeta potential of the liposomes prepared by the mixture of lipids 1 and 2 was 47.1±1.6 mV. Addition of DOPE in the mixture of the lipids 1 and 2, the zeta potential (42.9±1.1 mV) was not much decreased. As shown in Fig. 3b, the zeta potential was slightly decreased along with the increase in cationic liposome/DNA weight ratio. Most of the cell membranes usually show negative charge, so it is expected that the high positively charged liposomes formulated by the mixture lipids 1 and 2 alone or with the combination of DOPE will significantly enhance the interaction between liposomes and cells and facilitate cellular uptake.

Transfection Activity Most of the cationic lipid carriers studied so far are liposomes composed of cationic lipid alone or a mixture of cationic lipid and a helper lipid, which was usually DOPE.²⁹⁾ DOPC³⁰⁾ or cholesterol.³¹⁾ The alternative approach can be the use of combination of cationic lipids having the same headgroup but with tails of different chain lengths¹⁵ or cationic lipids with different polarhead and hydrophobic tails. 16) To study the synergistic effect of cationic lipids with different polarheads, central core structures and hydrophobic tails, the lipids 1 and 2 were mixed at various weight ratios and tested for DNA delivery to human embryonic kidney cells (HEK293) using β -galactosidase as a reporter gene. The liposomes prepared from the lipids 1 and 2 were also evaluated for transfection efficiency. The transfection activity was reported as number of transfected cells per cm². Figure 4 displays data generated from an assay employing plasmid DNA (0.1 µg/well) at liposomes/DNA weight ratio of 20 under serum-free condition. Liposomes comprises of the lipid 1 and 2 alone exhibited low transfection efficiency than the Lipofectamine™ 2000. As shown in Fig. 4, the weight ratio of 1 to 2 is important for higher transfection efficiency; the optimal ratio was 1:1. Combining the lipid 1 with 2 at weight ratio of

September 2014 1539



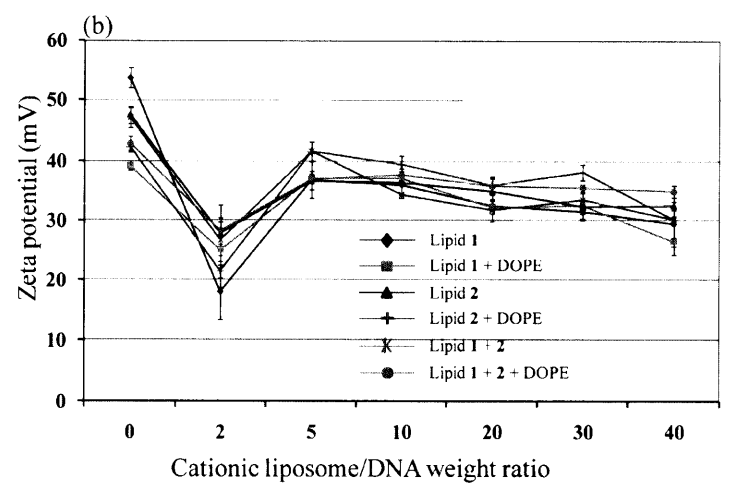


Fig. 3. (a) Particle Size and (b) Zeta Potential at Varying Weight Ratios of Liposomes/DNA Complexes

(♦) liposomes-lipid 1. (■) liposomes-lipid 1+DOPE (1:1), (♠) liposomes-lipid 2, (+) liposomes-lipid 2+DOPE (1:1), (*) liposomes-lipids 1+2 (1:1), and (●) liposomes-lipids 1+2+DOPE (0.5:0.5:1). Each value represents the mean±S.D. of three measurements.

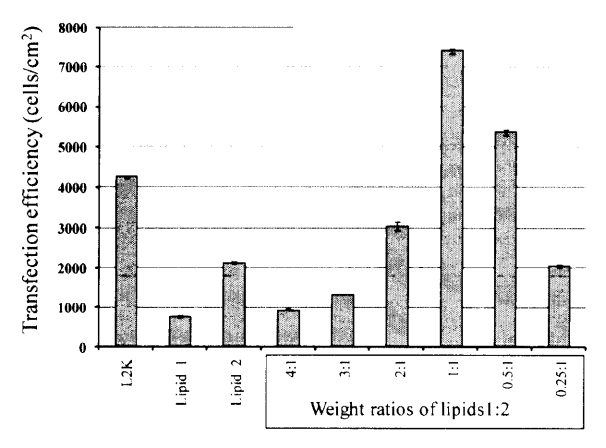


Fig. 4. In Vitro Transfection Efficiency of Liposomes/DNA Complexes with Weight Ratio of 20 in HEK293 Cells

The transfection efficiencies (cells/cm²) of the liposomes were compared to that of the commercially available reagent, the Lipofectamine™ 2000 (L2K). Each value represents the mean±S.D. of triplicate experiments.

1:1 enhances about 10 and 3.5-fold the extent of transfection of HEK293 cells, compared with liposomes prepared from each of lipids 1 and 2, respectively. At this ratio, the transfection efficiency was about 2-fold higher than that of the com-

mercially available transfection agent, Lipofectamine™ 2000. When the ratio of the lipids 1 to 2 decreases the transfection efficiency was also decreased. It has been shown that the synergistic effect of cationic liposomes on treansfection efficiency depended on the lipid composition. The minor change in cationic lipid component significantly effected on the transfection efficiency.¹⁷⁾ Thus, our finding confirmed this observation. It has also been revealed that liposomes compose of very different lipid headgroups and/or aliphatic tails has been shown to produce asymmetric liposomes. 18) This was expected to increase the biocompatibility and flexibility of liposomes as delivery system. The liposomes comprised of lipids 1 and 2 which have different polarheads, central core structures and hydrophobic tails may be constructed asymmetric liposomes, in particular at weight ratio of 1:1, and resulted in highly transfection efficiency. On the basis of the results (Fig. 4), the mixture of lipids 1 and 2 at weight ratio of 1:1 was chosen to further optimize transfection.

The helper lipid, DOPE, has been known to increase the transfection efficiency of cationic liposomes to transfer and release DNA into the cytoplasm.³²⁾ To evaluate the effect of DOPE on gene delivery of the mixture of cationic lipids 1 and 2, this mixture lipids (1/2 at weight ratio of 1:1) was mixed with different amounts of DOPE to form cationic liposomes.

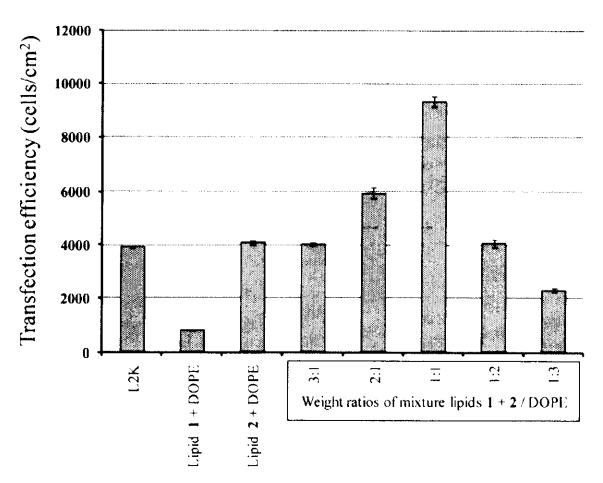


Fig. 5. In Vitro Transfection Efficiency of Liposomes/DNA Complexes with Weight Ratio of 20 in HEK293 Cells

The liposomes were formulated at various weight ratios of mixture lipids 1+2 and DOPE. The transfection efficiencies (cells/cm²) of the liposomes were compared to that of the commercially available reagent, the Lipofectamine™ 2000 (L2K). Each value represents the mean±S.D. of triplicate experiments.

In order to find out the most effective formulation, transfection with identical liposomes/DNA weight ratio of 20 was used. Their ability to deliver a plasmid encoding β -galactosidase into HEK293 cells was studied (Fig. 5). A synergistic effect on the transfection efficiency was clearly demonstrated by the combined use of mixture of lipids 1 and 2 with the helper lipid, DOPE. The highest transfection efficiency was achieved by using the combination of mixture of lipids 1 and 2/DOPE at the weight ratio of 1:1. This formulation dramatically increased the transfection efficiency for 11.5- and 2.3-fold, which was higher than those of liposomes comprised of lipid 1-DOPE and lipid 2-DOPE formulations, respectively. This optimal formulation exhibited 2.5-fold higher transfection efficiency than that of Lipofectamine™ 2000. Thus, the liposomes composed of mixture lipids/DOPE at weight ratio of 1:1 was chosen for further study.

The transfection efficiency of the cationic liposome also depends on the cationic lipisomes/DNA ratio as previously reported by our group^{19,33,34)} and others.^{35–37)} To find out the optimal liposomes/DNA ratio, transfection experiments were performed against HEK293 cells by using mixture lipids/DOPE ratio of 1:1. As shown in Fig. 6, the liposomes formulations with mixture lipids/DOPE at 1:1 weight ratio showed maximum transfection efficiency at liposomes/DNA weight ratio of 5 and transfection profiles followed a bell-shaped graph. At this optimal liposomes/DNA weight ratio, liposome comprised of mixture lipids having different polarheads, central core structures and hydrophobic tails showed nearly 3-fold higher transfection efficiency than Lipofectamine[™] 2000.

One of the major drawbacks of cationic liposomes for their *in vivo* use is the inhibition of the transfection efficiency in the presence of serum. Most of cationic liposomes including many commercially available transfection reagents which exhibited high transfection activity in the absence of serum lost their efficiency when transfected in the presence of serum. ^{34,38)} In order to investigate the effect of serum on gene transfection efficiencies of mixture lipids, transfection experiments with our optimized lipid formulations were therefore performed in the presence of 10, 20, 30 and 40% serum. The results are

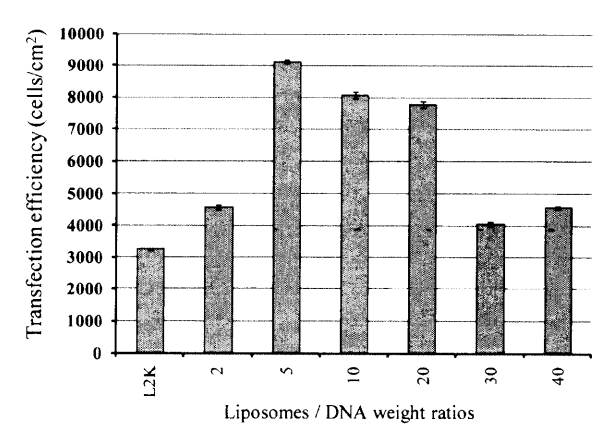


Fig. 6. In Vitro Transfection Efficiency of Liposomes/DNA Complexes across the Cationic Liposome/DNA Weight Ratios of 2 to 40 in HEK293 Cells

Transfection efficiency (cells/cm²) of the mixture lipids was compared to that of the commercial reagent, Lipofectamine™ 2000 (L2K). Each value represents the mean±S.D. of triplicate experiments.

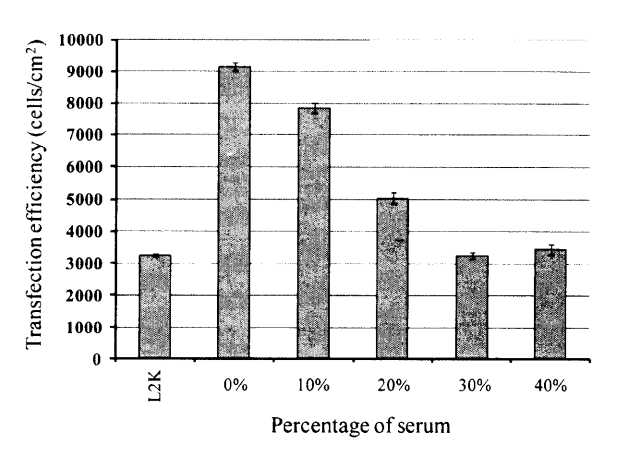


Fig. 7. Transfection Efficiency of Mixture Lipids Using Optimized Mixture Lipids/DOPE Ratio of 1:1 and Liposome/DNA Ratio of 5 in HEK293 Cells at Various Amount of Serum

Transfection efficiency (cells/cm²) of the mixture lipids was compared to that of the commercial reagent, Lipofectamine™ 2000 (L2K). Each value represents the mean±S.D. of triplicate experiments.

shown in Fig. 7. The transfection efficiency of mixture lipids gradually decreased when the amount of serum increase. Interestingly, the transfection efficiency of mixture lipids at high serum condition (30−40%) showed comparable transfection efficiency to Lipofectamine[™] 2000. It has been reported that size of the lipoplexes may be one of the factors contributing the serum resistance.^{39,40)} Large lipoplexes (>700 nm) showed transfection efficiency in the presence or absence of serum, but small lipoplexes (<250 nm) exhibited transfection efficiency only in the absence of serum.³⁹⁾ Thus, high transfection efficiency of optimized lipoplexes formulation, total lipids/DNA ratio of 5, under high serum condition may be due to the large size of our lipoplexes aggregates (1428±46 nm, Fig. 3a).

It is known that transfection agents have the ability to specifically deliver DNA into different cell types. ^{19,33,34)} To evaluate the transfection efficiency of these mixture lipids toward the different cell lines, human breast adenocarcinoma (MCF-7) and cervical epithelial adenocarcinoma (HeLa) cells, the experiments were performed by using optimum condition under serum-free conditions. The transfection efficiency of mixture lip-

September 2014

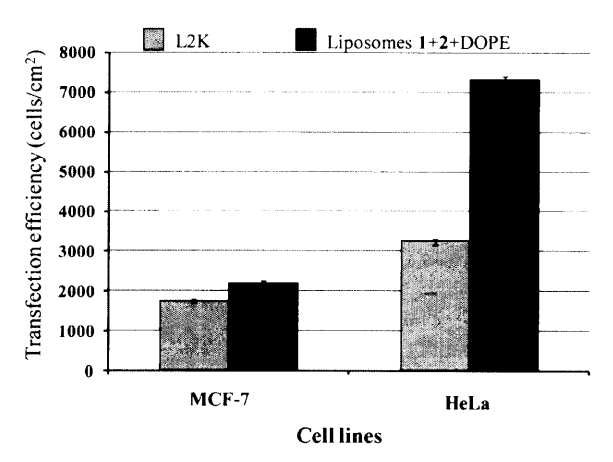


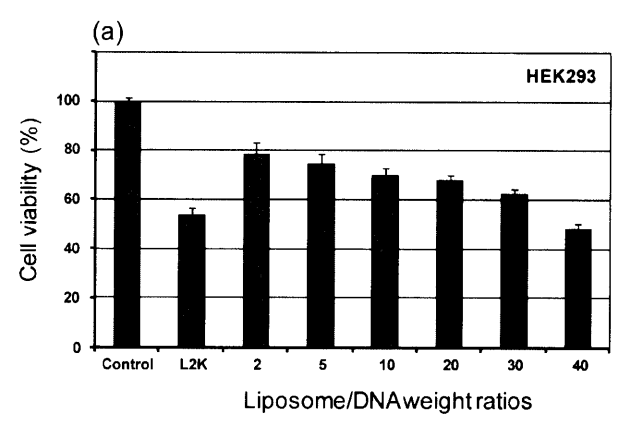
Fig. 8. In Vitro Transfection Efficiency of Liposomes Comprised of Mixture Lipids 1 and 2/DOPE (1:1 Weight Ratio) in MCF-7 and HeLa Cells Using Optimum Conditions

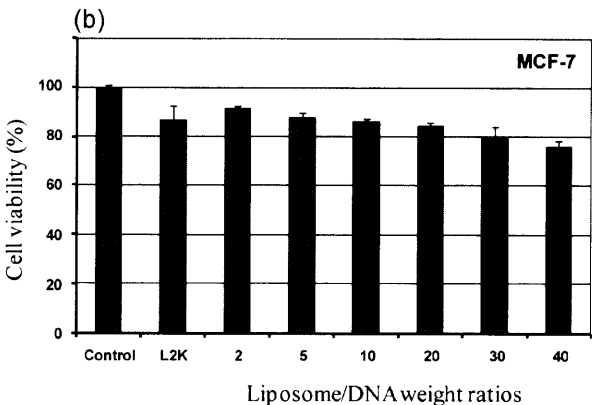
Transfection efficiency (cells/cm²) of the mixture lipids was compared to that of the commercial reagent, Lipofectamine™ 2000 (L2K). Each value represents the mean±S.D. of triplicate experiments.

ids was compared with the commercially available transfection agent, Lipofectamine[™] 2000, which was calculated as 100%. The results are illustrated in Fig. 8. The optimal liposome and lipoplexes formulations of mixture lipids that work well in HEK293 cells can be applied to MCF-7 and HeLa cells. The liposome comprised of mixture lipids 1 and 2/DOPE at 1:1 weight ratio exhibited 2-fold higher transfection efficiency to deliver DNA into HeLa cells than that of the Lipofectamine[™] 2000. However, the ability of these lipids and Lipofectamine[™] 2000 to transfer DNA into MCF-7 cells was comparable.

Transfection Toxicity Two mostly concerned criteria for gene delivery carriers are transfection efficiency and their cytotoxicity. To assess the relationship between cytotoxicity and gene expression efficiency, the toxicity of the liposomes/ DNA complexes at weight ratios of 2 to 40 was determined by measuring changes in cell metabolic activity (MTT assay) and was shown as % cell viability as compared to the control cells in the presence of DNA. The results are shown in Fig. 9. It was found that the optimal lipoplexes formulation (liposomes/ DNA weight ratio of 5) of the mixture lipids showed low toxicity (cell viability more than 80%) in MCF-7 and HeLa cells. The cell viability of these lipids against HEK293 cell was slightly lower than 80%. This result was in contrast to the high transfection efficiency of these lipids. The cell viability of Lipofectamine2000™ against MCF-7 and HeLa cell was higher and slightly lower than 80%, respectively. However, the cytotoxicity of the Lipofectamine™ 2000 was relatively high for HEK293 cell line and the cell viability was approximately 60%. Thus, a slight reduction in metabolic activity of these mixture lipids should not prevent it from further in vivo study as tranfection agent.

In conclusion we have demonstrated that the combination of lipids with different polarheads, central core structures and hydrophobic tails in the presence of helper lipid, DOPE, has allowed the discovery of highly efficient transfection agents with minimal cytotoxicity. These mixture lipids showed high efficiency to deliver DNA into HEK293, MCF-7 and HeLa cells than that of a commercially available transfection agent. We hope that the strategy illustrated here is useful for the development of cationic lipid-based gene delivery. Employing





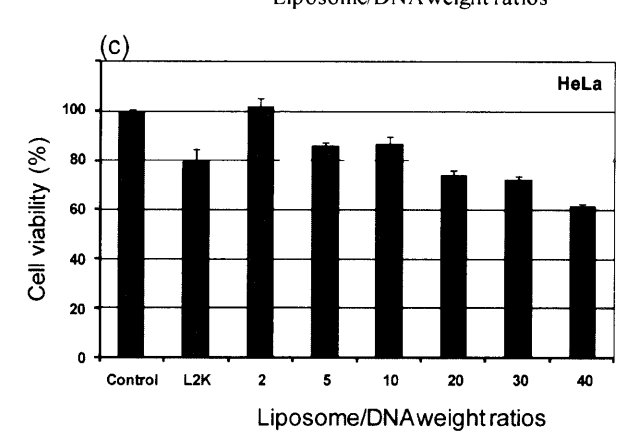


Fig. 9. Cell Viability of (a) HEK293, (b) MCF-7 and (c) HeLa Cells in the Presence of Lipoplexes Formulated at Various Liposome/DNA Weight Ratios of 2 to 40 Using the Constant Amount of DNA at $0.1\,\mu g$ per Well

The commercially available agent, Lipofectamine™ 2000 (L2K) was also tested for comparison. Cell metabolic activity was determined by an MTT assay. Each value represents the mean±S.D. of triplicate experiments.

the synergistic effect of these lipids may be a promising approach for successful non-viral gene transfection.

Acknowledgments This work was supported by Office of the Higher Education Commission (OHEC), Ministry of Education and The Thailand Research Fund (TRF) (RMU5480003). NN acknowledges the Royal Golden Jubilee Ph.D. program of TRF for studentship (Grant No. PHD/0217/2552). Supports from TRF (DBG5680006) and the Center of Excellence for Innovation in Chemistry (PERCH-CIC), OHEC, Ministry of Education are gratefully acknowledged.

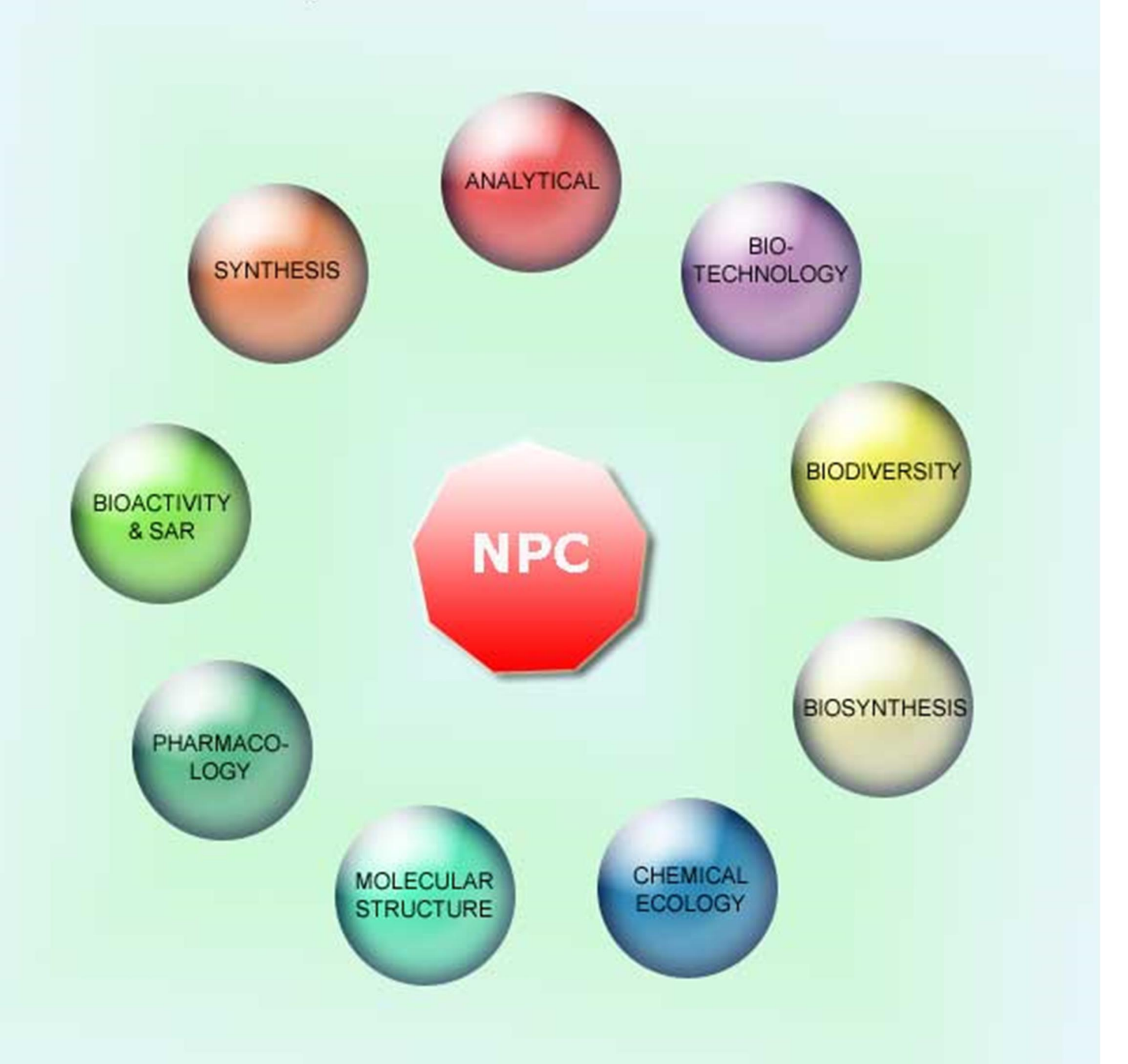
REFERENCES

- Cavazzana-Calvo M, Hacein-Bey S, de Saint Basile G, Gross F, Yvon E, Nusbaum P, Selz F, Hue C, Certain S, Casanova JL, Bousso P, Deist FL, Fischer A. Gene therapy of human severe combined immunodeficiency (SCID)-X1 disease. *Science*, 288, 669-672 (2000).
- Kaplitt MG, Feigin A, Tang C, Fitzsimons HL, Mattis P, Lawlor PA, Bland RJ, Young D, Strybing K, Eidelberg D, During MJ. Safety and tolerability of gene therapy with an adeno-associated virus (AAV) borne GAD gene for Parkinson's disease: an open label, phase I trial. *Lancet*, 369, 2097–2105 (2007).
- Yang ZR, Wang HF, Zhao J, Peng YY, Wang J, Guinn BA, Huang LQ. Recent developments in the use of adenoviruses and immunotoxins in cancer gene therapy. *Cancer Gene Ther.*, 14, 599–615 (2007).
- Niven R, Pearlman R, Wedeking T, Mackeigan J, Noker P, Simpson-Herren L, Smith JG. Biodistribution of radiolabeled lipid-DNA complexes and DNA in mice. J. Pharm. Sci., 87, 1292-1299 (1998).
- Dunbar CE. Gene transfer to hematopoietic stem cells, implications for gene therapy of human disease. Annu. Rev. Med., 47, 11–20 (1996).
- Anderson WF, Canning EU, Okamura B. Human gene therapy. Nature, 392 (Suppl.), 25–30 (1998).
- Lundstrom K. Latest development in viral vectors for gene therapy. Trends Biotechnol., 21, 117–122 (2003).
- Edelstein ML, Abedi MR, Wixon J. Gene therapy clinical trials worldwide to 2007—an update. J. Gene Med., 9, 833–842 (2007).
- Mintzer MA, Simanek EE. Nonviral vectors for gene delivery. Chem. Rev., 109, 259–302 (2009).
- Xu D, Hong J, Sheng K, Dong L, Yao S. Preparation of polyethyleneimine nanogels via photo-Fenton reaction. Radiat. Phys. Chem., 76, 1606–1611 (2007).
- Xu DM, Yao SD, Liu YB, Sheng KL, Hong J, Gong PJ, Dong L. Size-dependent properties of M-PEIs nanogels for gene delivery in cancer cells. *Int. J. Pharm.*, 338, 291–296 (2007).
- Kopatz I, Remy JS, Behr JP. A model for non-viral gene delivery: through syndecan adhesion molecules and powered by actin. J. Gene Med., 6, 769-776 (2004).
- 13) Mounkes LC, Zhong W, Cipres-Palacin G, Heath TD, Debs RJ. Proteoglycans mediate cationic liposome-DNA complex-based gene delivery in vitro and in vivo. J. Biol. Chem., 273, 26164-26170 (1998).
- 14) Felgner PL, Gadek TR, Holm M, Roman R, Chan HW, Wenz M, Northrop JP, Ringold GM, Danielsen M. Lipofection: a highly efficient, lipid-mediated DNA-transfection procedure. *Proc. Natl. Acad.* Sci. U.S.A., 84, 7413-7417 (1987).
- Wang L, MacDonald RC. New strategy for transfection: mixtures of medium-chain and long-chain cationic lipids synergistically enhance transfection. *Gene Ther.*, 11, 1358–1362 (2004).
- 16) Wang L, MacDonald RC. Synergistic effect between components of mixtures of cationic amphipaths in transfection of primary endothelial cells. *Mol. Pharm.*, 4, 615–623 (2007).
- Caracciolo G, Pozzi D, Caminiti R, Marchini C, Montani M, Amici A, Amenitsch H. Transfection efficiency boost by designer multicomponent lipoplexes. *Biochim. Biophys. Acta*, 1768, 2280–2292 (2007).
- Pautot S, Frisken BJ, Weitz DA. Engineering asymmetric vesicles. Proc. Natl. Acad. Sci. U.S.A., 100, 10718–10721 (2003).
- Yingyongnarongkul B, Radchatawedchakoon W, Krajarng A, Watanapokasin R, Suksamrarn A. High transfection efficiency and low toxicity cationic lipids with aminoglycerol-diamine conjugate. *Bioorg. Med. Chem.*, 17, 176–188 (2009).
- 20) Paecharoenchai O, Niyomtham N, Ngawhirunpat T, Rojanarata T, Yingyongnarongkul B, Opanasopit P. Cationic niosomes composed of spermine-based cationic lipids mediate high gene transfection efficiency. J. Drug Target., 20, 783-792 (2012).
- 21) Paecharoenchai O, Niyomtham N, Apirakaramwong A, Ngawhirunpat T, Rojanarata T, Yingyongnarongkul B, Opanasopit P. Structure relationship of cationic lipids on gene transfection mediated by cationic liposomes. AAPS PharmSciTech, 13, 1302–1308 (2012).

- 22) Eisenführ A, Arora PS, Sengle G, Takaoka LR, Nowick JS, Famulok M. A ribozyme with michaelase activity: Synthesis of the substrate precursors. *Bioorg. Med. Chem.*, 11, 235–249 (2003).
- Gershon H, Ghirlando R, Guttman SB, Minsky A. Mode of formation and structural features of DNA-cationic liposome complexes used for transfection. *Biochemistry*, 32, 7143-7151 (1993).
- Xu Y, Szoka FC Jr. Mechanism of DNA release from cationic liposome/DNA complexes used in cell transfection. *Biochemistry*, 35, 5616–5623 (1996).
- Unciti-Broceta A, Diezmann F, Ou-Yang CY, Fara MA, Bradley M. Synthesis, penetrability and intracellular targeting of fluoresceintagged peptoids and peptide-peptoid hybrids. *Bioorg. Med. Chem.*, 17, 959–966 (2009).
- Oliver M, Jorgensen MR, Miller A. The facial solid-phase synthesis of cholesterol-based polyamine lipids. *Tetrahedron Lett.*, 45, 3105–3107 (2004).
- 27) Yingyongnarongkul B, Apiratikul N, Aroonrerk N, Suksamrarn A. Solid phase synthesis and antibacterial activity of hydroxycinnamic acid amides and analogues against methicillin-resistant Staphylococcus aureus and vancomycin-resistant S. aureus. Bioorg. Med. Chem. Lett., 16, 5870–5873 (2006).
- 28) Nash IA, Bycroft BW, Chan WC. Dde—a selective primary amine protecting group: A facile solid phase synthetic approach to polyamine conjugates. *Tetrahedron Lett.*, 37, 2625–2628 (1996).
- Farhood H, Serbina N, Huang L. The role of dioleoyl phosphatidylethanolamine in cationic liposome-mediated gene-transfer. *Biochim. Biophys. Acta*, 1235, 289–295 (1995).
- Caracciolo G, Pozzi D, Caminiti R, Marchini C, Montani M, Amici A, Amenitsch H. Transfection efficiency boost by designer multicomponent lipoplexes. *Biochim. Biophys. Acta*, 1768, 2280–2292 (2007).
- 31) Li S, Tseng WC, Stolz DB, Wu SP, Watkins SC, Huang L. Dynamic changes in the characteristics of cationic lipidic vectors after exposure to mouse serum: implications for intravenous lipofection. *Gene Ther.*, 6, 585–594 (1999).
- 32) Hui SW, Langner M, Zhao Y-L, Ross P, Hurley E, Chan K. The role of helper lipids in cationic liposome-mediated gene transfer. *Biophys. J.*, 71, 590-599 (1996).
- 33) Radchatawedchakoon W, Watanapokasin R, Krajarng A, Yingyongnarongkul B. Solid phase synthesis of novel asymmetric hydrophilic head cholesterol-based cationic lipids with potential DNA delivery. Bioorg. Med. Chem., 18, 330-342 (2010).
- 34) Radchatawedchakoon W, Krajarng A, Niyomtham N, Watanapokasin R, Yingyongnarongkul B. Transfection efficiency of cationic lipids with asymmetric acyl-cholesteryl hydrophobic tails. Chem. Eur. J., 17, 3287-3295 (2011).
- 35) Bajaj A, Kondaiah P, Bhattacharya S. Effect of the nature of the spacer on gene transfer efficacies of novel thiocholesterol derived gemini lipids in different cell lines: A structure-activity investigation. J. Med. Chem., 51, 2533-2540 (2008).
- 36) Kim B-K, Bae Y-U, Doh K-O, Hwang G-B, Lee S-H, Kang H, Seu Y-B. The synthesis of cholesterol-based cationic lipids with trimethylamine head and the effect of spacer structures on transfection efficiency. *Bioorg. Med. Chem. Lett.*, 21, 3734–3737 (2011).
- 37) Goldring WPD, Jubeli E, Downs RA, Johnston AJS, Abdul Khalique N, Raju L, Wafadari D, Pungente MD. Novel macrocyclic and acyclic cationic lipids for gene transfer: Synthesis and in vitro evaluation. Bioorg. Med. Chem. Lett., 22, 4686–4692 (2012).
- Ghosh YK, Visweswariah SS, Bhattacharya S. Nature of linkage between the cationic headgroup and cholesteryl skeleton controls gene transfection efficiency. FEBS Lett., 473, 341–344 (2000).
- Turek J, Dubertret C, Jaslin G, Antonakis K, Scherman D, Pitard B. Formulations which increase the size of lipoplexes prevent serum-associated inhibition of transfection. J. Gene Med., 2, 32–40 (2000).
- Lian T, Ho RJY. Design and characterization of a novel lipid–DNA complex that resists serum-induced destabilization. *J. Pharm. Sci.*, 92, 2373–2385 (2003).

NATURAL PRODUCT COMMUNICATIONS

An International Journal for Communications and Reviews Covering all Aspects of Natural Products Research



10th Anniversary Issue

Volume 10. Issue 1. Pages 1-232. 2015 ISSN 1934-578X (printed); ISSN 1555-9475 (online) www.naturalproduct.us

NPC

Natural Product Communications

EDITOR-IN-CHIEF

DR. PAWAN K AGRAWAL

Natural Product Inc. 7963, Anderson Park Lane, Westerville, Ohio 43081, USA agrawal@naturalproduct.us

EDITORS

PROFESSOR ALEJANDRO F. BARRERO

Department of Organic Chemistry, University of Granada, Campus de Fuente Nueva, s/n, 18071, Granada, Spain afbarre@ugr.es

PROFESSOR ALESSANDRA BRACA

Dipartimento di Chimica Bioorganicae Biofarmacia, Universita di Pisa, via Bonanno 33, 56126 Pisa, Italy braca@farm.unipi.ti

PROFESSOR DE-AN GUO

State Key Laboratory of Natural and Biomimetic Drugs, School of Pharmaceutical Sciences, Peking University, Beijing 100083, China gda5958@163.com

PROFESSOR YOSHIHIRO MIMAKI

School of Pharmacy, Tokyo University of Pharmacy and Life Sciences, Horinouchi 1432-1, Hachioji, Tokyo 192-0392, Japan mimakiy@ps.toyaku.ac.jp

PROFESSOR STEPHEN G. PYNE

Department of Chemistry University of Wollongong Wollongong, New South Wales, 2522, Australia spyne@uow.edu.au

PROFESSOR MANFRED G. REINECKE

Department of Chemistry, Texas Christian University, Forts Worth, TX 76129, USA m.reinecke@tcu.edu

PROFESSOR WILLIAM N. SETZER

Department of Chemistry
The University of Alabama in Huntsville
Huntsville, AL 35809, USA
wsetzer@chemistry.uah.edu

PROFESSOR YASUHIRO TEZUKA

Faculty of Pharmaceutical Sciences Hokuriku University Ho-3 Kanagawa-machi, Kanazawa 920-1181, Japan y-tezuka@hokuriku-u.ac.jp

PROFESSOR DAVID E. THURSTON

Department of Pharmaceutical and Biological Chemistry, The School of Pharmacy, University of London, 29-39 Brunswick Square, London WCIN IAX, UK david.thurston@pharmacy.ac.uk

HONORARY EDITOR

PROFESSOR GERALD BLUNDEN

The School of Pharmacy & Biomedical Sciences, University of Portsmouth, Portsmouth, PO1 2DT U.K. axuf64@dsl.pipex.com

ADVISORY BOARD

Prof. Viqar Uddin Ahmad Karachi, Pakistan
Prof. Giovanni Appendino Novara, Italy
Prof. Yoshinori Asakawa Tokushima, Japan
Prof. Roberto G. S. Berlinck

Prof. Anna R. Bilia Florence, Italy Prof. Maurizio Bruno Palermo, Italy

São Carlos, Brazil

Prof. César A. N. Catalán Tucumán, Argentina Prof. Josep Coll Barcelona, Spain Prof. Geoffrey Cordell Chicago, IL, USA Prof. Fatih Demirci Eskişehir, Turkey

Prof. Ana Cristina Figueiredo Lisbon, Portugal

Lisbon, I ortugu

Prof. Cristina Gracia-Viguera Murcia, Spain Dr. Christopher Gray

Saint John, NB, Canada Prof. Dominique Guillaume Reims. France

Prof. Duvvuru Gunasekar

Tirupati, India

Prof. Hisahiro Hagiwara Niigata, Japan Prof. Tsukasa Iwashina Tsukuba, Japan Prof. Leopold Jirovetz Vienna, Austria Prof. Vladimir I Kalinin Vladivostok, Russia Prof. Phan Van Kiem

Hanoi, Vietnam

Prof. Niel A. Koorbanally Durban, South Africa Prof. Chiaki Kuroda Tokyo, Japan Prof. Hartmut Laatsch Gottingen, Germany

Prof. Marie Lacaille-Dubois

Dijon, France

Prof. Shoei-Sheng Lee

Prof. Shoei-Sheng Lee Taipei, Taiwan Prof. Imre Mathe Szeged, Hungary

Prof. M. Soledade C. Pedras Saskatoon, Canada Prof. Luc Pieters Antwerp, Belgium Prof. Peter Proksch Düsseldorf, Germany

Tahiti, French Polynesia Prof. Luca Rastrelli Fisciano, Italy Prof. Stefano Serra Milano, Italy

Prof. Phila Rahariyelomanana

Prof. Monique Simmonds *Richmond, UK*Dr. Bikram Singh

Palampur, India
Prof. John L. Sorensen
Manitoba, Canada
Prof. Johannes van Staden
Scottsville, South Africa
Prof. Valentin Stonik
Vladivostok, Russia
Prof. Winston F. Tinto
Barbados, West Indies
Prof. Sylvia Urban
Melbourne, Australia

Prof. Karen Valant-Vetschera

Vienna, Austria

INFORMATION FOR AUTHORS

Full details of how to submit a manuscript for publication in Natural Product Communications are given in Information for Authors on our Web site http://www.naturalproduct.us.

Authors may reproduce/republish portions of their published contribution without seeking permission from NPC, provided that any such republication is accompanied by an acknowledgment (original citation)-Reproduced by permission of Natural Product Communications. Any unauthorized reproduction, transmission or storage may result in either civil or criminal liability.

The publication of each of the articles contained herein is protected by copyright. Except as allowed under national "fair use" laws, copying is not permitted by any means or for any purpose, such as for distribution to any third party (whether by sale, loan, gift, or otherwise); as agent (express or implied) of any third party; for purposes of advertising or promotion; or to create collective or derivative works. Such permission requests, or other inquiries, should be addressed to the Natural Product Inc. (NPI). A photocopy license is available from the NPI for institutional subscribers that need to make multiple copies of single articles for internal study or research purposes.

To Subscribe: Natural Product Communications is a journal published monthly. 2015 subscription price: US\$2,595 (Print, ISSN# 1934-578X); US\$2,595 (Web edition, ISSN# 1555-9475); US\$2,995 (Print + single site online); US\$595 (Personal online). Orders should be addressed to Subscription Department, Natural Product Communications, Natural Product Inc., 7963 Anderson Park Lane, Westerville, Ohio 43081, USA. Subscriptions are renewed on an annual basis. Claims for nonreceipt of issues will be honored if made within three months of publication of the issue. All issues are dispatched by airmail throughout the world, excluding the USA and Canada.



Natural Product Communications

Diarylheptanoids of *Curcuma comosa* with Inhibitory Effects on Nitric Oxide Production in Macrophage RAW 264.7 Cells

Nilubon Sornkaew^a, Yuan Lin^b, Fei Wang^b, Guolin Zhang^b, Ratchanaporn Chokchaisiri^c, Ailian Zhang^d, Kanjana Wongkrajang^e, Parichat Suebsakwong^a, Pawinee Piyachaturawat^f and Apichart Suksamrarn^{a,*}

s apichart@ru.ac.th; asuksamrarn@yahoo.com

Received: September 21st, 2014; Accepted: November 9th, 2014

Eight new diarylheptanoids, a 1.2:1 mixture of (3S)- and (3R)-1-(4-hydroxyphenyl)-7-phenyl-(4E,6E)-4,6-heptadien-3-ol (1a and 1b), a racemic mixture of (3S)- and (3R)-1-(4-hydroxyphenyl)-3-methoxy-7-phenyl-(4E,6E)-4,6-heptadiene (2a and 2b), a ca. 1:1 mixture of (3S)- and (3R)-1-(4-hydroxy-3-methoxyphenyl)-3-methoxy-7-phenyl)-(4E,6E)-4,6-heptadiene (3a and 3b), 3-acetoxy-1-(3,4-dihydroxyphenyl)-7-phenylheptan-5-ol (4), (3R)-1-(4,5-dihydroxyphenyl)-7-phenyl-(6E)-6-hepten-3,2'-epoxide (5), and thirteen known diarylheptanoids, 6–12, a 3:1 mixture of 13a and 13b, and 14–17, were isolated from the rhizomes of *Curcuma comosa* from Sakon Nakhon, northeastern part of Thailand. The isolated compounds were evaluated for their anti-inflammatory activities on the inhibition of lipopolysaccharide-induced nitric oxide production in macrophage RAW 264.7 cells and the diarylheptanoids 1a and 1b mixture and 14 exhibited potent inhibitory activity.

Keywords: Curcuma comosa, Zingiberaceae, Diarylheptanoids, NO inhibitory activity.

Curcuma comosa Roxb. (Zingiberaceae) has been used in indigenous medicine of Thailand. The rhizome of this plant species has been used for the treatment of postpartum uterine bleeding and also as an aromatic stomachic. A number of diarylheptanoids with nematocidal [1], estrogenic activity [2], and a phloracetophenone glucoside with choleretic activity [3] have been isolated. The aerial parts of the plant contain labdane diterpenes [4], flavonoid glycosides and diarylheptanoids [5]. Unlike C. longa, this species exists with high biodiversity. Investigations on the chemotaxonomy of C. comosa collected from cultivation sites in different parts of Thailand revealed that their rhizome morphologies are highly variable. Chromosome numbers, together with inflorescent, floral and leaf morphology were used for identification and classification of this species into different cultivars. The study revealed that chromosome numbers can be used to verify accurately the taxonomic identification of C. comosa [6]. The amplified fragment length polymorphism (AFLP) marker was also used to identify and elucidate the phylogenetic relationships of this species [7].

We have recently investigated the constituents of the *C. comosa* rhizomes collected from Kampaengsaen district, Nakhon Pathom province, in the central part of Thailand [2]. Further phytochemical studies of this plant species collected from different regions of the country have been made. Preliminary investigation of the chemical constituents of the rhizomes collected from Sawangdaendin district, Sakon Nakhon province, northeastern part of Thailand revealed different diarylheptanoid contents from those previously reported, especially the minor components [2]. The present work describes the isolation and structural elucidation of eight new and thirteen known diarylheptanoids from the rhizomes of *C. comosa* from Sakon Nakhon province and their inhibitory activities on lipopolysaccharide (LPS)-induced nitric oxide (NO) production in macrophage RAW 264.7 cells.

The hexane and ethanol extracts of *C. comosa* rhizomes from Sakon Nakhon province were subjected to repeated column chromatography and eight new (1–5), together with thirteen known



Professor Apichart Suksamrarn received his B.Sc. with honors in Chemistry and M.Sc. in Organic Chemistry from Mahidol University, Thailand. He obtained his Ph.D. in Organic Chemistry from the University of Cambridge, U.K. He received his postdoctoral training at CSIRO, Division of Applied Organic Chemistry, Melbourne, Australia. His major recognitions include: Outstanding Scientist Award from the Foundation for the Promotion of Science and Technology under the Patronage of His Majesty the King, National Outstanding Researcher Award from the National Research Council of Thailand, and TRF Senior Research Scholar Award from The Thailand Research Fund. He is now working at the Department of Chemistry, Faculty of Science, Ramkhamhaeng University, Bangkok. His fields of research are bioactive natural products, structural modification of natural products, and natural product-based drug discovery. Professor Suksamrarn has published about 150 papers in peer-reviewed journals including 4 textbooks and 11 patent applications.

^aDepartment of Chemistry and Center for Innovation in Chemistry, Faculty of Science, Ramkhamhaeng University, Bangkok 10240, Thailand

^bChengdu Institute of Biology, Chinese Academy of Sciences, Chengdu 610041, China

^cDepartment of Chemistry, School of Science, University of Phayao, Muang, Phayao 56000, Thailand

^dSchool of Forestry and Biotechnology, Zhejiang A & F University, Hangzhou 311300, China

^eDepartment of Chemistry, Faculty of Science and Technology, Pibulsongkram Rajabhat University, Phitsanulok 65000, Thailand

^fDepartment of Physiology, Faculty of Science, Mahidol University, Bangkok 10400, Thailand

2" 7 5
$$\frac{R^1}{3}$$
 $\frac{R^2}{6}$ $\frac{R^3}{6}$ $\frac{R^2}{6}$ $\frac{R^3}{6}$ $\frac{R^3}{6}$ $\frac{R^2}{6}$ $\frac{R^3}{6}$ $\frac{R^3}{6}$ $\frac{R^2}{6}$ $\frac{R^3}{6}$ $\frac{R^3}{6}$

Figure 1: Structures of new compounds 1-5 and known compounds 6-17.

diarylheptanoids were isolated (Figure 1). These were 1,7-diphenyl-(6E)-6-hepten-3-one (6), (5R)-1,7-diphenyl-5-hydroxy-(6E)-6hepten-3-one (7) [1,8], 1,7-diphenyl-(4E,6E)-4,6-heptadien-3-one (8) [2], (3R)-1,7-diphenyl-(4E,6E)-4,6-heptadien-3-ol (9), 1-(4hydroxyphenyl)-7-phenyl-(6E)-6-hepten-3-one 1-(4-(10),hydroxyphenyl)-7-phenyl-(4E,6E)-4,6-heptadien-3-one (11) [2], (3S,5S)-1,7-diphenylheptan-3,5-diol (12) [9], a 3:1 mixture of (3S)and (3R)-1-(4-hydroxyphenyl)-7-phenyl-(6E)-6-hepten-3-ol (13a and 13b), (3S)-1-(3,4-dihydroxyphenyl)-7-phenyl-(6E)-6-hepten-3-ol (14) [2], 1-(3-methoxy-4-hydroxyphenyl)-7-phenylheptan-3,5-diol (15) [10], 1-(4-hydroxyphenyl)-7-phenylheptan-3,5-diol [10,11], and 1,7-bis-(4-hydroxyphenyl)-(4*E*,6*E*)-4,6-heptadien-3one (17) [12]. The configurations of 7 and 9 were determined to be R by the modified Mosher's method (data not shown) [2]. The absolute configurations of compounds 13 and 14 were determined to be a 3:1 mixture of 3S and 3R (13a and 13b) and 3S, respectively (data not shown). It is noteworthy that the absolute stereochemistry and enantiomeric ratio of compounds 9, 13 and 14 is the same as those isolated from Nakhon Pathom province.

Compound 1 was obtained as a white solid, mp 110-112°C. The HR-TOFMS (ES⁻) showed the $[M-H]^-$ peak at m/z 279.1835, compatible with the molecular formula $C_{19}H_{20}O_2$. The IR absorption band at 3233 cm⁻¹ revealed the presence of a hydroxyl group. The presence of $\alpha, \beta, \gamma, \delta$ -unsaturated system was evident from the ¹H NMR signals (Table 1) at $\delta_{\rm H}$ 5.83 (dd, J = 15.1, 6.8 Hz, 1H, H-4), $\delta_{\rm H}$ 6.37 (dd, J = 15.1, 10.6 Hz, 1H, H-5), 6.54 (d, J = 15.6 Hz, 1H, H-7), and 6.76 (partially overlapping signal, 1H, H-6), which corresponded with the 13 C NMR signals at $\delta_{\rm C}$ 136.1, 131.0, 132.6 and 128.1, respectively (Table 1). The COSY spectrum correlations between H-1 (δ_H 2.65, m, 2H) and H-2 (δ_H 1.87, m, 2H), H-2 and H-3 ($\delta_{\rm H}$ 4.21, m, 1H), and H-3 and H-4 determined the presence of a hydroxyl at C-3. The attachment of the phenyl group to the 7-position of the heptyl chain was confirmed from the HMBC correlations between H-6 and C-1" (δ_C 137.0), H-7 and C-2"/C-6" $(\delta_{\rm C}\ 126.3)$, and H-2"/H-6" $(\delta_{\rm H}\ 7.38,\ {\rm br}\ {\rm d},\ J=7.5\ {\rm Hz},\ 2{\rm H})$ and C-7 $(\delta_C 132.6)$, whereas that of the 4-hydroxyphenyl moiety to the 1-position was confirmed by the HMBC correlations between H-1 and C-2 (δ_C 38.8), C-3 (δ_C 72.0), C-1' (δ_C 133.7), C-2'/6' (δ_C 129.4), and H-2'/H-6' ($\delta_{\rm H}$ 7.05, d, J = 8.2 Hz, 2H) and C-1 ($\delta_{\rm C}$ 30.7) (Table 1). The low optical rotation, $[\alpha]_D^{29}$ –3.8, c 1.37 (EtOH), suggested that this compound existed as a mixture of two enantiomers, since it has

Figure 2: $\Delta \delta = (\Delta \delta_S - \Delta \delta_R)$ values obtained from the MTPA esters of compounds **1a** and **1b** mixture in CDCl₃.

been observed that diarylheptanoids with a 4,6-dien-3-ol system exhibited high optical rotation [2]. The absolute stereochemistry at C-3 and the enantiomeric ratio were determined by the modified Mosher's method [2]. Thus, upon treatment with (R)-(-)-MTPA chloride and (S)-(+)-MTPA chloride, the **1a** and **1b** mixture was transformed to a mixture of the corresponding (S)-MTPA esters **1ax** and **1bx**, and (R)-MTPA esters **1ay** and **1by**, respectively (Figure 2). Analysis of the 1 H NMR spectra of the two Mosher ester mixtures established the absolute configuration at C-3 of the diarylheptanoid mixture as S and R in a ratio of 1.2:1. The diarylheptanoid **1** was thus concluded as a 1.2:1 mixture of (3S)- and (3R)-1-(4-hydroxyphenyl)-7-phenyl-(4E,6E)-4,6-heptadien-3-ol (1a and (1b).

Compound **2** was obtained as a colorless sticky solid. The HR-TOFMS (ES⁻) showed the [M–H]⁻ peak at m/z 293.1541, consistent with the molecular formula $C_{20}H_{22}O_2$. The IR spectrum showed an absorption band for a hydroxyl group at 3321 cm⁻¹. The ¹H NMR data (Table 1) of **2** were similar to those of **1** except that **2** showed the presence of a methoxyl signal at δ_H 3.29 (3H, s) and δ_C 56.1, which could be placed at C-3 (δ_C 81.2) from the HMBC correlations between OCH₃-3/C-3, and between H-3/C-1 (δ_C 30.5), C-2 (δ_C 37.3), OCH₃, and C-5 (δ_C 132.9). Compound **2** exhibited low optical rotation, $[\alpha]_{29}^{29}$ –0.3 (c 0.68 EtOH), suggesting that this compound should exist as a racemic mixture. Compound **2a** and **2b** was thus assumed to exist as a racemic mixture of (3S)- and (3R)-1-(4-hydroxyphenyl)-3-methoxy-7-phenyl-(4E,6E)-4,6-heptadiene.

Compound 3 was isolated as a colorless sticky solid. The molecular formula was determined as C₂₁H₂₄O₃ by HR-TOFMS (ES⁻) at m/z 323.1698 [M-H]. The IR spectrum showed an absorption band for a hydroxyl group at 3308 cm⁻¹. The ¹H and ¹³C NMR spectra of 3 (Table 1) were found to be similar to those of 2, with an additional signal for a methoxyl group at C-3' ($\delta_{\rm C}$ 143.6). The aromatic proton signals at $\delta_{\rm H}$ 6.67 (s, 1H, H-2'), 6.81 (d, J = 7.6 Hz, 1H, H-5') and 6.66 (d, J = 7.6 Hz, 1H, H-6') revealed a 1,3,4-trisubstituted aromatic ring. The location of a methoxyl group at C-3' and a hydroxyl group at C-4' were confirmed by the HMBC correlations between H-2'/C-3', C-4' (δ_C 146.3), and C-6' (δ_C 121.0), H-5'/C-1' (δ_C 133.8), C-3', C-4', and C-6', H-6'/C-2' (δ_C 111.0), C-3', and C-4'. Diaryheptanoid 3 exhibited low optical rotation ($[\alpha]_D^{25}$ +2.2, c 1.52, EtOH) indicating that this compound should exist as a ca. 1:1 mixture of (3S)- and (3R)-1-(4-hydroxy-3-methoxyphenyl)-3-methoxy-7-phenyl-(4E,6E)-4,6-heptadiene (**3a** and **3b**).

Compound **4** was isolated as a colorless sticky solid. The HRTOFMS (ES⁻) at m/z 357.1716 [M–H]⁻ established the molecular formula as $C_{21}H_{26}O_5$. The IR spectrum showed an absorption band for hydroxyl and acetoxyl groups at 3370 and 1705 cm⁻¹, respectively. The ¹H NMR assignments (Table 1) for the proton signals at δ_H 6.63 (br s, 1H, H-2'), 6.74 (d, J=8.0 Hz, 1H, H-5') and 6.54 (br d, J=8.0 Hz, 1H, H-6') revealed a 1,3,4-trisubstitued benzene ring system. The ¹³C NMR data (Table 1) displayed 21 signals including two carbinolic (δ_C 66.8, and 71.4), five methylene (δ_C 31.1, 32.0, 36.4, 38.4, and 42.6), one acetoxy (δ_C 21.0 and 173.0), and twelve aromatic ring carbons, suggesting an acetylated

Table 1: ¹H and ¹³C NMR data of compounds 1-5 (CDCl₃).^a

Position	1		2		3	3		4		5	
	δ_{H}	δ_{C}	δ_{H}	$\delta_{\rm C}$	δ_{H}	δ_{C}	$\delta_{\rm H}$	$\delta_{\rm C}$	δ_{H}	δ_{C}	
1	2.65 (m)	30.7	2.61 (m)	30.5	2.62 (m)	31.2	2.49 (m)	31.1	2.62, 2.69 (m)	24.0	
2	1.87 (m)	38.8	1.77, 1.94 (m)	37.3	1.77, 1.91 (m)	37.5	1.75, 1.66 (m)	36.4	1.70, 1.92 (m)	27.5	
3	4.21 (m)	72.0	3.60 (m)	81.2	3.59 (m)	81.2	5.05 (m)	71.4	3.94 (br s)	74.9	
4	5.83 (dd, 15.1, 6.8)	136.1	5.65 (dd, 15.0, 8.0)	134.1	5.65 (dd, 15.2, 8.0)	134.2	1.60 (m)	42.6	1.72, 1.87 (m)	34.8	
5	6.37 (dd, 15.1, 10.6)	131.0	6.32 (dd, 15.0, 10.7)	132.9	6.32 (dd, 15.2, 10.8)	132.9	3.46 (m)	66.8	2.39 (m)	28.7	
6	6.76 ^b	128.1	6.78 (dd, 15.7, 10.7)	128.1	6.78 (dd, 15.6, 10.8)	128.1	1.88, 1.76 (m)	38.4	6.23 (dt, 15.9, 7.2)	130.0	
7	6.54 (d, 15.6)	132.6	6.55 (d, 15.7)	132.6	6.53 (d, 15.6)	132.6	2.64, 2.77 (m)	32.0	6.41 (d, 15.9)	130.2	
1'	-	133.7	-	133.9	-	133.8	-	142.1	-	142.6	
2'	7.05 (d, 8.2)	129.4	7.03 (d, 7.9)	129.4	6.67 (s)	111.0	6.63 (br s)	115.5	-	113.7	
3'	6.74 (d, 8.2)	115.2	6.74 (d, 7.6)	115.1	-	143.6	-	143.7	6.37 (s)	103.8	
4'	-	153.7	-	153.6	-	146.3	-	133.5	-	137.0	
5'	6.74 (d, 8.2)	115.2	6.74 (d, 7.6)	115.1	6.81 (d, 7.6)	114.1	6.74 (d, 8.0)	115.3	-	148.7	
6'	7.05 (d, 8.2)	129.4	7.03 (d, 7.9)	129.4	6.66 (d, 7.6)	121.0	6.54 (br d, 8.0)	120.4	6.52 (s)	115.5	
1"	-	137.0	-	137.0	-	137.1	-	141.8	-	137.6	
2"	7.38 (br d, 7.5)	126.3	7.39 (br d, 7.3)	126.3	7.30 (d, 7.4)	126.3	7.15°	128.3	7.32 (d, 7.3)	125.9	
3"	7.30 (br t, 7.5)	128.5	7.30 (dd, 7.3, 7.2)	128.5	7.25 (t, 7.6)	128.6	7.24 (m)	128.4	7.27 (t, 7.3)	128.4	
4"	7.22 (m)	127.5	7.23 (m)	127.5	7.22 (m)	127.6	7.15°	125.7	7.17 (t, 6.9)	126.8	
5"	7.30 (br t, 7.5)	128.5	7.30 (dd, 7.3, 7.2)	128.5	7.25 (t, 7.6)	128.6	7.24 (m)	128.4	7.27 (t, 7.3)	128.4	
6"	7.38 (br d, 7.5)	126.3	7.39 (br d, 7.3)	126.3	7.30 (d, 7.4)	126.3	7.15°	128.3	7.32 (d, 7.3)	125.9	
3-OMe	-	-	3.29 (s)	56.1	3.28 (s)	56.2	-	-	-	-	
3-OAc	-	-	-	-	-	-	2.02 (s)	21.0, 173.0	-	-	
3'-OMe	-	-	-	-	3.85 (s)	55.8	-	-	-	-	
4'-OH	=	-	-	-	5.46 (s)	-	-	-	-	-	

^aAssignments were based on DEPT, HMQC, and HMBC experiments. ^bPartially overlapping signal. ^cOverlapping signals with the same superscript.

diarylheptanoid structure. The structure deduction of **4** was confirmed by COSY, DEPT, HMQC, and HMBC spectra. The attachment of the phenyl group to the 7-position of the heptyl chain was confirmed by the HMBC correlations between H-7 ($\delta_{\rm H}$ 2.64 and 2.77, m, 2 × 1H) and C-1" ($\delta_{\rm C}$ 141.8) and C-2"/C-6" ($\delta_{\rm C}$ 128.3). However, the absolute stereochemistry at C-5 could not be determined by the modified Mosher's method and this was due to the complex ¹H NMR spectra of the Mosher salts of **4**. Also, the existing data did not permit the assignment of the absolute configuration at C-3. Compound **4** was therefore identified as 3-acetoxy-1-(3,4-dihydroxyphenyl)-7-phenylheptan-5-ol.

Compound 5 was isolated as a colorless amorphous solid, mp 52–53°C, $[\alpha]_{\rm D}^{21}$ –43.1 (*c* 0.48, EtOH). The molecular formula was determined as $C_{19}H_{20}O_3$ by HR-TOFMS (ES⁻) at m/z 295.1338 [M-H]. The IR spectrum showed an absorption band for hydroxyl groups at 3328 cm⁻¹. The ¹³C NMR data (Table 1) displayed 19 signals including a carbinolic (δ_C 74.9), four methylene (δ_C 24.0, 27.5, 28.7, and 34.8), two methine ($\delta_{\rm C}$ 130.0 and 130.2), and twelve aromatic ring carbons, suggesting a diarylheptanoid structure. The presence of the trans-olefinic protons was evident from the double triplet signal at $\delta_{\rm H}$ 6.23 (J=15.9, 7.2 Hz, H-6) and the doublet signal at δ_C 6.41 (J = 15.9 Hz, H-7) in the ¹H NMR spectrum, which corresponded to the 13 C NMR signals at $\delta_{\rm C}$ 130.0 and 130.2, respectively. The ¹H NMR spectrum of compound 5 was similar to that of (3S)-1-(3,4-dihydroxyphenyl)-7-phenyl-(6E)-6-hepten-3-ol (14). However, the significant differences were their molecular weights and the presence of aromatic singlet signals of H-3' at $\delta_{\rm H}$ 6.37 ($\delta_{\rm C}$ 103.8), and H-6' at δ_H 6.52 (δ_C 115.5), which indicated the connectivity between an aromatic ring at C-3 with an ether bond. The large W_{1/2} value (24 Hz) of H-3 suggested its axial relationship with H-1ax. The absolute configuration at C-3 of 5 was investigated by circular dichroism (CD) spectroscopy. C-3 was determined to have an Rconfiguration based on the helicity rule for P-helicity of the chiral chromane ring system [13], which showed a negative Cotton effect for the 1L_b band at 250-270 nm [14]. Moreover, the NOE correlation of H-3 and H-1 (Figure 3) also confirmed the C-3 configuration. Compound 5 was thus elucidated as (3R)-1-(4,5)dihydroxyphenyl)-7-phenyl-(6E)-6-hepten-3,2'-epoxide.

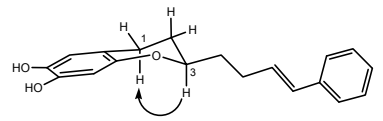


Figure 3: NOE correlation of H-3 with H-1 of compound 5.

The high biodiversity of the chemical constituents of *C. comosa* should be noted. The contents of a number of diarylheptanoids from *C. comosa* rhizomes collected from Sakon Nakhon province according to the present work were found to be different from those isolated from *C. comosa* from Kampaengsaen district, Nakhon Pathom province, central part of Thailand [2]. Apart from the new compounds 1–5, the known compounds 12, and 15–17 have not been reported previously in the Kampaengsaen cultivar.

To examine the biological effect of the isolated compounds, mouse macrophage RAW 264.7 cells were treated with different concentrations of the diarylheptanoids. Compounds 1a and 1b mixture and 14 were found to be active (IC₅₀ <10 μ M). LPS treatment significantly promoted the production of NO, a wellknown cytokine involving in various biological processes including inflammation and immunoregulation [15]. BAY 11-7082, a NF-κB inhibitor, which was used as a positive control, significantly inhibited the production of NO in the LPS-treated RAW 264.7 cells. Furthermore, compounds 1a and 1b mixture and 14 could inhibit the production of NO in the LPS-treated RAW 264.7 cells in a concentration-dependent manner. The calculated IC₅₀ concentration of compounds 1a and 1b mixture and 14 for the inhibition of NO production in LPS-stimulated RAW 264.7 cells was $0.66 \pm 0.32 \mu M$ and $0.42 \pm 0.16 \mu M$, respectively. The anti-inflammatory effect of the diarylheptanoids does not only clarify our understanding of the traditional medicinal use of C. comosa rhizomes, but also implicate further potential development of compounds 1a and 1b mixture and 14 as therapeutic tools for the prevention and treatment of inflammatory diseases.

Experimental

General: Melting points were determined with an electrothermal melting point apparatus and are uncorrected. Optical rotations were measured on a JASCO-1020 polarimeter. IR spectra were obtained

using a Perkin-Elmer Frontier FT-IR spectrophotometer. ¹H and ¹³C NMR spectra were recorded on a Bruker AVANCE 400 FT-NMR spectrometer, operating at 400 MHz (¹H) and 100 MHz (¹³C). ESMS and ESTOFMS spectra were measured with Finnigan LC-Q and Bruker micrOTOF Q II mass spectrometers. The CD spectrum was determined with a JASCO J-810 spectrophotometer. Unless indicated otherwise, column chromatography was carried out using Merck silica gel 60 (<0.063 mm). Merck Lichrolut RP-18 (0.040-0.060 mm) and Pharmacia Sephadex LH-20 were used for reversed phase and size exclusion column chromatography. For TLC, Merck precoated silica gel 60 F₂₅₄ plates were used. Compounds on TLC were detected under UV light and by spraying with anisaldehyde-H₂SO₄ reagent followed by heating.

Plant material: The rhizomes of Curcuma comosa were collected from Sawangdaendin district, Sakon Nakorn province in June 2008. A voucher specimen of this plant is deposited at the Department of Plant Sciences, Faculty of Science, Mahidol University, Bangkok.

Extraction and isolation: The pulverized, dry rhizomes of the plant (19.9 kg) were macerated successively with n-hexane and EtOH to yield the hexane (brownish syrup, 822.1 g) and EtOH extracts (dark brownish sticky solid, 1.4 kg), respectively. A portion of the hexane extract (463.8 g) was subjected to column chromatography (CC) eluting with a gradient of *n*-hexane–EtOAc to give 3 fractions. Fraction 1 (195.8 g) was fractionated by CC, eluting with n-hexane-EtOAc (0:100 to 100:0), to give sub-fractions 1.1-1.4. Sub-fraction 1.3 was recrystallized with CH₂Cl₂-n-hexane to give 8 (6.1 g) as pale yellow needles, mp 62–64°C. The filtrate was further purified by CC (n-hexane-EtOAc, 100:0.7) to give 4 sub-fractions (1.3.1-1.3.4). Subfraction 1.3.4 was purified by CC (n-hexane-EtOAc, 200:0.7) to afford 2 sub-fractions (1.3.4.1–1.3.4.2). Sub-fraction 1.3.4.2 was further subjected to CC (*n*-hexane–CH₂Cl₂, 50:50) to give **6** (216.8 mg). Fraction 2 (235.5 g) was recrystallized with *n*-hexane–CH₂Cl₂ to give 9 (100.1 g), mp 79–80°C, $[\alpha]_D^{29}$ –38.2 (*c* 0.60, MeOH). A portion of the EtOH extract (759.5 g) was fractionated by CC using a gradient of n-hexane-EtOAc to EtOAc-MeOH to obtain 12 fractions. Fraction 6 (10.1 g) was further purified by CC (silica gel, n-hexane-EtOAc, 90:10) to yield 7 sub-fractions (6.1-6.7). Subfraction 6.5 was further chromatographed (CH₂Cl₂–MeOH, 100:0.1) to give 4 sub-fractions (6.5.1-6.5.4). Sub-fraction 6.5.2 was purified using Sephadex LH-20 CC (100% MeOH), followed by silica CC $(CH_2Cl_2-MeOH, 100:0.1)$ to give 7 (4 mg), $[\alpha]_D^{29}$ +6.0 (c 0.82, MeOH), and 10 (1.0 g), mp 49-50°C. Fraction 9 was purifided by CC (n-hexane-EtOAc, 90:10) to afford 6 sub-fractions (9.1-9.6). Subfraction 9.4 was further purified by CC (CH₂Cl₂-MeOH, 200:0.5) to give 4 sub-fractions (9.4.1-9.4.4). Sub-fraction 9.4.4 was further chromatographed (n-hexane-EtOAc, 100:20) to furnish 12 (42.3 mg), $[\alpha]_D^{29}$ -8.4 (c 0.38, MeOH), a mixture of **13a** and **13b** (274.7 mg), mp 94–95°C, $[\alpha]_{\rm D}^{\rm 29}$ –1.6 (c 1.48, MeOH), and a mixture of ${\bf 1a}$ and 1b (35.5 mg). Fraction 10 was subjected to CC using n-hexane-EtOAc (90:10) to obtain 7 sub-fractions (10.1-10.7). Sub-fraction 10.4 was further separated on Sephadex LH-20 (100% MeOH) to give 5 sub-fractions (10.4.1–10.4.5). Sub-fraction 10.4.3 was further purified $(CH_2Cl_2-MeOH, 200:0.5)$ to give 3 sub-fractions (10.4.3.1-10.4.3.3). Sub-fraction 10.4.3.2 was purified by CC (n-hexane-EtOAc, 90:10) to yield a mixture of 3a and 3b (21.0 mg). Subfraction 10.4.3.3 was further purified (CH₂Cl₂-MeOH, 200:0.5) to give a mixture of 2a and 2b (221.3 mg). Sub-fraction 10.7 after further purified by Sephadex LH-20 column (100% MeOH), followed by silica CC (n-hexane-EtOAc, 90:10) furnished 11 (278.1 mg) as colorless prisms, mp 129-130°C. Fraction 11 was chromatographed (n-hexane–EtOAc, 90:10) to give 3 sub-fractions (11.1–11.3).

Sub-fraction 11.2 was then subjected to CC (CH₂Cl₂-MeOH, 100:0.1) to give 5 sub-fractions (11.2.1–11.2.5). Sub-fraction 11.2.2 was chromatographed (n-hexane–EtOAc, 70:30) to give 5 (26.1 mg). Sub-fraction 11.2.2.3 was chromatographed (silica gel, n-hexane-EtOAc, 70:30) to give 3 sub-fractions (11.2.2.3.1-11.2.2.3.3). Subfraction 11.2.2.3.3 was then purified by CC (CH₂Cl₂-MeOH, 100:0.3) to **4** (16.8 mg) and **15** (14.9 mg), $[\alpha]_D^{29}$ -3.3 (*c* 0.35, EtOH). Sub-fraction 11.2.4 was purified by CC (CH₂Cl₂-MeOH, 100:0.3) to give 6 sub-fractions (11.2.4.1-11.2.4.6). Sub-fraction 11.2.4.5 was subjected to Sephadex LH-20 CC (100% MeOH) to give 14 (443.5 mg), mp 100–101°C, $[\alpha]_{\rm D}^{29}$ +1.2 (c 1.39, MeOH), and **16** (96.6 mg), $[\alpha]_{\rm D}^{29}$ -14.6 (c 0.35, EtOH). Fraction 12 was chromatographed (nhexane-EtOAc, 90:10) to give 8 sub-fractions (12.1-12.8). Subfraction 12.5 was further separated on Sephadex LH-20 CC (100% MeOH) to yield 3 sub-fractions, the second of which was purified in the usual manner to give 17 (3.2 mg).

and (3R)-1-(4-Hydroxyphenyl)-7-phenyl-(4E,6E)-4,6heptadien-3-ol (1a, 1b)

White solid.

MP: 110 –112°C (EtOAc–n-hexane).

 $[\alpha]_{D}^{29}$: -3.8 (*c* 1.37, EtOH).

IR (KBr): 3233, 3022, 2924, 2849, 1612, 1596, 1447, 1228, 990, 825, 748, 692 cm⁻¹.

¹H and ¹³C NMR: Table 1.

HR-TOFMS (ES, negative ion mode): m/z 279.1835 [M-H]⁻. Calcd for $C_{19}H_{20}O_2$ –H, 279.1835.

(3S)and (3R)-1-(4-Hydroxyphenyl)-3-methoxy-7-phenyl-(4E,6E)-4,6-heptadiene (2a, 2b)

Colorless sticky solid.

 $[\alpha]_{\rm D}^{29}$: -0.3 (*c* 0.68, EtOH).

IR (KBr): 3321, 3024, 2930, 1613, 1513, 1447, 1224, 990, 828 cm⁻¹. ¹H and ¹³C NMR: Table 1.

HR-TOFMS (ES, negative ion mode): m/z 293.1541 [M-H]⁻. Calcd for C₂₀H₂₂O₂-H, 293.1542.

(3S)- and (3R)-1-(4-Hydroxy-3-methoxyphenyl)-3-methoxy-7phenyl-(4E,6E)-4,6-heptadiene (3a, 3b)

Colorless sticky solid.

 $[\alpha]_{D}^{29}$: +2.2 (*c* 1.52, EtOH).

IR (KBr): 3308, 3023, 2930, 1613, 1513, 1447, 1224, 990 cm⁻¹. ¹H and ¹³C NMR: Table 1.

HR-TOFMS (ES, negative ion mode): m/z 323.1698 [M-H]⁻. Calcd for $C_{21}H_{24}O_3$ –H, 323.1641.

3-Acetoxy-1-(3,4-dihydroxyphenyl)-7-phenylheptan-5-ol (4)

Colorless sticky solid.

 $[\alpha]_{D}^{29}$: +5.3 (*c* 1.31, EtOH).

IR (KBr): 3370, 3027, 2924, 2860, 1705, 1518, 1444, 1248, 1024, 698 cm⁻¹

¹H and ¹³C NMR: Table 1.

HR-TOFMS (ES, negative ion mode): m/z 357.1716 [M-H]⁻. Calcd for $C_{21}H_{26}O_5$ –H, 357.1702.

(3R)-1-(4,5-Dihydroxyphenyl)-7-phenyl-(6E)-6-hepten-3,2'epoxide (5)

Colorless amorphous solid.

MP: 52-53°C (EtOAc-*n*-hexane).

 $[\alpha]_{D}^{29}$: -43.1 (*c* 0.48, EtOH).

CD (CH₂Cl₂) λ max: $\Delta\epsilon_{251}$ -1.98, $\Delta\epsilon_{275}$ +0.32.

IR (KBr): 3328, 3024, 2933, 2859, 1596, 1515, 1453, 1227, 1186, 957, 794 cm⁻¹.

¹H and ¹³C NMR: Table 1.

HR-TOFMS (ES, negative ion mode): m/z 295.1338 [M–H]⁻. Calcd for $C_{19}H_{20}O_3$ –H, 295.1334.

Determination of the absolute configuration of 1: The absolute configuration at the 3-position of 1 was performed as described previously [2], and the results are summarized in Figure 2.

Cell culture and measurement of NO production from RAW 264.7 cells: Mouse macrophage RAW 264.7 cells (ATCC at Shanghai Institutes for Biological Science, Shanghai, China) were maintained in DEME/High Glucose medium (Invitrogen, Carlsbad, CA, U.S.A.) supplemented with 10% (v/v) FBS and antibiotics (100 U/mL penicillin and 0.1 g/L streptomycin) under a humidified atmosphere containing 5% CO₂ at 37°C. The RAW 264.7 cells were seeded in 96-well plates with 1 × 10⁴ cells/well and allowed to adhere for 6 h at 37°C in 5% CO₂. After that, the cells were pretreated with various concentrations of compounds for 2 h,

followed by 1 μ g/mL LPS and incubated for another 24 h. The cell culture medium was taken for NO measurement by using a commercially available kit based on the Griess reaction (Beyotime, Haimen, China). Nitrite production was measured with a microplate reader at OD 550 nm. Percent inhibition was calculated.

Statistical analysis: All statistical calculations were carried out using GraphPad Prism 5.01. The results were expressed as the mean \pm standard error of means of three independent experiments.

Acknowledgements - This work was supported by The Thailand Research Fund. GZ and FW acknowledge support from the National Natural Science Foundation of China (No. 20911140472). NS and PS are grateful for scholarships from the Center of Excellence for Innovation in Chemistry (PERCH-CIC), Office of the Higher Education Commission, Ministry of Education. AZ acknowledges a research fellowship from Ramkhamhaeng University. We thank Dr Thaya Jenjittikul, Department of Plant Sciences, Mahidol University for the identification of the plant species.

References

- [1] Jurgens TM, Frazier EG, Schaeffer JM, Jones TE, Zink DL, Borris RP, Nanakorn W. (1994) Novel nematocidal agents from *Curcuma comosa*. *Journal of Natural Products*, 57, 230-235.
- [2] Suksamrarn A, Ponglikitmongkol M, Wongkrajang K, Chindaduang A, Kittidanairak S, Jankam A, Yingyongnarongkul B, Kittipanumat N, Chokchaisiri R, Khetkam P, Piyachaturawat P. (2008) Diarylheptanoids, new phytoestrogens from the rhizomes of *Curcuma comosa*: Isolation, chemical modification and estrogenic activity evaluation. *Bioorganic & Medicinal Chemistry*, 16, 6891-6902.
- [3] Suksamrarn A, Eiamong S, Piyachaturawat P, Byrne LT. (1997) A phloracetophenone glucoside with choleretic activity from *Curcuma comosa*. *Phytochemistry*, 45, 103-105.
- [4] Chokchaisiri R, Chaneiam N, Svasti S, Fucharoen S, Vadolas J, Suksamrarn A. (2010) Labdane diterpenes from the aerial parts of *Curcuma comosa* enhance fetal hemoglobin production in an erythroid cell line. *Journal of Natural Products*, 73, 724-728.
- [5] Chokchaisiri R, Innok P, Suksamrarn A. (2012) Flavonoids glycosides from the aerial parts of *Curcuma comosa. Phytochemistry Letters*, 5, 361-366.
- [6] Soontornchainaksaeng P, Jenjittikul T. (2010) Chromosome number variation of phytoestrogen-producing Curcuma (Zingiberaceae) from Thailand. Journal of Natural Medicine, 64, 370-377.
- [7] Keeratinijakal V, Kladmook M, Laosatit K. (2010) Identification and characterization of *Curcuma comosa* Roxb., phytoestrogens-producing plant, using AFLP markers and morphological characteristics. *Journal of Medicinal Plants Research*, 4, 2651-2657.
- [8] Kuronayaki M, Noro T, Fukushima S, Aimaya R, Ikuta A, Itokawa H, Morita M. (1983) Studies on the constituents of the seeds of *Alpinia katsumadai* Hayata. *Chemical & Pharmaceutical Bulletin*, 31, 1544-1550.
- [9] Hashimoto T, Tori M, Asakawa Y. (1986) Five new diarylheptanoids from the male flowers of *Alnus sieboldiana*. *Chemical & Pharmaceutical Bulletin*, 34, 1846-1849.
- [10] Shin D, Kinoshita K, Koyama K, Takahashi K. (2002) Antiemetic principles of Alpinia officinarum. Journal of Natural Products, 65, 1315-1318.
- [11] Uehara SI, Yasuda I, Akiyama K, Morita H, Takeya K, Itokawa H. (1987) Diarylheptanoids from the rhizomes of *Curcuma xanthorrhiza* and *Alpinia officinarum. Chemical & Pharmaceutical Bulletin*, 35, 3298-3304.
- [12] Li J, Zhao F, Li MZ, Chen LX, Qiu F. (2010) Diarylheptanoids from the rhizomes of *Curcuma kwangsiensis*. *Journal of Natural Products*, 73, 1667-1671.
- [13] (a) Antus S, Kurtan T, Juhasz L, Kiss L, Hollosi M, Majer ZS. (2001) Chiroptical properties of 2,3-dihydrobenzo[b]furan and chromone chromophores in naturally occurring O-heterocycles. Chirality, 13, 493-506; (b) Slade D, Ferreira D, Marais JPJ. (2005) Circular dichroism, a powerful tool for the assessment of absolute configuration of flavonoids. Phytochemistry, 66, 2177-2215; (c) Mazzani F, Pescitelli G, Bari LD, Netscher T, Salvadori P. (2009) Circular dichroism of tocopherols versus tocotrienols. Chirality, 21, 35-43.
- [14] Cardillo G, Merlini L, Nasini G. (1971) Constituents of Dragon's blood. Part I. Structure and absolute configuration of new optically active flavans. Journal of the Chemical Society (C), 3967-3970.
- [15] (a) Mendes SDS, Candi A, Vansteenbrugge M, Pignon MR, Bult H, Boudjeltia KZ, Munaut C, Raes M. (2009) Microarray analyses of the effects of NF-kappaB or PI3K pathway inhibitors on the LPS-induced gene expression profile in RAW264.7 cells: synergistic effects of rapamycin on LPS-induced MMP9-overexpression. *Cellular Signalling*, 21, 1109-1122; (b) Guzik TJ, Korbut R, Adamek-Guzik T. (2003) Nitric oxide and superoxide in inflammation and immune regulation. *Journal of Physiology and Pharmacology*, 54, 469-487.

Diarylheptanoids of <i>Curcuma comosa</i> with Inhibitory Effects on Nitric Oxide Production in Macrophage RAW 264.7 Cells Nilubon Sornkaew, Yuan Lin, Fei Wang, Guolin Zhang, Ratchanaporn Chokchaisiri, Ailian Zhang, Kanjana Wongkrajang, Parichat Suebsakwong, Pawinee Piyachaturawat and Apichart Suksamrarn	89			
Rapid Dereplication and Identification of the Bioactive Constituents from the Fungus, <i>Leucocoprinus birnbaumii</i> Robert Brkljača and Sylvia Urban				
Pterandric Acid – its Isolation, Synthesis and Stereochemistry Muhammad A. Haleem, Simone C. Capellari, Beryl B. Sympson and Anita J. Marsaioli	99			
Cardanols, Long Chain Cyclohexenones and Cyclohexenols from Lannea schimperi (Anacardiaceae) Dorothy A. Okoth and Neil A. Koorbanally	103			
Pulvinulin A, Graminin C, and <i>cis</i> -Gregatin B – New Natural Furanones from <i>Pulvinula</i> sp. 11120, a Fungal Endophyte of <i>Cupressus arizonica</i>	40=			
E. M. Kithsiri Wijeratne, Yaming Xu, A. Elizabeth Arnold and A. A. Leslie Gunatilaka Potent Anti-Calmodulin Activity of Cyclotetradepsipeptides Isolated from Isaria fumosorosea Using a Newly Designed Biosensor Abraham Madariaga-Mazón, Martín González-Andrade, Conchita Toriello, Hortensia Navarro-Barranco and Rachel Mata	107			
Mutagenesis of Lysines 156 and 159 in Human Immunodeficiency Virus Type 1 Integrase (IN) Reveals Differential Interactions between these Residues and Different IN Inhibitors	113			
David C. Crosby, Xiangyang Lei, Charles G. Gibbs, Manfred G. Reinecke, and W. Edward Robinson, Jr.	117			
Herbal Medicinal Products versus Botanical-Food Supplements in the European market: State of Art and Perspectives Anna Rita Bilia	125			
Chemical Composition and Biological Activity of Essential Oils of <i>Dracocephalum heterophyllum</i> and <i>Hyssopus officinalis</i> from Western Himalaya				
Iris Stappen, Jürgen Wanner, Nurhayat Tabanca, David E. Wedge, Abbas Ali, Vijay K. Kaul, Brij Lal, Vikas Jaitak, Velizar K. Gochev, Erich Schmidt and Leopold Jirovetz	133			
Cytotoxic Active Constituents of Essential Oils of Curcuma longa and Curcuma zanthorrhiza Erich Schmidt, Boris Ryabchenko, Juergen Wanner, Walter Jäger and Leopold Jirovetz	139			
Antimicrobial Activity of Nerolidol and its Derivatives against Airborne Microbes and Further Biological Activities Sabine Krist, Daniel Banovac, Nurhayat Tabanca, David E. Wedge, Velizar K. Gochev, Jürgen Wanner, Erich Schmidt and Leopold Jirovetz	143			
Chemical Composition and Antifungal Activity of <i>Aaronsohnia pubescens</i> Essential Oil from Algeria Ahmed Makhloufi, L. Ben Larbi, Abdallah Moussaoui, Hamadi A. Lazouni, Abderrahmane Romane, Jürgen Wanner, Erich Schmidt, Leopold Jirovetz and Martina Höferl	149			
Radical Scavenging and Antioxidant Activities of Essential Oil Components – An Experimental and Computational Investigation Farukh S. Sharopov, Michael Wink and William N. Setzer	153			
<u>Accounts/Reivews</u>				
Enzyme-Mediated Synthesis of Sesquiterpenes Stefano Serra	157			
Triterpenoids as Neutrophil Elastase Inhibitors Dom Guillaume, Thi Ngoc Tram Huynh, Clément Denhez, Kim Phi Phung Nguyen and Azzaq Belaaouaj	167			
Mechanistic Insights to the Cytotoxicity of Amaryllidaceae Alkaloids Jerald J. Nair, Lucie Rárová, Miroslav Strnad, Jaume Bastida and Johannes van Staden	171			
Review of β-carboline Alkaloids from the Genus Aspidosperma Tanya H. Layne, Joy S. Roach and Winston F. Tinto	183			
Natural Flavonoids as Potential Herbal Medication for the Treatment of Diabetes Mellitus and its Complications Jian Chen, Sven Mangelinckx, An Adams, Zheng-tao Wang, Wei-lin Li and Norbert De Kimpe	187			
Lignins of Bioenergy Crops: a Review Yadhu N. Guragain, Alvaro I. Herrera, Praveen V. Vadlani and Om Prakash	201			
Plant Chemical Defenses: Are all Constitutive Antimicrobial Metabolites Phytoanticipins? M. Soledade C. Pedras and Estifanos E. Yaya	209			
Sponge Derived Bromotyrosines: Structural Diversity through Natural Combinatorial Chemistry Hendrik Niemann, Andreas Marmann, Wenhan Lin and Peter Proksch	219			

Natural Product Communications 2015

Volume 10, Number 1

Contents

10th Anniversary issue

Annivarsory Message	i-ii
Editorial Board Members	iii-vi
Original Paper ANALYTICAL	
Expedient Access to Enantiopure Cyclopentanic Natural Products: Total Synthesis of (-)-Cyclonerodiol Carmen Pérez Morales, M. Mar Herrador, José F. Quílez del Moral and Alejandro F. Barrero	1
Identification of Sesquiterpene Lactones in the Bryophyta (Mosses) Takakia: Takakia Species are Closely Related Chemically to the Marchantiophyta (Liverworts) Yoshinori Asakawa, Kaeko Nii and Masanobu Higuchi	5
Chemotypes of <i>Ligularia vellerea</i> , its Hybrids, and <i>L. melanothyrsa</i> Anna Shimizu, Kyosuke Inoue, Mayu Ichihara, Ryo Hanai, Yoshinori Saito, Yasuko Okamoto, Motoo Tori, Xun Gong and Chiaki Kuroda	9
neo-Clerodane Diterpenoids from Scutellaria altissima Petko I. Bozov and Josep Coll	13
Phytotoxicity of Triterpenes and Limonoids from the Rutaceae and Meliaceae. 5α,6β,8α,12α-Tetrahydro-28-norisotoonafolin – a Potent Phytotoxin from <i>Toona ciliata</i> Liliane Nebo, Rosa M. Varela, José M. G. Molinillo, Vanessa G. P. Severino, André L. F. Sarria, Cristiane M. Cazal, Maria Fátima das Graças Fernandes, João B. Fernandes and Francisco A. Macías	TY 17
Triterpene Glycosides of Sea Cucumbers (Holothuroidea, Echinodermata) as Taxonomic Markers Vladimir I. Kalinin, Sergey A. Avilov, Alexandra S. Silchenko and Valentin A. Stonik	21
Amurensiosides L-P, Five New Cardenolide Glycosides from the Roots of Adonis amurensis Satoshi Kubo, Minpei Kuroda, Akihito Yokosuka, Hiroshi Sakagami and Yoshihiro Mimaki	27
UV-protective Effects of Phytoecdysteroids from <i>Microsorum grossum</i> Extracts on Human Dermal Fibroblasts Raimana Ho, Taivini Teai, Alain Meybeck and Phila Raharivelomanana	33
Spirostane-type Saponins from <i>Dracaena fragrans</i> « Yellow Coast » Abdelmalek Rezgui, Anne-Claire Mitaine-Offer, Tomofumi Miyamoto, Chiaki Tanaka and Marie-Aleth Lacaille-Dubois	37
Secondary Metabolites from a Strain of Alternaria tenuissima Isolated from Northern Manitoba Soil Chukwudi S. Anyanwu and John L. Sorensen	39
Chemical Prospection of Important Ayurvedic Plant <i>Tinospora cordifolia</i> by UPLC-DAD-ESI-QTOF-MS/MS and NMR SYNTHE! Manju Bala, Praveen Kumar Verma, Shiv Awasthi, Neeraj Kumar, Brij Lal and Bikram Singh	43
Kopsiyunnanines J1 and J2, New Strychnos-type Homo-Monoterpenoid Indole Alkaloids from Kopsia arborea Mariko Kitajima, Tetsuya Koyama, Yuqiu Wu, Noriyuki Kogure, Rongping Zhang and Hiromitsu Takayama	49
Diversity in the Flavonoid Composition of Stellera chamaejasme in the Hengduan Mountains Kei Shirai, Yasuko Okamoto, Motoo Tori, Takayuki Kawahara, Xun Gong, Teruaki Noyama, Eiji Watanabe and Chiaki Kuroda	53
Constituents of Indonesian Medicinal Plant Averrhoa bilimbi and Their Cytochrome P450 3A4 and 2D6 Inhibitory Activities Lidyawati Auw, Subehan, Sukrasno, Shigetoshi Kadota and Yasuhiro Tezuka	57
Flavonoids from Curcuma longa Leaves and their NMR Assignments Chia-Ling Jiang, Sheng-Fa Tsai and Shoei-Sheng Lee	63
Phytochemical Analysis and Biological Evaluation of Selected African Propolis Samples from Cameroon and Congo Danai Papachroni, Konstantia Graikou, Ivan Kosalec, Harilaos Damianakos, Verina Ingram and Ioanna Chinou	67
Improved Chromatographic Fingerprinting Combined with Multi-components Quantitative Analysis for Quality Evaluation of <i>Penthorum chinense</i> by UHPLC-DAD Wangping Deng, Tongtong Xu, Min Yang, Yajun Cui and De-an Guo	71
Anthocyanins of <i>Hibiscus sabdiffera</i> Calyces from Sudan Lucie Cahlíková, Badreldin H. Ali, Lucie Havlíková, Mirek Ločárek, Tomáš Siatka, Lubomír Opletal and Gerald Blunden	77
Maqui berry vs Sloe berry – Liquor-based Beverage for New Development Amadeo Gironés-Vilaplana, Diego A. Moreno and Cristina García-Viguera	81
Phytochemical Profile of the Aerial Parts of Sedum sediforme and Anti-inflammatory Activity of Myricitrin Daniel Winekenstädde, Apostolis Angelis, Birgit Waltenberger, Stefan Schwaiger, Job Tchoumtchoua, Stefanie König, Oliver Werz, Nektorios Aligiannis, Alexios Leandros Skaltsounis and Harmann Stuppner	93

FISEVIER

Contents lists available at ScienceDirect

Neurochemistry International

journal homepage: www.elsevier.com/locate/nci



Di-O-demethylcurcumin protects SK-N-SH cells against mitochondrial and endoplasmic reticulum-mediated apoptotic cell death induced by $A\beta_{25-35}$



Decha Pinkaew ^a, Chatchawan Changtam ^b, Chainarong Tocharus ^c, Sarinthorn Thummayot ^c, Apichart Suksamrarn ^d, Jiraporn Tocharus ^{a,*}

- ^a Department of Physiology, Faculty of Medicine, Chiang Mai University, Chiang Mai 50200, Thailand
- b Division of Physical Science, Faculty of Science and Technology, Huachiew Chalermprakiet University, Samutprakarn 10540, Thailand
- c Department of Anatomy, Faculty of Medicine, Chiang Mai University, Chiang Mai 50200, Thailand
- d Department of Chemistry and Center of Excellence for Innovation in Chemistry, Faculty of Science, Ramkhamhaeng University, Bangkok 10240, Thailand

ARTICLE INFO

Article history: Received 2 July 2014 Received in revised form 20 October 2014 Accepted 21 October 2014 Available online 24 October 2014

Keywords: Alzheimer's disease Amyloid beta Apoptosis Di-O-demethylcurcumin Endoplasmic reticulum stress Mitochondrial death pathway

ABSTRACT

Alzheimer's disease (AD) is a neurodegenerative and progressive disorder. The hallmark of pathological AD is amyloid plaque which is the accumulation of amyloid β (A β) in extracellular neuronal cells and neurofibrillary tangles (NFT) in neuronal cells, which lead to neurotoxicity via reactive oxygen species (ROS) generation related apoptosis. Loss of synapses and synaptic damage are the best correlates of cognitive decline in AD. Neuronal cell death is the main cause of brain dysfunction and cognitive impairment. Aß activates neuronal death via endoplasmic reticulum (ER) stress and mitochondria apoptosis pathway. This study investigated the underlying mechanisms and effects of di-O-demethylcurcumin in preventing A β -induced apoptosis. Pretreatment with di-O-demethylcurcumin for 2 h, which was followed by A β ₂₅-35 (10 μM) in human neuroblastoma SK-N-SH cells improved cell viability by using MTS assay and decreased neuronal cell apoptosis. Pretreatment with di-O-demethylcurcumin attenuated the number of nuclear condensations and number of apoptotic cells in $A\beta_{25-35}$ -induced group in a concentration-dependent manner by using transmission electron microscope (TEM) and flow cytometry, respectively. Di-O-demethylcurcumin also increased the ratio of Bcl-X_L/Bax protein, and reduced intracellular ROS level, cytochrome c protein expression, cleaved caspase-9 protein expression, and cleaved caspase-3 protein expression. Additionally, di-O-demethylcurcumin treatment also reduced the expression of ER stress protein markers, including protein kinase RNA like endoplasmic reticulum kinase (PERK) phosphorylation, eukaryotic translation initiation factor 2 alpha (eIF2\alpha) phosphorylation, inositol-requiring enzyme 1 (IRE1) phosphorylation, X-box-binding protein-1 (XBP-1), activating transcription factor (ATF6), C/EBP homologous protein (CHOP), and cleaved caspase-12 protein. CHOP and cleaved caspase-12 protein are the key mediators of apoptosis. Our data suggest that di-O-demethylcurcumin is a candidate protectant against neuronal death through its suppression of the apoptosis mediated by mitochondrial death and ER stress pathway.

© 2014 Elsevier Ltd. All rights reserved.

1. Introduction

Alzheimer's disease (AD) is a progressive neurodegenerative disease of the central nervous system (CNS), affecting, generally, elderly people. AD is one of the most common forms of dementia, which is determined clinically by diagnosing for multiple cognitive deficits including memory loss, emotional disturbance, etc. (Hauptmann et al., 2006). The pathological hallmarks of AD are amyloid plaques and neurofibrillary tangles (NFT) (Hardy and Selkoe,

2002; Selkoe, 2001) that cause loss of neurons and synapses in the brain. Amyloid β (β) is derived from the proteolytic cleavage of the amyloid precursor protein (APP) by β - and γ -secretase enzymes, and accumulate in the extracellular neuronal cells (Sisodia et al., 2001). NFT is accumulated within the neurons as a result of abnormal phosphorylation of the microtubules-associated tau-protein. Recent studies suggest that β accumulation has been causatively implicated in the neuronal dysfunction and neuronal loss that underlie the clinical manifestations of AD (Dante et al., 2003). Furthermore, several lines of research have suggested that β exerts neuronal toxicity through the production of reactive oxygen species (ROS) (Behl et al., 1994; Butterfield et al., 2007), which leads to neuronal apoptosis (Ramalingam and Kim, 2012) due to the involvement of the mitochondrial death pathway and the endoplasmic reticulum (ER) stress (Takuma et al., 2005). ER is an intracellular organelle

^{*} Corresponding author. Department of Physiology, Faculty of Medicine, Chiang Mai University, Chiang Mai 50200, Thailand. Tel.: +66 53 945362; fax: +66 53 945365. E-mail address: jtocharus@gmail.com (J. Tocharus).

related to protein folding, intracellular calcium homeostasis, lipid synthesis, steroids and cholesterol. Cellular conditions in ER, such as depletion of calcium, alter glycosylation, and the oxidative stress leads to unfolded protein. Unfolded protein accumulation in ER lumen is termed as ER stress (Nakagawa et al., 2000); this accumulation activates unfolded protein response (UPR), thereby signaling responses for ER homeostasis by decreasing protein synthesis, and increasing chaperone and degradation (Schroder and Kaufman, 2005; Vembar and Brodsky, 2008). However, prolonged ER stress is associated with apoptotic cell death (Boyce and Yuan, 2006), which is caused by activating three signal transducers that are protein kinase RNA like endoplasmic reticulum kinase (PERK), activating transcription factor (ATF6) and inositol-requiring enzyme 1 (IRE1); then, upregulates the expression of the C/EBP homologous protein (CHOP) (Chen et al., 2012), caspase-12 protein (Nakagawa et al., 2000), and glucose related protein 78 (Grp78) (Kim et al., 2008). Moreover, apoptosis mainly involves excessive ROS-induced mitochondrial dysfunction upon the increase in the permeability of mitochondria membrane (Chen and Yan, 2007). These results in the inducing of proapoptotic protein such as Bax translocate from the cytoplasm to the mitochondria membrane and a decrease in the antiapoptotic proteins (Bcl-2, Bcl-X_L). Thereafter, cytochrome c gets released to the cytoplasm and combines with apoptotic protease activating factor 1 (APAF-1) and procaspase-9 to become the active form of caspase-9 protein which stimulates the caspase-3 protein, and this leads to cell death (Li et al., 1997; Slee et al., 1999). Therefore, evidences suggest that suppression of Aβ-mediated neuronal apoptosis would be a target to attenuate progressive neuronal damages and provide a strategy for the given approach to the development and treatment of AD.

Curcumin is the major constituent of curcuminoids isolated from turmeric (Curcuma longa L.), with demethoxycurcumin and bisdemethoxycurcumin being the minor constituents. Previous studies have shown that curcumin has a wide range of beneficial properties, including antioxidant activity, anti-inflammatory activity, anticancer activity, neuroprotective effects, and antiviral activity (Bandgar et al., 2014; Belviranli et al., 2013; Bhullar et al., 2013; Morsy and El-Moselhy, 2013; Rath et al., 2013). Several groups of researchers are engaged in the design and synthesis of new curcuminoid analogs that exhibit higher physiological activities and pharmacological activities than the parent curcumin itself (Aroonrerk et al., 2012; Changtam et al., 2010; Sandur et al., 2007). Recently, we reported our research finding that di-O-demethylcurcumin, a chemically modified analog of curcumin, showed a potent antiinflammatory activity greater than that of the parent curcumin (Tocharus et al., 2012). However, it remains unclear whether di-Odemethylcurcumin exerts neuroprotection against Aβ-induced neuronal damage. Considering the important role of $A\beta$ in the pathogenesis of AD, elucidation of the effects of di-O-demethylcurcumin against Aβ-induced toxicity may provide a new insight into its potential application to the prevention or treatment of AD. It is, therefore, of interest to investigate whether di-O-demethylcurcumin would protect against Aβ-induced cytotoxicity in SK-N-SH cells. In the present study, we explored the possible mechanisms underlying the neuroprotective effects of di-O-demethylcurcumin against Aβ₂₅₋₃₅-induced apoptosis in SK-N-SH cells. We evaluated the protective effect of the production of ROS, and mitochondrial disruption, as well as ER stress.

2. Materials and methods

2.1. Materials

SK-N-SH cells (human neuroblastoma cells) were obtained from American Type Culture Collection (ATCC, Manassas, VA, USA). A β_{25-35} was obtained from Sigma (St. Louis, MO, USA). Minimum essential

medium (MEM), fetal bovine serum (FBS), penicillin, and streptomycin were purchased from GIBCO-BRL (Gaithersburg, MD, USA). The following antibodies were used for the western blot analysis: anti-Bcl-X_L, anti-Bax, anti-cytochrome c, anti-cleaved caspase-3, anti-cleaved caspase-9, anti- β -actin, anti-mouse IgG peroxidase-conjugated secondary antibody, anti-rabbit IgG peroxidase-conjugated secondary antibody (Millipore, Bedford, MA, USA), anti-Grp78, anti-CHOP, anti-PERK, anti-phospho-PERK, anti-phospho-IF2 α (Cell Signaling Technology, MA, USA), anti-ATF6, anti-XBP-1 (Santa Cruz Biotechnology, CA, USA), anti-phospho-IRE1 α and anticaspase-12 (Abcam, Cambridge, UK) and anti- β -actin.

2.2. Methods

 $A\beta_{25-35}$ was dissolved in deionized distilled water at concentration of 1 mM and storage at -80 °C. Before it was used in each of the experiments, it was aggregated at 37 °C for a week, after which it was diluted to the required concentration with sterile water.

2.2.1. Cell culture

The SK-N-SH cells were cultured in MEM supplemented with 10% heat inactivated FBS, 100 units/ml penicillin, and 100 μ g/ml streptomycin in humidified 95% air, at 37 °C and 5% CO₂ in an incubator. The cells were passaged by trypsinization every 2–3 days.

2.2.2. Preparation of di-O-demethylcurcumin

Curcumin (850 mg, 2.30 mmol), obtained from *Curcuma longa* as described previously (Changtam et al., 2010), was dissolved in dry CH₂Cl₂ (90 ml); the mixture was stirred at 0 °C or 5 min and BBr₃ (1 ml) was slowly added. The reaction mixture was stirred at 0 °C for 30 min and more BBr₃ (1 ml) was slowly added. After stirring at 0 °C for 1 h, water (200 ml) was added and the mixture was extracted with EtOAc. The combined organic phase was washed with water, dried over anhydrous Na₂SO₄ and the solvent was removed under vacuum. The crude products were separated by column chromatography using CH₂Cl₂-MeOH (10:1) as eluting solvent to yield mono-O-demethylcurcumin 240 mg (29%) and di-O-demethylcurcumin 450 mg (57%). The spectroscopic (¹H NMR and mass spectra) data were consistent with the reported values (Venkateswarlu et al., 2005).

2.2.3. Cell viability using MTS assay

The SK-N-SH cells were plated at a density of 2×10^5 cells/ml into 96 well plates (Corning Inc., Corning, NY, USA) and then incubated for 24 h at 37 °C in a CO₂ incubator. The cells were pretreated with di-O-demethylcurcumin (1 μ M, 2 μ M, 4 μ M and 8 μ M) for 2 h, which was followed by the addition of 10 μ M A β_{25-35} for 24 h. Thereafter, PrestoBlue reagent was added to each well and incubated additionally for 2 h at 37 °C under a humidified condition of 5% CO₂. The absorbance was measured using a microplate reader (Bio-Tek, Instruments, Winoaski, VT, USA) at the wavelength of 540 nm from three independent experiments. The background absorbance was measured at 600 nm and subtracted.

2.2.4. Determination of intracellular ROS by DCF assay

The cells at a density of 2×10^4 cells/well were plated in 96 well plates and then incubated for 24 h at 37 °C in CO₂ incubator. The cells were pretreated with di-O-demethylcurcumin (2 μ M, 4 μ M and 8 μ M) for 2 h, and then treated with A β_{25-35} for 24 h. The medium was removed, and DCFH-DA solutions were added for 25 min. The absorbance was measured using a fluorescence microplate reader (DTX800, Beckman Coulter, Austria) at an excitation wavelength of

485 nm and an emission wavelength of 535 nm. Fluorescent images were observed and collected by a fluorescence microscope from three independent experiments (Olympus AX-70, Olympus, Tokyo, Japan).

2.2.5. Cell apoptosis analysis

The cell death was investigated using fluorescein isothiocyanate (FITC) annexin V apoptosis detection kit (BD Bioscience, Canada) by following the manufacturer's instructions. Briefly, the SK-N-SH cells were plated at a density of 5×10^5 cells/well in six well plate and pretreated with di-O-demethylcurcumin for 2 h, which was followed by treatment in the presence or absence of $A\beta_{25-35}$ for 24 h; thereafter, the cells were collected and resuspended in $1\times$ binding buffer and incubated with annexin V-FITC and propidium iodide for 15 min in the dark. The cells were analyzed using FACS canto ii flow cytometry. The percentage of the apoptotic cells from three independent experiments was calculated using Diva software (FAC BIVA).

2.2.6. Assessment of nuclear morphological change

For the assessment of the nuclear morphological change of the apoptotic cells in the SK-N-SH cells, the cells were plated at a density of 2×10^4 cells/well in six well plates. The cells were pretreated with di-O-demethycurcumin for 2 h, and then treated in the presence or absence of A β_{25-35} for 24 h; the cells were then fixed with 2.5% glutaraldehyde in phosphate buffer saline (PBS), pH 7.4 at 4 °C until embedding. Thereafter, the cells were post-fixed with 1% osmium tetroxide for 2 h. Following this, they were dehydrated in a graded series (20–100%) of ethanol, and then embedded in araldite. Ultrathin sections were cut on an ultra microtome, using diamond knives collected on copper grids, and stained with 4% uranyl acetate and Reynolds lead citrate. The images from three independent experiments were detected with the help of an electron microscope (JEM-2200 FS; JEOL, Tokyo, Japan).

2.2.7. Western blot

The SK-N-SH cells were cultured in a density of 5×10^5 cells/ml in a 60 mm culture dish, at 37 °C, overnight. The cells were pretreated with di-O-demethylcurcumin at concentrations of 2 μ M, 4 μ M and 8 μ M for 2 h in the presence or absence of A β_{25-35} and lysed in a lysis buffer containing NP-40, 1% sodium deoxycholate, 0.1% sodium dodecyl sulfate, 40 mM β-glycerophosphate, 50 mM sodium fluoride, 2 mM sodium orthovanadate and 1× protease inhibitors at 4 °C for 15 min. The protein concentration was determined using the Bradford protein assay (Bio-Rad Laboratories, Hercules, CA, USA) and equal amounts of proteins were electrophoresed in a 10-15% SDS polyacrylamide gel and then transferred to a polyvinylidene fluoride (PVDF) membrane (Immobilon-P, Millipore, Bedford, MA, USA) at 400 mA for 30 min. Thereafter, it was incubated with the indicated antibodies (anti-p-PERK, anti-PERK, anti-ATF6, anti-Grp78, antip-eIF2α, anti-eIF2α, anti-CHOP, anti-IRE1, anti-p-IRE1, anti-cleaved caspase 12, anti-XBP-1, anti-Bax, anti-Bcl-X_L, anti-cytochrome c, anticleaved caspase-3 protein and anti-cleaved caspase-9 protein) in 1:1000–1:2000 dilution with phosphate-buffered saline with Tween 20 (PBST) at 4 °C, overnight. The blots were incubated with horseradish peroxidase-conjugated secondary antibodies for 1 h at room temperature. The signal was visualized as blots using the Immobilon Western (Millipore, MA, USA) and exposed to an X-ray film. The densitometry from three independent experiments was analyzed using the Image-J® software.

2.3. Statistical analysis

All the data are represented as the mean ± SD. Statistical significance was determined using one-way ANOVA, followed by Post Hoc

Dunnett's test. Values of P < 0.001, P < 0.01, P < 0.05 were considered as statistically significant.

3. Results

3.1. Di-O-demethylcurcumin increases cell viability against $A\beta_{25-35}$

The cells were pretreated with di-O-demethylcurcumin (2 μ M, 4 μ M and 8 μ M) for 2 h prior to the addition of 10 μ M of A β_{25-35} , and the protective effect was determined after 24 h of treatment. The result showed that 10 μ M of A β_{25-35} induced significantly the cell death of approximately 30% of the cells (P < 0.05) compared to the control group (Fig. 1). Di-O-demethylcurcumin attenuated the cytotoxicity of A β_{25-35} and significantly increased (P < 0.001) the cell viability in a concentration-dependent manner. The cell viability upon pretreatment with di-O-demethylcurcumin at concentrations of 2 μ M, 4 μ M and 8 μ M for 2 h before being treated with A β_{25-35} for 24 h were 84.31 \pm 1.07%, 88.96 \pm 1.30%, and 93.24 \pm 2.30%, respectively. At these concentrations, di-O-demethylcurcumin alone did not show any obvious effects on the viability of the SK-N-SH cells (Fig. 1).

3.2. Di-O-demethylcurcumin attenuated $A\beta_{25-35}$ induced production of ROS in SK-N-SH cells

An investigation was carried out to examine whether di-O-demethylcurcumin could inhibit the ROS generation induced by A β_{25-35} . We determined the effects of di-O-demethylcurcumin on ROS production by measuring the redox-sensitive dye DCFH-DA. As demonstrated in Fig. 2A,B, exposure to 10 μ M of A β_{25-35} of the SK-N-SH cells for 24 h resulted in a significant increase in the amount of ROS, by 238.44 \pm 10.67%, as compared to the control group. After the pretreatment with 2 μ M, 4 μ M and 8 μ M of di-O-demethylcurcumin in SK-N-SH cells before being treated with A β_{25-35} , the ROS levels were found to have significantly decreased (P< 0.001) in comparison with the A β_{25-35} -treated SK-N-SH group. At these concentrations, it was observed that di-O-demethylcurcumin alone did not show any

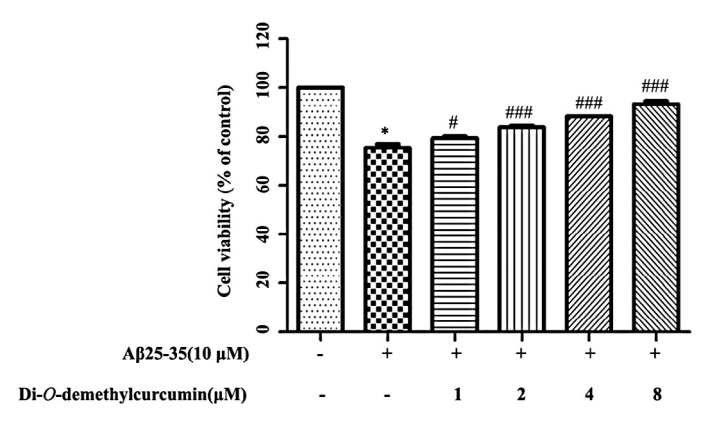


Fig. 1. Di-O-demethylcurcumin improves the cell viability of the SK-N-SH cells induced by Aβ₂₅₋₃₅. The SK-N-SH cells were pretreated with various concentrations (2–8 μM) of di-O-demethylcurcumin for 2 h, which was followed by treatment with 10 μM Aβ₂₅₋₃₅ for 24 h. The cell viability was measured using the 3-(4,5-dimethylthiazol-2-yl)-5-(3-carboxymethoxyphenyl)-2-(4-sulfophenyl)-2H-tetrazolium (MTS) assay. The data were normalized by using a control group. The values are presented as mean percent of control \pm SD of three independent experiments. *P<0.05 vs. control group; *P<0.05, **P<0.001 vs. group treated with Aβ₂₅₋₃₅ alone.

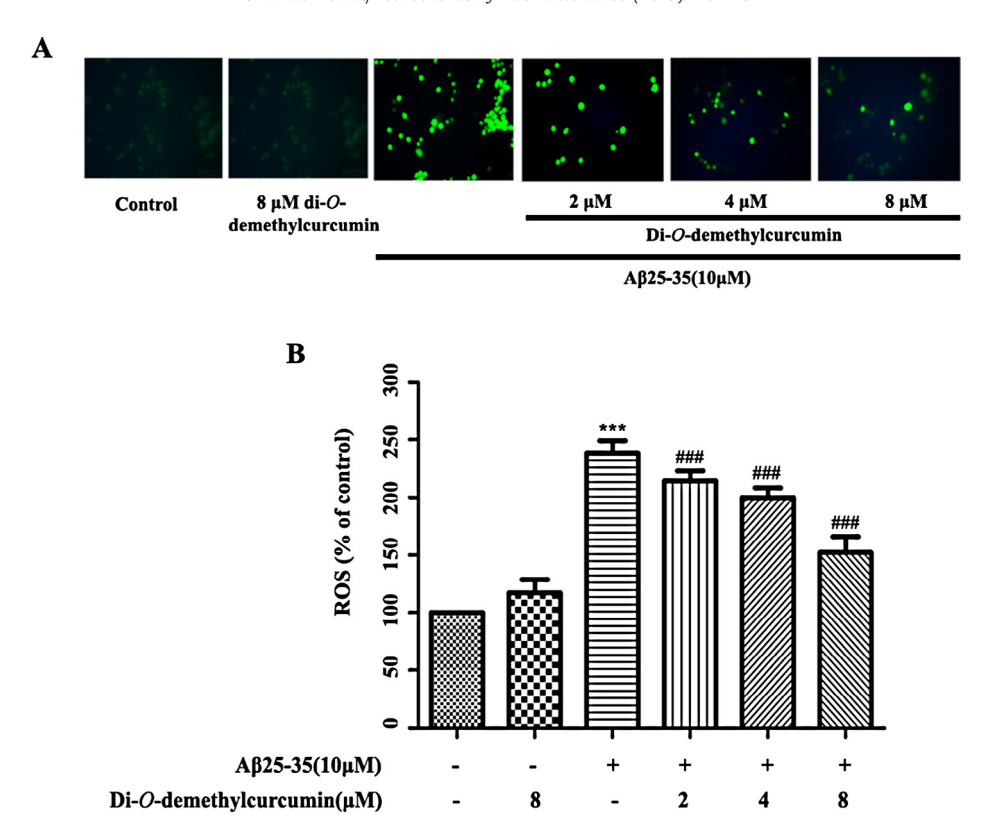


Fig. 2. The effect of di-*O*-demethylcurcumin on $Aβ_{25-35}$ -induced ROS production in SK-N-SH cells. **A:** Scanning Confocal Microscopy detected $Aβ_{25-35}$ -induced ROS production in SK-N-SH cells. **a:** The control group. b: The SK-N-SH cells treated with di-*O*-demethylcurcumin alone. c: The SK-N-SH cells treated with $10 \,\mu\text{M}$ of $Aβ_{25-35}$ alone. d-f: SK-N-SH cells pretreated with di-*O*-demethylcurcumin at the concentration of $2 \,\mu\text{M}$, $4 \,\mu\text{M}$ and $8 \,\mu\text{M}$ for $2 \,h$ prior to treatment with $10 \,\mu\text{M}$ $Aβ_{25-35}$ for $24 \,h$. **B:** The values of ROS are presented as the mean percent of control \pm SD of three independent experiments. ***P<0.001 vs. control group; ###P<0.001 vs. group treated with $Aβ_{25-35}$ alone.

obvious effects on the basal level of ROS (Fig. 2A,B). These results imply that di-O-demethylcurcumin has free radical scavenging effect in SK-N-SH cells activated by $A\beta_{25-35}$.

3.3. Di-O-demethylcurcumin prevents cell apoptosis caused by $A\beta_{25-35}$

In order to confirm the protective effect of di-Odemethylcurcumin against Aβ₂₅₋₃₅-induced SK-N-SH cells death, we investigated the nuclear morphological change in the apoptotic cells by using transmission electron microscope (TEM). As illustrated in Fig. 3A, $A\beta_{25-35}$ treatment alone showed nuclear condensation and cell shrinkage compared to the control. On the other hand, treatment with di-O-demethylcurcumin was found to decrease the apoptotic morphological change, and the morphology was observed to be similar to that of the control group. In addition, the number of apoptotic cells was also quantitatively analyzed using flow cytometry with Annexin V-FITC/PI double staining. The A β_{25-35} -treated cells significantly increased (P < 0.001) the number of apoptotic cells as compared to the control group. However, pretreatment with di-O-demethylcurcumin was observed to significantly reduce (P < 0.001) the number of apoptotic cells as compared to the cells treated with the $A\beta_{25-35}$ group in a dosedependent manner (Fig. 3B,C). The apoptotic cells at the time of pretreatment with di-O-demethylcurcumin (at concentrations of $2 \mu M$, $4 \mu M$ and $8 \mu M$) were $62.60 \pm 2.35\%$, $38.73 \pm 1.35\%$, and 14.77 ± 1.63%, respectively. These results suggest that di-Odemethylcurcumin suppresses $A\beta_{25-35}$ -induced cell apoptosis in SK-N-SH cells.

3.4. Effects of di-O-demethylcurcumin on A $\beta_{25\text{-}35}$ -induced ER stress in SK-N-SH cells

To investigate whether di-O-demethylcurcumin could suppress the apoptosis mediated by the ER stress pathway, we first determined whether $A\beta_{25-35}$ could induce ER stress. With this purpose, we investigated the expression of Grp78, a marker of ER stress in SK-N-SH cells. The SK-N-SH cells were treated with 10 μM of $A\beta_{25-35}$ for 0 h, 3 h, 6 h, 9 h, 12 h and 24 h, following which the cells were harvested. The results revealed that $A\beta_{25-35}$ had significantly increased the expression of the Grp78 proteins in the SK-N-SH cells (P < 0.001), with the maximum level being observed at the 12th h. Thereafter, we investigated the expression of the three major sensors of the ER stress pathway, including PERK, IRE1 and ATF6, using the western blot analysis. The activation of the PERK signal pathway was determined using the phosphorylated form of eIF2 α and PERK in the SK-N-SH cells was treated with $A\beta_{25-35}$. The presence of $A\beta_{25-35}$ increased the phosphorylated form of eIF2 α and the PERK proteins in a time-dependent manner, with the maximum level being observed at the 12th h in the SK-N-SH cells (Fig. 4A). Next, we investigated the effects of $A\beta_{25-35}$ activation on the IRE1 signal pathway, which was found out by determining the expression levels of XBP-1 and the phosphorylation form of p-IRE1 using the western blotting analysis. It was observed that $A\beta_{25-35}$ had increased the expression of phosphorylated IRE1 in a time-dependent manner (Fig. 4A). As XBP-1 mRNA is a specific substrate of IRE1, the splicing of XBP-1 is commonly used as a marker for IRE1 activation. We determined the activation of IRE1 by detecting the XBP-1 protein in the SK-N-SH cells. It was found that $A\beta_{25-35}$ had significantly

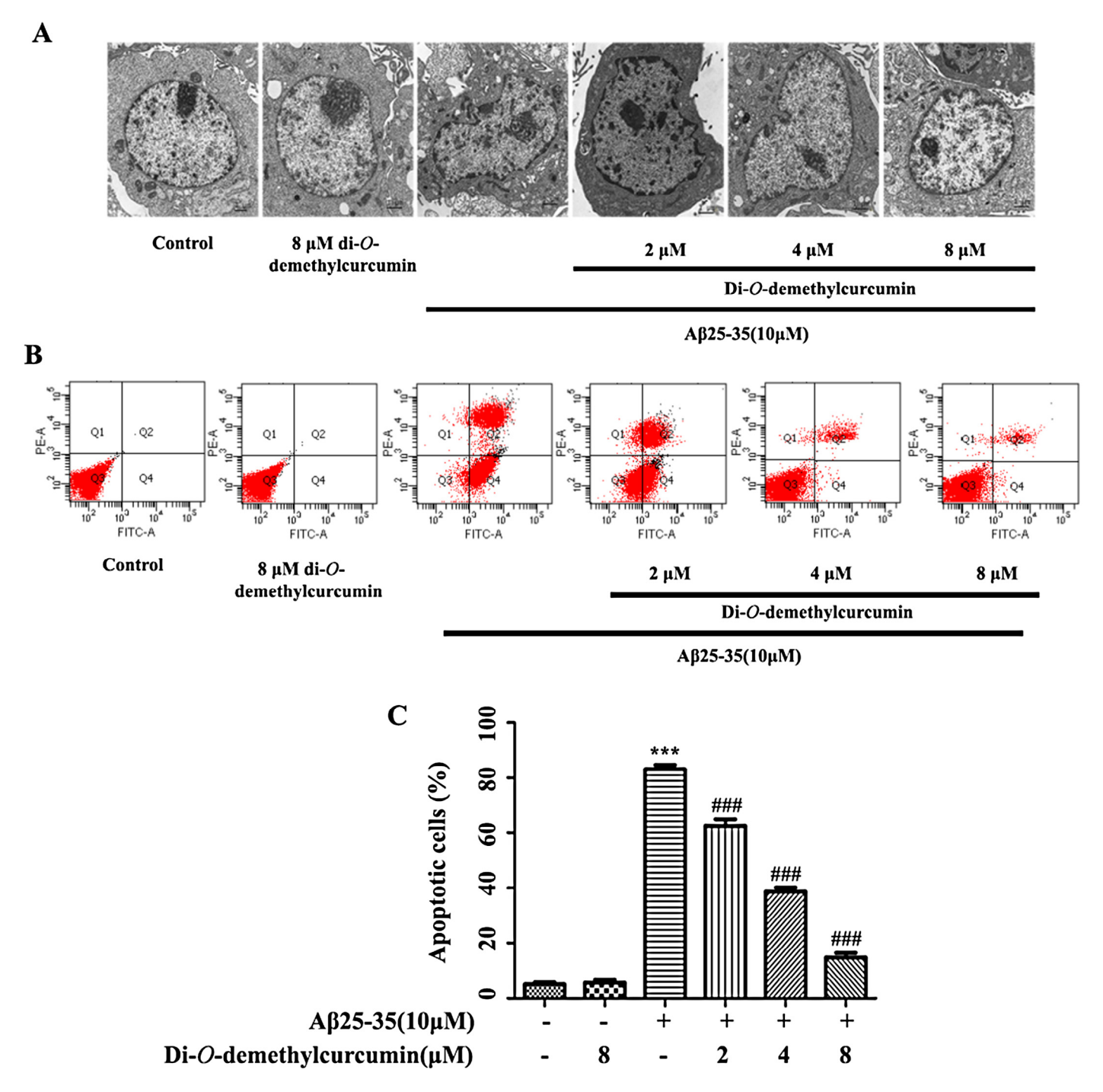


Fig. 3. Di-O-demethylcurcumin attenuated $Aβ_{25-35}$ -induced apoptosis in SK-N-SH cells. **A:** The morphological changes of SK-N-SH cells were detected using TEM. The effect of di-O-demethylcurcumin on $Aβ_{25-35}$ induced apoptosis in SK-N-SH cells. a: The control group. b: The SK-N-SH cells treated with di-O-demethylcurcumin alone. c: SK-N-SH cells treated with 10 μM of $Aβ_{25-35}$ alone. d-f: SK-N-SH cells pretreated with di-O-demethylcurcumin at the concentration of 2 μM, 4 μM and 8 μM for 2 h prior to treatment with 10 μM of $Aβ_{25-35}$ for 24 h. **B:** SK-N-SH cells were labeled with Annexin V-FITC and Pl. The apoptotic SK-N-SH cells were analyzed using flow cytometry. The numbers indicate the percentage of the cells in each quadrant (lower left: FITC-/Pl⁻, intact cells; lower right:FITC*/Pl⁻, apoptotic cells; upper left: FITC-/Pl⁺, necrotic cells; upper right: FITC-/Pl⁺, late apoptotic cells). **C:** The percentage of apoptotic cells are presented as the mean percent of control ± SD of three independent experiments. ****P<0.001 vs. control group; *##P<0.001 vs. group treated with $Aβ_{25-35}$ alone.

increased (P < 0.001) the XBP-1 protein in response to the exposed time in a time-dependent manner, with the maximum increase observed at the 24th h (Fig. 4A). In addition, we investigated the expression of the ER stress proteins of ATF6, CHOP and cleaved caspase 12 using the western blotting analysis, and showed that the optimal time expressions of these three are at the 12th h, 24th h and 9th h, respectively, after being exposed to A β ₂₅₋₃₅ (Fig. 4A). Altogether, the result suggested that the expression of the ER stress

proteins increased in a time-dependent manner, with the maximum level being observed between the 9th h and 24th h in the SK-N-SH cells treated with A β_{25-35} . Based on these results, the investigation for the determination of the further effects of di-O-demethy-lcurcumin in A β_{25-35} -induced ER stress was subsequently carried out at this time point. In order to determine the cytoprotective effect of di-O-demethylcurcumin in A β_{25-35} -induced ER stress, the SK-N-SH cells were pretreated with various concentrations of

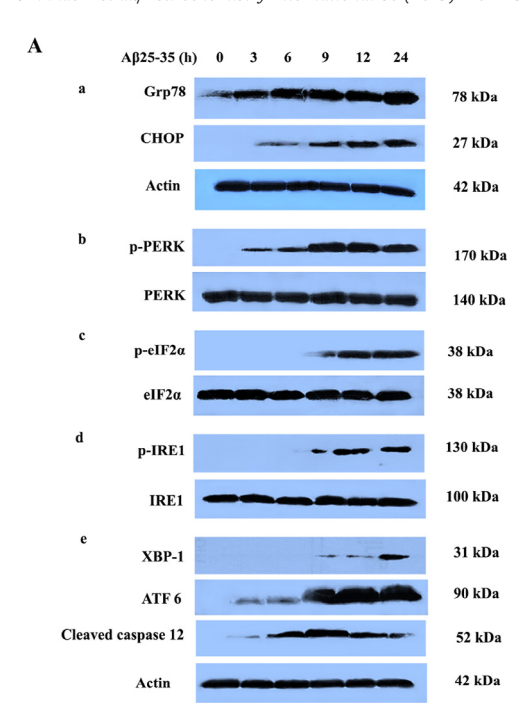


Fig. 4. Di-O-demethylcurcumin suppresses $A\beta_{25-35}$ -induced ER stress in SK-N-SH cells. **A:** SK-N-SH cells were treated with 10 μM $A\beta_{25-35}$ for 0 h, 3 h, 6 h, 9 h, 12 h, and 24 h. The expression of Grp78, p-PERK, p-eIF2α, eIF2α, p-IRE1, IRE1, XBP-1, ATF6, CHOP, cleaved caspase 12 protein were examined using the western blot analysis. The β-actin antibody was used as an internal control. **B:** A representative western blot showing the expression of p-PERK, p-eIF2α, eIF2α, p-IRE1, IRE1 and XBP-1 in SK-N-SH cells. The cells were pretreated with di-O-demethylcurcumin (at concentrations of 2 μM, 4 μM and 8 μM) for 2 h, which was followed by treatment with 10 μM of $A\beta_{25-35}$ for 24 h. a: The quantitative analysis of p-IRE1 was normalized to the eIF2α. c: The quantitative analysis of p-IRE1 was normalized to the IRE1. d: The quantitative analysis of $A\beta_{25-35}$ for 24 h. a: The cells were pretreated with di-O-demethylcurcumin (at concentrations of 2 μM, 4 μM and 8 μM) for 2 h, which was followed by treatment with 10 μM $A\beta_{25-35}$ for 24 h. a: The quantitative analysis of Grp78 was normalized to the $A\beta_{25-35}$ for 24 h. a: The quantitative analysis of Grp78 was normalized to the $A\beta_{25-35}$ for 24 h. a: The quantitative analysis of Grp78 was normalized to the $A\beta_{25-35}$ for 24 h. a: The quantitative analysis of Grp78 was normalized to $A\beta_{25-35}$ for 24 h. a: The quantitative analysis of Grp78 was normalized to $A\beta_{25-35}$ for 24 h. a: The quantitative analysis of Grp78 was normalized to $A\beta_{25-35}$ for 24 h. a: The quantitative analysis of Grp78 was normalized to $A\beta_{25-35}$ for 24 h. a: The quantitative analysis of Grp78 was normalized to $A\beta_{25-35}$ for 24 h. a: The quantitative analysis of Grp78 was normalized to $A\beta_{25-35}$ for 24 h. a: The quantitative analysis of Grp78 was normalized to $A\beta_{25-35}$ for 24 h. a: The quantitative analysis of Grp78 was normalized to $A\beta_{25-35}$ for 24 h. a: The quantitative analysis of Grp78 was normalized to $A\beta_{25-35}$ for 24 h. a: The quantitative an

di-O-demethylcurcumin (2 μ M, 4 μ M and 8 μ M) for 2 h, prior to A β_{25-35} activation. The expressions of the phosphorylated forms of eIF2 α , PERK, IRE1, and the expression of XBP-1, ATF6, CHOP, cleaved caspase-12 protein and Grp78, were observed to have significantly decreased (P<0.001) in a concentration-dependent manner (Fig. 4B,C). These data suggest that di-O-demethylcurcumin attenuated apoptosis through the ER stress pathway in SK-N-SH cells.

3.5. Effects of di-O-demethylcurcumin on $A\beta_{25-35}$ -induced mitochondria apoptosis pathway in SK-N-SH cells

An analysis was conducted to determine the protective effect of di-O-demethylcurcumin against $A\beta_{25-35}$ -induced mitochondrial death pathway in SK-N-SH cells. We investigated the expression of Bcl-X_L, Bax, cytochrome c, cleaved caspase-9 protein, and cleaved caspase-3 proteins at 0 h, 3 h, 6 h, 9 h, 12 h and 24 h in SK-N-SH cells activated using 10 μ M of A β_{25-35} . As presented in Fig. 5A, the expression of Bcl-X_L was found to have significantly decreased in a time-dependent manner (P < 0.001). On the other hand, the expression of Bax was observed to have significantly increased in a time-dependent manner (P < 0.001). The release of cytochrome c to cytosol was also found to have significantly increased (P < 0.001) in a time-dependent manner, with the maximum level being observed at the 12th h in the SK-N-SH cells activated by A β_{25-35} . Next, we carried out an investigation to confirm that the relevant mitochondria apoptosis pathway was affected by the overexpression of the cleaved caspase-9 protein and the cleaved caspase-3 protein, which shows the presence of the apoptosis cells. We found that both the cleaved caspase-9 protein and the cleaved caspase-3 protein had the optimal time of expression at the 24th h after the treatment with 10 μ M of A β_{25-35} (Fig. 5A). Pretreatment with various concentration of di-O-demethylcurcumin for 2 h prior to the treatment with 10 μ M of A $\beta_{25\text{-}35}$ was found to significantly increase (P<0.001) the Bcl-X_L/Bax ratio in a concentration-dependent manner (Fig. 5B,C). In addition, it was observed that di-O-demethylcurcumin also markedly decreased (P<0.001) the expression of cytochrome c, cleaved caspase-9 protein, and cleaved caspase-3 protein in a concentration-dependent manner (Fig. 5D,E,F).

4. Discussion

It is now well known that Aβ is neurotoxic and contributes to the pathogenesis of AD. The toxicity of AB is associated with senile plagues formed in AD brains, which is attributable to the amino acid located in position 25-35 of the full length length, containing the functional domain that is involved in the neurotoxic effects in AD (Kubo et al., 2002; Millucci et al., 2010). The $A\beta_{25-35}$ is widely used to as an experimental model of AD, thus, we implied that cultured SK-N-SH cells treated with $A\beta_{25-35}$ as used in the present study would provide a suitable approach to determine the effects of di-O-demethylcurcumin on AB toxicity. Previous studies have reported that Aβ induces oxidative stress by producing excessive amount of ROS (Shearman et al., 1994), which lead to cell membrane lipid destruction, DNA damage, oxidation of proteins, and, finally, apoptosis (Zawia et al., 2009). Thus, suppression of oxidative stress brings with it the benefit of preventing AD (Calabrese et al., 2008). Di-O-demethylcurcumin, a demethylated analog of curcumin, has been reported to be a strong anti-inflammatory agent greater than its parent compound, as demonstrated in our previous study (Tocharus et al., 2012). In this study, we further investigated the protective role of di-O-demethylcurcumin against $A\beta_{25-35}$ induced apoptosis mediated by mitochondrial death pathway and

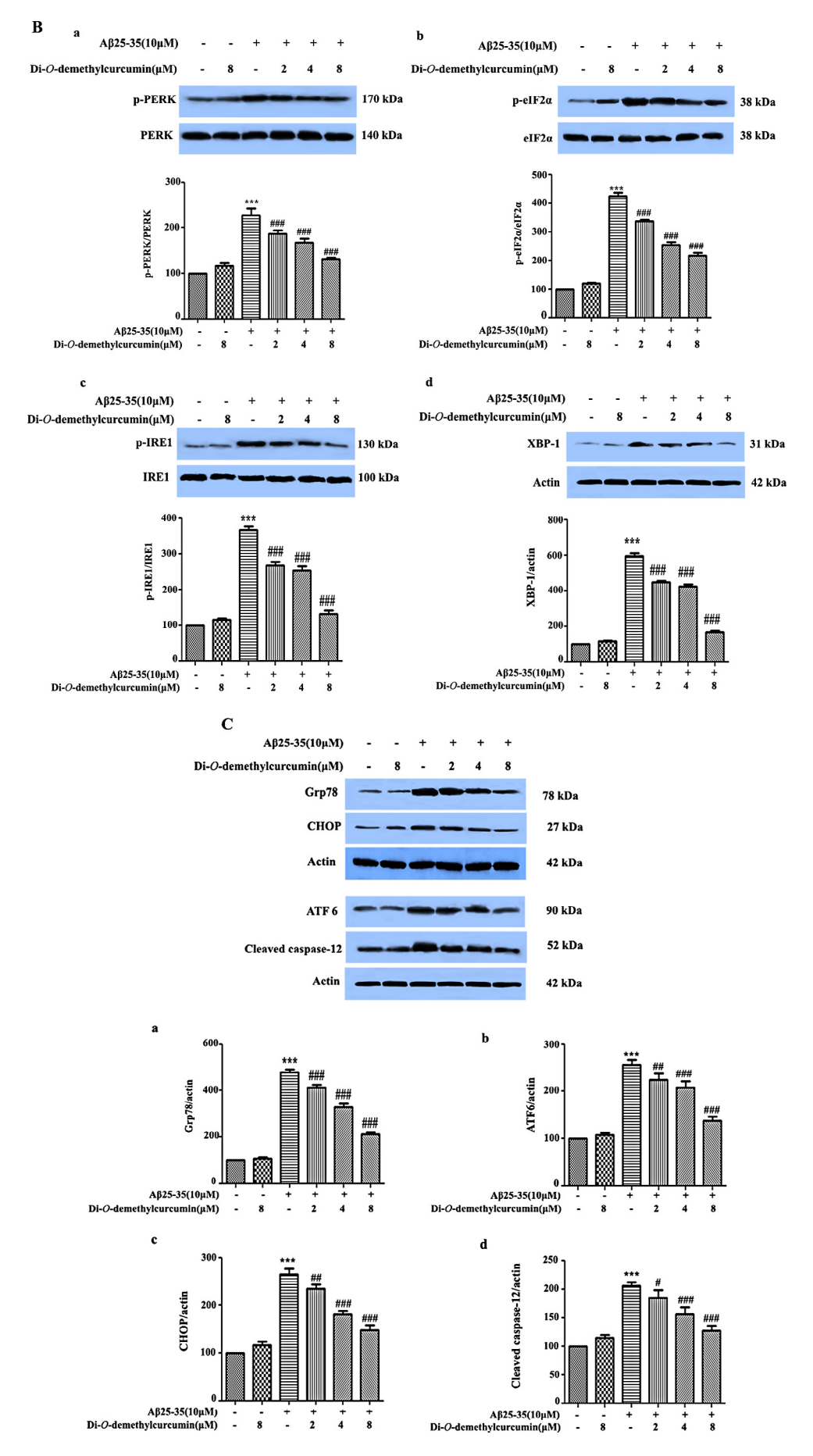


Fig. 4. (continued)

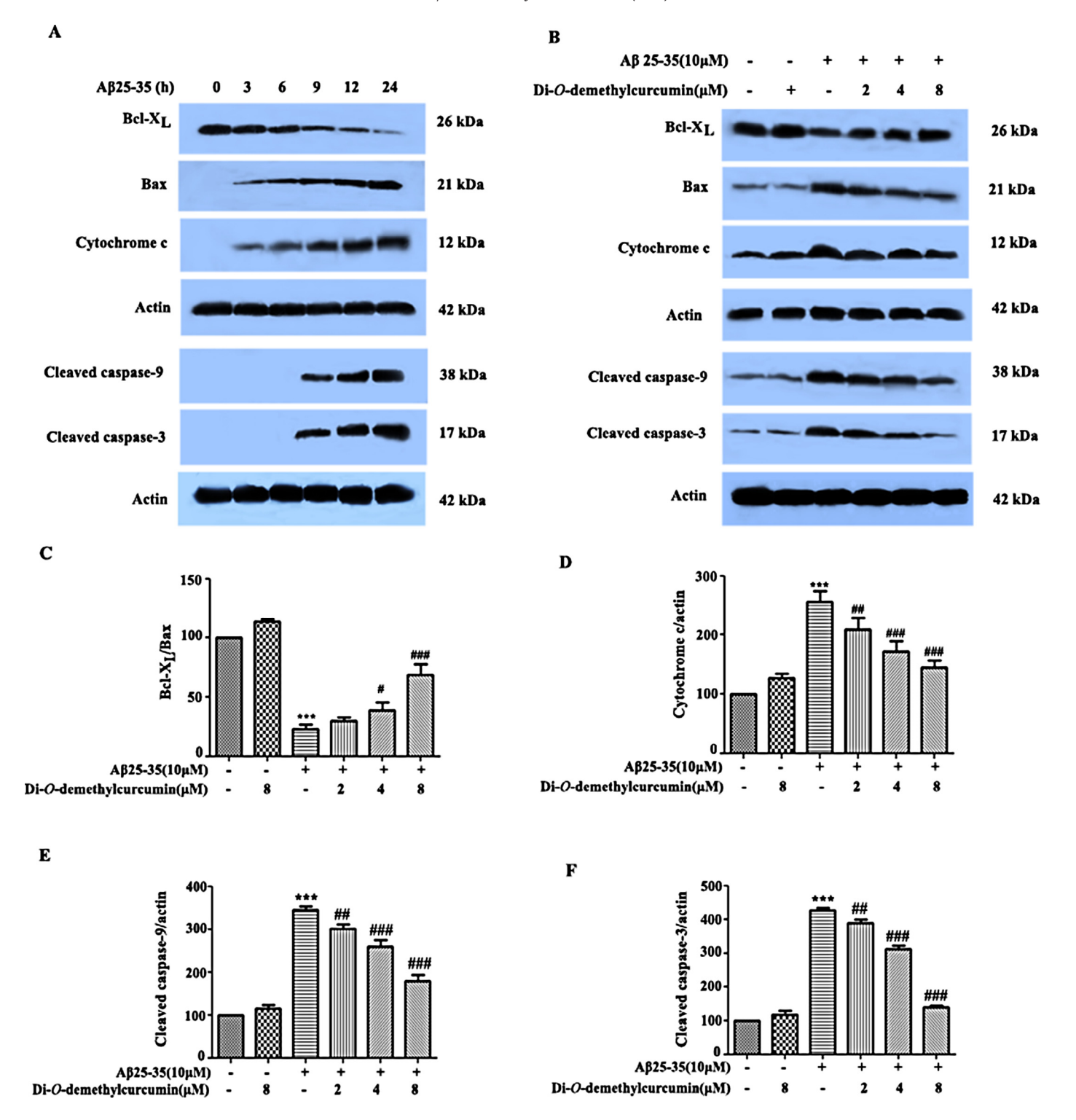


Fig. 5. The effects of di-O-demethylcurcumin on $Aβ_{25-35}$ -induced mitochondria apoptosis pathway in SK-N-SH cells. **A:** A representative western blot showing the expression of Bcl-X_L, Bax, cytochrome c, the cleaved caspase-9 protein and the cleaved caspase-3 protein. The SK-N-SH cells were treated with $10 \mu M$ $Aβ_{25-35}$ for 0 h, 3 h, 6 h, 9 h, 12 h, and 24 h. The β-actin antibody was used as an internal control. **B:** A representative western blot showing the expression of Bcl-X_L, Bax, cytochrome c, cleaved caspase-9 and cleaved caspase-3 protein in the SK-N-SH cells. The cells were pretreated with di-O-demethylcurcumin (at concentrations of $2 \mu M$, $4 \mu M$ and $8 \mu M$) for 2 h, which was followed by treatment with $10 \mu M$ of $Aβ_{25-35}$ for 24 h. **C:** The quantitative analysis of Bcl-X_L was normalized to the Bax. **D:** The quantitative analysis of cytochrome c was normalized to β-actin. **E:** The quantitative analysis of cleaved caspase-3 protein was normalized to β-actin. The values are presented as mean ± SD of three independent experiments. ***P < 0.001 vs. control group; **P < 0.05, **#P < 0.01, ***#P < 0.001 vs. group treated with $Aβ_{25-35}$ alone.

ER stress pathway. We first investigated A β_{25-35} -induced cytotoxicity in SK-N-SH cells using the MTS assay. It was observed that pretreatment with various concentrations of di-O-demethylcurcumin had markedly increased the cell viability in a concentration-

dependent manner. We next explored if di-O-demethylcurcumin has protective effects against A β_{25-35} -induced neuronal cell apoptosis. A β_{25-35} -treated cells were investigated using TEM, and the results of the investigation revealed typical morphological

features of apoptosis with chromatin condensation and nucleus fragmentation. We next carried out the quantitative analysis for the number of apoptotic cells using flow cytometry. The results showed that di-O-demethylcurcumin can protect SK-N-SH cells against Aβ-induced apoptosis. Simultaneously, we found out that $A\beta_{25-35}$ is able to induce mitochondrial dysfunction (Costa et al., 2012) as determined by its ability to increase ROS accumulation, whereas di-O-demethylcurcumin has the ability to reverse these events. A large number of experiments have demonstrated that Aβ₂₅₋₃₅ plays an important role in cell apoptosis mediated by mitochondrial death pathway and ER stress pathway (Alberdi et al., 2013; Costa et al., 2012; Takuma et al., 2005). It is well known that $A\beta_{25-35}$ induces mitochondria dysfunction by increasing the intracellular ROS production (Shearman et al., 1994), depolarizing the mitochondrial membrane, opening the mitochondrial permeability transition pore (MPTP), and inducing the release of cytochrome c, which, in turn, activates caspase-3 protein which plays an important role in cell apoptosis (Budihardjo et al., 1999; Manczak et al., 2010; Zhang and Armstrong, 2007). Our findings are consistent with previous reports showing that treatment with Aβ₂₅₋₃₅ induced mitochondrial dysfunction by increasing free radicals and reducing the mitochondrial membrane potential, thereby upregulating cytochrome c, caspase-9 protein and caspase-3 protein and downregulating the ratio of Bcl-X_L/Bax, and also that di-Odemethylcurcumin suppressed this activation (Budihardjo et al., 1999; Manczak et al., 2010; Zhang and Armstrong, 2007). Accumulations of ROS can result in oxidative stress, impairment of cell function, and apoptosis. It is a widely accepted fact that long periods of accumulation of unfolded protein in ER corresponds to apoptosis in AD (Boyce and Yuan, 2006). We therefore investigated the molecular events associated with A β_{25-35} -induced ER stress (Ferreiro et al., 2006). ER plays an important role in protein folding and modification. Protein biosynthesis in ER can be interfered with because of a variety of toxic conditions, including hypoxia, nutrient deprivation, Ca²⁺ overload, etc., which initiate the unfold protein response (UPR) that causes ER stress. ER stress triggers several specific signaling pathways, such as ER-associated protein degradation and UPR (Hoozemans et al., 2005). UPR is initiated by three ERresident transmembrane proteins known as sensors of ER stress (Ron and Walter, 2007), namely, PERK, ATF6 and IRE1, which are activated by the ER-resident chaperone glucose-regulated protein of 78 kDa (Grp78 or BiP) (Calfon et al., 2002; Kim et al., 2008). This study provides evidence that $A\beta_{25-35}$ activates ER stress signaling pathways in SK-N-SH cells, and that the induction of ER stress is implicated in $A\beta_{25-35}$ -induced apoptosis. We demonstrated that $A\beta_{25-35}$ induced the up-regulation of Grp78, p-PERK, p-elF2 α , and cleaved ATF6 α , and increased the expression of CHOP and the caspase-12 protein which are important apoptotic inducers. All the same, it was also demonstrated that pretreatment with di-Odemethylcurcumin suppressed the activation of ER stress signaling pathway by inhibiting the Grp78, p-PERK, p-elF2α, and cleaved ATF 6α , and also decreased the expression of CHOP and the caspase-12 protein. A number of studies have demonstrated that prolonged activation of ER stress can activate the expression of CHOP and the caspase-12 protein, the key mediators of ER stress-induced cell death pathways in AD (Chen et al., 2012; Paschen and Mengesdorf, 2005). CHOP, a transcription factor induced by ATF6, PERK or IRE1, regulates cell death by suppressing the expression of the Bcl-2 protein (Hacki et al., 2000; McCullough et al., 2001) as well as by increasing the Bax protein (Gotoh et al., 2004; Paradis et al., 1996). Additionally, caspase-12 protein is an ER stress specific protein which activates the caspase-9 protein (Ishige et al., 2007; Morishima et al., 2002), a process that would lead to the activation of the caspase-3 pathways during apoptosis in AD. Thus, this study confirms that increased levels of CHOP and caspase-12 protein in neuronal cells leads to ER-stress-associated apoptosis. Therefore, di-O-

demethylcurcumin-mediated inhibition of the CHOP and caspase-12 expression may be a key strategy in the efforts toward preventing ER stress-induced effects by $A\beta_{25-35}$.

In conclusion, it can be stated that the results here show that $A\beta_{25-35}$ -treated SK-N-SH cells undergo apoptosis and di-O-demethylcurcumin exerts neuroprotective, antioxidative and antiapoptotic effects by attenuating the mitochondrial death pathway and the ER stress pathway. Thus, the protective effects of di-O-demethylcurcumin against neuronal neurotoxins may help to provide the pharmacological basis of its clinical usage in the prevention or palliation of neurodegeneration in AD.

Acknowledgments

This work was supported by the Faculty of Medicine Research Fund, Chiang Mai University (grant no. 72/2557), and the Graduate School, Chiang Mai University, Chiang Mai, Thailand. Partial supports from The Thailand Research Fund (grant no. DBG5680006) and the Center of Excellence for Innovation in Chemistry, Office of the Higher Education Commission, are gratefully acknowledged.

References

- Alberdi, E., Wyssenbach, A., Alberdi, M., Sanchez-Gomez, M.V., Cavaliere, F., Rodriguez, J.J., et al., 2013. Ca(2+)-dependent endoplasmic reticulum stress correlates with astrogliosis in oligomeric amyloid beta-treated astrocytes and in a model of Alzheimer's disease. Aging Cell 12, 292–302.
- Aroonrerk, N., Changtam, C., Kirtikara, K., Suksamrarn, A., 2012. Inhibitory effects of di-*O*-demethylcurcumin on interleukin-1B-induced interleukin-6 production from human gingival fibroblasts. J. Dent. Sci. 7, 350–358.
- Bandgar, B.P., Kinkar, S.N., Chavan, H.V., Jalde, S.S., Shaikh, R.U., Gacche, R.N., 2014. Synthesis and biological evaluation of asymmetric indole curcumin analogs as potential anti-inflammatory and antioxidant agents. J. Enzyme Inhib. Med. Chem. 29, 7–11.
- Behl, C., Davis, J.B., Lesley, R., Schubert, D., 1994. Hydrogen peroxide mediates amyloid beta protein toxicity. Cell 77, 817–827.
- Belviranli, M., Okudan, N., Atalik, K.E., Oz, M., 2013. Curcumin improves spatial memory and decreases oxidative damage in aged female rats. Biogerontology 14, 187–196.
- Bhullar, K.S., Jha, A., Youssef, D., Rupasinghe, H.P., 2013. Curcumin and its carbocyclic analogs: structure-activity in relation to antioxidant and selected biological properties. Molecules 18, 5389–5404.
- Boyce, M., Yuan, J., 2006. Cellular response to endoplasmic reticulum stress: a matter of life or death. Cell Death Differ. 13, 363–373.
- Budihardjo, I., Oliver, H., Lutter, M., Luo, X., Wang, X., 1999. Biochemical pathways of caspase activation during apoptosis. Annu. Rev. Cell Dev. Biol. 15, 269–290.
- Butterfield, D.A., Reed, T., Newman, S.F., Sultana, R., 2007. Roles of amyloid beta-peptide-associated oxidative stress and brain protein modifications in the pathogenesis of Alzheimer's disease and mild cognitive impairment. Free Radic. Biol. Med. 43, 658-677.
- Calabrese, V., Cornelius, C., Mancuso, C., Pennisi, G., Calafato, S., Bellia, F., et al., 2008. Cellular stress response: a novel target for chemoprevention and nutritional neuroprotection in aging, neurodegenerative disorders and longevity. Neurochem. Res. 33, 2444–2471.
- Calfon, M., Zeng, H., Urano, F., Till, J.H., Hubbard, S.R., Harding, H.P., et al., 2002. IRE1 couples endoplasmic reticulum load to secretory capacity by processing the XBP-1 mRNA. Nature 415. 92–96.
- Changtam, C., de Koning, H.P., Ibrahim, H., Sajid, M.S., Gould, M.K., Suksamrarn, A., 2010. Curcuminoid analogs with potent activity against Trypanosoma and Leishmania species. Eur. J. Med. Chem. 45, 941–956.
- Chen, C.M., Wu, C.T., Chiang, C.K., Liao, B.W., Liu, S.H., 2012. C/EBP homologous protein (CHOP) deficiency aggravates hippocampal cell apoptosis and impairs memory performance. PLoS ONE 7, e40801.
- Chen, J.X., Yan, S.D., 2007. Amyloid-beta-induced mitochondrial dysfunction. I. Alzheimers Dis. 12. 177–184.
- Costa, R.O., Ferreiro, E., Martins, I., Santana, I., Cardoso, S.M., Oliveira, C.R., et al., 2012. Amyloid beta-induced ER stress is enhanced under mitochondrial dysfunction conditions. Neurobiol. Aging 33, 824.e5–e16.
- Dante, S., Hauss, T., Dencher, N.A., 2003. Insertion of externally administered amyloid beta peptide 25-35 and perturbation of lipid bilayers. Biochemistry 42, 13667–13672
- Ferreiro, E., Resende, R., Costa, R., Oliveira, C.R., Pereira, C.M., 2006. An endoplasmic-reticulum-specific apoptotic pathway is involved in prion and amyloid-beta peptides neurotoxicity. Neurobiol. Dis. 23, 669–678.
- Gotoh, T., Terada, K., Oyadomari, S., Mori, M., 2004. Hsp70-DnaJ chaperone pair prevents nitric oxide- and CHOP-induced apoptosis by inhibiting translocation of Bax to mitochondria. Cell Death Differ. 11, 390–402.

- Hacki, J., Egger, L., Monney, L., Conus, S., Rosse, T., Fellay, I., et al., 2000. Apoptotic crosstalk between the endoplasmic reticulum and mitochondria controlled by Bcl-2. Oncogene 19, 2286–2295.
- Hardy, J., Selkoe, D.J., 2002. The amyloid hypothesis of Alzheimer's disease: progress and problems on the road to therapeutics. Science 297, 353–356.
- Hauptmann, S., Keil, U., Scherping, I., Bonert, A., Eckert, A., Muller, W.E., 2006. Mitochondrial dysfunction in sporadic and genetic Alzheimer's disease. Exp. Gerontol. 41, 668–673.
- Hoozemans, J.J., Veerhuis, R., Van Haastert, E.S., Rozemuller, J.M., Baas, F., Eikelenboom, P., et al., 2005. The unfolded protein response is activated in Alzheimer's disease. Acta Neuropathol. 110, 165–172.
- Ishige, K., Takagi, N., Imai, T., Rausch, W.D., Kosuge, Y., Kihara, T., et al., 2007. Role of caspase-12 in amyloid beta-peptide-induced toxicity in organotypic hippocampal slices cultured for long periods. J. Pharmacol. Sci. 104, 46–55.
- Kim, I., Xu, W., Reed, J.C., 2008. Cell death and endoplasmic reticulum stress: disease relevance and therapeutic opportunities. Nat. Rev. Drug Discov. 7, 1013–1030.
- Kubo, T., Nishimura, S., Kumagae, Y., Kaneko, I., 2002. In vivo conversion of racemized beta-amyloid ([D-Ser 26]A beta 1-40) to truncated and toxic fragments ([D-Ser 26]A beta 25-35/40) and fragment presence in the brains of Alzheimer's patients. J. Neurosci. Res. 70, 474–483.
- Li, P., Nijhawan, D., Budihardjo, I., Srinivasula, S.M., Ahmad, M., Alnemri, E.S., et al., 1997. Cytochrome c and dATP-dependent formation of Apaf-1/caspase-9 complex initiates an apoptotic protease cascade. Cell 91, 479–489.
- Manczak, M., Mao, P., Calkins, M.J., Cornea, A., Reddy, A.P., Murphy, M.P., et al., 2010. Mitochondria-targeted antioxidants protect against amyloid-beta toxicity in Alzheimer's disease neurons. J. Alzheimers Dis. 20, s609–s631.
- McCullough, K.D., Martindale, J.L., Klotz, L.O., Aw, T.Y., Holbrook, N.J., 2001. Gadd153 sensitizes cells to endoplasmic reticulum stress by down-regulating Bcl2 and perturbing the cellular redox state. Mol. Cell. Biol. 21, 1249–1259.
- Millucci, L., Ghezzi, L., Bernardini, G., Santucci, A., 2010. Conformations and biological activities of amyloid beta peptide 25-35. Curr. Protein Pept. Sci. 11, 54-67.
- Morishima, N., Nakanishi, K., Takenouchi, H., Shibata, T., Yasuhiko, Y., 2002. An endoplasmic reticulum stress-specific caspase cascade in apoptosis: cytochrome c-independent activation of caspase-9 by caspase-12. J. Biol. Chem. 277, 34287–34294.
- Morsy, M.A., El-Moselhy, M.A., 2013. Mechanisms of the protective effects of curcumin against indomethacin-induced gastric ulcer in rats. Pharmacology 91, 267–274.
- Nakagawa, T., Zhu, H., Morishima, N., Li, E., Xu, J., Yankner, B.A., et al., 2000. Caspase-12 mediates endoplasmic-reticulum-specific apoptosis and cytotoxicity by amyloidbeta. Nature 403, 98–103.
- Paradis, E., Douillard, H., Koutroumanis, M., Goodyer, C., Le Blanc, A., 1996. Amyloid beta peptide of Alzheimer's disease downregulates Bcl-2 and upregulates bax expression in human neurons. J. Neurosci. 16, 7533–7539.

- Paschen, W., Mengesdorf, T., 2005. Endoplasmic reticulum stress response and neurodegeneration. Cell Calcium 38, 409–415.
- Ramalingam, M., Kim, S.J., 2012. Reactive oxygen/nitrogen species and their functional correlations in neurodegenerative diseases. J. Neural Transm. 119, 891–910.
- Rath, K.S., McCann, G.A., Cohn, D.E., Rivera, B.K., Kuppusamy, P., Selvendiran, K., 2013. Safe and targeted anticancer therapy for ovarian cancer using a novel class of curcumin analogs. J. Ovarian Res. 11, 35–47.
- Ron, D., Walter, P., 2007. Signal integration in the endoplasmic reticulum unfolded protein response. Nat. Rev. Mol. Cell Biol. 8, 519–529.
- Sandur, S.K., Pandey, M.K., Sung, B., Ahn, K.S., Murakami, A., Sethi, G., et al., 2007. Curcumin, demethoxycurcumin, bisdemethoxycurcumin, tetrahydrocurcumin and turmerones differentially regulate anti-inflammatory and anti-proliferative responses through a ROS-independent mechanism. Carcinogenesis 28, 1765– 1773.
- Schroder, M., Kaufman, R.J., 2005. The mammalian unfolded protein response. Annu. Rev. Biochem. 74, 739–789.
- Selkoe, D.J., 2001. Alzheimer's disease: genes, proteins, and therapy. Physiol. Rev. 81, 741–766.
- Shearman, M.S., Ragan, C.I., Iversen, L.L., 1994. Inhibition of PC12 cell redox activity is a specific, early indicator of the mechanism of beta-amyloid-mediated cell death. Proc. Natl. Acad. Sci. U.S.A. 91, 1470–1474.
- Sisodia, S.S., Annaert, W., Kim, S.H., De Strooper, B., 2001. Gamma-secretase: never more enigmatic. Trends Neurosci. 11, 2–6.
- Slee, E.A., Harte, M.T., Kluck, R.M., Wolf, B.B., Casiano, C.A., Newmeyer, D.D., et al., 1999. Ordering the cytochrome c-initiated caspase cascade: hierarchical activation of caspases-2, -3, -6, -7, -8, and -10 in a caspase-9-dependent manner. J. Cell Biol. 144. 281–292.
- Takuma, K., Yan, S.S., Stern, D.M., Yamada, K., 2005. Mitochondrial dysfunction, endoplasmic reticulum stress, and apoptosis in Alzheimer's disease. J. Pharmacol. Sci. 97, 312–316.
- Tocharus, J., Jamsuwan, S., Tocharus, C., Changtam, C., Suksamrarn, A., 2012. Curcuminoid analogs inhibit nitric oxide production from LPS-activated microglial cells. J. Nat. Med. 66, 400–405.
- Vembar, S.S., Brodsky, J.L., 2008. One step at a time: endoplasmic reticulum-associated degradation. Nat. Rev. Mol. Cell Biol. 9, 944–957.
- Venkateswarlu, S., Ramachandra, M.S., Subbaraju, G.V., 2005. Synthesis and biological evaluation of polyhydroxycurcuminoids. Bioorg. Med. Chem. 13, 6374–6380.
- Zawia, N.H., Lahiri, D.K., Cardozo-Pelaez, F., 2009. Epigenetics, oxidative stress, and Alzheimer disease. Free Radic. Biol. Med. 46, 1241–1249.
- Zhang, D., Armstrong, J.S., 2007. Bax and the mitochondrial permeability transition cooperate in the release of cytochrome c during endoplasmic reticulum-stress-induced apoptosis. Cell Death Differ. 14, 703–715.



Contents lists available at ScienceDirect

Bioorganic & Medicinal Chemistry Letters

journal homepage: www.elsevier.com/locate/bmcl



Synthesis and in vitro transfection efficiency of spermine-based cationic lipids with different central core structures and lipophilic tails



Nattisa Niyomtham ^a, Nuttapon Apiratikul ^b, Kanoknetr Suksen ^c, Praneet Opanasopit ^d, Boon-ek Yingyongnarongkul ^{a,*}

- ^a Department of Chemistry and Center of Excellence for Innovation in Chemistry, Faculty of Science, Ramkhamhaeng University, Bangkapi, Bangkok 10240, Thailand
- ^b Department of Chemistry, Faculty of Science, Siam University, Phasi-Charoen, Bangkok 10160, Thailand
- Department of Physiology and Research Center of Transport Proteins for Medical Innovation, Faculty of Science, Mahidol University, Bangkok 10400, Thailand
- d Pharmaceutical Development of Green Innovations Group (PDGIG), Faculty of Pharmacy, Silpakorn University, Nakhon Pathom 73000, Thailand

ARTICLE INFO

Article history: Received 12 August 2014 Revised 24 November 2014 Accepted 12 December 2014 Available online 19 December 2014

Keywords: Cationic lipids Gene delivery Spermine derivatives Solid phase synthesis

ABSTRACT

Twelve spermine-based cationic lipids with four different central core structures (di(oxyethyl)amino, di(oxyethyl)amino carboxy, 3-amino-1,2-dioxypropyl and 2-amino-1,3-dioxypropyl) and three hydrophobic tails (lauric acid, myristic acid and palmitic acid) were synthesized. The liposomes containing lipids and DOPE showed moderate to good in vitro DNA delivery into HeLa cells. GFP expression experiments revealed that liposomes composed of lipids with 3-amino-1,2-dioxypropyl as a central core structure exhibited highest transfection efficiency under serum-free condition. Whereas, lipid with 2-amino-1,3-dioxypropyl core structure showed highest transfection under 10% serum condition. Moreover, the liposomes and lipoplexes composted of these cationic lipids exhibited low cytotoxicity.

 $\ensuremath{\text{@}}$ 2015 Published by Elsevier Ltd.

Gene therapy has been receiving much attention due to its promise to prevent and treat many acquired and inherited diseases such as cancers, cystic fibrosis and AIDS. 1-3 Viruses are the most effective DNA delivery vehicle for gene therapy, but they suffer from a number of undesirable properties for therapeutic applications, such as uncertainties about safety, immunogenicity, limited packaging capacity for genetic material and manufacturing difficulties. Non-viral DNA delivery vehicles have, therefore, also been under development in an effort to overcome these barriers. There are many classes of compounds used for the non-viral delivery of DNA including cationic polymers, cationic peptides, cationic dendrimers and cationic lipids. 4

Cationic lipids are small molecules which can easily be designed and studied structure—activity relationships.^{5–7} Cationic lipids are commonly comprised of three main parts including polarhead, linker and lipophilic domain. Cationic lipids with double hydrocarbon chains as lipophilic tails have been widely studied and used as the non-viral gene delivery. These lipids usually have glycerol or aminoglycerol as central core structure.^{8–11} Since the first reported of cationic lipid having aminoglycerol backbone, *N*-[1-(2,3dioleol-

yloxy)propyl]-*N*,*N*,*N*-trimethylammonium chloride (DOTMA),⁸ numerous aminoglycerol-based cationic lipids have been synthesized for gene delivery. These include 1,2-dimyristyloxypropyl-3-dimethyl-hydroxyethyl ammonium bromide (DMRIE),⁹ 1,2-dioleoyloxypropyl-3-dimethyl-hydroxyethyl ammonium bromide (DORIE),⁹ *N*-(1-(2,3-dioleoyloxy)propyl)-*N*,*N*,*N*-trimethylammonium methyl sulfate (DOTAP)¹⁰ and 2,3-dioleyloxy-*N*-[2(spermine-carboxamido)ethyl]-*N*,*N*-dimethyl-1-propanaminium pentatrifluoroacetate (DOSPA).¹¹

Previously, structure–activity relationship study of cationic lipids having aminoglycerol as a central core structure has been investigated. The polarhead of aminoglycerol-based cationic lipids was mainly monocationic group. Naturally occurring polyamine, especially spermine, has been used as polarhead of numerous cationic lipids due to its ability to condense with DNA. However, the use of spermine as a polarhead of aminoglycerol-based cationic lipid has not been reported. Moreover, the central core structure of cationic lipid, rather than aminoglycerol, has not been much attention. We are therefore interested to synthesize new cationic lipids which exhibit high transfection efficiency. Thus, spermine-based cationic lipids bearing different central core structures including di(oxyethyl)amino (Ax–Az), di(oxyethyl)amino carboxy (Bx–Bz), 3-amino–1,2-dioxypropyl or aminoglycerol

^{*} Corresponding author. Tel.: +66 2 3190931; fax: +66 2 3191900. E-mail address: boonek@ru.ac.th (B.-e. Yingyongnarongkul).

(**Cx-Cz**) and 2-amino-1,3-dioxypropyl (**Dx-Dz**) (Fig. 1), together with different length of fatty acid tails have been synthesized and evaluated their transfection efficiency in HeLa cells.

Since the highly polar nature of polyamine-based cationic lipids, the final products were difficult to purify and they were usually obtained in low overall yields. 16,17 The synthesis of these lipids in solution is a laborious task since it involves extensive use of protective group strategy and requires tedious purification steps due to the polarity of the compounds. Solid phase organic synthesis has emerged as a powerful technology with several advantages including simplification of reaction procedures, easy separation of supported species and products and application to automation system. We then desired to use the solid phase synthesis to construct the spermine-based cationic lipids with various central core structure and different chain length of fatty acids.

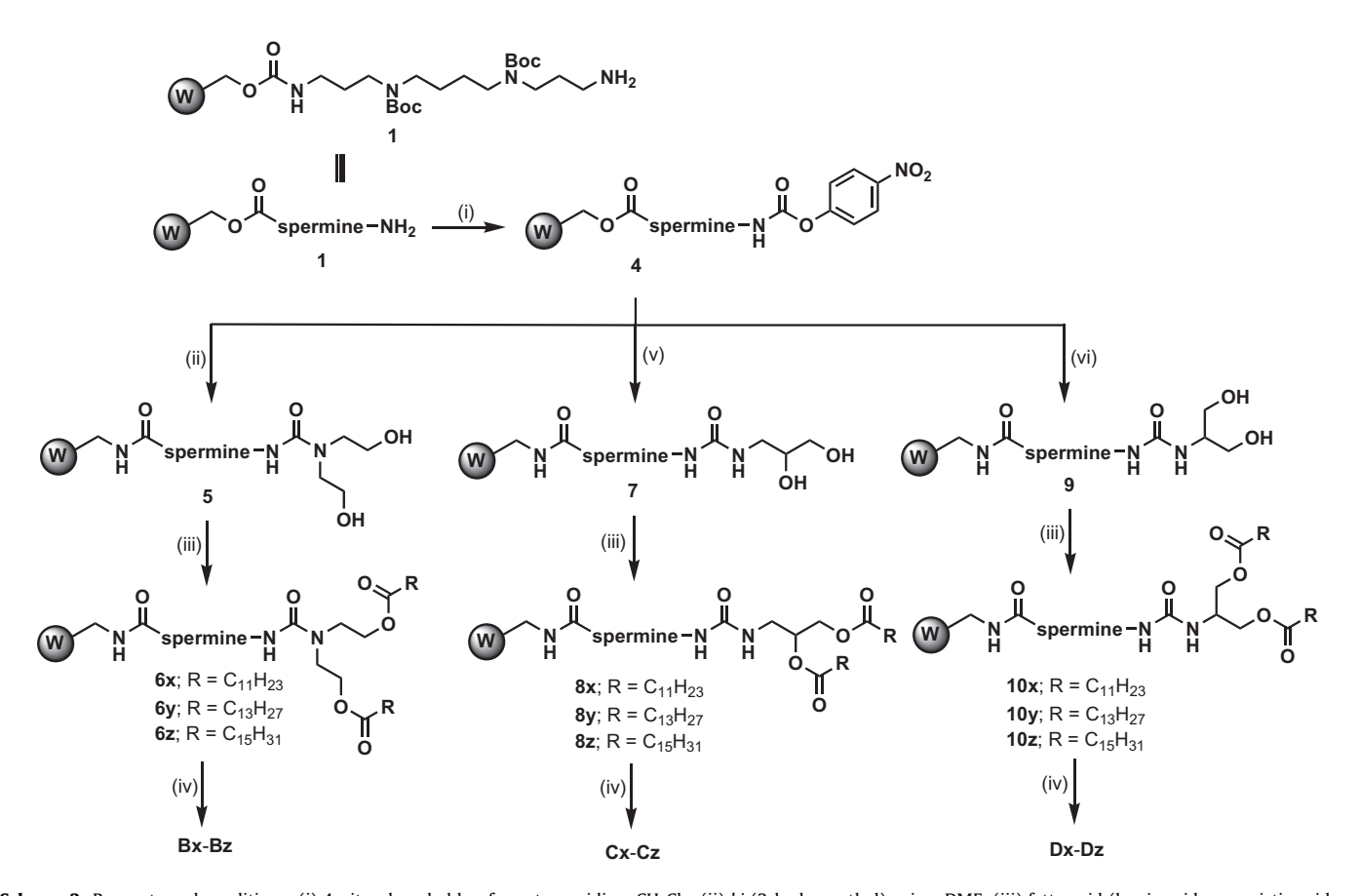
Our approach to generate a spermine-based cationic lipids library via solid phase parallel synthesis is shown in Schemes 1 and 2. Spermine was anchored on the Wang resin following literature method^{15b} with some modification to give the resin **1**. Reaction of the resin-bound protected-spermine 1 with 2-bromoethanol using diisopropylethylamine (DIPEA) as a base yielded the diol resin 2. Three different fatty acids (lauric acid, myristic acid and palmitic acid) were separately coupled with the diol resin 2 using diisopropylcarbodiimide (DIC) as coupling agent to generate compounds 3x-3z. The tert-butyloxycarbonyl (Boc) protection groups were removed and the lipids Ax-Az were cleaved from the solid support by trifluoroacetic acid (TFA) in CH₂Cl₂. The lipids Bx-Dz were also synthesized from the resin 1 through the active carbamate resin 4 (Scheme 2). The readily available agents, bis (2-hydroxyethyl)amine, 3-amino-1,2-propanediol and 2-amino-1,3-propanediol, were used to generate lipids having di(oxyethyl)aminocarboxy (lipids Bx-Bz), 3-amino-1,2-dioxypropyl (lipids **Cx–Cz**) and 2-amino-1,3-dioxypropyl (lipids **Dx–Dz**) core structures, respectively. Thus, the primary amino group of the resin **1** was reacted with 4-nitrophenylchloroformate to generate the active carbamate resin **4**. The resins **5**, **7** and **9** were generated by replacing 4-nitrophenol with bis(2-hydroxyethyl)amine, (\pm)-3-amino-1,2-propanediol and 2-amino-1,3-propanediol, respectively. The hydroxyl groups of resins **5**, **7** and **9** were then coupled with various fatty acids followed by treatment with TFA in CH₂Cl₂ to obtain lipids **Bx–Dz**. The synthesized lipids **Ax–Dz** were obtained as TFA salts and were directly used for further studies.

In order to determine the effect of central core structures and the chain length of hydrophobic tails of liposomes Ax-Dz on the ability to form complex with DNA, they were mixed with DNA at weight ratios of 5, 10 and 20. The lipoplexes formation was monitored by gel electrophoresis. As shown in Figure 2, all the cationic liposomes could bind with DNA to form lipoplexes. Liposomes Av. Az. Bx-Bz. Cx-Cz. Dx and Dv completely bound DNA using liposome/DNA ratio of 5. For the liposomes Ax and Dz, the liposome/ DNA ratio had to be increased to 10 and 20, respectively. Liposomes Ax with di(oxyethyl)amino core structure and lauric acid tails did not bind DNA at liposome/DNA weight ratio of 5. In contrast, liposome Dz with 2-amino-1,3-dioxypropyl core structure did not bind DNA at the liposome/DNA weight ratio lower than 10 when the longer hydrocarbon chains was used as lipophilic tails. Results in Figure 2, it was suggested that the central core structures and the chain length of the tails of spermine-based cationic lipids would affect the DNA binding ability.

Further investigations of the particle size and zeta potentials of the liposomes and liposomes/DNA complexes, dynamic light scattering assay was utilized across the entire liposomes/DNA weight ratios of 2–40. As shown in Figure 3a, the particle size of the liposomes are around 500–700 nm. The fully DNA condensation to

Figure 1. Structures of cationic lipids having different central core structures and lipophilic tails.

Scheme 1. Reagents and conditions: (i) 2-bromoethanol (20 equiv), DIPEA, DMF; (ii) fatty acids (lauric acid or myristic acid or palmitic acid) (6 equiv), DIC (6 equiv), DMAP (cat. amount), CH₂Cl₂/DMF (1:1); (iii) 20% TFA/CH₂Cl₂.



Scheme 2. Reagents and conditions: (i) 4-nitrophenyl chloroformate, pyridine, CH₂Cl₂; (ii) bis(2-hydroxyethyl)amine, DMF; (iii) fatty acid (lauric acid or myristic acid or palmitic acid) (6 equiv), DIC (6 equiv), CH₂Cl₂/DMF (1:1); (iv) 20% TFA/CH₂Cl₂; (v) (±)-3-amino-1,2-propanediol, DMF; (vi) 2-amino-1,3-propanediol, DMF.

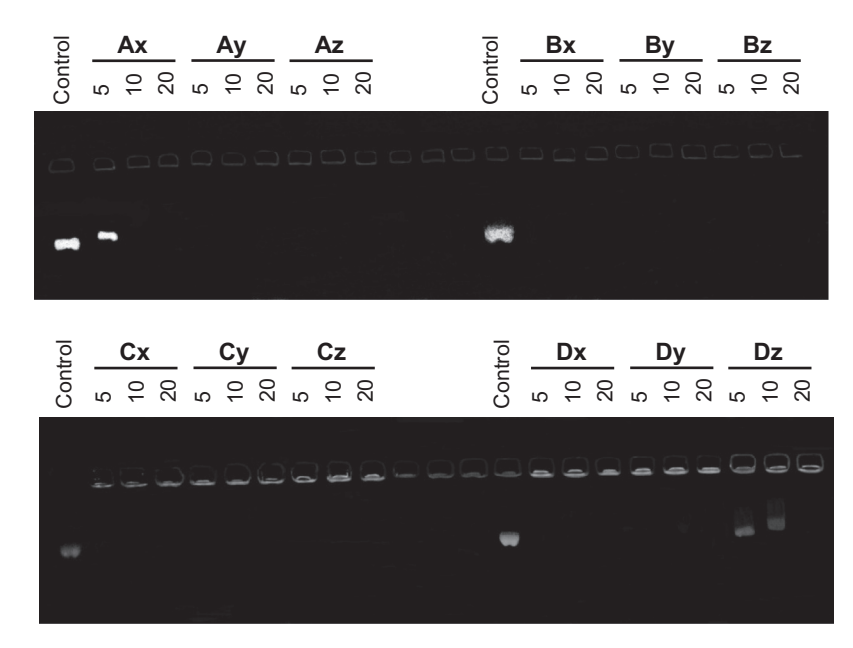


Figure 2. Electrophoretic gel retardation assays of cationic liposomes/DNA complexes at weight ratios of 5, 10 and 20.

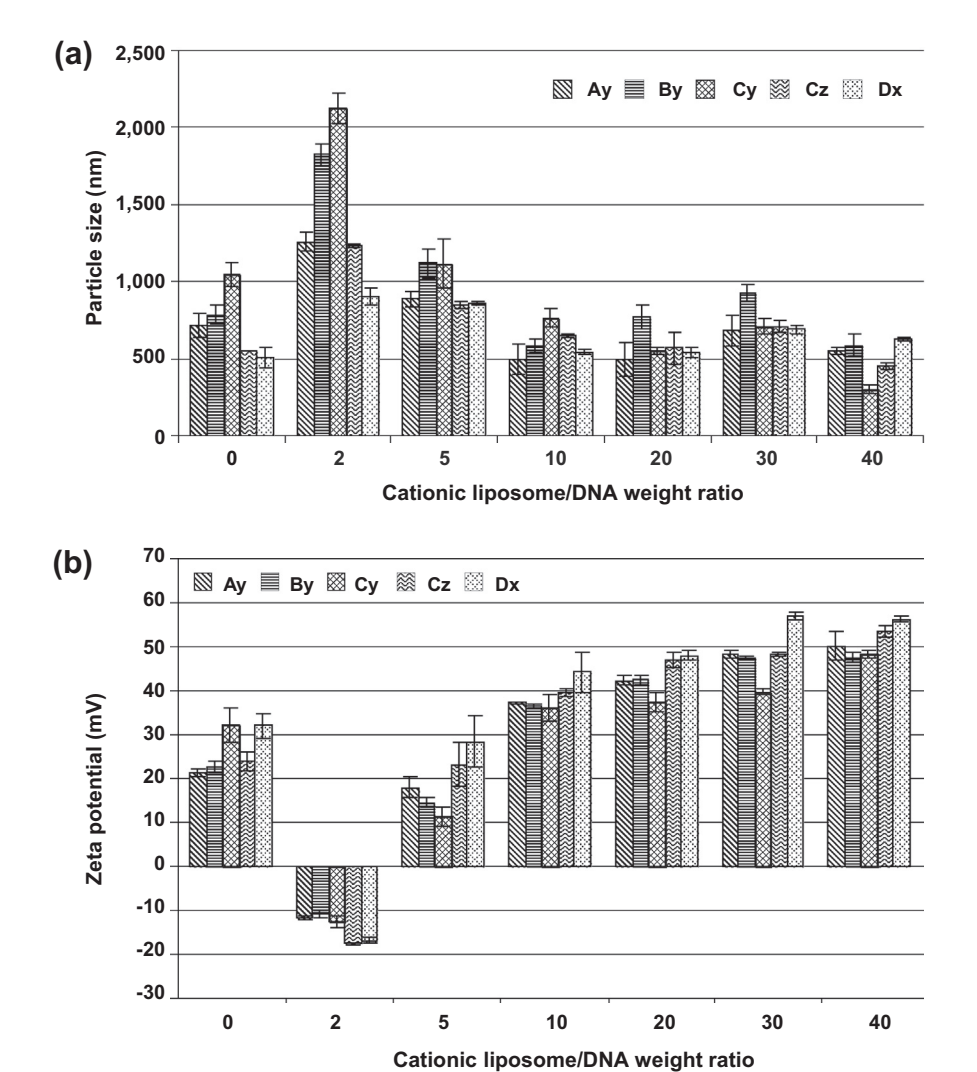


Figure 3. (a) Mean particle size and (b) zeta potential of the lipoplexes formed from each lipid under various liposomes/DNA weight ratios. Each value represents the mean ± standard deviation of three measurements.

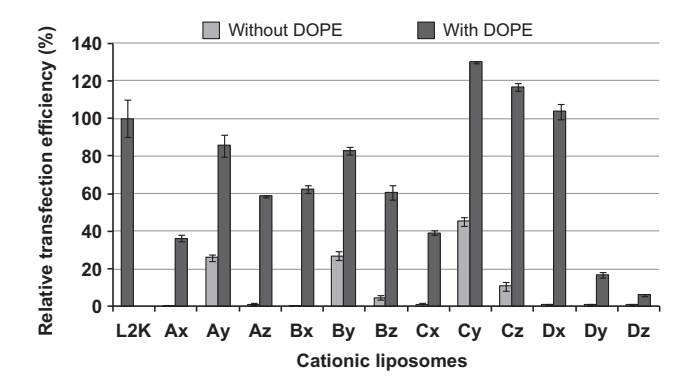


Figure 4. Relative transfection efficiency (%) of each cationic liposomes relative to LipofectamineTM 2000 (L2K). Cationic liposomes were mixed with plasmid DNA (β-Gal, 0.1 μ g/ μ L per well) at weight ratios (cationic lipid/DNA) of 20 and used for transfection into HeLa cells.

form lipoplexes was observed at liposomes/DNA weight ratio of 10. At this point, the diameters of the lipoplexes were found to be approximately 500–700 nm. The zeta potential, which is a measure of the electrical field of cationic liposomes in an aqueous environment, is one of the important factors that controls their DNA binding ability. High zeta potential is preferred for higher DNA binding ability. It was found that the zeta potentials of the liposomes were around 20–30 mV (Fig. 3b). The zeta potential of the lipoplexes increased along with the increase of liposome/DNA ratio and surface charges of the complete lipoplexes formation were found to be 37–45 mV. Most of the cell membranes usually show negative charge, hence the high positively charged lipoplexes will significantly enhance the interaction between lipoplexes and cells and facilitate cellular uptake.

In order to evaluate the transfection efficiency of synthesized lipids, the plasmid DNA encoding β -galactosidase as a reporter gene and *ortho*-nitrophenyl- β -galactoside (ONPG) as a substrate were used. This method allowed rapid identifies the lead compounds from the library synthesis. This Helper lipid, usually dioleoylphosphatidyl ethanolamine (DOPE) or cholesterol, is often used in the combination of cationic lipid to form liposome with optimal transfection efficiency. Thus, cationic liposomes are formed from either individual cationic lipid or with a combination

of neutral lipid, DOPE, at weight ratio of 1:1. Lipoplexes composed of each cationic liposomes and DNA were prepared at the liposomes/DNA weight ratio of 20 with the DNA concentration of 0.1 µg per well. The lipoplexes were then transfected into HeLa cells in 96-well plate format. The transfection efficiency of cationic liposomes was evaluated in comparison with the commercially available transfection reagent, Lipofectamine™ 2000. The transfection activity of each cationic liposome was reported as percentage relative transfection efficiency to that of the Lipofectamine™ 2000 control. The transfection results are shown in Figure 4. It was found that liposome formation with a combination of lipid and DOPE exhibited much higher transfection efficiency than the liposome formation with lipid alone. It has been suggested that DOPE play a role in facilitating the disassembly of the lipid-based DNA formulations after their internalization, and the escape of DNA from the endocytotic vesicle.¹⁹ Cationic lipids **Cy** and **Cz** with 3-amino-1, 2-dioxypropyl core structure and **Dx** having 2-amino-1.3-dioxypropyl core structure gave relative transfection levels of 130%, 117% and 104%, respectively, to delivery DNA into HeLa cells (Fig. 4). Compounds Ay, Az, Bx-Bz, were also identified as active transfection agents, but the levels of gene expression were slightly lower than those for Cy, Cz and Dx.

The results revealed that the central core structure of sperminebased cationic lipids is essential factor to affect the transfection efficiency. The chain length of fatty acid is also important for this class of lipid to exhibit high transfection. The chain length of 14-carbon tail (myristic acid) was optimal for most of the lipids, except Dx, which required shorter hydrocarbon chain for high transfection efficiency. To obtain absolute transfection efficiency, the green fluorescence protein (GFP) expression of liposomes containing lipids Av, By, Cy, Cz and Dx were examined using plasmid DNA encoding GFP as a reporter gene. One of the major drawbacks of cationic lipids for their in vivo applications is the inhibition of the transfection efficiency of cationic liposomes in the presence of serum. Most of cationic lipids which exhibited high transfection activity in the absence of serum lost their efficiency when transfected in the presence of serum.^{7,20} The transfection experiment was performed under serum free and with 10% serum conditions. The transfection efficiency of synthesized cationic lipids was compared with Lipofectamine™ 2000 by observing the transfected cells under fluorescence microscope (Fig. 5) and the transfected cells were counted. The transfection activity was reported as number

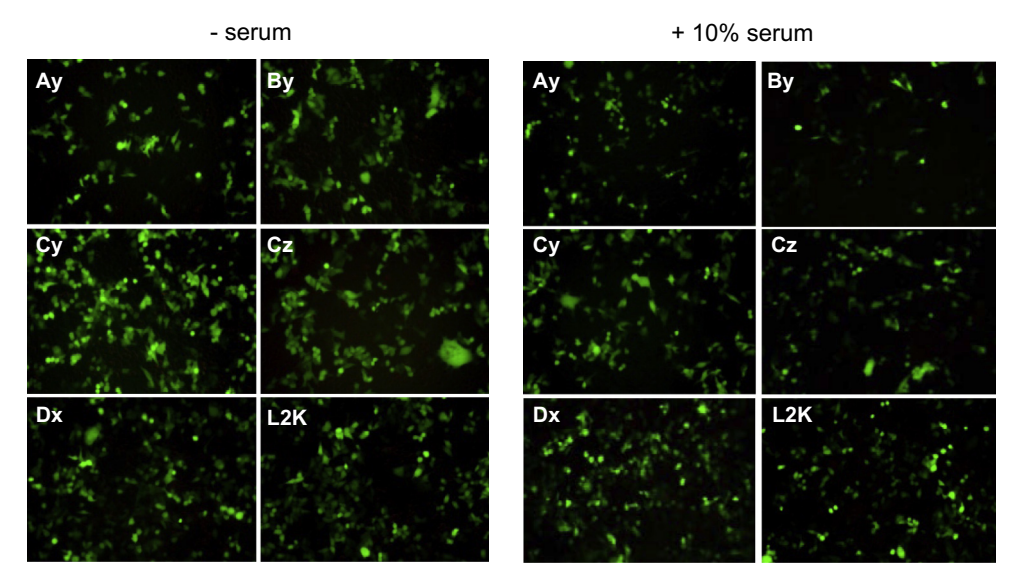


Figure 5. Expression of GFP using lipids Ay, By, Cy, Cz, Dx and Lipofectamine™ 2000 (L2K) under serum-free and 10% serum conditions. The lipoplexes was used at liposomes/DNA weight ratio of 20.

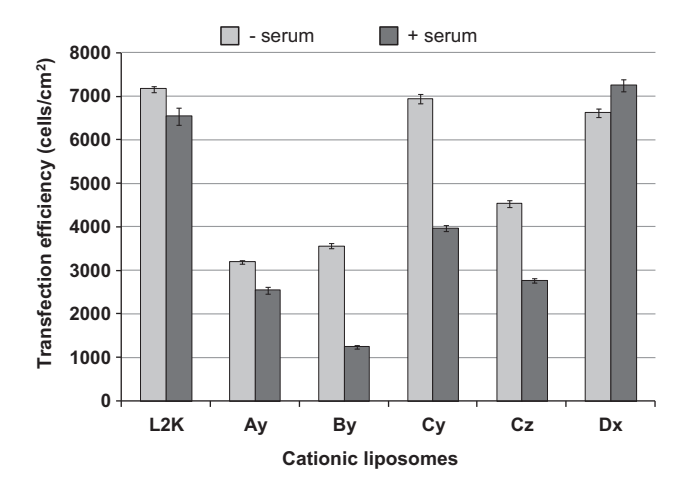


Figure 6. In vitro transfection efficiency of liposomes/DNA weight ratio of 20 in HeLa cells. The transfected cells were counted under fluorescence microscope. Each value represents the mean ± standard deviation of three wells.

of transfected cells per square centimeter (cells/cm²) (Fig. 6). As shown in Figures 5 and 6, lipids Cy²¹ (6947 ± 104 cells/cm²) and Dx²¹ (6629 ± 97 cells/cm²) showed comparable in vitro transfection efficiency to that of Lipofectamine™ 2000 (7165 ± 75 cells/cm²) under serum-free condition. Interestingly, lipid Dx having 2-amino-1,3-dioxypropyl core structure gave slightly higher transfection efficiency in the presence of 10% serum. The remaining lipids exhibited lower efficiency under serum-containing condition. As shown in Figure 6, the transfection efficiency of Lipofectamine™ 2000 (6546 ± 195 cells/cm²) under 10% serum condition was slightly lower than that under serum-free media. It has been

reported that size of the lipoplexes may be one of the factors contributing the serum resistance. Large lipoplexes (>700 nm) showed transfection efficiency in the presence or absence of serum, but small lipoplexes (<250 nm) exhibited transfection efficiency only in the absence of serum. The liposome **Dx**/DNA weight ratio of 20 formed large lipoplexes (539 ± 34 nm) which showed high transfection efficiency both under serum-free and 10% serum conditions. However, lipoplexes composed of liposome **Cy**/DNA at weight ratio of 20 which was larger size (560 ± 177 nm) than that of **Dx** exhibited lower transfection efficiency under 10% serum. Thus, the central core structure of cationic lipid may be one of the factors that causes high transfection efficiency under serum-containing condition.

The exonucleolytic degradation of deoxy oligonucleotide by serum has been previously reported.²⁴ Cationic liposome²⁴ and some other gene delivery carriers^{25,26} have been used to protect deoxy oligonucleotide from nuclease degradation. To see whether cationic lipids Cy and Dx have such properties to protect DNA degradation, the liposomal and free DNA were incubated with 10% fetal bovine serum at 37 °C for various time intervals. The incubation of the free DNA with 10% serum resulted in complete DNA degradation within 8 h (Fig. 7a). As shown in Figure 7b and d, only the control band can be seen when liposomal DNA was incubated with 10% serum up to 24 h. The results indicated that these liposomes were fully condensed DNA and stable under serum condition. After liposome/DNA complexes were broken by treating with 0.5% SDS, the encapsulated DNA was released from the liposomes and DNA bands were observed (Fig. 7c and e). It was found that the intensity of all released DNA bands close to that of the control DNA. To this end, both liposomes Cy and Dx could protect DNA from serum-mediate degradation even after 24 h. The serum stability of Lipofectamine™ 2000 to protect DNA degradation was

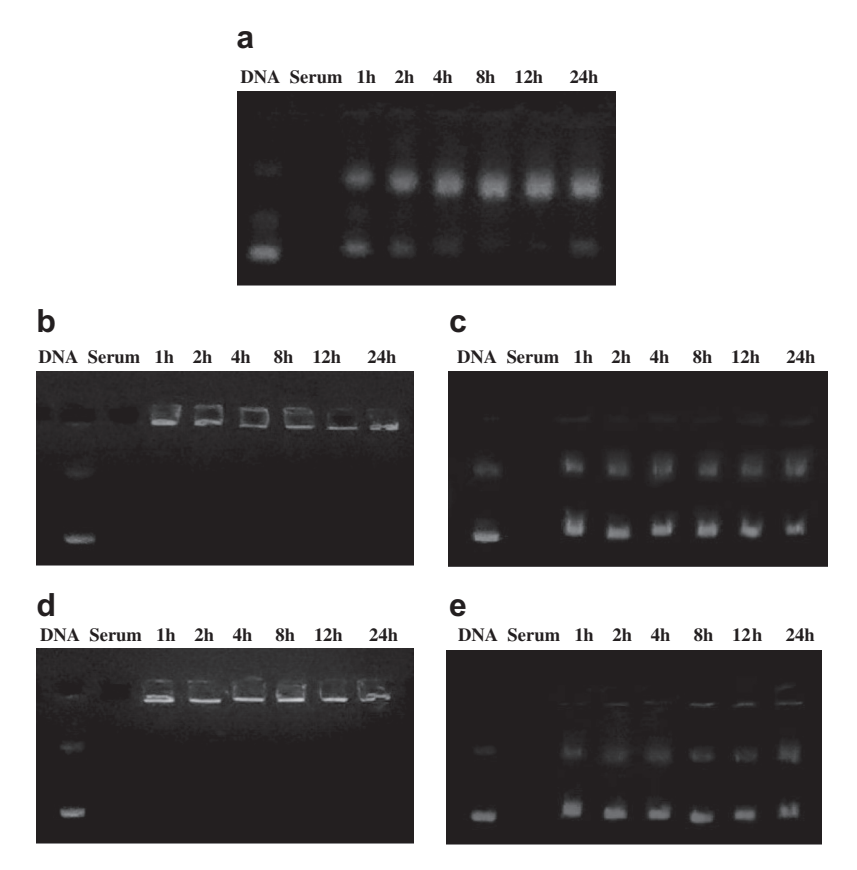


Figure 7. Serum stability of DNA in different lipid preparations. (a) Free DNA treated with 10% serum, (b) liposome **Cy**/DNA complexes and (c) after treated with 0.5% SDS at 37 °C for 10 min, (d) liposome **Dx**/DNA complexes and (e) after treated with 0.5% SDS at 37 °C for 10 min.

Table 1Relative cell viability of cationic liposomes in HeLa cells (% ± SD)

		Liposomes/DNA weight ratio					
		5	10	20	30	40	50
Control	100 ± 3.1						
Lipofectamine™ 2000	89.2 ± 0.3						
Cy/DOPE (1:1)		102.0 ± 0.3	100.5 ± 1.9	102.8 ± 1.1	100.6 ± 0.1	97.8 ± 1.2	95.4 ± 2.9
Cz/DOPE (1:1)		102.8 ± 0.1	107.0 ± 2.6	102.4 ± 0.7	98.8 ± 3.3	93.3 ± 0.1	86.6 ± 0.6
Dx /DOPE (1:1)		97.8 ± 1.4	90.8 ± 0.3	81.8 ± 0.5	80.7 ± 0.9	74.4 ± 0.8	70.6 ± 0.1

not performed in this study. However, having a report revealed that Lipofectamine $^{\text{TM}}$ 2000 cannot protect siRNA from degradation for longer times under serum condition. 24

Since toxicity of the gene carrier must be concerned prior to development for in vivo application. The cytotoxicity of cationic liposomes and lipoplexes was performed by measuring changes in cell metabolic activity (MTT assay)²⁷ on HeLa cells. The results are shown as percentage cell viability as compared to the control cells in the presence of DNA. As could be seen from Table 1, the central core of cationic lipids is an important factor to affect the cytotoxicity. The cell viability of cationic liposomes Cy and Cz having aminoglycerol as a central core structure was above 85%. Whereas, the cytotoxicity of caionic liposomes $\mathbf{D}\mathbf{x}$ with 2-amino-1,3-propanediol as core structure was relatively higher. The cell viability at the liposome/DNA weight ratio of 50 was about 70%. However, the cell viability at the liposome/DNA weight ratio of 20, which showed comparable or greater transfection efficiency than Lipofectamine™ 2000 was above 80%. It is thus concluded that spermine-based cationic lipids can produce high levels of transfection without inducing significant cell death. Most importantly, lipid $\mathbf{D}\mathbf{x}$ was compatible for serum condition that make it promising non-viral transfection vector for further in vivo study.

In conclusion, a series of spermine-based cationic lipids having different central core structures and lipophilic tails were synthesized and their structure-activity relationships were studied. The cationic liposomes comprised of cationic lipid Cy having 3-amino-1,2-dioxypropyl core structure and helper lipid, DOPE, showed high transfection efficiency to deliver DNA into HeLa cells. Most of the cationic liposomes decrease the transfection efficiency and intracellular gene expression under serum-containing condition. However, lipid Dx with 2-amino-1,3-dioxypropyl core structure effectively delivered DNA into HeLa cells in the presence of serum. We hope that the strategy illustrated here is useful for the development of cationic lipid-based gene delivery. Transfection biology and physical characterization of these lipids are now under investigation. It was also suggested that investigation of further compounds containing different central core structures for their transfection potency is warranted.

Acknowledgments

This work was supported by Office of the Higher Education Commission (OHEC), Ministry of Education and The Thailand Research Fund (TRF) (RMU5480003). N.N. acknowledges the Royal Golden Jubilee PhD program of TRF for studentship (Grant No. PHD/0217/2552). Supports from TRF (DBG5680006) and the Center of Excellence for Innovation in Chemistry (PERCH-CIC), OHEC, Ministry of Education are gratefully acknowledged.

Supplementary data

Supplementary data associated with this article can be found, in the online version, at http://dx.doi.org/10.1016/j.bmcl.2014.12. 043.

References and notes

- Yang, Z. R.; Wang, H. F.; Zhao, J.; Peng, Y. Y.; Wang, J.; Guinn, B.-A.; Huang, L. Q. Cancer Gene Ther. 2007, 14, 599.
- Caplen, N. J.; Alton, E. W.; Middleton, P. G.; Dorin, J. R.; Stevenson, B. J.; Gao, X.; Durham, S. R.; Jeffery, P. K.; Hodson, M. E.; Coutelle, C.; Huang, L.; Porteous, D. J.; Williamson, R.; Geddes, D. M. Nat. Med. 1995, 1, 39.
- 3. El-Aneed, A. J. Control. Release 2004, 94, 1.
- 4. Mintzer, M. A.; Simanek, E. E. Chem. Rev. 2009, 109, 259.
- Kim, B.-K.; Doh, K.-O.; Nam, J. H.; Kang, H.; Park, J.-G.; Moon, I.-J.; Seu, Y.-B. Bioorg. Med. Chem. Lett. 2009, 19, 2986.
- Zhang, Q.-F.; Yang, W.-H.; Yi, W.-J.; Zhang, J.; Ren, J.; Luo, T.-Y.; Zhu, W.; Yu, X.-Q. Bioorg. Med. Chem. Lett. 2011, 21, 7045.
- (a) Yingyongnarongkul, B.; Radchatawedchakoon, W.; Krajarng, A.; Watanapokasin, R.; Suksamrarn, A. Bioorg. Med. Chem. 2009, 17, 176; (b) Radchatawedchakoon, W.; Watanapokasin, R.; Krajarng, A.; Yingyongnarongkul, B. Bioorg. Med. Chem. 2010, 18, 330; (c) Radchatawedchakoon, W.; Krajarng, A.; Niyomtham, N.; Watanapokasin, R.; Yingyongnarongkul, B. Chem. Eur. J. 2011, 17, 3287.
- Felgner, P. L.; Gadex, T. R.; Holm, M.; Roman, R.; Chan, H. W.; Wenz, M.; Northrop, J. P.; Ringold, G. M.; Danielsen, M. Proc. Natl. Acad. Sci. U.S.A. 1987, 84, 7413
- Felgner, J. H.; Kumar, R.; Sridhar, C. N.; Wheeler, C. J.; Tsai, Y. J.; Border, R.; Ramsey, P.; Martin, M.; Felgner, P. L. J. Biol. Chem. 1994, 269, 2550.
- 10. Leventis, R.; Silvius, J. R. Biochim. Biophys. Acta 1990, 1023, 124.
- 11. Gebeyehu, G.; Jessee, J. A.; Ciccarone, V. C.; Hawley-Nelson, P.; Chytil, A. U.S. Patent 5,334,761, 1994.
- Heyes, J. A.; Niculescu-Duvaz, D.; Cooper, R. G.; Springer, C. J. J. Med. Chem. 2002, 45, 99.
- Liu, D.; Qiao, W.; Li, Z.; Chen, Y.; Cui, X.; Li, K.; Yu, L.; Yan, K.; Zhu, L.; Guo, Y.; Cheng, L. Chem. Biol. Drug Des. 2008, 71, 336.
- Zhi, D.; Zhang, S.; Qureshi, F.; Zhao, Y.; Cui, S.; Wang, B.; Chen, H.; Wang, Y.;
 Zhao, D. Bioorg. Med. Chem. Lett. 2012. 22. 3837.
- (a) Blagbrough, I. S.; Al-Hadithi, D.; Geall, A. J. Tetrahedron 2000, 56, 3439; (b) Oliver, M.; Jorgensen, M. R.; Miller, A. Tetrahedron Lett. 2004, 45, 3105; (c) Randazzo, R. A. S.; Bucki, R.; Janmey, P. A.; Diamond, S. L. Bioorg. Med. Chem. 2009, 17, 3257; (d) Maslov, M. A.; Medvedeva, D. A.; Rapoport, D. A.; Serikov, R. N.; Morozova, N. G.; Serebrennikova, G. A.; Vlassov, V. V.; Zenkova, M. A. Bioorg. Med. Chem. Lett. 2011, 21, 2937; (e) Markov, O. O.; Mironova, N. L.; Maslov, M. A.; Petukhov, I. A.; Morozova, N. G.; Vlassov, V. V.; Zenkova, M. A. J. Control. Release 2012, 160, 200; (f) Byk, G.; Dubertret, C.; Escriou, V.; Frederic, M.; Jaslin, G.; Rangara, R.; Pitard, B.; Crouzet, J.; Wils, P.; Schwartz, B.; Scherman, D. J. Med. Chem. 1998, 41, 224; (g) Byk, G.; Wetzer, B.; Frederic, M.; Dubertret, C.; Pitard, B.; Jaslin, G.; Scherman, D. J. Med. Chem. 2000, 43, 4377.
- Geall, A. J.; Taylor, R. J.; Earll, M. E.; Eaton, M. A. W.; Blagbrough, I. S. Bioconjugate Chem. 2000, 11, 314.
- Keller, M.; Jorgensen, M. R.; Perouzel, E.; Miller, A. D. Biochemistry 2003, 42, 6067.
- (a) Kim, B.-K.; Bae, Y.-U.; Doh, K.-O.; Hwang, G.-B.; Lee, S.-H.; Kang, H.; Seu, Y.-B. Bioorg. Med. Chem. Lett. 2011, 21, 3734; (b) Golding, W. P. D.; Jubeli, E.; Downs, R. A.; Johnston, A. J. S.; Khalique, N. A.; Raju, L.; Wafadari, D.; Pungente, M. D. Bioorg. Med. Chem. Lett. 2012, 22, 4686.
- (a) Harvie, P.; Wong, F. M. P.; Bally, M. B. Biophys. J. 1998, 75, 1040; (b) Simoes, S.; Slepushkin, V.; Gasper, R.; Pedroso de Lima, M. C.; Duzgunes, N. Gene Ther. 1999, 6, 1798.
- 20. Ghosh, K. Y.; Visweswariah, S. S.; Bhattacharya, S. FEBS Lett. 2000, 473, 341.
- 21. IR, NMR and mass spectral characterizations of active compounds. **Lipid Cy**: IR: ν_{max} 3444, 2923, 2853, 1734, 1670, 1467, 1160, 1134 cm⁻¹; ¹H NMR (400 MHz, CD₃OD): δ 0.88 (br t, J = 6.2 Hz, 6H, 2 × CH₃), 1.28 (s, 40H, 20 × CH₂), 1.58 (br m, 4H, 2 × OCOCH₂CH₂), 1.80 (br m, 6H, NHCH₂CH₂CH₂CH₂CH₂NH and NHCH₂CH₂CH₂N), 2.07 (m, 2H, NH₂CH₂CH₂CH₂NH), 2.30 (m, 4H, 2 × OCOCH₂CH₂), 3.03–3.10 (m, 10H, NH₂CH₂CH₂CH₂NH, NHCH₂CH₂CH₂CH₂NH and NHCH₂CH₂CH₂N), 3.20 (m, 1H, NHCH₃H_bCH(OCO)CH₂(OCO)), 3.24 (m, 2H, NHCH₂CH₂CH₂N), 3.38 (dd, J = 14.3, 4.8 Hz, 1H, NHCH₃H_bCH(OCO)CH₂(OCO)), 4.03 (dd, J = 12.0, 7.1 Hz, 1H, NHCH₂CH(OCO)CH₃H_b(OCO)), 4.34 (dd, J = 12.0, 2.7 Hz, 1H, NHCH₂CH(OCO)CH₃H_b(OCO)), 5.17 (br s, 1H, NHCH₂CH(OCO)CH₃(OCO)); ¹³C NMR (100 MHz, CD₃OD): δ 14.4 (CH₃), 23.7, 24.3, 30.2, 30.4, 30.6, 33.0 (CH₂), 24.1, 24.2, 28.1 (NHCH₂CH₂CH₂CH₂NH, NHCH₂CH₂CH₂N), 36.9 (NHCH₂CH₂CH₂NH, NHCH₂CH(OCO)CH₂(OCO)CH₂(NH₂N), 37.8, 46.0, 48.0, 48.1, 48.3 (NH₂CH₂CH₂CH₂NH, NHCH₂CH₂CH₂CH₂NH, NHCH₂CH₂CH₂CH₂NH NHCH₂CH₂CCOO)CH₃(NH NHCH₂CH₂CH₂NH NHCH₂CH₂CCOO)CH₃(NH NHCH₂CH₃CCOO)CH₃(NH NHCH₃CH₃CCOO)CH₃(NH H₃CH₃CCOO)CH₃(NHCH₃CH₃CCOO)CH₃(NHCH₃CH₃CCOO)CH₃(NHCH₃CH₃CCOO)CH₃(NHCH₃CH₃CCOO)CH₃(NHCH₃CH₃CCO

(NHCH₂CH₁(OCO)CH₂(OCO)), 161.7 (NHCONH), 174.8 and 175.0 (OCOCH₂); MS(ES): m/z: 740 ([M+H]⁺ 100%); HRESIMS (+ve) m/z calcd for $C_{42}H_{86}N_5O_5$ [M+H]⁺ 740.6623, found 740.6624; **Lipid Dx**: IR: v_{\max} 3407, 2922, 2852, 1740, 1680, 1432, 1293, 1204, 1138 cm⁻¹; ¹H NMR (400 MHz, CD₃OD): δ 0.89 (br t, g = 6.4 Hz, 6H, g × CH₃), 1.28 (s, 32H, g 16 × CH₂), 1.59 (br m, 4H, g × OCO CH₂CH₂), 1.81 (br m, 6H, NHCH₂CH₂CH₂CH₂NH and NHCH₂CH₂CH₂NH), 2.07 (m, 2H, NH₂CH₂CH₂PNH), 2.32 (m, 4H, g × OCOCH₂CH₂), 3.03-3.12 (m, 10H, NH₂CH₂CH₂CH₂NH, NHCH₂CH₂CH₂CH₂NH and NHCH₂CH₂CH₂NH, 3.25 (br m, 2H, NHCH₂CH₂CH₂CH₂NH, 3414 (br s, 5H, NHCH(CH₂OCO)₂); ¹³C NMR (100 MHz, CD₃OD): δ 14.3 (CH₃), 23.7, 24.3, 30.2, 30.4, 30.5, 30.7, 33.0 (CH₂), 24.17, 24.18, 28.4 (NHCH₂CH₂CH₂CH₂NH, NHCH₂CH₂CH₂NH, NHCH₂CH₂CH₂CH₂NH, 34.95 (2 × OCOCH₂CH₂), 3.70 (NHCH₂CH₂CH₂NH) 16.0 (2 × OCOCH₂CH₂), 34.94, 34.95 (2 × OCOCH₂CH₂), 3.70 (NHCH₂CH₂CH₂NH) NHCH₂CH₂CH₂N), 49.6, 64.0, 64.2 (NHCH(CH₂OCO)₂), 162.9 (NHCONH), 175.0

- (OCOCH₂); MS(ES): m/z: 684 ([M+H]⁺ 100%); HRESIMS (+ve) m/z calcd for $C_{38}H_{78}N_5O_5$ [M+H]⁺ 684.5997, found 684.5997. The spectroscopic data of the synthesized lipids are reported in Supplementary data.
- Turek, J.; Dubertret, C.; Jaslin, G.; Antonakis, K.; Scherman, D.; Pitard, B. J. Gene Med. 2000, 2, 32.
- 23. Lian, T.; Ho, R. J. Y. J. Pharm. Sci. 2003, 92, 2373.
- Zhang, C.; Tang, N.; Liu, X. J.; Liang, W.; Xu, W.; Torchilin, V. P. J. Control. Release 2006, 112, 229.
- Semple, S. C.; Klimuk, S. K.; Dos Harasym, T. O.; Santos, N.; Ansell, S. M.; Wong, K. F.; Maurer, N.; Stark, H.; Cullis, P. R.; Hope, M. J.; Scherrer, P. Biochem. Biophys. Acta 2001, 1510, 152.
- Peng, J.; He, X.; Wang, K.; Tan, W.; Li, H.; Xing, X.; Wang, Y. Nanomedicine 2006, 2, 113.
- 27. Denizot, F.; Lang, R. J. Immunol. Methods 1986, 89, 271.



Contents lists available at ScienceDirect

NeuroToxicology



Suppression effects of O-demethyldemethoxycurcumin on thapsigargin triggered on endoplasmic reticulum stress in SK-N-SH cells



Adchara Janyou ^a, Chatchawan Changtam ^b, Apichart Suksamrarn ^c, Chainarong Tocharus ^a, Jiraporn Tocharus ^{d,*}

- ^a Department of Anatomy, Faculty of Medicine, Chiang Mai University, Chiang Mai 50200, Thailand
- ^b Faculty of Science and Technology, Huachiew Chalermprakiet University, Samutprakarn 10540, Thailand
- ^c Department of Chemistry and Center of Excellence for Innovation in Chemistry, Faculty of Science, Ramkhamhaeng University, Bangkok 10240, Thailand
- ^d Department of Physiology, Faculty of Medicine, Chiang Mai University, Chiang Mai 50200, Thailand

ARTICLE INFO

Article history: Received 31 May 2015 Received in revised form 5 August 2015 Accepted 6 August 2015 Available online 8 August 2015

Keywords: ER stress Thapsigargin O-demethyldemethoxycurcumin Neurodegenerative diseases Neuronal cells

ABSTRACT

Endoplasmic reticulum (ER) stress is involved in neurodegenerative diseases, including Alzheimer's disease and Parkinson's disease. Therefore, interventions that attenuate ER stress may contribute to induction in apoptotic cell death. This study aimed to evaluate the potential involvement of O-demethyldemethoxycurcumin, an analog of curcuminoids, on thapsigargin-induced apoptosis in cultured neuroblastoma (SK-N-SH) cells through the ER stress signaling pathway. The results showed that O-demethyldemethoxycurcumin reduced thapsigargin induced cell death in SK-N-SH cells and the release of lactate dehydrogenase (LDH) by decreasing the apoptotic cell death induced by thapsigargin. Consistent with these findings, O-demethyldemethoxycurcumin inhibited the thapsigargin-induced activation of cleavagecaspase-12. Moreover, O-demethyldemethoxycurcumin attenuated the intracellular Ca²⁺ level and the expression of the calpain protein. O-demethyldemethoxycurcumin also downregulated the expression of ER stress signaling proteins, including the phosphorylation of PKR-like endoplasmic reticulum kinase (p-PERK), the phosphorylation of inositol-requiring enzyme 1 (p-IRE1), activating transcription factor 6 (ATF6), binding immunoglobulin protein (BiP) and C/EBP homologous protein (CHOP). Our findings suggest that O-demethyldemethoxycurcumin could protect against thapsigargin-induced ER stress in SK-N-SH cells.

© 2015 Elsevier Inc. All rights reserved.

1. Introduction

Neurodegenerative diseases, such as Alzheimer's disease (AD), Parkinson's disease (PD) and Huntington's disease (HD), account

Abbreviations: 6-OHDA, 6-hydroxydopamine; AD, Alzheimer's disease; ATF6, activating transcription factor 6; BiP, binding immunoglobulin protein; BSA, bovine serum albumin; CHOP, C/EBP homologous protein; CNS, central nervous system; DMSO, dimethyl sulfoxide; DNA, deoxyribonucleic acid; ER, endoplasmic reticulum; FBS, fetal bovine serum; H₂O₂, hydrogen peroxide; HD, Huntington's disease; IRE1, inositol-requiring protein-1; LDH, lactate dehydrogenase; MEM, minimal essential medium; MTT, A-3-(4,5-dimethyl-thiazol-2-yl)-2,5-diphenyl-tetrazolium bromide; PD, Parkinson's disease; PERK, PKR-like ER kinase; PI, propidium iodide; PKR, double-stranded RNA-activated protein kinase; SDS-PAGE, sodium dodecyl sulfate-polyacrylamide gel electrophoresis; SERCA, sarcoplasmic/endoplasmic reticulum calcium ATPase.

* Corresponding author.

 $\hbox{\it E-mail address:} \ jtocharus@gmail.com \ (J.\ Tocharus).$

for a significant and increasing proportion of morbidity and mortality worldwide (Mercado et al., 2013; Alzheimer's Association, 2014; Tanner et al., 2014). Several lines of evidence suggest that endoplasmic reticulum (ER) stress plays a critical role in the development or pathology of many neurodegenerative diseases (Emerit et al., 2004; Costa et al., 2010; Hetz, 2012; Nagai, 2012). These diseases share a common pathogenetic mechanism the aggregation and deposition of unfolded proteins that leads to progressive central nervous system (CNS) degeneration (Emerit et al., 2004; Brown and Naidoo, 2012; Hugo and Hetz, 2013; Halliday and Mallucci, 2014). The ER is a main organelle that regulates protein folding and calcium signaling (Hamman et al., 1998; Kleizen and Braakman, 2004). When the ER is disturbed, unfolded proteins accumulate in the ER lumen and Ca²⁺ is released from the ER to the cytoplasm, leading to ER stress on the cells (Kass and Orrenius, 1999). Several stimuli, such as glucose deprivation, interference with N-linked protein glycosylation, viral infection and depletion of Ca²⁺ in the ER, lead to an accumulation of unfolded proteins in the ER that triggers the unfolded protein response (UPR) (Oyadomari and Mori, 2004; Bernales et al., 2012). The UPR is mediated through ER transmembrane receptors, including double-stranded RNA-activated protein kinase (PKR), the PKR-like ER kinase (PERK), inositol-requiring protein-1 (IRE1) and activating transcription factor 6 (ATF6). Excessive and prolonged stresses ultimately lead to apoptosis by inducing expression of the C/EBP homologous protein (CHOP), a Bcl-2 inhibitor (Harding et al., 2003; Xu et al., 2005; Hetz et al., 2006; Lai et al., 2007). Therefore, interventions that attenuate ER stress may contribute to reduced apoptosis (Nagai, 2012; Bernales et al., 2012; Costa et al., 2013).

Curcumin is a major chemical component of curcuminoids, which is isolated from turmeric (Curcuma longa L). Curcumin and its analogs have been reported to have pharmacological potential as antimutagenic, anticancer, antioxidant, antibacterial and neuroprotective agents (Mazumder et al., 1995; Jiang et al., 2007; Parvathy et al., 2009; Zhao et al., 2011; Fang et al., 2013; Kou et al., 2013; Bhullar et al., 2013; Son et al., 2013; Yang et al., 2014; Yoon et al., 2014). Our study reported that the analogs of curcumin exhibited higher physiological and pharmacological activities than the parent curcumin itself by inhibiting nitric oxide and proinflammatory cytokines production. Among them, O-demethyldemethoxycurcumin was a more potent anti-inflammatory than its parent compounds (Tocharus et al., 2012). It is therefore of interest to investigate whether chemical modification of the curcuminoids would improve their neuroprotective property. In this study, we evaluated whether O-demethyldemethoxycurcumin, the demethylated analog of the natural demethoxycurcumin, protects SK-N-SH cells from thapsigargin-induced cell death mediated by ER stress. Using this model, we determined the effects of O-demethyldemethoxycurcuminon on expression of proteins involved in ER stress-induced cell death.

2. Materials and methods

2.1. Cell culture

SK-N-SH cells, human neuroblastoma cells, were obtained from American Type Culture Collection (ATCC, Manassas, VA, USA). SK-N-SH cells were cultured in Minimum Essential Media (MEM) (Gibco, Gaithersburg, MD, USA) containing 10% FBS, penicillin and streptomycin maintained in a humidified atmosphere of 5% $\rm CO_2$ and 95% air at 37 °C.

2.2. Chemicals

Thapsigargin was purchased from Sigma (St. Louis, MO, USA), and minimal essential medium (MEM), fetal bovine serum (FBS), penicillin, and streptomycin were sourced from GIBCO-BRL (Gaitherburg, MD, USA). The 5 Fluo-4 NW calcium assay kit was purchased from Molecular Probe (Molecular ProbeTM). The western blot analysis used the following antibodies: anti-p-PERK, anti-PERK, anti-CHOP, anti-calpain, anti-BiP, anti-actin (Cell Signaling Technology, MA, USA), anti-p-IRE1, anti-IRE1, anti-ATF6, anti-cleavage caspase-12 (Santa Cruz Biotechnology, CA, USA), anti-mouse IgG peroxidase-conjugated secondary antibody and anti-rabbit IgG peroxidase-conjugated secondary antibody (Millipore, Bedford, MA, USA).

2.3. Preparation of O-demethyldemethoxycurcumin

Demethoxycurcumin (300 mg, 0.89 mmol), obtained from *Curcuma longa* as described previously (Changtam et al., 2010), was dissolved in dry CH_2CI_2 (50 ml). The mixture was stirred at

 $0-5\,^{\circ}\text{C}$ for 5 min and then BBr₃ (1 ml) was slowly added. The reaction mixture was kept stirring at $0-5\,^{\circ}\text{C}$ for 1 h; water (100 ml) was added and the mixture was extracted with EtOAc. The combined organic phase was washed with water, dried over anhydrous Na₂SO₄ and the solvent was removed under vacuum. The crude product was purified by column chromatography using CH₂Cl₂–MeOH (10:1) as eluting solvent to yield *O*-demethyldemethoxycurcumin (180 mg, 62%). The spectroscopic (^{1}H NMR and mass spectra) data were consistent with the reported values (Venkateswarlu et al., 2005).

2.4. Measurement of cell viability using MTT assays

A-3-(4,5-dimethyl-thiazol-2-yl)-2,5-diphenyl-tetrazolium bromide (MTT) assay was used to assess cell viability. SK-N-SH cells were cultured in a 96-well plate at a density of 5×10^5 cells/ml for 24 h at 37 °C in a CO $_2$ incubator. The cells were pretreated with 1, 2 or 4 μ M O-demethyldemethoxycurcumin for 2 h and then treated in the presence or absence of 1 μ M thapsigargin for 24 h. After that 100 μ l of MTT solution (10 mg/ml) was added to each well and incubated at 37 °C for 2 h. The medium was aspirated and 100 μ l dimethyl sulfoxide (DMSO) was then added to dissolve the formazan crystals. The absorbance was measured at 570 nm using a microplate reader (Bio-Tek, Instruments, Winooaski, VT, USA).

2.5. Measurement of lactate dehydrogenase (LDH) release

To determined neurotoxicity of thapsigargin, LDH assay was performed by the LDH cytotoxicity assay kit according to the manufacturer's instruction. SK-N-SH cells were cultured in a 96-well plate at a density of 5×10^5 cells/ml for $24\,h$ at $37\,^{\circ}\text{C}$ in a CO_2 incubator. The cells were pretreated with 1, 2 or $4\,\mu\text{M}$ O-demethyldemethoxycurcumin for 2 h and then treated in the presence or absence of $1\,\mu\text{M}$ thapsigargin for $24\,h$. The culture medium was collected and transferred to a 96-well plate. The level of LDH was assessed by adding $100\,\mu\text{l}$ LDH reaction mix and incubated at $37\,^{\circ}\text{C}$ for $30\,\text{min}$. The absorbance was measured at $450\,\text{nm}$ using a microplate reader (Bio-Tek, Instruments, Winooaski, VT, USA).

2.6. Measurement of intracellular calcium level

SK-N-SH cells were plated at a density of 1 \times 10⁴ cells/well into a 96-well plate for 24 h. Cells were pretreated with 1, 2 or 4 μ M O-demethyldemethoxycurcuminfor 2 h, followed by treatment with 1 μ M thapsigargin for 24 h. Cells were loaded with Tyrode-HEPES (in mM: 145 NaCl, 2.7 KCl, 1 MgCl₂, 1.8 CaCl₂, 10 p-glucose, 10 HEPES, pH 7.4) containing 0.02% pluronic acid, 10 μ M fluo-4 AM and 1 mM probenecid in the dark for 45 min at 37 °C. Cells were washed with Tyrode-HEPES in the dark for 30 min at room temperature. Changes in fluorescence were measured at an excitation wavelength of 494 nm and emission wavelength of 516 nm by using a fluorescent plate reader (DTX800, Beck-man Coulter, Austria).

2.7. Assessment of apoptosis using flow cytometry

To determine the number of cell apoptosis, SK-N-SH cells were plated at a density of 1×10^5 cells/ml into a 96-well plate for 24 h. Cells were pretreated with 1, 2 or 4 μ M O-demethyldemethoxycurcumin for 2 h, followed by treatment with 1 μ M thapsigargin for 24 h; then cells were collected and resuspended in $1\times$ binding buffer and incubated with annexinV-FITC and propidium iodide (PI) for 15 min. Cells were analyzed with the MuseTM Cell Analyzer (Millipore, Bedford, MA, USA).

2.8. Western blot analysis

SK-N-SH cells were plated at a density of 5×10^5 cells/ml at 37 °C. The cells were then pretreated with O-demethyldemethoxycurcumin at concentrations of 1, 2 or 4 µM for 2 h, followed by treatment in the presence or absence of 1 µM thapsigargin for 9 h for detecting the expression of p-PERK, PERK, and CHOP or 24 h for detecting the expression of p-IRE1, IRE1, ATF6, BiP, calpain and cleavage caspase-12. After treatment, SK-N-SH cells were washed with cold phosphate-buffered saline (PBS; pH 7.4). SK-N-SH cells at a density of 5×10^5 cells/well were lysed in lysis buffer supplemented with protease inhibitor cocktail. The cell lysates were centrifuged at $11,000 \times g$ for 15 min at 4 °C. The supernatant was collected and assayed for determination of total protein concentrations using the Bradford assay with bovine serum albumin (BSA) as the standard. Extracted protein (50 µg) in each sample was separated by sodium dodecyl sulfate-polyacrylamide gel electrophoresis (SDS-PAGE) on 10–15% polyacrylamide gel. Separated proteins were transferred to polyvinylidenenedifluoride (PVDF) membrane and were incubated overnight in blocking solution containing 5% non-fat dry milk. Then, they were incubated overnight with primary antibodies (anti p-PERK, anti-PERK, anti-p-IRE1, anti-IRE1, anti-ATF6, anti-BiP, anticalpain, anti-cleavage caspase-12, anti-CHOP, and anti-actin) at 4 °C. The blots were then incubated for 1 h with horseradish peroxidaseconjugated secondary antibodies (Millipore, MA, USA). The signal was visualized blots using enhanced chemiluminescence. Densitometric analysis was performed using a scanning densitometer of X-ray films and the results were normalized using β -actin by using Image I[®] software.

2.9. Statistical analysis

All data were calculated as mean \pm SD of three independent experiments and the comparison between groups were performed by One-Way Analysis of Variance (ANOVA), followed by Post Hoc Dunnett's test. The level of significance was taken as p < 0.05.

3. Results

3.1. Effects of O-demethyldemethoxycurcumin on cell viability and apoptotic cell death induced by thapsigargin in SK-N-SH cells

We first investigated the effect of O-demethyldemethoxycurcumin on ER stress-induced cell death in SK-N-SH cells. In the preliminary experiment, we determined the viability of cells treated with thapsigargin at concentrations of 0.001, 0.01, 0.1, 1 or 2 μM were 92.8 ± 2.0 , 80.3 ± 6.0 , 75.3 ± 2.5 , 49.6 ± 2.5 and $44.0 \pm 1.2\%$, respectively (Fig. 1A). Based on these results, thapsigargin of 1 µM, at which thapsigargin significantly induced cell death in approximately 50% of the cells (p < 0.001) compared to the control group, was selected for use in subsequent studies to examine the protective effect of Odemethyldemethoxycurcumin. Cells were preincubated with 1, 2 or 4 µM of O-demethyldemethoxycurcumin for 2 h before being treated with 1 µM thapsigargin for an additional 24 h, a statistical increase in cell viability was observed when cells were exposed in a concentrationdependent manner. The cell viability values were 60.1 \pm 1.6, 76.1 \pm 3.7 and 85.9 \pm 1.9% when the cells were pretreated with 1, 2 or 4 μ M of 0demethyldemethoxycurcumin, respectively (Fig. 1B). The cytoprotective effect of O-demethyldemethoxycurcumin was also confirmed by LDH release assay (Fig. 1C). The results showed that thapsigargin induced releasing LDH at approximately $128 \pm 6.51\%$ of cell compared with the control group. The level of LDH following pretreatment with 1, 2 or 4 μ M O-demethyldemethoxycurcumin for 2 h and then treatment with 1 μ M thapsigargin were 125 \pm 4.71, 119 \pm 4.31 and 107 \pm 5.50%, respectively (Fig. 1C). To determine whether the observed inhibitory effect of thapsigargin on cell viability was caused by inducing apoptosis, we measured the number of apoptotic cells using a flow cytometer. Flow cytometric analysis (with FITC annexin-V and propidium iodide) revealed the increased number of apoptotic cells by thapsigargin were 37.82% (Fig. 1D–F). The numbers of apoptotic cells following pretreatment with 1, 2 or 4 μ M O-demethyldemethoxycurcumin for 2 h and then treatment with 1 μ M thapsigargin were 19.53%, 17.10% and 12.11%, respectively (Fig. 1F). O-demethyldemethoxycurcumin alone did not affect the number of apoptotic cells. Taken together, these results showed that O-demethyldemethoxycurcumin protected SK-N-SH cells against ER stress-induced apoptotic death.

3.2. Effects of O-demethyldemethoxycurcumin on intracellular calcium level induced by thapsigargin in SH-N-SH cells

Pretreatment of cells with *O*-demethyldemethoxycurcumin at concentrations of 1, 2 or 4 μM for 2 h, followed by 1 μM thapsigargin for 24 h, significantly decreased intracellular calcium accumulation by thapsigargin, the levels of intracellular calcium were $151.83\pm14.80,\ 141.87\pm11.45$ and $127.92\pm19.15\%$ compared to the group treated with thapsigargin alone (187.11%), respectively (Fig. 2). However, treatment with 4 μM of *O*-demethyldemethoxycurcumin alone did not affect the level of intracellular calcium compared to the control group.

3.3. Effects of O-demethyldemethoxycurcumin on thapsigargin induced ER stress signaling pathway in SH-N-SH cells

To determine the protective effect of O-demethyldemethoxvcurcumin on thapsigargin-induced apoptosis via the ER stress pathway, we first used western blot analysis to investigate the effect of thapsigargin on the expression of ER stress proteins, including p-PERK, PERK, p-IRE1, IRE1, ATF6, BiP, calpain, cleavage caspase-12 and CHOP expression proteins in SH-N-SH cells over various time periods. SK-N-SH cells were treated with 1 µM thapsigargin for 0, 3, 6, 9, 18 or 24 h. The results showed a significant increase in the relative expression of the p-PERK normalized to PERK protein at 9 h, together with the expression of CHOP normalized actin protein (Fig. 3A). The thapsigargin treatment resulted in a significantly increased expression of p-IRE1, ATF6, BiP, calpain and cleavage caspase-12 proteins in a time-dependent manner (Fig. 3A-C). These results suggested that the expression of ER stress proteins increased in a time-dependent manner from 3 to 24 h, with the maximum level at 24 h. The expression of p-PERK and CHOP proteins was observed from 9 to 24 h in SK-N-SH cells treated with 1 μM thapsigargin, with the maximum level at 9 h. Therefore, the expression of p-PERK and CHOP proteins at 9 h and the expression of p-IRE1, ATF6, BiP, calpain and cleavage caspase-12 at 24 h were chosen for subsequent studies. Pretreatment with 1, 2 or 4 µM O-demethyldemethoxycurcumin for 2 h before treatment with 1 µM thapsigargin for an additional 9 significantly attenuated the expression of p-PERK, PERK, and CHOP proteins in a concentration-dependent manner (Fig. 4A and E). Moreover, pretreatment with O-demethyldemethoxycurcumin prior to thapsigargin activation for 24 h significantly reduced the expression of p-IRE1, IRE1, ATF6, BiP, calpain and cleavage caspase-12 in a concentrationdependent manner (Fig. 4B-D). However, O-demethyldemethoxycurcumin alone did not affect the expression of these proteins. These findings indicated that O-demethyldemethoxycurcumin protected neuronal cells against thapsigargin-induced apoptosis by attenuating ER stress activating pathways.

4. Discussion

The present study demonstrated that O-demethyldemethoxycurcumin reduced thapsigargin induced cell death accompanied

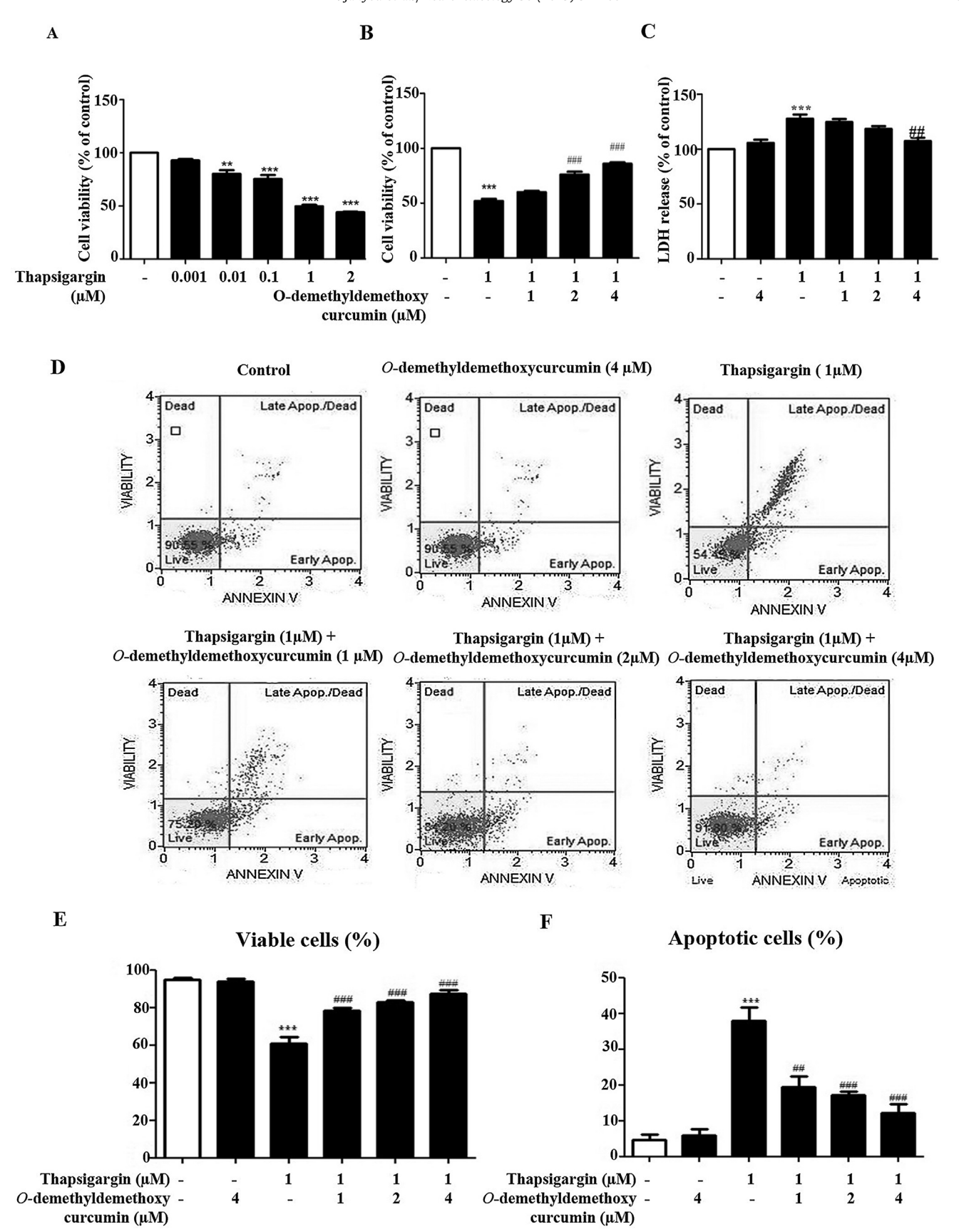


Fig. 1. The effect of O-demethyldemethoxycurcumin on thapsigargin-induced cell death in SK-N-SH cells. (A) Cells were pretreated with 1, 2 or 4 μ M O-demethyldemethoxycurcumin for 2 h and then exposed with 1 μ M thapsigargin for 24 h. Cell viability was measured by MTT assay and LDH release assay (B, C). The representative of FITC annexin-V and propidium iodide binding assay in flow cytometry (D). The comparative results of the percentage of viable cells and apoptotic cells by flow cytometry (E, F). The data are expressed as the mean \pm SD of 3 independent experiments. Means were significantly different: **p < 0.01, and ****p < 0.001 compared with the control group; **p < 0.01, and ***p < 0.001 compared with the 1 μ M thapsigargin-treated group.

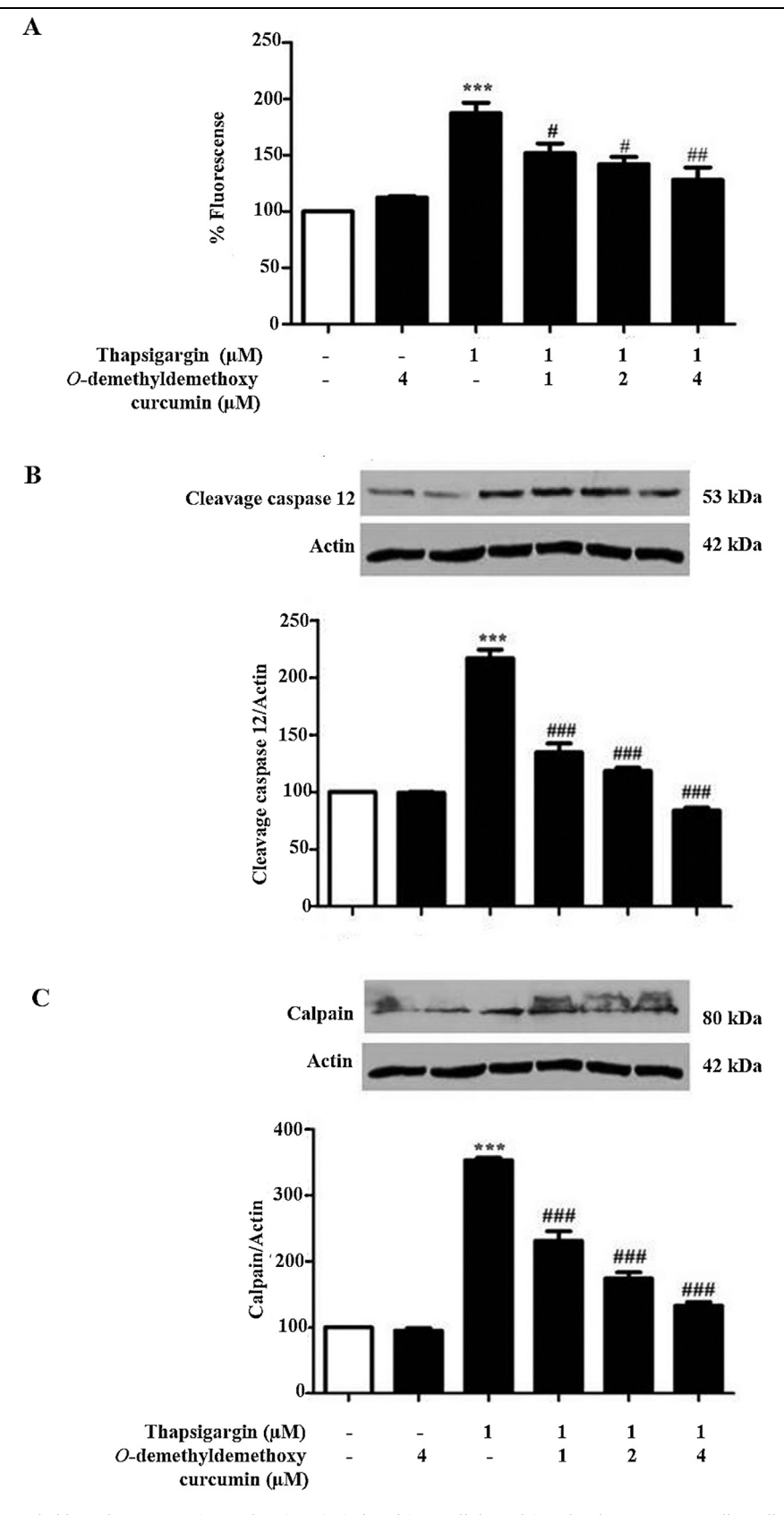


Fig. 2. Protective effect of O-demethyldemethoxycurcumin on thapsigargin-induced intracellular calcium level on SK-N-SH cells. Cells were pretreated with various concentrations of O-demethyldemethoxycurcumin (1, 2 or 4 μ M) for 2 h before treating with 1 μ M thapsigargin for 24 h. The level of intracellular Ca²⁺ was determined by the fluorescent intensity of fluo-4 AM. (A). The representative western blot analysis showing the expression and quantitative analysis of calpain and cleavage caspase-12 normalized to the actin. (B, C). The data show mean \pm SD of 3 independent experiments. Means were significantly different: ***p < 0.001 compared with control group; *p < 0.05, ***p < 0.01, and ***#p < 0.001 compared with 1 μ M thapsigargin-treated group.

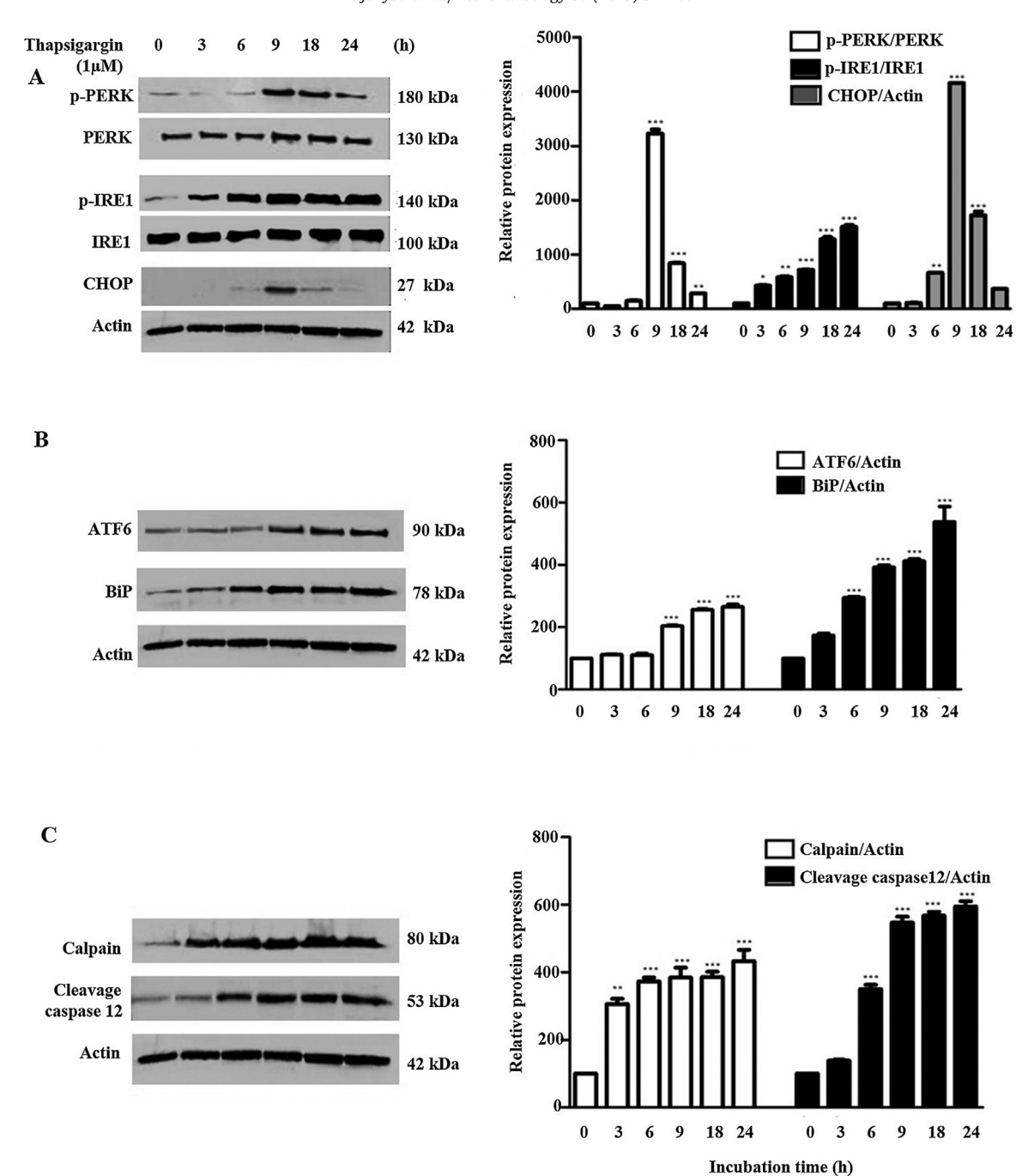


Fig. 3. The time course of the thapsigargin-induced expression of p-PERK, PERK, p-IRE1, IRE1, CHOP. (A) The quantitative analysis of ATF6 and BiP was normalized to the actin. (B) The quantitative analysis of calpain and cleavage caspase-12 was normalized to the actin. (C) in SK-N-SH cells. The cells were treated with 1 μ M thapsigargin for 0, 3, 6, 9, 18 or 24 h and then harvested; the proteins were extracted to determine the expression of indicated proteins by using western blot analysis. The data show mean \pm SD of 3 independent experiments. Means were significantly different: *p < 0.05, **p < 0.01, and ***p < 0.001 compared with control group.

by reducing LDH release in SK-N-SH cells. Based on our findings, we proposed that O-demethyldemethoxycurcumin has a neuroprotective effect against ER stress-induced cell death. Previous studies suggested cell death following exposure to amyloid β , hydrogen peroxide (H_2O_2), tunicamycin or thapsigargin are useful as models of neurodegenerative diseases (Yan Qin et al., 2010; Saito et al., 2007). Thapsigargin is a specific inhibitor of the ER calcium ATPase, causing an increase in cytoplasmic Ca^{2+} concentration (Thastrup et al., 1990; Lytton et al., 1991; Lervick et al., 1995; Nath et al., 1997). Dysfunction of calcium homeostasis can cause ER stress and cell death (Bernales et al.,

2012). There is crosstalk between the ER and mitochondria; ER stress induces mitochondrial dysfunction and caspase activation. ER-induced apoptosis is associated with early calpain-dependent activation of cleavage caspase-12, which can lead to caspase-3 cleavage. Finally, caspase-3 induces cell death via apoptosis (Nakagawa et al., 2000; Morishima et al., 2002). Calpain, a Ca²⁺-responsive cytosolic cysteine protease that is an important early mediator of ER-dependent cell death, is activated during ER stress. In the present study with SK-N-SH cells, we successfully produced the thapsigargin-induced ER stresses with increased Ca²⁺ concentrations, and increased expressions of calpain and cleavage

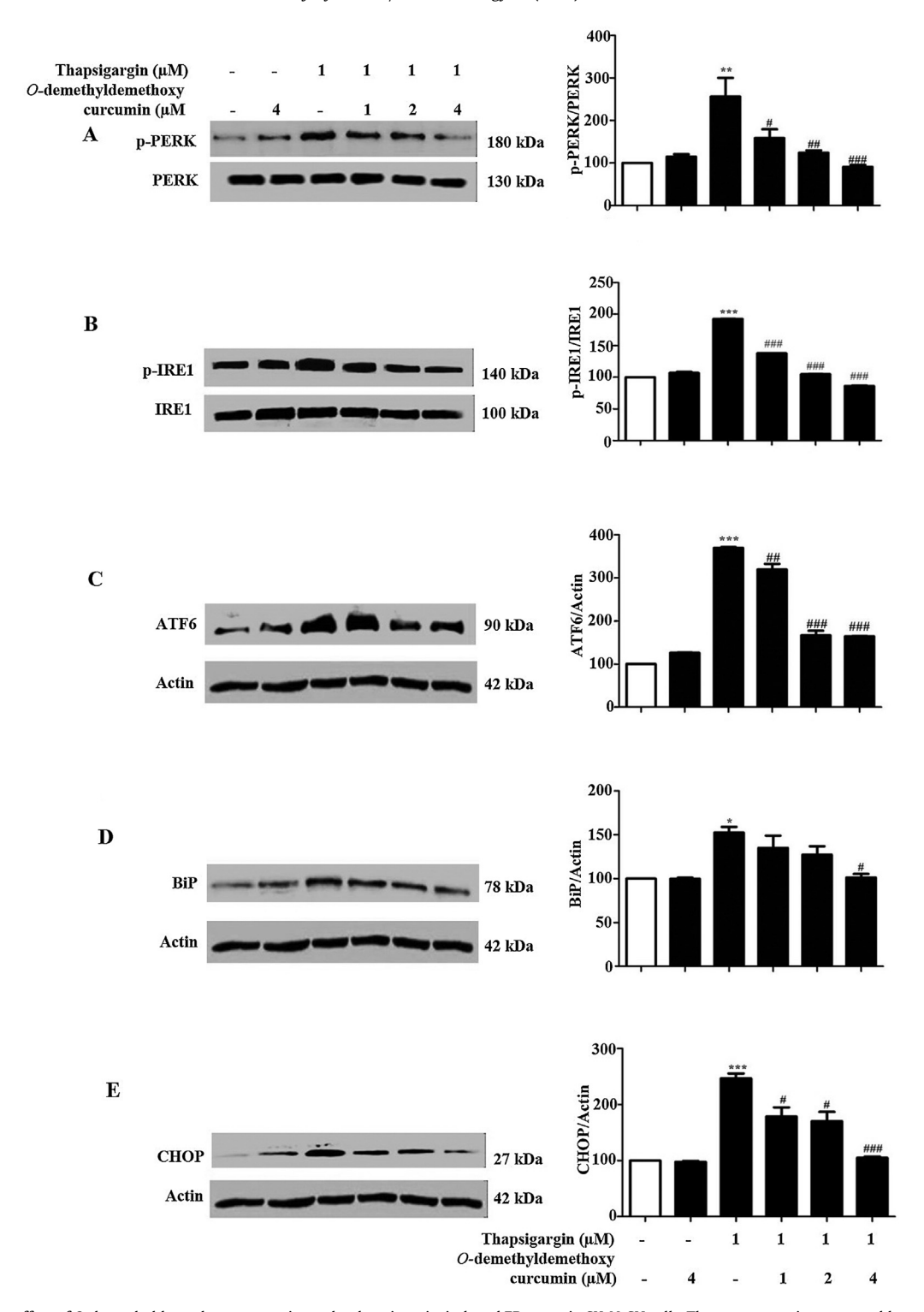


Fig. 4. The protective effect of *O*-demethyldemethoxycurcumin on the thapsigargin-induced ER stress in SK-N-SH cells. The representative western blot analysis showing the expression of p-PERK, p-IRE1, IRE1, Bip, ATF6, and CHOP proteins in SK-N-SH cells. The cells were pretreated with *O*-demethyldemethoxycurcumin (1, 2 or 4 μM) for 2 h and then treated with 1 μM thapsigargin for 9 h or 24 h. (A) The quantitative analysis of p-PERK was normalized to the PERK. (B) The quantitative analysis of p-IRE1 was normalized to the IRE.1 (C–E). The quantitative analysis of ATF6, BiP and CHOP were normalized to the actin. The data show mean \pm SD of 3 independent experiments. Means were significantly different: $^*p < 0.05$, $^{**}p < 0.01$ and $^{***}p < 0.01$ and $^{***}p < 0.001$ compared with 1 μM thapsigargin-treated group.

caspase-12. However, we found a significant decreased in cytosolic Ca²⁺ levels in *O*-demethyldemethoxycurcumin-treated neuronal cells and decreased expression of calpain and cleavage caspase-12. In addition, we observed by flow cytometer that *O*-demethyldemethoxycurcumin protected SK-N-SH cells from apoptosis that related to increased cell viability from the MTT

assay and LDH assay. These findings suggest that *O*-demethyldemethoxycurcumin prevented ER stress-induced apoptosis via the blockage the loss of Ca²⁺ homeostasis trigger apoptosis by decreasing calpain and cleavage caspase-12.

ER stress is associated with increased transcription of ER resident chaperon BiP and nuclear protein CHOP. BiP is a regulator of UPR and

widely used as an ER stress marker. In prolonged ER stress, unfolded proteins accumulate within the ER, BiP releases from three sensors for ER signaling in the transmembrane of the ER (PERK, IRE1 and ATF6) and bind misfolded proteins, thereby activating PERK, IRE1 and ATF6 (Halliday and Mallucci, 2014). In this study, we showed that O-demethyldemethoxycurcumin downregulated expression of BiP and all three arms of UPRs, including the phosphorylation of $eIF2\alpha$ and IRE1 α and the cleavage of ATF6 in thansigargin-treated cells. Sustained and excessive ER stress leads to ER stress-induced apoptosis that is facilitated by an increase in CHOP expression. CHOP is expressed at low levels under normal conditions. Overexpression of CHOP correlates well with the onset of ER stress-associated apoptosis, while CHOP deficiency can protect cells from ER stressinduced apoptosis. Moreover, elevated expression of CHOP has been found in various neurodegenerative diseases in animal models, such as Parkinson's disease and Alzheimer's disease (Milhavet et al., 2002; Chen et al., 2004). Therefore, CHOP is a molecular targeting of candidates for neuroprotective agents in ER stress-related neurodegenerative diseases. Our results showed that O-demethyldemethoxycurcumin protected neuronal cells during ER stress at least in part, through the suppression of CHOP expression by inhibiting PERK, IRE1 and ATF6 pathways.

Thus, O-demethyldemethoxycurcumin, a demethylated analog of demethoxycurcumin, reduces thapsigargin toxicity by decreasing the expression of ER stress, which attenuates the progression of neuronal cell degeneration.

5. Conclusion

In summary, our study provides evidence that *O*-demethyldemethoxycurcumin effectively inhibits thapsigargin-induced apoptosis associated with ER stress in neuronal cells.

Conflict of interest

The authors declare that there are no conflicts of interest.

Transparency document

The Transparency document associated with this article can be found in the online version.

Acknowledgements

This work was supported by the National Research Council of Thailand (NRCT). Support from The Thailand Research Fund is gratefully acknowledged.

References

- Alzheimer's Association, 2014. 2014 Alzheimer's disease facts and figures. Alzheimers Dement. 10, 47–92.
- Bernales, S., Soto, M.M., McCullagh, E., 2012. Unfolded protein stress in the endoplasmic reticulum and mitochondria: a role in neurodegeneration. Front. Aging Neurosci. 4, 1–13.
- Bhullar, K.S., Jha, A., Youssef, D., Rupasinghe, H.P.V., 2013. Curcumin and its carbocyclic analogs: structure–activity in relation to antioxidant and selected biological properties. Molecules 18, 5389–5404.
- Brown, M.K., Naidoo, N., 2012. The endoplasmic reticulum stress response in aging and age-related diseases. Front. Physiol. 3, 3389–3399.
- Changtam, C., De Koning, H.P., Ibrahim, H., Sajid, M.S., Gould, M.K., Suksamrarn, A., 2010. Curcuminoid analogs with potent activity against Trypanosoma and Leishmania species. Eur. J. Med. Chem. 45, 941–956.
- Chen, G., Bower, K.A., Ma, C., Fang, S., Thiele, C.J., Luo, J., 2004. Glycogen synthase kinase 3 beta (GSK3beta) mediates 6-hydroxydopamine-induced neuronal death. FASEB J. 18, 1162–1164.
- Costa, R.O., Ferreiro, E., Cardoso, S.M., Oliveira, C.R., Pereira, C.M.F., 2010. ER stress-mediated apoptotic pathway induced by Aβ peptide requires the presence of functional mitochondria. J. Alzheimers Dis. 20, 625–636.

- Costa, R.O., Ferreio, E., Oliveira, C.R., Pereira, C.M.F., 2013. Inhibition of mitochondrial cytochrome c oxidase potentiates Aβ-induced ER stress and cell death in cortical neurons. Mol. Cell Neurosci. 52, 1–8.
- Emerit, J., Edeas, M., Bricaire, F., 2004. Neurodegenerative diseases and oxidative stress. Biomed. Pharmacother. 58, 39–46.
- Fang, X., Fang, L., Gou, S., Cheng, L., 2013. Design and synthesis of dimethylaminomethyl-substituted curcumin derivatives/analogues: potent antitumor and antioxidant activity, improved stability and aqueous solubility compared with curcumin. Bioorg. Med. Chem. Lett. 23, 1297–1301.
- Halliday, M., Mallucci, G.R., 2014. Targeting the unfolded protein response in neurodegeneration: a new approach to therapy. Neuropharm 76, 169–174.
- Hamman, B.D., Hendershot, L.M., Johnson, A.E., 1998. Bip maintains the permeability barrier of the ER membrane by sealing the luminal end of the translocon pore before and early in translocation. Cell 92, 747–758.
- Harding, H.P., Zhang, Y., Zeng, H., Novoa, I., Lu, P.D., Calfon, M., Sadri, N., Yun, C., Popko, B., Paules, R., Stojdl, D.F., Bell, J.C., Hettmann, T., Leiden, J.M., Ron, D., 2003. An integrated stress response regulates amino acid metabolism and resistance to oxidative stress. Mol. Cell 11, 619–633.
- Hetz, C., Bernasconi, P., Fisher, J., Lee, A.H., Bassik, M.C., Antonsson, B., Brandt, G.S., Iwakoshi, N.N., Schinzel, A., Glimcher, L.H., Korsmeyer, S.J., 2006. Proapoptotic BAX and BAK modulate the unfolded protein response by a direct interaction with IRE1α. Science 312, 572–576.
- Hetz, C., 2012. The unfolded protein response: controlling cell fate decisions under ER stress and beyond. Nat. Rev. Mol. Cell Biol. 13, 89–102.
- Hugo, V., Hetz, C., 2013. The unfolded protein response in Alzheimer's disease. Semin. Immunophatol. 35, 277–292.
- Jiang, J., Wang, W., Sun, Y.J., Hi, M., Li, F., Zhu, D.Y., 2007. Neuroprotective effect of curcumin on focal cerebral ischemic rats by preventing blood-brain barrier damage. Eur. J. Pharmacol. 561, 54–62.
- Kass, G.E.N., Orrenius, S., 1999. Calcium signaling and cytotoxicity. Environ. Health Perspect. 107, 25–35.
- Kleizen, B., Braakman, I., 2004. Protein folding and quality control in endoplasmic reticulum. Curr. Opin. Cell Biol. 16, 343–349.
- Kou, M.C., Chiou, S.Y., Weng, C.Y., Wang, L., Ho, C.T., Wu, M.J., 2013. Curcuminoids distinctly exhibit antioxidant activities and regulate expression of scavenger receptors and heme oxygenase-1. Mol. Nutr. Food Res. 57, 1598-1610.
- Lai, E., Teodoro, T., Volchuk, A., 2007. Endoplasmic reticulum stress: signaling the unfolded protein response. Physiology 22, 193–201.
- Lervick, V., Coffey, H., D'Mello, S.R., 1995. Opposing effects of thapsigargin on the survival of developing cerebellar granule neurons in culture. Brain Res. 676, 325–335.
- Lytton, J., Westlin, M., Hanley, M.R., 1991. Thapsigargin inhibits the sarcoplasmic or endoplasmic reticulum Ca-ATPase Family of calcium pumps. J. Biol. Chem. 26, 17067–17071.
- Mazumder, A., Raghavan, K., Weinstein, J., Kohn, K.W., Pommier, Y., 1995.
 Inhibition of human immunodeficiency virus type-1 integrase bycurcumin.
 Biochem. Pharmacol. 49, 1165–1170.
- Mercado, G., Valdes, P., Hetz, C., 2013. An ERcentric view of Parkinson's disease.

 Trends Mol. Med. 19, 1471–1491.
- Milhavet, O., Martindale, J.L., Camandola, S., Chan, S.L., Gary, D.S., Cheng, A., Holbrook, N.J., Mattson, M.P., 2002. Involvement of Gadd153 in the pathogenic action of presenilin-1 mutations. J. Neurochem. 83, 673–681.
- Morishima, N., Nakanishi, K., Takenouchi, H., Shibata, T., Yasuhiko, Y., 2002. An endoplasmic reticulum stress-specific caspase cascade in apoptosis: cytochrome c-independent activation of caspase-9 by caspase-12. J. Biol. Chem. 277, 34287–34294.
- Nagai, K., 2012. Bovine milk phospholipid fraction protects Neuro2a cells from endoplasmic reticulum stress via PKC activation and autophagy. J. Biosci. Bioeng. 114, 466–471.
- Nakagawa, T., Zhu, H., Morishima, N., Li, E., Xu, J., Yankner, B.A., Yuan, J., 2000. Caspase-12 mediates endoplasmic reticulum specific apoptosis and cytotoxicity by amyloid-β. Nature 403, 98–103.
- Nath, R., Raser, K.J., Hajimohammadreza, I., Wang, K.K.W., 1997. Thapsigargin induces apoptosis in SH-SY5Y neuroblastoma cells and cerebrocortical cultures. Biochem. Mol. Biol. Int. 43, 197–205.
- Oyadomari, S., Mori, M., 2004. Roles of CHOP/GADD153 in endoplasmic reticulum stress. Cell Death Differ. 11, 381–389.
- Parvathy, K.S., Negi, P.S., Srinivas, P., 2009. Antioxidant, antimutagenic and antibacterial activities of curcumin-β-diglucoside. Food Chem. 115, 265–271.
- Saito, Y., Nishio, K., Ogawa, Y., Kinumi, T., Yoshida, Y., Masuo, Y., Niki, E., 2007. Molecular mechanisms of 6-hydroxydopamine-induced cytotoxicity in PC12 cells: involvement of hydrogen peroxide-dependent and-independent action. Free Radic. Biol. Med. 42, 675–685.
- Son, Y., Lee, J.H., Cheong, Y.W., Chung, H.T., Pae, H.O., 2013. Antidiabetic potential of the heme oxygenase-1 inducer curcumin analogues. Biomed. Res. Int. 10, 1155–1162.
- Tanner, C.M., Goldman, S.M., Ross, G.W., Grate, S., 2014. The disease intersection of susceptibility and exposure: chemical exposures and neurodegenerative disease risk. Alzheimers Dement. 10, 213–225.
- Thastrup, O., Cullen, P.J., Drobak, B.K., Hanley, M.R., Dawson, A.P., 1990. Thapsigargin, a tumor promoter, discharges intracellular Ca²⁺ stores by specific inhibition of the endoplasmic reticulum Ca²⁺-ATPase. Proc. Natl. Acad. Sci. U. S. A. 8, 2466–2470.

- Tocharus, J., Jamsuwan, S., Tocharus, C., Changtam, C., Suksamrarn, A., 2012. Curcuminoid analogs inhibit nitric oxide production from LPS-activated microglial cells. J. Nat. Med. 66, 400-405.
- Venkateswarlu, S., Ramachandra, M.S., Subbaraju, G.V., 2005. Synthesis and biological evaluation of polyhydroxycurcuminoids. Bioorg. Med. Chem. 13, 6374-6380.
- Xu, C., Maitre, B.B., Reed, J.C., 2005. Endoplasmic reticulum stress: cell life and
- death decisions. J. Clin. Invest. 115, 2656–2664. Yan Qin, X., Cheng, Y., Chuan Yu, L., 2010. Potential protection of curcumin against intracellular amyloid β -induced toxicity in cultured rat prefrontal cortical neurons. Neurosci. Lett. 480, 21-24.
- Yang, J., SongS, Li, J., Liang, T., 2014. Neuroprotective effect of curcumin on hippocampal injury in 6-OHDA-induced Parkinson's disease rat. Pathol. Res. Pract. 210, 357–362.
- Yoon, M.J., Kang, Y.J., Lee, J.A., Kim, I.Y., Lee, Y.S., Park, J.H., Lee, B.Y., Kim, I.A., Kim, H.S., Kim, S.A., Yoon, A.R., Yun, C.O., Kim, E.Y., Lee, K., Choi, K.S., 2014. Stronger proteasomal inhibition and higher CHOP induction are responsible for more effective induction of parapoptosis by demethoxycurcumin than curcumin. Cell Death Dis. 1112, 2041-2055.
- Zhao, X.C., Zhang, L., Yu, H.X., Sun, Z., Lin, X.F., Tan, C., Lu, R.R., 2011. Curcumin protects mouse neuroblastoma Neuro-2A cells against hydrogen-peroxideinduced oxidative stress. Food Chem. 129, 387-394.